Characterisation of *Pseudomonas putida* FNR proteins

Susan Abdulrahman Ibrahim

A thesis submitted to the University of Sheffield for the degree of Doctor of Philosophy.

Department of Molecular Biology and Biotechnology,

The University of Sheffield

June 2016

Abstract

Pseudomonas putida KT2440 is a Gram-negative obligate aerobic bacterium. It is found in very diverse habitats such as soil, plants and water. The *Escherichia coli* Fumarate-Nitrate reduction regulator (FNR) protein is the paradigm for bacterial O_2-sensing transcription factors. However, unlike *E. coli*, *Pseudomonas putida* KT2440 possesses three FNR proteins (ANR, PP_3233, and PP_3287). The functions and properties of these multiple FNR proteins are poorly understood, but it has been suggested that they have evolved to fulfill distinct roles.

Under anaerobic conditions, all three *P. putida* FNR proteins possessed iron-sulfur clusters. The iron-sulfur cluster of ANR reacted rapidly with O_2 and was converted from a [4Fe-4S] to a [2Fe-2S] cluster, similar to that of *E. coli* FNR. Furthermore, during cluster conversion sulfur was retained. Like ANR, reconstituted PP_3233 and PP_3287 were converted to [2Fe-2S] forms when exposed to O_2, but their [4Fe-4S] clusters reacted more slowly. Activities of *P. putida* FNR proteins *in vivo* were consistent with those observed *in vitro*. Transcription from an FNR-dependent promoter indicated that all three FNR proteins were O_2-senstive transcription factors *in vivo*. Overall, the experimental results suggested that the amino acid substitutions flanking the cysteine residues that coordinate the iron sulfur clusters of *P. putida* PP_3233 and PP_3287 influence reactivity with O_2, such that ANR resembles *E. coli* FNR and is highly responsive to low concentrations of O_2, whereas PP_3233 and PP_3287 have evolved to be less sensitive to O_2.

Reconstituted ANR, PP_3233 and PP_3287 were capable of specifically binding at an FNR box under anaerobic conditions, whereas the apo-proteins were not. Thus, it was concluded that the binding activities of three FNR proteins were enhanced by the iron-sulfur cluster under anaerobic conditions. The recognition of an FNR box by all *P. putida* FNR proteins indicated that the expressions of all three proteins are likely to be either spatially or temporally separated and they could control identical/overlapping regulons.

Similar to *P. putida*, *Desulfovibrio desulfuricans* possesses multiple FNR proteins. *Desulfovibrio desulfuricans* is sulfate-reducing bacterium that has the ability to utilize nitrate and sulfate as electron acceptors. *Desulfovibrio desulfuricans* possesses two

regulatory proteins associated with the response to nitrosative stress HcpR and HcpR2.

It is shown that HcpR2 is a transcription factor that responds to O_2 and nitric oxide, via a [4Fe-4S] cluster. Holo-HcpR2 reacted with O_2 via assembly and disassembly of its iron-sulfur cluster similarly to *E. coli* FNR.

Acknowledgements

Firstly and importantly, I would like to express my deepest gratitude to my supervisor Prof. Jeffrey Green for his support and guidance throughout my research and writing thesis. I would also like to thank my second supervisor Dr. Melanie Stapleton for her support and help especially in the first steps of my project. A great thanks also goes to everyone in F10 for their help and support all the time.

My sincere thanks also goes to our collaborators at the university of East Anglia for their help and advice specially Dr. Jason Crack for his help in CD and LMS spectroscopy, and data analysis and fitting. Thanks also go to our collaborators in Germany for their help *in vivo* work. I have to thank Dr. Ian cadby for his help in HcpR2 work and Dr. Rosemary Staniforth and Amy Irvine for gel filtration experiments.

I would like to thank my friend Nadal Al-Saryi for her support and encouragement during my PhD. Finally, great thanks go to my family (my parents, my brother and sisters) for their constant encouragement and support through this work.

Table of Contents

List of Figures

Chapter 1

Chapter 3

Chapter 4

Chapter 5

Chapter 6

Chapter 7

List of Tables

Chapter 2

Chapter 6

List of Abbreviations

Amp^R: Ampicillin resistance

ANR: Anaerobic Nitrate Regulator

APS: Ammonium persulfate

bp: base pairs

cAMP: Cyclic adenosine monophosphate

CD spectroscopy: Circular dichroism spectroscopy

CRP: cAMP receptor protein

DNR: dissimilatory nitrate respiration regulator

DTT: Dithiothreitol

EDTA: Ethylenediaminetetraacetic acid

EMSA: Electromobility shift assay

Fe-S: Iron-sulfur cluster

FNR: Fumarate and Nitrate reduction Regulator

Gm^R: Gentamycin resistance

GST: Glutathione *S*-transferase

HEPES: N-2-hydroxyethylpiperazine-N'-2-ethanesulfonic acid

IPTG: Isopropyl-β-D-thiogalactopyranoside

Kan^R: Kanamycin resistance

kDa: KiloDalton

LB: Lennox broth

LCMS: Liquid chromatography mass spectrometry

MS: Mass spectroscopy

NOC-7: 1-Hydroxy-2-oxo-3-(3-aminopropyl)-3-isopropyl-1-triazene

OD: optical density

ONPG: *o*-nitrophenyl-β-D-galactopyranoside

PAGE: Polyacrylamide gel electrophoresis

PCR: Polymerase chain reaction

psi: pound-force per square inch

RNAP: RNA Polymerase

qRT-PCR: Quantitative Polymerase Chain Reaction

rpm: Revolutions per minute

SDS: Sodium dodecyl sulfate

TBS: Tris-Buffered Saline

TCA: Trichloroacetic acid

TEMED: N,N,N',N'-tetramethylethylenediamine

Tet^R: Tetracycline resistance

TMAO: Trimethylamine N-oxide

Tris: Tris (hydroxymethyl) methylamine

UV: Ultraviolet

$^V/_V$: Volume by volume

$^W/_V$: Weight by volume

X-Gal: 5-bromo-4-chloro-3-indolyl-β-D-galactopyranoside

Chapter 1

Introduction

1.0 Introduction

Packages of DNA (chromosomes and plasmids) are the repositories of information required for bacteria to survive, replicate and adapt to environmental change. The enzyme RNA polymerase (RNAP) recognises specific DNA sequences (promoters) from which it can initiate transcription, a process that generates RNA molecules (e.g. messenger RNAs, ribosomal RNAs, transfer RNAs, small non-coding RNAs) from the DNA template. Messenger RNAs (mRNAs) are translated by the ribosomal machinery to synthesise the proteins that are essential components of cell structures, catalyze metabolism and maintain cell function. The ability of bacteria to adapt is rooted in their ability to re-distribute RNAP, in response to external and internal signals, to ensure that optimal patterns of gene expression are adopted for a particular environment. Several mechanisms to achieve this transcriptional re-programming have been recognised, including, the use of alternative sigma (σ) factors, transcriptional attenuation and transcription factors. The ability to regulate gene expression at the level of transcription is essential for bacteria to remain competitive.

1.1 Bacterial transcription

There is only one RNAP in bacteria and archaea, which synthesises cellular RNA using DNA as a template (Burgess, 1971, Ebright, 2000). This process involves interaction between RNAP holoenzyme and the promoter sites in genomic DNA (Doi and Wang, 1986, Helmann and Chamberlin, 1988). The specificity of this interaction is controlled by RNAP holoenzyme, consisting of the core enzyme and an associated σ factor that recognises the promoter site. The σ factor is required to initiate and control gene transcription involving promoter melting and inhibition of nonspecific transcription (Buck *et al*., 2000).

Holo-RNAP binds at the promoters and forms open complexes to initiate synthesis of RNA. Elongation of the RNA chain can proceed using the core enzyme only and hence the σ factor can be reused for initiating transcription of new RNA (Travers and Burgess, 1969, Gross *et al*., 1998, Murakami and Darst, 2003). Termination is the final step when RNAP interacts with termination factors that lead to release of polymerase and the RNA transcript (Figure 1.1; Zhang *et al*., 1999).

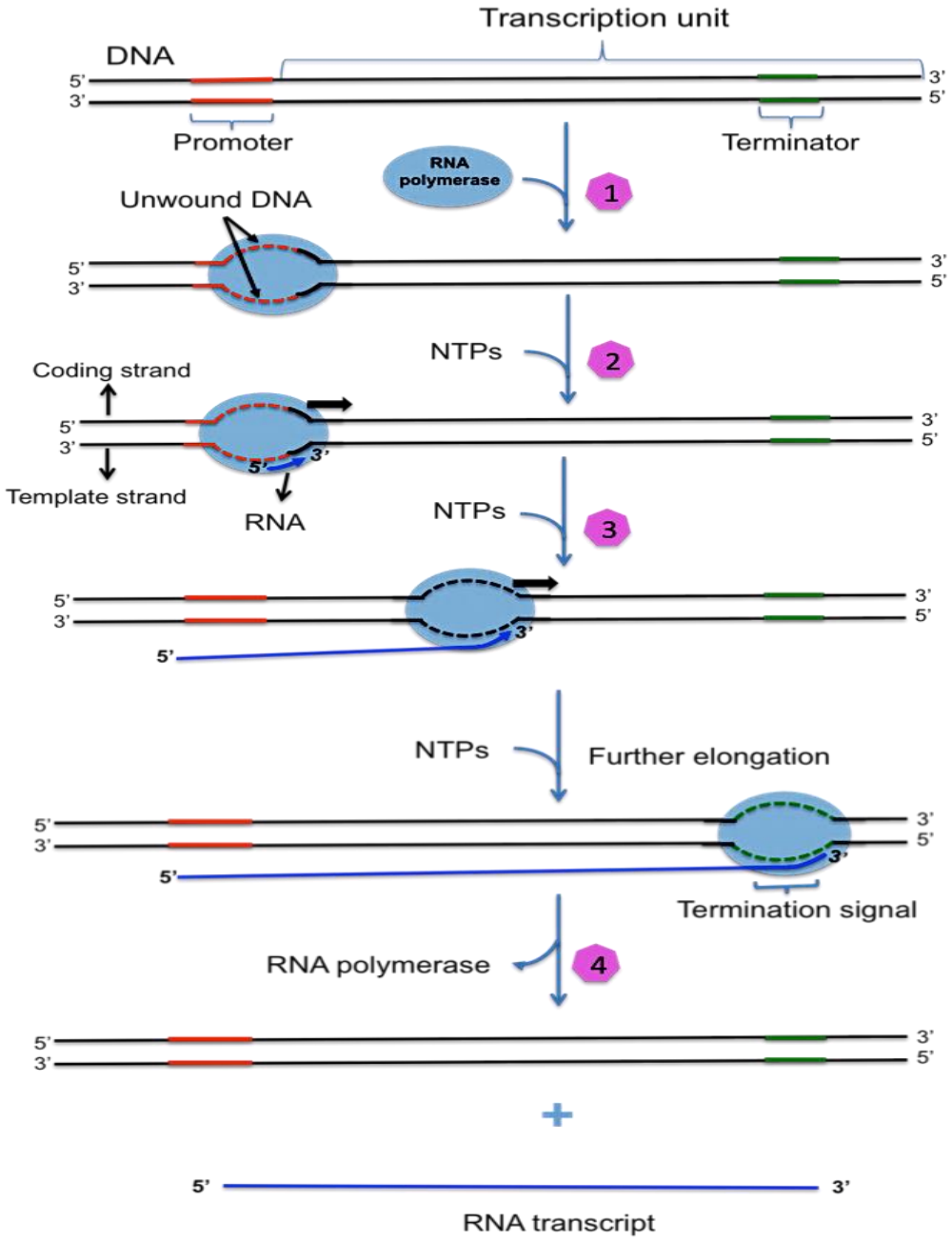

Figure 1.1: Transcription from a bacterial promoter. RNA polymerase (RNAP) holoenzyme interacts with promoter DNA to form open complex 'bubble' just upstream of transcription site in double stranded DNA (Unwound DNA) to initiate transcription using the template strand as shown by dashed red lines (Steps 1 and 2). Elongation starts to extend the RNA chain shown as a solid blue line (Step 3). Termination is the final step when RNAP interacts with termination factors that lead to release of polymerase and the RNA transcript (Step 4).

1.1.1 The structure of *E. coli* RNAP

The molecular weight of *E. coli* RNAP holoenzyme is ~440 kDa and is made up of β', β, σ, α2, ω subunits (Figure 1.2; Burgess *et al*., 1969, Burgess, 1971, Murakami, 2013). The crystal structural of RNAP has been solved and is "crab-claw" shaped with a channel that is appropriately sized to accommodate double stranded DNA (Burgess, 1971, Zhang *et al*., 1999, Ebright, 2000, Cramer *et al*., 2001, Darst, 2001).

The α subunit is a homodimer and is essential for binding β and β'. The C-terminal domain (250-329 residues) of α (αCTD) is a DNA-binding domain and an essential target for transcription factors (Igarashi and Ishihama, 1991, Ross *et al*., 1993). There is a flexible linker between αCTD and N-terminal domain αNTD (Ross *et al*., 1993). AT some promoters, there is another element called an UP element located upstream of the core -35 element that is bound by αCTD (Figure 1.3; Ross *et al*., 1993).

The largest subunits β and β' are involved in formation of the catalytic centre of RNAP by providing a binding site for DNA and DNA/RNA hybrid (Murakami, 2015). In the "crab-claw" the two pincers surround a cleft. One pincer is formed by the β subunit and is called the "clamp" and the other pincer is formed by the β` subunit. In addition, there is a narrow gap between the "clamp" and σ region 2 (Chakraborty *et al*., 2012).

The ω subunit is the smallest subunit (10 kDa) and is formed of five α helices (α1-α5). The C-terminal tail of ω subunit includes fully extended α4 and α5, but there is no interaction between it and C-terminal tail of β' subunit. The *E. coli* RNAP holoenzyme can respond to ppGpp (guanosine 5′-diphosphate, 3′-diphosphate) because of the link between ω subunit and ppGpp-dependent transcription (Vrentas *et al*., 2005).

Escherichia coli σ^{70} belongs the group I σ family and plays an important role in transcription of housekeeping genes. This primary σ factor contains four conserved domains: $\sigma_{1.1}$ (region 1.1), σ2 (regions 1.2-2.4), σ3 (regions 3.0-3.2), and σ4 (regions 4.1-4.2). The $\sigma_{1.1}$ locates between σ2, the β lobe, the β' clamp, and the β' cleft and functions as autoinhibition domain, which prevents binding between DNA and free σ^{70}. Regions 2.4 and 4.2 recognise the -10 and -35 DNA sequences respectively that are separated by 16-19 bp and region 2.3 is involved in melting of double stranded DNA (Figure 1.3; Mekler *et al*., 2002, Murakami and Darst, 2003).

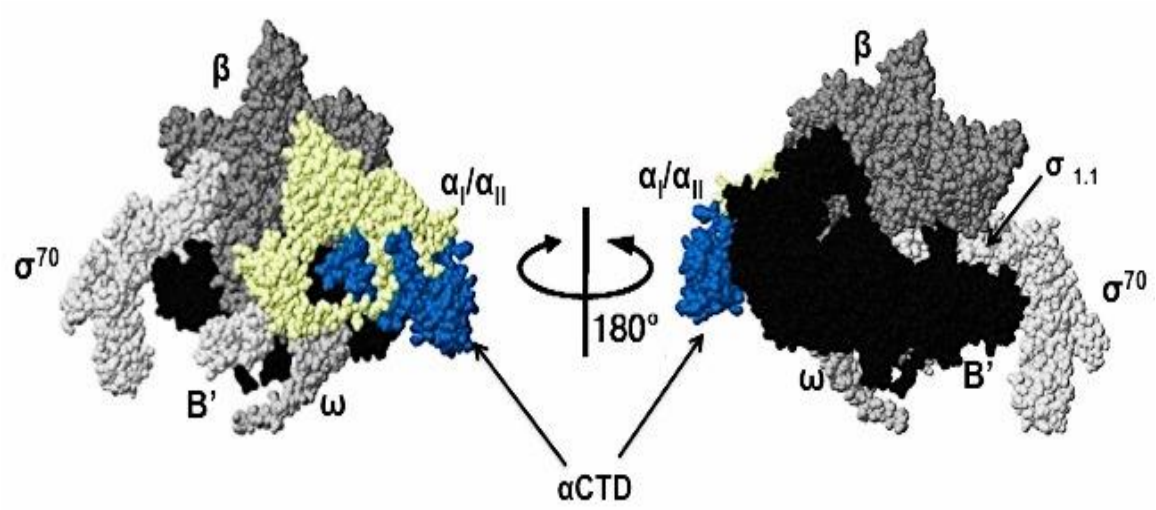

Figure 1.2: Structure of the *E. coli* RNAP holoenzyme. Interaction of the *E. coli* RNAP core enzyme with σ^{70} is shown (α subunits: blue and yellow; β subunit: dark gray; β' subunit: black; ω subunit: light gray; σ^{70} and σ region 1.1: white). Figure is generated by JSmol.

1.1.2 The function of *E. coli* RNAP

During transcription initiation, the σ factor plays an important role in recognition of the promoter to form the closed complex (RP_C). RNAP binds to UP element (via αCTD), -35 and -10 regions (via σ^{70}) and protects the DNA sequence -55 to -5 relative to the transcript start (+1) (Figure 1.3). The first change occurs upstream of the -35 region. Kinetic studies with the λP_R promoter and *E. coli* RNAP showed that enhancement in the reactivity of λP_R closed complex occurs on the template strand of DNA at -38 and the UP element region (-48 on the template and -45 on non-template DNA strands). This enhancement suggested bending and distortion of the DNA at these points (Davis *et al*., 2005). The mechanism of DNA bending is unclear, but the flexible linkers to αCTD allow specific binding to the UP element, which includes binding of one αCTD (centred at -42) with region 4 of the σ factor, or non-specific binding upstream of the -35 region in RPc. The second binding site of αCTD is centred at -52. Binding of both αCTDs are required for efficient transcription, indicating that the second αCTD must play a role in stability of the complex (Estrem *et al*., 1999, Gourse *et al*., 2000). These interactions between the αCTD and DNA upstream of the promoter have important roles in increasing transcription, efficient open complex formation at λP_R, and effective initiation at *lacUV5* (Figure 1.3; Davis *et al*., 2005, Ross and Gourse, 2005).

It has been shown that the downstream region (-5 to +20) in RP_C is protected by RNAP as it locates in the cleft (Hofer *et al*., 1985, Schickor *et al*., 1990, Kovacic, 1987, Mecsas *et al*., 1991). To form the open complex, the downstream region (-5 to +20) must bend by 90° to enter the cleft (Saecker *et al*., 2002, Vassylyev *et al*., 2002). The A base that locates at -11 flips out of the double strand and into a pocket of σ^{70} region 2. This flipping of the A base occurs before the -10 region bending, this adds more flexibility to the double strand leading to bending and capture of the double strand by the cleft. However, the -10 element may be bent initially by RNAP resulting in destabilisation the duplex and base flipping (Feklistov and Darst, 2011).

Opening the transcription bubble (entire ~13 bp) at λP_R happens in the rate-determining isomerization step. This step depends on the solution temperature with 1000-fold increased rate when the temperature was shifted from 7°C to 42°C (Roe *et al*., 1985, Saecker *et al*., 2002, Gries *et al*., 2010). Changes in conformation of DNA and RNAP are needed to convert the unstable open complex the I_2 to extremely stable open complex RP_O (Figure 1.4). These changes include repositioning of the discriminator region to be more reactive (Haugen *et al*., 2006, Gries *et al*., 2010). A

kinetic study discovered a I_3 pathway that involves conversion of I_2 to RP_O (Kontur *et al*., 2008). Figure 1.4 summarises the initiation of open complex formation at λP_R promoter.

In the early stages of elongation, σ factor is released, but this is a very slow step and thus some of σ^{70} may be retained by transcription elongation complexes (TECs) until termination when the RNA transcript and RNAP dissociate from template DNA (Harden *et al*., 2016).

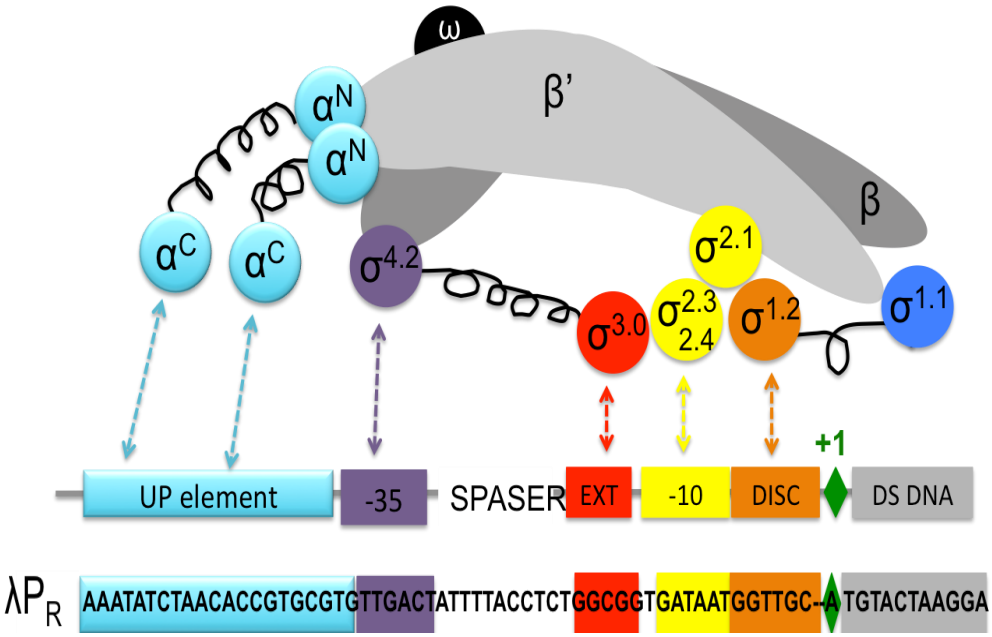

Figure 1.3: Interactions between RNAP holoenzyme and promoter regions. Diagrams present holo-RNAP and DNA promoter regions: RNAP: α2: cyan; β and β': gray; ω: black. σ regions are shown in purple, red, yellow, orange and blue. Promoter regions include: UP element (cyan), -35 element (purple), extended -10 (red), -10 element (yellow), discriminator (orange), transcription start site (green) and DNA downstream of the transcription start site (gray). Black springs showed the linkers in α and σ subunits. DNA sequence of λP_R is shown. Figure adapted from Ruff *et al*. (2015).

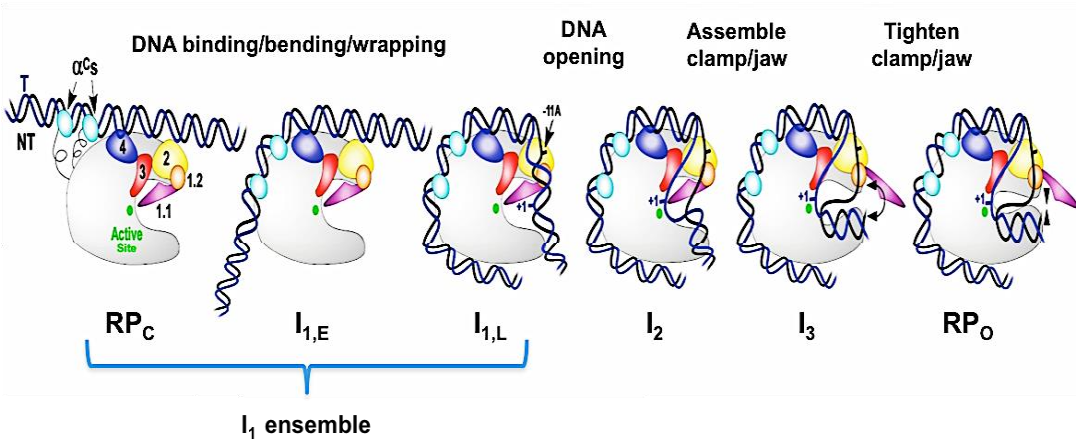

Figure 1.4: Formation of open complex at λP_R promoter. The "I_1" ensemble includes closed complex "RP_C, $I_{1,E}$ (early), or $I_{1,L}$ (late)". The αCTDs in cyan; β and β' in gray; σ regions in (pink, orange, yellow, red and blue) are shown. Figure is taken from Ruff *et al*. (2015).

1.1.3 Control of gene expression

There are hundreds of different housekeeping genes in bacteria, which are important for the cell under all conditions of growth, including those encoding DNA polymerase, RNA polymerase and DNA gyrase. Under specific conditions many enzymes are required for amino acid synthesis or response to specific conditions such as DNA damage. Expression of essential genes is required under all growth conditions but the expression of other genes is conditional. Thus, cells must regulate gene expression using transcription regulation to determine which genes are transcribed and to what extent. When the gene encodes a protein, translation regulation can be used as a second mechanism to regulate the expression. Post-translation or post-transcription regulation can be used to regulate the active amount of RNA and protein by degradation or modification, such as nucleoside methylation in rRNA and tRNA or protein phosphorylation. Transcription regulation is the most common mechanism to control gene expression in bacteria, such as the regulation of *lac* operon (repressed by Lac repressor and activated by cAMP-CAP) and *trp* operon (controlled by attenuation) (Figure 1.5; Trun and Trempy, 2009, Lodish, 2013).

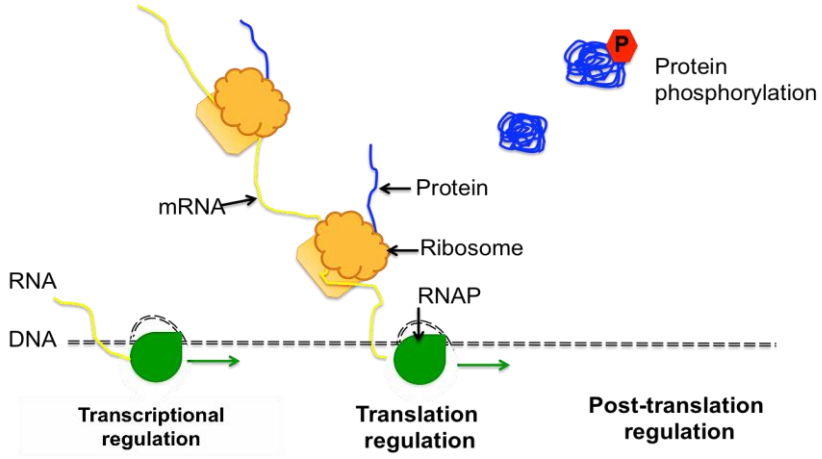

Figure 1.5: Control of gene expression. Cells regulate gene expression by using transcription, translation or post-translation regulation. Figure adapted from Lodish (2013).

1.2 Transcription regulation

Seven transcriptions factors (CRP, FNR, IHF, Fis, ArcA, NarL and Lrp) have been estimated to regulate the expression of 51% of *E. coli* genes. Most of these regulate large numbers of genes by binding to specific promoters (Martinez-Antonio and Collado-Vides, 2003, Browning and Busby, 2004). Transcription factors can be repressors or activators, but some can do both dependent on the promoter target (Perez-Rueda and Collado-Vides, 2000).

Escherichia coli FNR is a member of CRP/FNR family (Sharrocks *et al*., 1990). The name of this family is derived from the two key transcription regulator members: the cyclic AMP receptor protein (CRP or CAP; the catabolite gene activator protein) and the Fumarate and nitrate reduction regulator (FNR) (Kiley and Reznikoff, 1991, Botsford and Harman, 1992, Lawson *et al*., 2004, Kang *et al*., 2005). FNR is an O_2 responsive regulator that coordinates switching between aerobic and anaerobic metabolism (Guest *et al*., 1996).

1.2.1 The CRP/FNR family

The CRP/FNR family of transcription regulators shares a common structural framework. Members are found in many bacteria where they contribute to the regulation of genes and operons in response to diverse environmental signals (Green *et al*., 2001, Korner *et al*., 2003, Zhou *et al*., 2012), such as anoxia, CO and oxidative and nitrosative stresses (Aono *et al*., 1996, Green *et al*., 2001, Cruz-Ramos *et al*., 2002). In response to these signals they regulate many important metabolic processes, for example anaerobic respiration, anaerobic degradation of aromatic ring compounds and nitrogen fixation (Spiro and Guest, 1991, Egland and Harwood, 2000, Lopez *et al*., 2001). This superfamily contains three groups: FNR, CRP and NtcA (Fischer, 1994, Korner *et al*., 2003). The FNR group contains very diverse subgroups: FNR, FixK, FnrN and DNR/FLP. The CRP group contains proteins controlling the response to glucose starvation. The NtcA group contains cyanobacterial nitrogen and sulfur metabolic regulators (Vollack *et al*., 1999).

1.2.2 *Escherichia coli* FNR

Fumarate-nitrate reduction regulator (FNR) proteins are a major subgroup of the CRP/FNR family of bacterial transcription regulators (Korner *et al*., 2003). The major function of FNR proteins is the re-programming of gene expression to coordinate the switch from aerobic to anaerobic metabolism when facultative anaerobes like *E. coli* are starved of O_2 (Kang *et al*., 2005, Constantinidou *et al*., 2006, Partridge *et al*., 2006, Partridge *et al*., 2007). The N-terminal region of FNR contains four essential cysteine residues that coordinate an O_2-sensitive [4Fe-4S] cluster (Sharrocks *et al*., 1990, Khoroshilova *et al*., 1997). In the absence of O_2, the [4Fe-4S] cluster is stable, and FNR exists as a homodimer that is capable of high affinity, site-specific DNA binding to an FNR box (TTGAT(N4)ATCAA) (Lazazzera *et al*., 1996, Khoroshilova *et al*., 1997). When bound to target DNA, FNR activates the expression of genes encoding proteins required for anaerobic metabolism and represses those utilized under aerobic conditions (Constantinidou *et al*., 2006, Myers *et al*., 2013), such that when O_2 is available, anaerobic metabolism is shutdown in favor of the more energetically efficient aerobic respiratory metabolism (Crack *et al*., 2007, Reinhart *et al*., 2008). The crystal structure of *Aliivibrio fischeria* (*Af*) FNR has been solved recently by Volbeda *et al*. (2015; Figure 1.6).

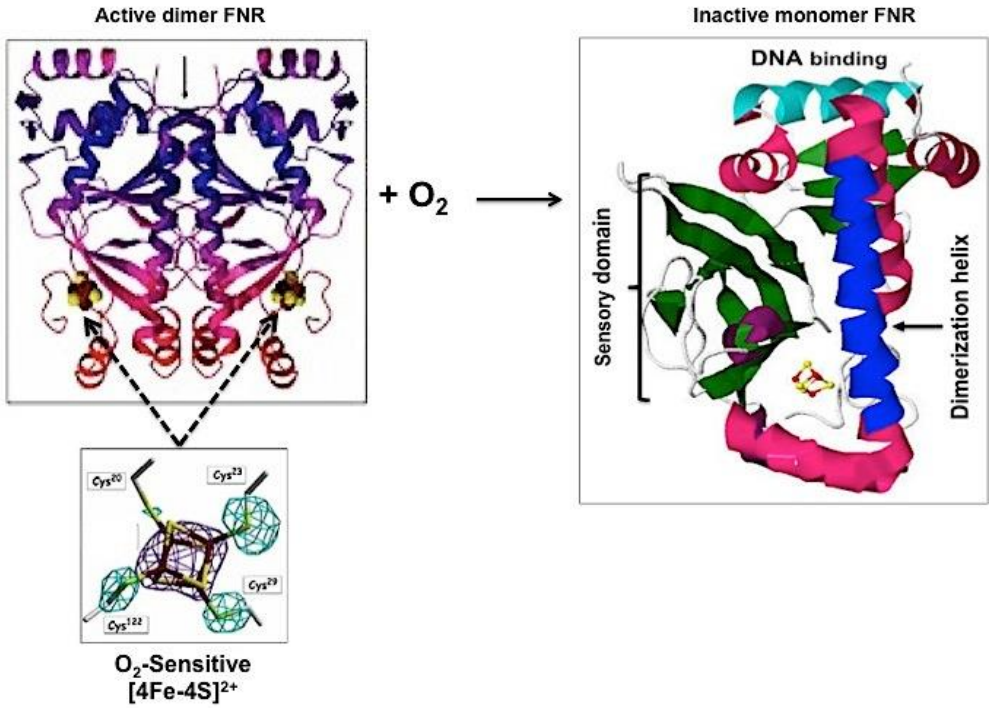

Figure 1.6: Structure of *Aliivibrio fischeria* FNR protein. Three-dimensional structure of *Af*FNR according to the reported structure by Volbeda *et al*. (2015). The active dimer FNR responds to O_2 via O_2 sensitive [4Fe-4S] clusters and is converted to inactive monomeric form. The DNA-binding helix (cyan), dimerization helix (blue) and sensing domain (green), are shown in inactive monomer FNR. Figures of dimeric FNR and the [4Fe-4S] cluster are taken from Volbeda *et al*. (2015) and the diagram of monomer FNR was generated by Pymol (DeLano, 2002).

1.2.3 DNA-FNR binding

Active FNR possesses the ability to bind to specific DNA sequences. A consensus sequence TT**G**AT----AT**C**AA has been determined (Eiglmeier *et al*., 1989, Spiro and Guest, 1990, Green and Guest, 1994). This palindrome contains an inverted repeat sequence that is recognised by the DNA-recognition helix (α_F) (Green *et al*., 2001); shown in cyan in Figure 1.6). The dimeric form of FNR can bind to this sequence to activate or repress transcription under anaerobic conditions (Bell *et al*., 1989, Spiro and Guest, 1990). The essential features in this sequence are: G-C bp **(bold)** and T-A bp (underlined) (Spiro, 1994). It has been shown that the FNR residues: Glu-209, Ser-212 and Arg-213 are important for binding FNR sites. Glu-209 interacts with the G-C bp, Ser-212 interacts with the first A-T bp and Arg-213 residue interacts C-G bp and A-T bp downstream (Figure 1.7A). Change of only one nucleotide in FNR site leads to transform the sequence to CRP site **G**TGAT----ATCA**C** (Figure 1.7B; Spiro *et al*., 1990, Green *et al*., 2001). The four base pairs between the two half-sites of the FNR site are called the non-conserved tetrad (NCT). Analysis of FNR-dependent promoters has indicated that NCT plays essential role in FNR mediated regulation transcription. NCT contributes to changing the level of expression from FNR-dependent promoters under anaerobic conditions (Scott *et al*., 2003).

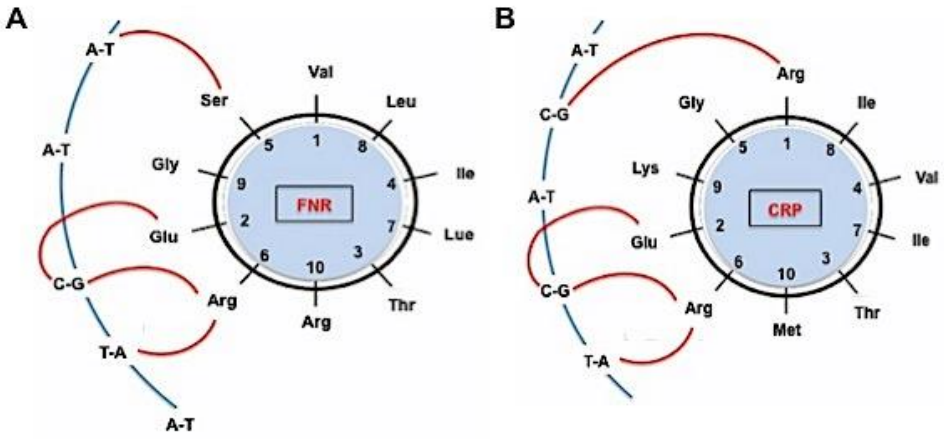

Figure 1.7: The FNR and CRP interactions with DNA binding sites. Helical wheels are shown for FNR and CRP recognition helices. Numbers represented the position of DNA recognition helices. Interactions of the Arg (position 6) and Glu (position 2) with conserved base pairs in DNA-binding site A-T and C-G for FNR (A) and CRP (B) are indicated by red lines. The interactions between Ser (position 5) and A-T for FNR, Arg in position 1 and C-G for CRP are indicated as well. Figures adapted from Spiro *et al*. (1990) and Green *et al.* (2001).

1.2.4 FNR mediated transcription regulation

FNR transcription activation begins when FNR binds to its binding site at a target promoter and recruits RNAP. FNR-dependent promoters have been arranged in to two classes: class I and class II promoters. Class I promoters have an FNR site located at -61.5, -71.5, -82.5 or -92.5 relative to transcription start (Figure 1.8A). However, in class II promoters the FNR site is located at -41.5 upstream of transcription start region (Figure 1.8B; Wing *et al*., 1995). FNR activity depends on the protein-protein interactions between FNR and RNAP to activate transcription (Lamberg and Kiley, 2000). FNR contains three activating regions (AR): AR1, AR2 and AR3 that play essential roles in transcription activation (Green *et al*., 2001, Blake *et al*., 2002).

Class II promoters are the most common FNR-activated promoters (Wing *et al*., 1995). Two interactions consisting of an activation contact and an anti-inhibition contact via AR3 and AR1 of FNR are made between FNR and RNAP. AR3 is a β4-β5 loop (residues 80-88) with negative charge that makes an activating contact with RNAP and σ^{70} (Williams *et al*., 1991, Bell and Busby, 1994, Ralph *et al*., 1998, Lamberg and Kiley, 2000). The FNR-AR1 consists of three surface-exposed loops located between 71-75, 116-121 and 184-192 residues with Thr-118 and Ser-187 providing side chains to contact RNAP αCTD in an anti-inhibition interaction thereby promoting open complex formation (Wing *et al*., 1995, Williams *et al*., 1997, Lamberg and Kiley, 2000, Wing *et al*., 2000, Lee *et al*., 2000). Besides AR1 and AR3, a third region (AR2) can be exposed under certain circumstances. AR2 is a positively charged surface, which contacts the N-terminal domain of the α-subunit of RNAP (Li *et al*., 1998, Ralph *et al*., 2001). However, AR2 has only a minor affect on the transcription activity of FNR at class II promoters, and it is not required for class I promoters (Blake *et al*., 2002).

FNR can repress target genes via protein-protein interaction between FNR and α-subunit of RNAP. Repression occurs when the αCTD of RNAP interacts with tandem FNR dimers (Green *et al*., 1996b, Meng *et al*., 1997, Browning *et al*., 2002). Barnard and colleagues determined the essential mechanism for FNR repression using artificial promoters that fixed one FNR binding site at -41.5 and placed a second site upstream at different locations. FNR could repress transcription when it was bound at tandem sites located at -41.5 and either -85.5 or -95.5. This suggested that optimal spacing between FNR tandem sites (44 or 53 bp) is required for repression. This

observation was confirmed by detecting FNR-mediated repression when sites were at -61.5 and either -104.5 or -105.5. This showed the requirement for the distance between the two sites should be ~44 bp for repression to occur. The *E. coli ndh* promoter is a natural example of repression via tandem binding of FNR at -50.5 and -94.5 with 44 bp spacing between two sites (Meng *et al*., 1997, Barnard *et al*., 2003).

Repression can also be simple when FNR was bound to a single site overlapping the -35 element (Williams *et al*., 1998).

A- Class I promoter

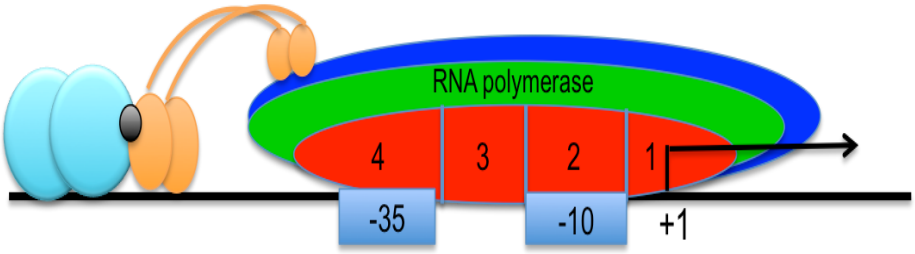

B- Class II promoter

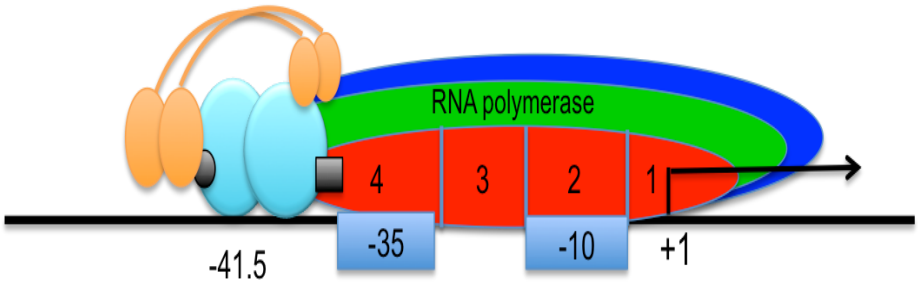

Figure 1.8: FNR-dependent promoters. Figures show the RNAP holoenzyme and a dimeric FNR-type activator (blue ovals). The RNAP αCTD and αNTD are shown as a yellow ovals joined by linkers, protein-protein interactions are shown as black shapes. **(A) Class I promoter.** The FNR binds at -61.5, -71.5, -82.5 or -92.5 (i.e. on the same face of the DNA helix) upstream of the transcript start (+1). An, AR1 interaction between αCTD and the downstream subunit of FNR is formed (black oval). **(B) Class II promoter.** FNR binds to target DNA at -41.5 and interacts with RNAP via two mechanisms: anti-inhibition involves protein-protein interaction between AR1 (black oval) and αCTD; and direct activation includes binding between AR3 (black square) and region 4 of the σ subunit. Figures adapted from Busby and Ebright (1997), Brown *et al.* (2003) and Browning and Busby (2004).

1.2.5 Mechanism of O_2- sensing by FNR

FNR responds to O_2 via a cysteine-rich N-terminal domain that contains five cysteine residues, four of which (Cys-20, 23, 29 and 122, but not Cys-16) are essential for the function of FNR (Sharrocks *et al*., 1990, Khoroshilova *et al*., 1997). Anaerobically, FNR is activated by acquiring one [4Fe-4S] cluster per protomer. The cluster is essential for enhancing dimerization and DNA-binding in response to low O_2 tension (Green *et al*., 1996a, Lazazzera *et al*., 1996, Crack *et al*., 2004, Crack *et al*., 2007). The conversion of $[4Fe\text{-}4S]^{2+}$ cluster to $[2Fe\text{-}2S]^{2+}$ cluster is triggered by O_2 via $[3Fe\text{-}4S]^{1+}$ intermediate leading to monomerization and loss of the DNA-binding activity (Crack *et al*., 2004, Crack *et al*., 2007). The FNR $[2Fe\text{-}2S]^{2+}$ cluster is relatively stable, but in the presence of O_2 it degrades to yield apo-FNR. *In vivo* apo-FNR is the main form under aerobic conditions (Achebach *et al*., 2004, Achebach *et al*., 2005). The amount of FNR protein is similar under anaerobic and aerobic (Unden and Duchene, 1987). Prior studies with *Clostridium pasteurianum* 8Fe-ferredoxin suggested a suitable model for the reaction of FNR with O_2. One-electron converts the $[4Fe\text{-}4S]^{2+}$ cluster to the superoxidised state $[4Fe\text{-}4S]^{3+}$ and than releases Fe^{2+} to yield $[3Fe\text{-}4S]^{1+}$ (Eq.1.1; Tilley *et al*., 2001).

$$[4Fe\text{-}4S]^{2+} - e^- \rightarrow [4Fe\text{-}4S]^{3+} \rightarrow [3Fe\text{-}4S]^{1+} + Fe^{2+} \qquad [1.1]$$

In the FNR reaction, the electron acceptor is O_2, generating superoxide ($O_2^{-\cdot}$). The released Fe^{2+} could react with $O_2^{-\cdot}$ to produce Fe^{3+} and hydrogen peroxide (H_2O_2). Hydrogen peroxide has been detected, suggesting that the products of FNR reaction with O_2 are superoxide and H_2O_2 (Crack *et al*., 2004). Experiments showed that 0.37 superoxide ions per cluster were produced during the reaction of [4Fe-4S] cluster with O_2. In the presence of catalase, the concentration of superoxide ion increased to ~0.58 ions per cluster, indicating that the superoxide ions disproportionate to O_2 and H_2O_2 (Crack *et al*., 2007).

The oxidation state of iron released in the first step of the reaction was investigated using a Ferene assay. The Ferene assay results were well fitted to single exponential demonstrating that the results described the first step of the reaction only and that one Fe^{2+} ion was released per cluster (Crack *et al*., 2007). The second step of the reaction is oxygen-independent and involves spontaneous cluster conversion from [3Fe-4S] to [2Fe-2S] with partial sulfide retention as cysteine persulfide. Only one Fe^{3+} ion is released in the second step (Figure 1.7; Crack *et al*., 2006, Zhang *et al*., 2012).

The superoxide generated in the first step of the reaction is harmful and may cause DNA damage (Imlay, 2002). The $1e^-$ reduction of O_2 to $O_2^{\cdot-}$ informing the hyperoxidised $[4Fe\text{-}4S]^{3+}$ cluster implies that up to 4[4Fe-4S] clusters could be oxidised by only one molecule of O_2. In *E. coli,* superoxide is recycled back to O_2 by superoxide dismutase (SOD) and catalase (Schellhorn and Hassan, 1988, Kargalioglu and Imlay, 1994). The recycling of superoxide and H_2O_2 provides a positive feedback loop that extends the O_2 sensitivity of the [4Fe-4S] cluster of FNR (Eq. 1.2 and 1.3; Figure 1.9; Crack *et al*., 2007).

$$4O_2^{\cdot-} + 4H^+ \rightarrow 2O_2 + 2H_2O_2 \qquad [1.2]$$

$$2H_2O_2 \rightarrow O_2 + 2H_2O \qquad [1.3]$$

In vitro, aerobic or anaerobic apo-FNR can be reconstituted to the [4Fe-4S] form under anaerobic conditions by incubation with cysteine and Fe^{2+} and cysteine desulfurase (NifS protein) under reducing conditions (Zheng *et al*., 1993, Green *et al*., 1996a, Khoroshilova *et al*., 1997, Schwartz *et al*., 2000). *Escherichia coli* possesses two mechanisms for biosynthesis of iron-sulfur clusters. Isc (Iron-sulfur cluster) is the general pathway for Fe-S cluster assembly and Suf (Sulfur formation) is utilized under oxidative stress and iron-limiting conditions. *In vivo*, only Isc pathway is required to convert the apo-FNR to [4Fe-4S] cluster under anaerobic conditions (Ayala-Castro *et al*., 2008, Mettert *et al*., 2008).

There are two major issues relating to the O_2-sensing mechanism of FNR. The first concerns the [4Fe-4S] to [2Fe-2S] conversion in response to O_2 and whether the reaction is metal-based oxidation, sulfur-based oxidation or a combination of both. The metal-based oxidation requires releasing one Fe^{2+}, one Fe^{3+} and two S^{2-} ions, via [3Fe-4S] cluster (Crack *et al*., 2004, Crack *et al*., 2006, Crack *et al*., 2007, Crack *et al*., 2008a, Jervis *et al*., 2009). A sulfur-based oxidation was suggested after finding that only ~70% of the sulfide of the [4Fe-4S] cluster was detected upon exposure to O_2, suggesting that ~30% had been oxidised (Khoroshilova *et al*., 1997). However, trying to detect the sulfur oxidation products, such as polysulfide, cysteine persulfide, or sulfinic acid, was not possible (Sutton *et al*., 2004). The second related issue concerned the possibility of reversible conversion of $[4Fe\text{-}4S]^{2+} \leftrightarrow [2Fe\text{-}2S]^{2+}$ forms (Zhang *et al*., 2012). Resonance Raman, UV-visible absorbance and CD, and MS studies of the conversion of [4Fe-4S] to [2Fe-2S] clusters in response to O_2 have been done. The results indicate a combination of iron and sulfur-based oxidation and formation of [2Fe-2S] cluster coordinated by one or two cysteine persulfides.

Furthermore, the conversion of the cluster was detected to be reversible under anaerobic conditions in presence of Fe^{2+} and reducing agent (DTT) and lack of sulfide. Thus, the mechanism of [4Fe-4S] repair proposed for *E. coli* FNR is likely to be a common feature of this family of regulators and probably other iron-sulfur cluster proteins (Zhang *et al*., 2012). Figure 1.9 summarises the reaction of [4Fe-4S] cluster with O_2.

As well as FNR's sensitivity to O_2, [4Fe-4S] clusters can sense nitric oxide. FNR serves primarily as an O_2 sensor with a secondary nitric oxide sensing role. Upon exposure to nitric oxide, the [4Fe-4S] cluster of FNR reacts with 8 molecules of NO to form a mixture of dinitrosyl iron complex (DNIC) and RRE-like species. Nitrosylation of the [4Fe-4S] cluster of FNR occurs via a very rapid multi-step reaction leading to monomerization of the protein and impaired DNA-binding activity (Cruz‐Ramos *et al*., 2002, Crack *et al*., 2013). Anaerobic exposure of *E. coli* to nitric oxide caused up-regulation of FNR-repressed genes such as *hmp* that encodes a flavohemoglobin (Poole, 2005).

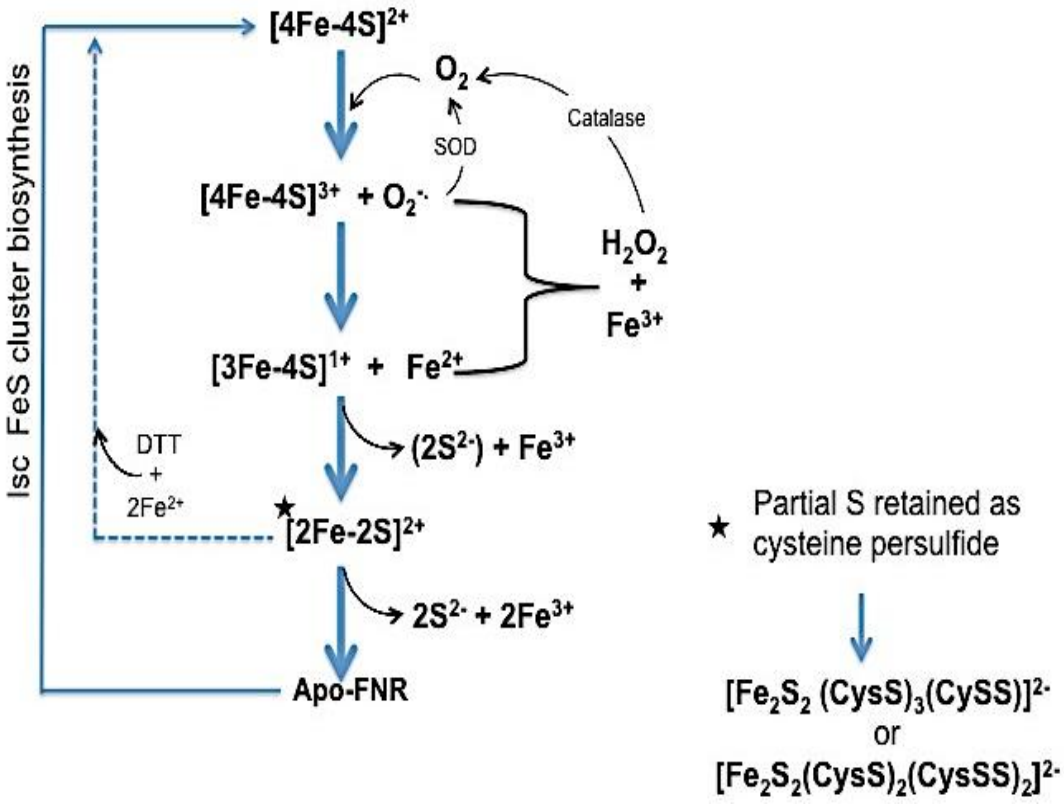

Figure 1.9: The reaction of the $[4Fe\text{-}4S]^{2+}$ cluster of FNR with O_2. One-electron converts the $[4Fe\text{-}4S]^{2+}$ cluster to the superoxidised state $[4Fe\text{-}4S]^{3+}$ and releases Fe^{2+} to yield $[3Fe\text{-}4S]^{1+}$. The second step is a slower and spontaneous reaction involving the conversion of intermediate $[3Fe\text{-}4S]^{1+}$ cluster to $[2Fe\text{-}2S]^{2+}$ cluster, which is an inactive form of FNR. Prolonged exposure to O_2 leads to degradation of the [2Fe-2S] cluster to apo-FNR that can be reactivated by incorporation [4Fe-4S] cluster under anaerobic conditions. Figure adapted from Crack *et al.* (2008a).

Escherichia coli is a facultative anaerobic bacterium capable of aerobic respiration, anaerobic respiration and fermentation. Therefore, O_2 sensing and the response to alterations in O_2 concentration are important in order to survive under different growth conditions. As discussed above, a transcription regulatory system has evolved in *E. coli* to sense O_2 and re-programme gene expression in response to O_2 availability. *Escherichia coli* FNR is the paradigm for direct O_2-responsive regulators (Green *et al*., 2009, Crack *et al*., 2012a, Crack *et al*., 2012b). Most bacteria such as *E. coli* and *Pseudomonas aeruginosa* have only one FNR protein. However, *Pseudomonas putida* and *Burkholderia* spp. possess multiple FNR family proteins that retain the characteristic cluster of cysteine residues in the N-terminal sensory domain. Transcriptomic analysis of the opportunistic pathogen *Burkholderia cenocepacia* revealed the presence of a 50-gene low oxygen-activated (*lxa*) locus that is associated with persistence of this obligate aerobe under anaerobic conditions. The *lxa* locus includes the FNR protein BCAM0287, which was induced 17-fold under low O_2 (micro-aerobic) conditions. In addition, two other FNR encoding genes were induced during growth under a 6% O_2 atmosphere, BCAM0049 (induced 77-fold, compared with aerobic conditions) and BCAM1483 (induced 3.5-fold) (Sass *et al*., 2013). Although an FNR box-like (FNR-binding site) motif was associated with many genes induced under microaerobic conditions, the functions of the multiple FNR regulators in *B. cenocepacia* remain poorly defined. Similarly, the properties and functions of the three FNR proteins of *P. putida* KT2440 are poorly understood. Thus, the starting point for the work reported in this thesis was the hypothesis that the three FNR proteins of *P. putida* have evolved to fulfill distinct but overlapping roles. This was suggested because the amino acids adjacent to the three N-termal cysteine residues that could coordinate an iron-sulfur cluster differ between the three *P. putida* FNR proteins and *E. coli* FNR variants in these positions (D22G and S24F) exhibit enhanced O_2 stability (Kiley and Reznikoff, 1991, Jervis *et al*., 2009). Thus, to better understand the reasons why *P. putida* has three FNR proteins the properties of the *P. putida* FNR proteins using molecular biology and biochemical methods were investigated to establish whether they operate as *bona fide* O_2-sensitive regulators like *E. coli* FNR and *P. aeruginosa* ANR. Three FNR proteins (PP_3233, PP_3287, and PP_4265, the last of which is also known as ANR) from a single bacterial species, *P. putida* KT2440, have been isolated, and their responses to O_2 *in vivo* and *in vitro* have been assessed. To place this work into content some information about *P. putida* is provided below.

1.3 *Pseudomonas* genus

Pseudomonads are Gram-negative, rod-shaped, polar flagellated and aerobic bacteria, belonging to the γ-proteobacteria (Blake *et al*., 2002). They can grow in different environments using diverse aerobic respiratory chains to adapt to different concentration of O_2. Some species can grow under anaerobic conditions such as *Pseudomonas aeruginosa* using arginine fermentation, pyruvate fermentation and nitrate as a terminal electron acceptor. This bacterium can use various sources of carbon such as glucose, aromatic compounds or amino acids (Williams *et al*., 2007). In *Pseudomonas*, the Entner-Doudoroff pathway is utilized to metabolise glucose (Lessie and Phibbs, 1984). Members of the *Pseudomonas* genus are capable of very rapid growth with simple requirements on standard laboratory media. Some of these bacteria are pathogenic such as *Pseudomonas aeruginosa* or *Pseudomonas syringae* (Preston, 2000, Stover *et al*., 2000, Timmis, 2002), and some are nonpathogenic such as *Pseudomonas fluorescens* or *Pseudomonas putida* (Klotz and Hutcheson, 1992).

1.3.1 *Pseudomonas putida* KT2440

Pseudomonas putida KT2440 is an obligate aerobic bacterium with an optimum growth temperature of 30°C, but it can grow at low temperature such as 4°C in soil or water (Fonseca *et al*., 2011). The glycolytic pathway is impaired in *P. putida* because of the lack of 6-Phosphofructokinase (Vicente and Canovas, 1973). However, similar to other pseudomonads the Entner-Doudoroff pathway is utilized to metabolise glucose and other sugars (del Castillo *et al*., 2007). 6-Phosphogluconate is the key compound in this pathway, which is generated via three pathways: the glucokinase branch, the gluconokinase branch, and the 2-ketogluconate loop (Vicente and Canovas, 1973).

As illustrated in Figure 1.10, after glucose enters the periplasm, it can be transported to cytoplasm by an ABC transporter or it can be oxidised to gluconate. In the cytoplasm, it is converted to glucose-6-phosphate by glucokinase and then to 6-phosphogluconate. Gluconate can enter the cytoplasm and be phosphorylated by gluconokinase to 6-phosphogluconate or can be oxidised to 2-ketogluconate. The latter can translocate to the cytoplasm and be reduced to 6-phosphogluconate. In the Entner-Doudoroff pathway (Edd/Eda enzymes) the 6-phosphogluconate is oxidised to 2-keto-3-deoxy-6-phosphogluconate to glyceraldehyde 3P and pyruvate. Pyruvate enters the Krebs cycle (del Castillo *et al*., 2007).

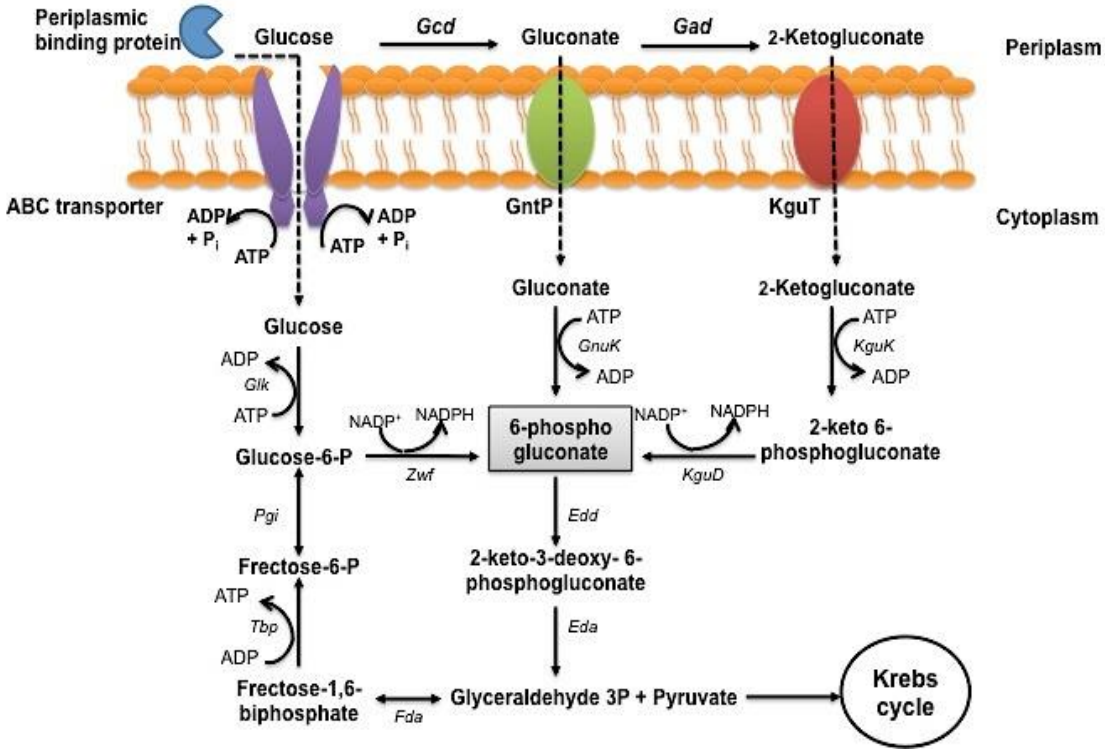

Figure 1.10: Glucose catabolism in *Pseudomonas putida* KT2440. Glucose catabolism in *P. putida* occurs in the periplasm and cytoplasm. Figure adapted from del Castillo *et al*. (2007).

The analysis of complete 6.18 Mb genome of *P. putida* KT2440 with ~ 62% content of G and C, 85% similarity to *P. aeruginosa*. In spite of similarity between these two species, *P. putida* lacks the virulence factors that include exotoxin A and type III secretion systems. Therefore, it is classified as a safe bacterium to utilize in different applications such as bioremediation, agriculture, production of bioplastic and biocatalysis (Nelson *et al*., 2002). *Pseudomonas putida* has the ability to grow aerobically, but it cannot thrive under anaerobic conditions. Under low O_2 concentration, *P. putida* KT2440 possesses genes allowing fermentative metabolism with substrates like pyruvate (dos Santos *et al*., 2004). For example, the *arcCIAD* operon is required for surviving under O_2-limited conditions by fermentation of arginine to ornithine and carbamoylphosphate to regenerate one ATP per arginine. Under low O_2 concentrations or depletion carbon and phosphate sources, the enzymes required for the arginine deiminase pathway are induced. *Pseudomonas putida arcA* deaminates arginine to citrulline in cytoplasm. The *argI* that is ortholog to *arcB* in *P. aeruginosa* encodes carbomoyltransferase that converts citrulline to ornithine and carbomoylphosphate. An antiporter system is encoded by *arcD*, which is essential for exporting ornithine out of the cell. Finally, conversion of carbomoylphosphate to NH_3 and CO_2 to generate ATP is required by *arcC* (Figure 1.11; Stalon and Mercenier, 1984).

The work described her has two parts: the first describes evidence that *P. putida* KT2440 possesses three FNR proteins (ANR, PP_3233 and PP_3287) with different O_2 sensitivities. ANR is similar to *E. coli* FNR but PP_3233 and PP_3287 are less O_2 sensitive. All three *P. putida* FNR proteins bind to the same DNA site (FF site). The second section describes experiments to investigate the properties of the HcpR2 protein of *D. desulfuricans*. This sulfate-reducing bacterium possesses two proteins HcpR and HcpR2 that are involved in regulating anaerobic respiration and the response to nitrate stress. The properties of HcpR2 were investigated and the results indicated that HcpR2 is likely to respond to O_2 and nitric oxide via reactions of its iron-sulfur cluster similar to *E. coli* FNR.

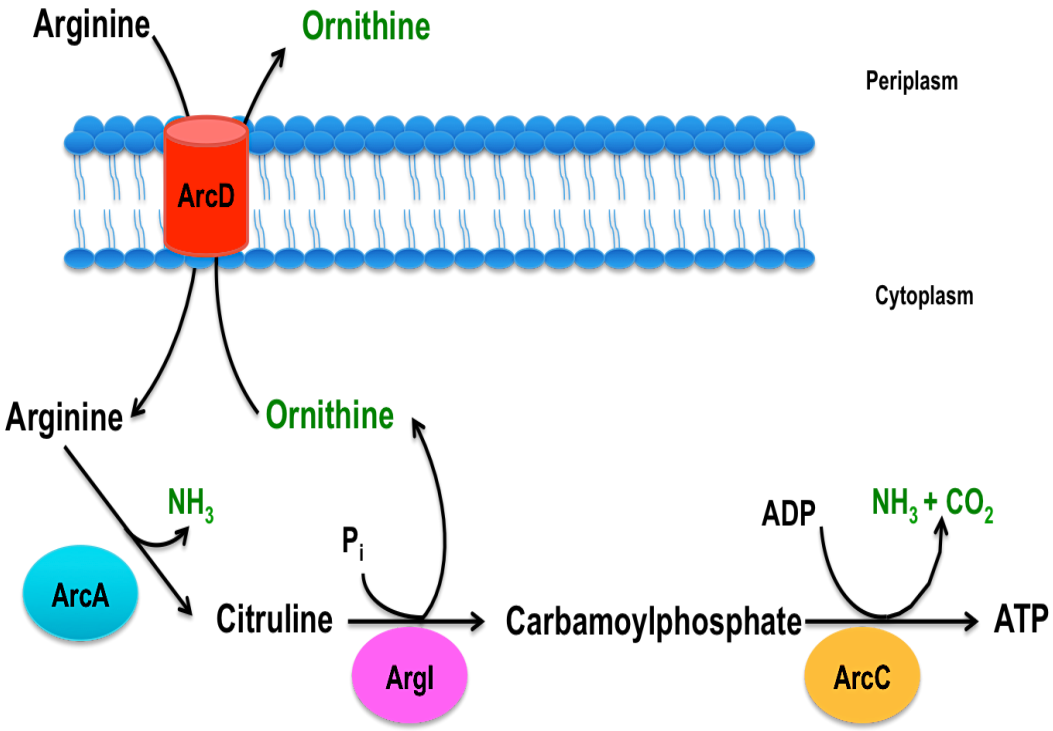

Figure 1.11: The arginine deiminase pathway in *Pseudomonas putida* KT2440. Arginine fermentation in cytoplasm is utilized under low O_2 concentration and depletion of carbon and phosphate sources to generate one molecule of ATP per one molecule of arginine. Figure adapted from Stalon and Mercenier (1984).

Chapter 2

Materials and Methods

2.0 Materials and Methods

2.1 Bacterial Strains

Table 2.1 shows the bacterial strains of *Escherichia coli* and *Pseudomonas putida* KT2440 that were used in this study.

Table 2.1: Bacterial strains used in this study

Strains	Characteristics	Provider or reference
JRG5302	*E. coli* BL21 λ (DE3) lysogen carries a chromosomal copy of the T7 RNA polymerase gene under control of the *lacUV5* promoter which induce by IPTG	Novagen
JRG6348	*E. coli* derivative of JRG1728 *lac*, *fnr* carrying a chromosomal FNR-dependent promoter-*lacZ* fusion; Cm^R	Dr. David Lee, University of Birmingham, UK
JRG2357	*E. coli DH5α supE44, ΔlacU169 (ϕ80lacZ ΔM15*), *hsdR17, recA1, endA1, gyrA96, relA1*	Lab collection
JRG6725	*P. putida* KT2440 (WT)	This work
JRG6721	*P. putida* KT2440Δ*anr* Δ*3233*	This work
JRG6722	*P. putida* KT2440Δ*anr* Δ*3287*	This work
JRG6723	*P. putida* KT2440Δ*3233* Δ*3287*	This work
JRG2499	*E. coli* DH5α (p547)	Lab collection
JRG2290	*E. coli* JM101 (pGS422)	Lab collection
JRG2855	*E. coli* JM101 (pGS649)	Lab collection
JRG2858	*E. coli* JM101 (pGS652)	Lab collection

JRG3802	*E. coli* MC1000 (pGS810)	Lab collection
JRG6444	JRG6348 (p2236)	This work
JRG6188	*E. coli* DH5α (pGS2268)	This work
JRG6445	JRG6348 (pGS2350)	This work
JRG6446	JRG6348 (pGS2351)	This work
JRG6447	JRG6348 (pGS2352)	This work
JRG6448	JRG6348 (pGS2353)	This work
JRG6555	*E. coli* DH5α (pGS2403)	This work
JRG6569	*E. coli* XL10Gold (pGS2413)	This work
JRG6570	*E. coli* XL10Gold (pGS2414)	This work
JRG6748	*E. coli* DH5α (p2490)	This work
JRG6765	*E. coli* DH5α (pGS2508)	This work
JRG6766	*E. coli* DH5α (pGS2509)	This work
JRG6502	*E. coli* DH5α (p2373)	This work

2.2 Plasmids

Table 2.2 shows the plasmids used in this work.

Table 2.2: Plasmids used in this study

Plasmids	Characteristics	Provider or reference
p2236	pBAD/ His B, 4.1 Kb, Amp^R	Invitrogen
p2490	pBB1-MCS-5, Gm^R	(Kovach *et al*., 1995)/ Dr. Jon Shaw, Medical School, University of Sheffield, UK.
p547	pGEX-KG, 5 Kb, Amp^R	(Guan and Dixon, 1991)/ Prof. Andy Sharrocks, University of Manchester, UK.
pGS810	pRW50 vector contains FNR promoter at – 41.5; Tet^R	(Wing *et al*., 1995)/ Lab collection
pGS2268	pGEX-KG containing *anr* for expression as a GST-fusion protein; Amp^R	This work
pGS2350	pBAD/ His B containing *fnr* from *E. coli* cloned as NcoI/ XhoI; Amp^R	This work
pGS2351	pBAD/ His B containing *anr* from *P. putida* cloned as NcoI/ XhoI; Amp^R	This work
pGS2352	pBAD/ His B containing *PP_3233* from *P. putida* cloned as NcoI/ XhoI; Amp^R	This work
pGS2353	pBAD/ His B containing *PP_3287* from *P. putida* cloned as NcoI/ XhoI; Amp^R	This work

pGS2403	As for pGS2414 but containing *PP_3233*; Amp^R	This work
pGS2413	As for pGS2414 but containing *PP_3287*; Amp^R	This work
pGS2414	pCOLD-TF (Takara Bio) containing *anr* for expression as a His_6-Tig-fusion protein; Amp^R	This work
pGS2508	*PP_3233* from *P. putida* cloned as EcoRI/XhoI into pBB1MSC-5; Gm^R	This work
pGS2509	*PP_3287* from *P. putida* cloned as EcoRI/XhoI into pBB1MSC-5; Gm^R	This work
pGS422	pUC13 containing the *melR* promoter with consensus FNR site FF at position -41.5 as a 340 bp EcoRI /HindIII fragment; Amp^R	(Sharrocks *et al*., 1991)/ Lab collection
pGS649	pBluescript containing the *melR* promoter with consensus CRP site CC as a 340 bp EcoRI/HindIII fragment; Amp^R.	Lab collection
pGS652	pBluescript containing the *melR* promoter with consensus NN site as a 340 bp EcoRI/HindIII fragment; Amp^R.	(Gostick *et al*., 1998) / Lab collection
p2373	pCOLD-TF DNA vector; Amp^R	Takara Bio Inc
pAS12	pEX18Ap containing gene replacement cassette for *PP_4265*, Amp^R, Gm^R	This work
pDelta_PP_3233	pEMG containing replacement cassette for *PP_3233*, Kan^R	This work

pDelta_PP_3287	pEMG containing replacement cassette for *PP_3287*, Kan^R	This work
pEMG	Gene replacement vector with two flanking I-SceI sites, Kan^R	(Martínez- García and de Lorenzo, 2011)/ This work
pEX18AP	Gene replacement vector; *sacB*, Amp^R	(Hoang *et al*., 1998)/ This work
pFLP2	Broad host range vector with FLP recombinase, Amp^R	(Hoang *et al*., 1998)/ This work
pPS858	Source of gentamicin resistance cassette; Amp^R, Gm^R	(Hoang *et al*., 1998)/ This work
pSWI	Broad host range vector with I-SceI endonuclease, Amp^R	(Wong and Mekalanos, 2000)/ This work

2.3 Media and reagent providers

The media used to grow the bacteria were supplied from Oxoid Ltd. DNA purification Kit, gel extraction, genomic DNA purification, Plasmid Midi kit and RNase Mini kit were obtained from Qiagen. Chemicals were purchased from Fisher Scientific, Bioline, BDH Chemicals Ltd. Light Shift Chemiluminescent EMSA Kits were provided by Thermo Scientific. Heparin and HiTrap columns were supplied by GE Healthcare. Ampicillin, gentamicin and tetracycline antibiotics were from Sigma and Melford Biolaboratories Ltd. The protein assay reagent was ordered from Bio-Rad. Green qRT-PCR master mix was ordered from Agilent Technology. Paraquat (N,N′-dimethyl-4,4′-bipyridinium dichloride) was from Sigma.

2.4 Bacterial media and culture conditions

2.4.1 Media

Strains of *E. coli* and *P. putida* were grown in Lennox Broth medium (LB).

	LB (g/L)	LB Agar (g/L)
Tryptone	10	10
NaCl	10	10
Yeast extract	5	5
Agar	-	15

For *E. coli* the minimal salt medium was M9. For *P. putida* the minimal medium was 154, supplemented with 0.4% ($^{w}/_{v}$) yeast extract and 30 mM L-arginine (Sigma) (Stalon *et al*., 1967, Vander Wauven *et al*., 1984).

	Medium 154 (L)	M9 medium (L)
KH_2PO_4	1.4 g	3 g
Na_2HPO_4	5.7 g	6 g
NaCl	0.6 g	0.5 g

K_2SO_4	1.7 g	-	
NH_4Cl	-	1 g	
$MnSO_4.4H_2O$	0.55 mg	-	Sterilized by filtration and added from stock solution just before use
$MgSO_4.7H_2O$	50 mg	493 mg	
$FeCl_3$	3 mg	-	
$CaCl_2$	-	11 mg	

All these components were dissolved in 1 L of distilled water and sterilized by autoclaving (121°C, 15 psi). The LB agar was cooled to 50°C, 200 µg/mL of ampicillin or tetracycline 35 µg/mL or gentamicin 20 µg/mL (final concentrations) were added and poured in to petri dishes (25 mL per plate). Plates were stored at 4°C.

2.4.2 Bacterial growth

Escherichia coli strains were cultured in LB medium with appropriate antibiotics at 37°C with shaking at 250 rpm. *Pseudomonas putida* was also cultured in LB medium with antibiotics, but at 30°C with shaking at 200 rpm until the desired optical density OD_{600} was reached. Primary cultures were prepared from a single colony from LB plate or frozen stock and 5 mL of LB and were used directly or to inoculate larger volume of media.

2.4.3 Bacterial growth measurement

The growth of *E. coli* and *P. putida* was estimated by reading the optical density at 600 nm (OD_{600}).

2.4.4 Growth supplements

To induce the protein expression, IPTG was added to final concentration 1 mM or 0.5 mM as indicated. Media (LB broth and agar) was supplemented with appropriate antibiotics such as ampicillin 200 µg/mL, tetracycline 35 µg/mL or gentamicin 20 µg/mL (final concentrations).

2.4.5 Storage of bacterial strains

For short-term storage, bacterial strains were saved on plates at 4°C. For long-term storage, strains were stored as glycerol stocks made by preparing primary cultures in 5 mL of LB (Section 2.4.2). The overnight culture was then centrifuged at 4020 *xg*, 5 min and the pellet re-suspended in 1 mL of LB. Following this 200 µl of 100% ($^{v}/_{v}$) sterile glycerol was added to 800 µl of primary culture and mix was stored at - 70°C.

2.4.6 Preparation of electrocompetent cells

Primary cultures were prepared from a single colony of JRG5302 or JRG6348 (Table 2.1) taken from an LB plate or 50 µl of a frozen glycerol stock and grown in 5 mL of LB (Section 2.4.2). The culture was incubated overnight at 37°C with shaking. Secondary cultures were grown in 250 mL flasks by incubating 50 mL of LB and 0.5 mL of the primary culture for 2 h at 37°C with shaking at 250 rpm. After incubation, usually until the OD_{600} had reached 0.5 – 0.6 (mid log phase) (Section 2.4.3) the cells were harvested by centrifugation in 50 mL pre-cooled universal tubes on 2790 *xg* for 10 min at 4°C. The supernatant was discarded and the bacterial pellet was washed 3 times (for 10 min each) in 25 mL of ice-cold 10% ($^{v}/_{v}$) glycerol solution. After the last washing, the pellet of bacteria was re-suspended gently in 1/100 starting volume of ice-cold 10% ($^{v}/_{v}$) glycerol. Aliquots (50 µl) of the cell suspension was dispensed into microfuge tubes and stored it at -80°C.

2.4.7 Transformation of electrocompetent cells

Plasmid DNA (up to 1 µg/µl) was added to the microfuge tube containing 50 µl of freshly prepared *E. coli* competent cells on ice. Then the mixture was transferred to pre-cooled electroporation cuvette at -20°C and voltage was applied using Hybaid Cell Shock unit (1800 V, 1 mm path length). Immediately, 1 mL of LB medium was added and mixed with the bacteria by pipetting, before transfer after shocking to microfuge tube and incubation at 37°C for 60 min. After incubation, 100 µl of the transformation mixture was spread on LB agar plates containing the appropriate antibiotic and incubated at 37°C overnight.

2.4.8 Preparing *P. putida* KT2440 electrically competent cells

Strains JRG6725, JRG6723, JRG6722 and JRG6721 (Table 2.1) were cultured in 5 mL of LB medium and incubated overnight at 30°C/200 rpm (Section 2.4.2). Secondary cultures were then prepared by inoculating 0.5 mL of the primary culture

into 50 mL of LB medium in 250 mL flasks at 30°C/200 rpm until the OD_{600} reached 1.0-2.0 (Section 2.4.3). The cells were harvested in 50 mL pre-cooled tubes by centrifugation at 2790 *xg* for 10 min and washed twice with 5 mL of cold electroporation buffer (1 mM HEPES pH 7.0). The final cell pellets were re-suspended in 100 µl of electroporation buffer and 9 µl of these cell suspensions were dispensed in microfuge tubes and stored at -80°C (Cho *et al*., 1995).

2.4.9 Transformation of *P. putida* KT2440 electrically competent cells

Plasmid DNA (1 µl, 5 ng/µl) was added into microfuge tube containing 9 µl of the freshly thawed electrocompetent *P. putida* KT2440 cells. The mixture was transferred into a pre-cooled electroporation cuvette and placed in the electroporation device and shocked (1800 V, 1 mm path length). SOC medium (1 mL); 2% ($^{w}/_{v}$) Bacto tryptone, 0.5% ($^{w}/_{v}$) Bacto yeast extract, 10 mM NaCl, 2.5 mM KCl, 10 mM $MgSO_4$, 20 mM glucose) was added immediately and mixed thoroughly before transfer into microfuge tube for incubation at 30°C for 30 min with shaking. After 30 min incubation, 100 µl of the transformation mixture were spread on LB and X-gal /IPTG agar plates containing appropriate antibiotics. The plates were incubated at 30°C overnight.

2.4.10 Growth curve of *P. putida*

The primary cultures of the *P. putida* KT2440 strains (wild type and mutants) were grown in 5 mL of LB containing tetracycline (35 µg/mL) when necessary (Section 2.4.2). The primary cultures were used to inoculate (1% ($^{v}/_{v}$) 50 mL flasks, containing 10 mL (aerobic conditions) and 40 mL (O_2-limited conditions) of LB medium containing tetracycline (35 µg/mL) when indicated 30°C/200 rpm. The OD_{600} was measured in each hour for 8 h (Section 2.4.3).

2.5 Nucleic acid methods

2.5.1 Nucleic acid storage

Purified genomic DNA and plasmids were stored in Qiagen EB buffer (10 mM Tris-HCl, pH 8.5) or deionized water at -20°C.

2.5.2 Plasmid DNA purification

Plasmid DNA was purified from 5 mL of *E. coli* overnight culture using the Qiagen QIAprep® Spin Miniprep kit, according to the manufacturer's instructions.

2.5.3 Polymerase Chain Reaction (PCR)

A Typical PCR reaction was assembled as below:

Plasmid DNA (50-100 ng/µl)	1 µl
Forward primer (100 µM)	1 µl
Reverse primer (100 µM)	1 µl
2x Extensor Master Mix enzyme (Thermo Scientific)	10 µl
ddH_2O	7 µl
Total volume	20 µl

Techne TC-3000 was used to carry out the PCR with the reaction setting as shown below.

	Temperature (°C)	Time min:s	Cycles
Initial denaturation	95	05:00	1
Denaturation	95	00:30	25
Annealing	58	00:30	25
Extension	72	00:33	25
Final extension	72	05:00	1
Final hold	4	∞	1

The PCR products were analyzed by agarose gel electrophoresis (Section 2.5.6).

2.5.4 DNA concentration measurement

The concentration of DNA was measured using the Nanodrop (Thermo Fisher Scientific) (double strand programme) with dH_2O as a blank.

2.5.5 Restriction endonucleases to digest the DNA

The DNA (~1 µg) was digested with restriction enzymes (1:10 of reaction volume) and 10x buffer according to the manufacturer's instructions. Digestions were carried out in 20 µl. Reactions were incubated at 37°C for 2 h. The resulting DNA fragments were analysed by agarose gel electrophoresis (Section 2.5.6).

2.5.6 Agarose gel electrophoresis

Agarose gel electrophoresis was used to view DNA fragments. Agarose was added to 1x TAE buffer (see below) to form 1% ($^{w}/_{v}$) suspension and then dissolved by heating in a microwave. Ethidium bromide solution (Bio-Rad) was added to the gel after cooling at 0.5 µg/mL before pouring. DNA samples were mixed with 5x loading dye (Qiagen) before loading to the gel. DNA HyperLadder I (1 Kb) was used to calibrate the size of the DNA fragments (provided by Bioline). Gels were developed in 1x TAE buffer for 1 h at 100 V. After this the UVtech photo document system was used to view the DNA fragments.

50x TAE (Tris-Acetate-EDTA) buffer

Tris	242 g
Glacial acetic acid	57.1 mL
0.5 M EDTA pH 8.0	100 mL
dH_2O to 1 L	

2.5.7 Gel Extraction

Required DNA fragments were cut from agarose gels (Section 2.5.6) and purified by the QIAquick® Gel Extraction Kit from Qiagen, according to manufacturer's instructions.

2.5.8 Genomic DNA purification

The ~2X10^9 bacterial cells were collected from the primary culture (Section 2.4.2) in microfuge tube by centrifugation for 10 min at 5000 *xg* and the supernatant was discarded. Genomic DNA was purified from the cell pellet using the Qiagen DNeasy®Tissue purification kit, according to manufacturer's instructions.

2.5.9 DNA purification

DNA was purified using the Qiagen QIAquick® Purification Kit, according to manufacturer's instructions.

2.5.10 Quantitative Polymerase Chain Reaction (qRT-PCR)

A-Preparing the cells

The JRG6725, JRG6721, JRG6722 and JRG6723 (Table 2.1) cultures were prepared by inoculating 1% ($^v/_v$) of a primary culture into 50 mL flasks containing 10, 20, 30, 40 or 50 mL of LB medium. The cultures were incubated at 30°C/200 rpm for ~3 h until OD_{600} reached 0.6-0.8 (Section 2.4.3). After incubation, aliquots (5 mL) were transferred into pre-cooled 50 mL Falcon tube and 2 mL of cold (5% ($^v/_v$) phenol pH 4.3 and 95% ($^v/_v$) ethanol) was added to the culture and left on ice for 30 min.

Cultures of JRG6348 (Table 2.1) transformed with the pBAD-HisB-derivatives pGS2350, pGS2351, pGS2352 or pGS2353 (Table 2.2; encoding FNR, PP_4265 (ANR), PP_3233 and PP_3287 all expressed under the control of the pBAD promoter to eliminate any differential transcriptional control over the production of the regulators) were grown under anaerobic conditions (sealed tubes filled to the neck) in M9 minimal medium supplemented with L-broth (5% ($^v/_v$), glycerol (0.4% ($^v/_v$), TMAO (20 mM), sodium fumarate (20 mM) and ampicillin (100 µg/mL) at 37°C until the OD_{600} reached 0.175- 0.200 (Constantinidou *et al*., 2006). Aliquots (5 mL) were removed and mRNA was stabilised by the addition of 2 mL of an ice-cold ethanol (95% ($^v/_v$) phenol (5% ($^v/_v$) pH 4.5 mix. The cultures were then exposed to air by shaking, and incubation was continued for 20 min before taking further samples for total RNA preparation.

After incubation in ice for 30 min, the cells were harvested by centrifugation at 3220 *xg* for 10 min at 4°C and the supernatant discarded. The cells pellet were re-suspended by residual liquid in tubes and transferred to 1.5 mL microfuge tube and

centrifuged at 16060 *xg* for 60 s in a bench-top microcentrifuge. Remaining liquid was discarded and the cell pellet was stored at -80°C before RNA extraction.

B- The RNA purification

The RNA samples were purified from cell pellets using the Qiagen RNeasy Plus Mini Kit according to the manufacturer's instructions. The RNA samples were stored at -70°C. The concentrations of RNA samples were measured using the Nanodrop spectrophotometer (Thermo Fisher Scientific) with free RNase water as a blank and 1% ($^{w}/_{v}$) of agarose gel electrophoresis was used to analyse the samples before dilution to 20 ng/µl.

C- Primer design

Primers were designed for qRT-PCR using the primers web tool (http://primer3.ut.ee/). The length of the primers were 19-22 base pairs with a T_m ~60°C and GC > 65%. The primers were ordered from Sigma-Aldrich. Table 2.3 shows the sequence of the primers used for qRT-PCR

Table 2.3: Sequences of qRT-PCR primers

Primers		Sequences 5´ →3´
	For *P. putida*	
ANR	F	TCTTTCGCTGAACCTGGAAG
	R	AGCCAAAACTGTCACCCTG
3233	F	ACGAAGTGGACAAACTGGAG
	R	GAAAATTCTTGATCGCCCCA
3287	F	GAATTTCTACCAACCTGCCATG
	R	TTGCGGATGTCTCGTGAAG
gyrA	F	GTCAACGGTTCCAGCGGTA
	R	TTCCGGGTTGTCGATGAGC
gyrB	F	GCAGCCGAGGTCATCATGA
	R	GCGTTCACAACCGACACAC
gap-1	F	AGCAAGGCCTGATGACCAC
	R	CGGGATCATCGACTGGGTG
rpoD	F	AAGGAAAGCATCGAGGCCC
	R	CACGCTCGACCAGTACCTC
	For *E. coli*	
gyrA	F	ACCTTGCGAGAGAAATTACACC
	R	AATGACCGACATCGCATAATC
lacZ	F	CGTGACGTCTCGTTGCTG
	R	GTACAGCGCGGCTGAAAT

F= Forward, R = Reverse

D- The qRT-PCR reaction

Reactions were carried out in 96-well plate format, each well contained

RNA sample (20 ng/µl)	5 µl
2x Brilliant III SYBR Green qRT-PCR mastermix (Sigma)	10 µl
Primers (5 pmol/µl)	2 µl
RT/ RNase Block enzyme	1 µl
DTT (100 mM)	0.2 µl
Free-RNase H_2O (Sigma)	1.8 µl

The qRT-PCR was carried out using the following settings:

Segment	Cycle No.	Time	Temperature (°C)
1	1	10 min	50
2	1	3 min	95
3	40	15 s	95
		20 s	60
4	1	1 min	95
		30 s	55
		30 s	95

2.6 Protein methods

2.6.1 Protein concentration measurement

Bio-Rad reagent was used to calculate the concentration of protein (Bradford, 1976). The Unicam HEλIOS spectrophotometer was used to measure the absorbance at 595 nm and standard curve was used to calculate protein concentration of samples. In addition, the concentrations of specific purified proteins were calculated by using their extinction coefficients, which were estimated by using Protparam tool (http://web.expasy.org/protparam/).

2.6.2 SDS-PAGE

SDS-PAGE was carried out as explained in Laemmli (1970). The analysis was carried out using 15% ($^{w}/_{v}$) resolving gel, and 5% ($^{w}/_{v}$) stacking gel as described below.

	15% Resolving gel (mL)	**5% Stacking gel (mL)**
30% ($^{w}/_{v}$) acrylamide	3.75	0.415
3 M Tris pH 8.3	0.95	-
0.5 M Tris pH 6.8	-	0.625
dH_2O	2.68	1.44
SDS 10% ($^{w}/_{v}$)	0.075	0.025
APS 10% ($^{w}/_{v}$)	0.01	0.025
TEMED	0.02	0.0025

The glass plates were organized in the clamps and the resolving gel was poured to full ¾ of the gel volume. Isopropanol was added on the top of the gel. When the gel had set, the isopropanol was removed by rinsing with dH_2O. The stacking gel was then poured on top of the resolving gel and a comb was inserted to make the wells. Once the gel had set the comb was removed and the gel was moved to in to the tank with 1x SDS running buffer (see below). Protein samples were mixed with 6x loading buffer (see below) and boiled for 10 min at 95°C before loading into the gel wells. Protein standard marker (Precision Plus Protein™ Standards from Bio-Rad) was loaded to calibrate the gels. After loading, the SDS-PAGE was run at 150 V for 60 min.

1x SDS running buffer		**6x SDS loading buffer**	
Tris	3 g	Tris-HCl (0.125 M, pH 6.8)	2.5 mL
Glycine	14.4 g	Sucrose 10% ($^{w}/_{v}$)	1 g
SDS	1 g	SDS 4% ($^{w}/_{v}$)	4 mL
dH_2O to 1 L		Bromophenol blue	0.1% ($^{w}/_{v}$)
		β-Mercaptoethanol	7% ($^{v}/_{v}$)

When the bromophenol blue dye reached the bottom of the gel. The gel was removed from the glass plates and stained with Coomassie blue stain (see below) for 30 min and then destained for overnight.

	Coomassie Blue stain	**Destained**
Coomassie Brillient Blue (R250)	1.15 g/L	-
Methanol	400 mL	400 mL
Acetic acid	100 mL	100 mL
dH_2O to 1 L		

2.6.3 Aerobic overproduction of *P. putida* ANR

The coding region of *anr,* which had been amplified from *P. putida* KT2440 genomic DNA using the primers MS87 (5´-TTTTTCTAGACATGTCCGAGCCAGTCAAACT-3´) and MS88 (5´-TTTTCTCGAGTCAGGCCTCGATTGCACCACA-3´) and ligated into p547 (Table 2.2; engineered XbaI and XhoI sites respectively (underlined)). The plasmid pGS2268 was purified and used to transform JRG5302 (Table 2.1, Section 2.4.7). Overproduction cultures were grown aerobically at 37℃ for 2 h until the OD_{600} reached 0.6-0.8 (Section 2.4.3). Then IPTG (1 mM) was added to the culture to induce GST-ANR production. Incubation with shaking 250 rpm was continued at in 25°C for 3 h. The cells were then harvested by centrifugation in a 500 mL centrifuge tube at 17696 *xg* for 15 min at 4°C. The supernatant was discarded and the bacterial pellet stored at -20 °C overnight or used directly to prepare cell-free extracts (Section 2.6.4).

2.6.4 Cell-free extract

The cell pellets were resuspended in 10 mL of 25 mM HEPES, 100 mM NaCl, 100 mM $NaNO_3$, 2.5 mM $CaCl_2$, pH 7.5. The cell pellets then were passed through a French pressure cell at 16000 psi three times or sonicated for 10 s (10 Microns) three times to lyse the cells. Cell debris was removed by centrifugation at 39191 *xg* for 30

min at 4°C. The supernatant was filtered through a syringe filter with a pore size of 0.45 µm.

2.6.5 Purification of GST- ANR

The GST-ANR protein was purified from cell-free extracts by affinity chromatography using Glutathione Sepharose 4B (GE Healthcare) equilibrated with 25 mM HEPES, 100 mM NaCl, 100 mM $NaNO_3$, 2.5 mM $CaCl_2$ at pH 7.5. The ANR protein was released from GST by treatment with thrombin (Thrombin from human plasma, Sigma) 10 units per 100 nmole of fusion protein after incubation at 4°C overnight.

2.6.6 Overproductions of Tig-ANR, Tig-PP_3233 and Tig-PP_3287

The *anr*, *PP_3233* and *PP_3287* were amplified from *P. putida* KT2440 genomic DNA, using the following primers: ANR, MS140 (5´-TTTTCATATGTCCGAGCCAGTCAAACTGCG-3´) and MS150 (5´-TTTTTCTAGATCAGGCCTCGATTGCACCAC-3´) containing engineered NdeI and XbaI sites respectively (underlined); PP_3233, MS141 (5´-TTTTCATATGTCAGGCTCTGCAGAAATGGG-3´) and MS92 (5´-TTTTCTCGAGTCAAGTGGGCTCCTCCAGGC-3´) containing engineered NdeI and XhoI restrictions sites (underlined) respectively; PP_3287, MS142 (5´-TTTTCATATGCCTGGCCAGCTGAAGGTCAC-3´) and MS151 (5´-TTTTTCTAGATCAGGGGCCCTTGGCCTCAC-3´) containing engineered NdeI and XbaI sites respectively (underlined) and ligated into p2373 (pCOLD-TF DNA vector) to give pGS2414, pGS2403 and pGS2413 respectively; Table 2.2.

The His_6-Tig-ANR, -PP_3233 and -PP_3287 proteins were overproduced aerobically in JRG5302 (Table 2.1) using 2 L flasks each one containing 300 mL of LB broth and ampicillin (200 µg/mL) at 37°C until the OD_{600} reached 0.6–0.8 (Section 2.4.3). The cultures were chilled to 15°C for 30 min and then IPTG (0.5 mM) was added and the cultures were incubated at 15°C for 24 h with shaking (250 rpm). The cell pellets were harvested by centrifugation at 17696 *xg* for 20 min at 4°C. Pellets were then stored at -20°C overnight or used directly for cell-free extract production (Section 2.6.7).

2.6.7 Purification of cell-free extract of Tig-ANR, -PP_3233 and -PP_3287.

The cell pellets were resuspended in 10 mL of buffer A (Section 2.6.8). Resuspended cells were passed three times through the Franch pressure cell at 16000 psi after

incubation with 200 µg/mL of lysozyme at room temperature for 30 min. The extracts were clarified by centrifugation at 39191 *xg* at 4°C for 30 min. The soluble fraction was used to purify the proteins.

2.6.8 Purification of Tig-ANR, -PP_3233 and -PP_3287 by affinity chromatography

The proteins Tig-ANR, -PP_3233 and -PP_3287 were purified from cell-free extracts using their engineered Histidine tags. Purification was achieved using 1 mL Hi-Trap™ chelating columns (GE Healthcare) and the His-tag purification programme on the AKTA™ prime machine (GE Healthcare). The machine was set and the reagents were prepared according to manufacturer's instruction. Cell-free extract (10 mL) was injected and 1 mL eluting fractions were collected. The fractions were analyzed by SDS-PAGE to identify those containing the purified protein.

Binding buffer A (pH 7.4)

Sodium phosphate	20 mM
NaCl	0.5 M
dH_2O to 1 L	

Elution buffer B (pH 7.4)

Sodium phosphate	20 mM
NaCl	0.5 M
Imidazole	1 M
dH_2O to 1 L	

Ni-loading eluent

$NiSO_4$	100 mM

The protein fractions were desalted into 25 mM HEPES, 100 mM NaCl, 100 mM $NaNO_3$ pH 7.5 using Vivaspin column (10 kDa) at 4000 *xg* for 20 min at room temperature. Protein solutions were stored at -20°C until required.

2.6.9 Amino acid analysis

The complete amino acid analysis of ANR was done by Alta Bioscience (University of Birmingham, UK) via acid hydrolysis for 24 h at 110°C of an ANR sample which had previously been subject to protein measurement by the Bradford assay (Section 2.6.1).

2.6.10 Size-exclusion chromatography

Superdex 200 column (10x300 mm, GE Healthcare) was equiliperated with 25 mM Tris-HCl pH 7.5, 2 mM EDTA pH 7.5 containing 0.5 M NaCl and 1 mM azide buffer was used to investigate the oligomeric state of apo-ANR, Apo-FNR and apo-HcpR2. Apo-ANR (~250 µM), apo-FNR (~159 µM) and apo-HcpR2 (~69 µM) samples were purified by heparin column chromatography (Section 2.7.2) and eluted with 25 mM Tris-HCl pH 7.5 containing 0.5 M NaCl. The elution volumes of the test proteins were compared to the standard curve consisting of: Blue dextran, haemoglobin, ovalbumin, cytochrome *c*, and aprotinin.

2.6.11 *Pseudomonas putida* KT2440 strains that only expressed one of the three FNR proteins

To investigate the relative responses of the three *P. putida* FNR proteins *in vivo*, it was necessary to create *P. putida* KT2440 strains that only expressed one of the three FNR proteins encoded by the genome. These strains were created by our colleagues José Manuel Borrero-de Acuña and Dr. Max Schobert at Technische Universität, Braunschweig, Germany. Two different strategies were used to create unmarked deletion mutants. The *P. putida* gene *PP_4265 encoding* ANR was deleted using *sacB* counter selection and FLP recombinase excision as described by Hoang *et al*., (1998). The primer pairs oAS23 (5´-GGAATTCAGCCAGATCGGCGACCTGTA-3´), oAS24 (5´-CGGGATCCTGTAGGCCAGTGTGCGCGAT-3´), oAS25 (5´-CGGGATCCACCTTGGCCTGGCGGTAGAA-3´) and oAS26 (5´-GCTCTAGACTGTCGGCATGCACTTCCAG-3´) containing engineered EcoRI, BamHI, BamHI and XbaI restrictions sites (underlined), respectively, were used to amplify 511 bp and 533 bp DNA fragments flanking the *PP_4265* gene. The fragments were cloned into the suicide vector pEX18Ap flanking the gentamicin resistance cassette from plasmid pPS858 and used to generate the unmarked *P. putida PP_4265* mutant strain (Hoang *et al*., 1998). For the generation of unmarked

gene deletion mutants of the genes encoding the FNR proteins PP_3233 and PP_3287, we used the I-SceI endonuclease based knockout strategy for *P. putida* described by Martinez-Garcia and de Lorenzo (2011). The following primers were used to amplify upstream and downstream regions of *PP_3233* and join both fragments by sewing PCR: PP_3233 Upstream-Forward (5´-GAATTCAAGGCTTTTTCGCGTTCTC-3´, engineered EcoRI site (underlined), PP_3233 Upstream-Reverse (5´-GAGACCTGCATGGACGAAGGACGATGCCTCCGCTTTTTTC-3´), PP_3233 Downstream-Forward (5´-CTTCGTCCATGCAGGTCTC-3´) and PP_3233 Downstream-Reverse (5´-AAGCTTATTTATCGTCAGCACCCAGAGT-3´, engineered HindIII site underlined). For *PP_3287 the* following primers: PP_3287 Upstream-Forward (5´- GAATTCTGCGATACGTAGGTAGAGCATC-3´, engineered EcoRI site (underlined), PP_3287 Upstream1-Reverse (5´-AGACATCCGCAACATGAAGCTTTCAGGCCTCCTTCGCATTACG-3´), PP_3287 Downstream-Forward (5´-GCTTCATGTTGCGGATGTCT-3´) and PP_3287 Downstream-Reverse (5´-GGATCCCCACGTTGCATGATCTTGAG-3´, engineered BamHI site (underlined) were used.

The PCR products were ligated into the suicide vector pEMG and used to generate double knockout mutants *P. putida PP_4265 PP_3233* (JRG6721) and *P. putida PP_4265 PP_3287* (JRG6722) as well as *P. putida PP_3233 PP_3287* (JRG6723) following the protocol described by Martínez- García and de Lorenzo (2011).

2.6.12 PP_3233 and PP_3287 overexpression in *P. putida*

The *PP_3233* and *PP_3287* open reading frames with their promoter regions were amplified from *P. putida* KT2440 genomic DNA using the primers: PP_3233 (5´-TTTTGAATTCGGCCTGATCAACACGTGAAC-3´) and (5´-TTTTCTCGAGTCGTCAGCACCCAGAGTGC-3´) containing engineered EcoRI and XhoI sites respectively (underlined); PP_3287 (5´-TTTTGAATTCGCCAGCTACACGTTGCGAA-3´) and (5´-TTTTCTCGAGATGATCTTGAGGCGGGCGA-3´) containing engineered EcoRI and XhoI respectively (underlined) and ligated into p2490 (pBBR1MCS-5) to give pGS2508 and pGS2509 respectively (Table 2.2).

For the heterologous *E. coli* reporter system, expression plasmids for use in the strain *E. coli* JRG6348 as well as an equivalent *E. coli* FNR expression plasmid to act as a

control were created by Dr. M.R. Stapleton. The open reading frames corresponding to FNR, ANR, PP_3233 and PP_3287 were amplified by PCR using oligonucleotide primers incorporating NcoI and XhoI restriction sites (underlined): MS125 (5´-TTTTCCATGGATCCCGGAAAAGCGAATTAT-3´) and MS126 (5´-TTTTCTCGAGTCAGGCAACGTTACGCGTAT-3´) for *fnr*; MS122 (5´-TTTTCCATGGTCCGAGCCAGTCAAACTGCG-3´) and MS88 (5´-TTTTCTCGAGTCAGGCCTCGATTGCACCACA-3´) for *anr*; MS124 (5´-TTTTCCATGGTCAGGCTCTGCAGAAATGGG-3´) and MS92 (5´-TTTTCTCGAGTCAAGTGGGCTCCTCCAGGC-3´) for *PP_3233*; MS123 (5´-TTTTCCATGGCCTGGCCAGCTGAAGGTCAC-3´) and MS90 (5´-TTTTCTCGAGTCAGGGGCCCTTGGCCTCAC-3´) for *PP_3287*. The products were then ligated into pBAD-HisB (Invitrogen) following NcoI and XhoI digestion and 'filling-in' the NcoI site so that the ATG start codon was provided by the vector and the encoded proteins lacked His-tags to give plasmids pGS2350, pGS2351, pGS2352 and pGS2353 encoding FNR, PP_4264 (ANR), PP_3233 and PP_3287 respectively (Table 2.2). The authenticity of all constructs was confirmed by DNA sequencing.

2.7 Iron –sulfur cluster methods

2.7.1 Anaerobic reconstitution of [4Fe-4S] –proteins

The purified ANR (Section 2.6.5), Tig-ANR, -PP_3233 and -PP_3287 (Section 2.6.8) and apo-HcpR2 protein, which was kindly provided by Dr. Ian Cadby, Birmingham University, were used for protein reconstitution. All the reagents, including the protein solutions, used in the reconstitution of the iron-sulfur clusters were made anaerobic by incubation in a DW Scientific Anaerobic Workstation. Protein samples (typically 2.5 mg/mL; 0.5-1.0 mL) were incubated with L-cysteine (0.5 mM), ammonium ferrous sulfate (0.2 mM), dithiothreitol (250 mM) and the cysteine desulfurase NifS (~0.3 µM) under anaerobic conditions. After 16 h incubation at 25°C, the reactions attained a straw-brown colour. Reconstituted protein was cleaned as described in Section 2.7.2.

2.7.2 Separation of [4Fe-4S]–proteins from reconstitution reaction components by heparin column chromatography

Generally, proteins that bind DNA bind to heparin, thus heparin chromatography can be used to separate such proteins from other reconstitution reaction components. All the following procedures were carried out in the anaerobic workstation. An aliquot (1 mL) of reconstituted protein was diluted 2-fold using anaerobic 25 mM Tris-HCl buffer

(pH 7.5). The diluted sample was applied to a 1 mL HiTrap heparin column (GE Healthcare) equilibrated in the same buffer. The heparin column was washed with 3 mL of anaerobic 25 mM Tris-HCl buffer (pH 7.5) to remove low molecular weight reaction components. The reconstituted protein was then eluted by applying anaerobic 25 mM Tris-HCl (pH 7.5) buffer supplemented with 0.5 M NaCl from the bottom of the column to minimize dilution of the protein. Coloured eluate was collected by hand into microfuge tubes. Coloured fractions could then be transferred to cuvettes which were closed with a screw cap containing a septa made from rubber and coated with Teflon.

2.7.3 Iron assay

The protein concentrations of the reconstituted and heparin purified protein samples were measured using the Bradford assay (Bradford, 1976; Section 2.7.1 and 2.7.2). Samples were then boiled in 1% ($^{w}/_{v}$) trichloroacetic acid for 5 min. After centrifugation in a bench top microcentrifuge (16060 *xg* for 5 min) the supernatant was removed and retained. The supernatant was used in the following reaction

Sample and dH_2O	480 µl
Saturated sodium acetate	400 µl
10% ($^{w}/_{v}$) Bathophenothroline sulfonic acid	30 µl
20% ($^{w}/_{v}$) Fresh sodium ascorbate	90 µl

After adding sodium ascorbate all the iron present in the sample was reduced to the ferrous state and formed a complex with the bathophenanthroline, resulting in a red colouration. Absorbance of the complex was then measured at 535 nm and compared to a standard curve to calculate the iron content of the protein. The standard curve was prepared using dilutions of an iron standard solution at 17.86 mM (Alfa Aesar).

2.7.4 Circular dichrosium (CD) of the $[4Fe\text{-}4S]^{2+}$ to $[2Fe\text{-}2S]^{2+}$ conversion in ANR.

Circular dichrosium (CD) spectroscopy was carried out by Dr. Jason Crack, University of East Anglia. Measurements were made with a Jasco J-810 spectropolarimeter. An aliquot of ANR (680 µl) was diluted to 29.8 µM [4Fe-4S] in a 1 cm anaerobic cuvette. The sample was treated with an aliquot of oxygenated buffer (~220 µM O_2) to give

approximately a 2-fold molar excess of O_2. The buffer was 9 mM Tris, 17 mM HEPES, 1.7 mM $CaCl_2$, 236 mM NaCl, 66 mM $NaNO_3$, pH 7.5. The sample was incubated for 15 min prior to measurement.

2.7.5 Liquid chromatography mass spectrometry (LCMS) study of the [4Fe-4S]$^{2+}$ to [2Fe-2S]$^{2+}$ cluster conversion in ANR.

Liquid chromatography mass spectrometry (LCMS) was carried out at the University of East Anglia by Dr. Jason Crack. An aliquot of ANR (20 µl, 80 µM [4Fe-4S]) was combined with ~2.8-fold molar excess of air-saturated buffer (~220 µM O_2), or aerobic buffer, and allowed to react for 15 min. Samples were diluted to 2.9 µM final concentration, with an aqueous mixture of 1% ($^v/_v$) acetonitrile, 0.3% ($^v/_v$) formic acid, sealed, removed from the anaerobic cabinet and loaded (5 □l) onto a ProSwift RP-1S column (4.6x50 mm) (Thermo Scientific) on a Ultimate 3000 UHLPC system (Dionex, Leeds, UK). Bound proteins were eluted (0.2 mL/min) using a linear gradient (15 min) from 1% to 100% ($^v/_v$) acetonitrile, 0.1% ($^v/_v$) formic acid. The eluent was continuously infused into a Bruker microQTOF-QIII mass spectrometer, running Hystar (Bruker Daltonics, Coventry, UK), using positive mode electrospray ionisation (ESI). Compass Data Analysis, with Maximum Entropy v1.3, (Bruker Daltonics, Coventry) was used for processing of spectra under LC peak. The mass spectrometer was calibrated with ESI-L tuning mix (Agilent Technologies).

2.7.6 Cary UV Visible spectroscopy

The Cary 50 Bio UV-visible spectroscopy was used to scan protein samples in a quartze Hellma® 10 mm cuvette with a screw cap lid to maintain anaerobic conditions. Appropriate buffer was used to obtain baseline. Scanning was carried out between 250-750 nm. Reagents that react with iron-sulfur clusters were injected in to the cuvette by Hamilton syringe through the lid which contained a Hellma® silicone seal.

2.7.7 Repair of cysteine persulfide [2Fe-2S]$^{2+}$ clusters

The O_2-induced [4Fe-4S]$^{2+}$ to [2Fe-2S]$^{2+}$ cluster conversion in ANR was monitored by UV-visible spectroscopy of samples after exposure to air-saturated buffer for 30 min. Repair of persulfide-ligated [2Fe-2S]$^{2+}$ clusters was monitored by obtaining UV-visible spectra in a Cary 50 Bio UV-visible spectrophotometer (Section 2.7.6) after addition of 3 mM DTT at 0 min and a 4-fold molar excess of Fe^{2+} under reducing conditions

without exogenous sulfide. The spectra were recorded after 50 min and 160 min.

2.7.8 Determination of protein extinction coefficients

To measure the extinction coefficients of reconstituted proteins, 1mL (100 µM) of the apo-protein sample was reconstituted under anaerobic conditions and cleaned using a heparin column chromatography (Section 2.7.1 and 2.7.2). The reconstituted sample was transferred to anaerobic cuvette. The UV-visible spectrum was recorded (Section 2.7.6). Then air-saturated buffer was added to the reconstituted protein sample. The spectrum was rerecorded. Then the cap of the cuvette was removed for 16 h at room temperature until the spectrum was that of the apo-protein. The final volume of the sample was measured and 200 µl was used in the Bradford assay to determine the protein concentration. The protein extinction coefficient was calculated using the equation

$$A = \varepsilon cL$$

Where is:

A = Absorbance at 420 nm and 550 nm

ε = Extinction coefficients

c = Concentration of the sample (µM)

L = Light path length in centimeters

2.7.9 Sensitivity of iron-sulfur cluster to O_2

To investigate iron-sulfur cluster reactivity with O_2, apo-proteins were reconstituted and purified under anaerobic conditions using a heparin column chromatography (Section 2.7.1 and 2.7.2). The UV-visible spectra (250-750 nm) of the reconstituted proteins were then recorded using a Cary Spectrophotometer (Section 2.7.6). Changes in the spectra following titration of the protein solution with increasing volumes of air-saturated (~220 µM O_2) buffer (25 mM Tris-HCl pH 7.5 containing 0.5 M NaCl) were recorded. The reactions were allowed to proceed for 10 min at room temperature after each successive addition of air-saturated buffer before the spectra were obtained. These spectra were used to plot $[O_2]$: $[4Fe\text{-}4S]^{2+}$ ratio against ΔA_{405}.

The rate of reaction of O_2 with [4Fe-4S] clusters was investigated. Typically, 0.5 mL of reconstituted protein solution (Section 2.7.1) in Hellma® cuvette was used. An equal volume of aerobic buffer was added to the cuvette by Hamilton syringe to give a known O_2 concentration (~110 µM) and mixed. The cuvette was then transferred to a

Cary spectrophotometer (Section 2.7.6). The absorbance at 420 nm were recorded every 1s to follow the conversion of [4Fe-4S] to [2Fe-2S] cluster. The data were fitted to a single or double-exponential function (as appropriate) under pseudo-first order reaction conditions using the equation $y = y_0 + (y_{max} - y_0)(1 - e^{[-k_{obs} .x]})$ by computing fits for the parameters y_0, K_{obs} and y_{max} (Sutton *et al*., 2004) by Dr. Jason Crack, Centre for Molecular and Structural Biochemistry, School of Chemistry, University of East Anglia, UK.

2.7.10 Nitric oxide preparation

Proli NONOate (Cayman Chemicals) was used as a source of nitric oxide. It releases 2 molecules of nitric oxide with half-life ~13 s at 25°C and pH 7.4 (Cruz-Ramos *et al*., 2002). Proli NONOate (500 µM) was dissolved in 10 mM NaOH was prepared just before use. In addition, NOC-7 (1-Hydroxy-2-oxo-3-(3-aminopropyl)-3-isopropyl-1-triazene, Enzo Life Sciences) (20 mM) was dissolved in 0.1 M NaOH and used to release nitric oxide.

2.7.11 Sensitivity of iron-sulfur clusters to nitric oxide

The reaction of reconstituted proteins (Section 2.7.1 and 2.7.2) with nitric oxide was investigated using a reconstituted proteins, Cary 50 Bio UV-Vis spectrophotometer and quartz Hellma® 10 mm cuvettes under anaerobic conditions (Section 2.7.6). A known concentration of nitric oxide was injected using a Hamilton syringe through the silicone seal in the lid of the cuvette containing the protein and mixed. After incubation for 10 min at room temperature the absorbance spectra at (250–750 nm) were recorded. To determine the rate of the reaction of iron-sulfur cluster reaction with nitric oxide, 0.5 mL (~10 µM) of reconstituted proteins were used. An equal amount (0.5 mL) of 100 µM of Proli NONOate was added to the cuvette and mixed. Then the cuvette was transferred to the spectrometer and the change in the absorbance at 350 nm was recorded. Data were fitted to a single or double-exponential function (as appropriate) under pseudo-first order reaction conditions using the equation $y = y_0 + (y_{max} - y_0)(1 - e^{[-k_{obs} .x]})$ by computing fits for the parameters y_0, K_{obs} and y_{max} (Sutton *et al*., 2004) by Dr. Jason Crack, University of East Anglia, UK.

2.7.12 β-Galactosidase assay

The β-galactosidase assay was carried out according to Miller (1992). The primary cultures of *P. putida* (wild type and mutants) were grown in LB medium containing tetracycline (35 µg/mL) at 30°C/ 200 rpm (Section 2.4.2). The primary cultures provided 1% ($^{v}/_{v}$) inocula for 10, 20, 30, 40 or 50 mL of medium in 50 mL conical flasks and incubated at 30°C/200 rpm until the OD_{600} reached 0.5-0.8 (Section 2.4.3). Three replicates cultures from each strain were assayed in triplicate. After incubation for 3 h volume of growth was measured by recording the $OD_{600.}$ Appropriate ANR, PP_3233 and PP_3287 cultures were added to 780 µl Z-buffer (see below), 20 µl chloroform and 10 µl of 0.1% ($^{v}/_{v}$) SDS. The mixtures were vortexed for 10 s and incubated at 28°C for 5 min.

The reactions were started by adding 200 µl of ONPG (4 mg/mL O-nitrophenyl-β-D-galactopyranoside stock solution). The reactions were stopped when the colour turned pale yellow by addition of 500 µl 1 M $Na_2CO_{3.}$ The time of the reactions were recorded. The samples were clarified in a bench top microcentrifuge at 16060 *xg* for 5 min and the supernatants were transferred to 1 mL cuvettes. The A_{420} were measured using the Unicam HEλIOS spectrophotometer. Miller units were calculated using the following equation:

$$(A_{420}/ v * t * A_{600}) * 1000$$

V is the volume of the culture in an mL

T is the time of the reaction in min at 28°C after the addition of ONPG until the reaction was terminated (Miller, 1992).

Z-buffer /L

Na_2HPO_4	60 mM
NaH_2PO_4	40 mM
KCl	10 mM
$MgSO_4.7H_2O$	1 mM
β-Mercaptoethanol	50 mM (added immediately prior to use).

2.7.13 Western blot analysis

A- Preparation of whole bacterial cell lysates

Primary cultures were grown in 5 mL of LB and ampicillin (200 µg/mL) or tetracycline (35 µg/mL) and gentamicin (20 µg/mL) (Section 2.4.2). The primary cultures were used to provide 1% ($^{v}/_{v}$) inocula for 10, 20, 30, 40 or 50 mL of LB medium in 50 mL conical flasks. Cultures were incubated at 37°C with shaking (275 rpm) overnight for *E. coli* strains and at 30°C with shaking (200 rpm) for 3 h for *P. putida* strains.

The OD_{600} of cultures were measured (Section 2.4.3) and 2 OD_{600} units were harvested by centrifugation in bench-top microcentrifuge at 16060 *xg* for 10 min and the supernatant was removed. The pellets were resuspended in 100 µl of 6x SDS loading buffer (Section 2.6.2) and heated at 100°C for 10 min.

SDS-PAGE was used to separate the samples (Section 2.6.2). Aliquots (15 µl) of each sample were loaded into each well and 10 µl of the protein standard marker (Precision plus protein™ standard from Bio-Rad) was used (Section 2.6.2).

B- Blotting the gel

After electrophoresis, the gels were transferred into square petri dishes containing 1x wet transfer buffer (see below) and incubated for 15 min. In addition, two pads of blotting paper, sponge pads and nitrocellulose membrane provided by Amersham Biosciences were placed into clean bowl containing pre-cooled 1x wet transfer buffer to soak for 15 min. After that proteins were transferred onto nitrocellulose membranes using a Trans Blot Mini Cell (Bio-Rad) for 1 h at 100 V. The membranes were removed from the blotting tanks and incubated in freshly prepared blocking solution (10% ($^{w}/_{v}$) Marvel in TBS-Tween-20) for 60 min at room temperature with shaking. After 1 h the membranes were transferred to TBS-Tween-20 (see below) containing an appropriate dilution of primary antibody (1:5000) for 2 h with shaking at room temperature. The membrane was washed three times in TBS-Tween-20 for 15 min on an orbital shaker. After the final wash, the membrane was incubated for 60 min in TBS-Tween-20 (see below) containing a 1/15000 dilution of ECL™ peroxidase labelled anti-rabbit antibody (Amersham Bioscienences). The membranes were washed twice with TBS (see below) for 15 min and proteins detected by Enhanced Chemiluminescence (ECL) (Thermo Scientific), according to manufacturer's instructions.

Wet transfer buffer

25 mM Tris base	3 g
150 mM glycine	11.3 g
20 % ($^{v}/_{v}$) methanol	200 mL
dH_2O to 1 L	

Blocking solution (10 mL)

TBS	10 mL
Dried milk powder (10% ($^{w}/_{v}$)	1 g
Tween-20 (0.05% ($^{v}/_{v}$)	5.0 µl

Tris-Buffered Saline (TBS) (pH 7.4)(10x)

Tris	30 g
NaCl	80 g
KCl	2 g
dH_2O to 1 L	

TBS-Tween 20 (1x)

TBS (10x)	100 mL
Tween-20 (0.1% ($^{v}/_{v}$)	1 mL
dH_2O to 1 L	

C- Sources of antibodies

The antiserum raised against FNR protein used in section 2.7.13(B) was kindly provided by Dr. Matthew Rolfe, University of Sheffield, UK.

2.7.14 Response of *P. putida* FNR proteins to nitric oxide and oxidative stress *in vivo*

The primary cultures of *P. putida* strains JRG6723, JRG6722 and JRG6721 (Table 2.2, encoding only ANR, PP_3233 or PP_3287) were grown in 5 mL of LB medium containing tetracycline (35 µg/mL) and gentamicin (20 µg/mL) (Section 2.4.2). The primary cultures were provided 1% ($^{v}/_{v}$) inocula for 10 mL of LB medium in 50 mL flasks for aerobic growth without and with paraquat (PQ, 200 µM, Section 2.3). In addition, the strains were grown under anaerobic conditions (sealed tube filled to the nick) in medium 154 (Section 2.4.1) supplemented with 0.4% ($^{w}/_{v}$) yeast extract (Sigma-Aldrich) and 30 mM L-arginine (Sigma) without and with NOC-7 (20 µM) (Section 2.7.10). Culture supplement with NOC-7 was incubated in the anaerobic cabinet and the fixed concentration was injected with a Hamilton syringe through the seal and mixed. The cultures were incubated at 30°C/200 rpm for 3 h. After incubation, the β-galactosidase activities were measured in triplicate (Section 2.7.12).

2.8 DNA-Protein interaction

2.8.1 Biotin-labelled DNA

To investigate the ability of ANR, PP_3233 and PP_3287 to recognise and bind to specific DNA sequences, biotin labelled DNA was amplified from pGS422 (FF site), pGS649 (CC site) and pGS652 (NN site) using PCR (Section 2.5.3) and 5`-biotin labelled M13 Forward (5´-CACGACGTTGTAAAACGAC-3´), and M13 Reverse (5´-GGATAACAATTTCACACAGG-3´) primers. In addition, biotin labelled p1827cTERM (5´-CAACGGAAAAAACATCTCCC-3´), and p1827cTERM-Reverse (5´-GGGCAGCGCGGTGGCGTAATCC-3´) were used to amplify a ~200 bp fragment of Ddes_1825 DNA for use in EMSAs (Electrophoretic Mobility Shift Assays). The gDNA used as the template was provided by Dr. Ian Cadby, Birmingham University, UK.

2.8.2 Electrophoretic Mobility Shift Assays (EMSA)

Various FNR family proteins (Section 2.7.1 and 2.7.2) were incubated with ~20 fmol of 5'-biotin labelled DNA in EMSA buffer (10 mM Tris-HCl pH 7.5, 50 mM KCl, 0.1 mM EDTA, 1 mM DTT and 5 mM $MgCl_2$). Samples were incubated for 5-10 min at room temperature. Loading buffer 6x (15% ($^{w}/_{v}$) Ficoll 400, 0.25% ($^{w}/_{v}$) Bromophenol blue, 0.25 % ($^{w}/_{v}$) Xylene cyanol and 1x TBE) was added to the samples prior to loading onto a 7.5% ($^{v}/_{v}$) polyacrylamide Tris-glycine gels (see below) while it was running. Electrophoresis was carried out by pre-run for 60 min at 100 V and then for 2 h at 100 V for sample separation. The gels were transferred to nylon membrane, provided by GE Healthcare using cooled 0.5x TBE buffer (see below) at 380 mA for 30 min. UV-light (120 mJ/cm^2 for 60 s) (Amersham) was used to crosslink the DNA to membrane. The Chemiluminescent Nucleic Acid Detection Module kit was used to detect biotin label DNA according to manufacturer's instructions (Thermo Scientific).

7.5% Tris-glycine gels

Acrylamide (30% ($^{w}/_{v}$)	2.5 mL
3 M Tris pH 8.3	1.26 mL
dH_2O	6.1 mL
APS (10% ($^{w}/_{v}$)	100 µl
TEMED	10 µl

Running buffer

Glycine	14.4 g
Tris	3 g
dH_2O to 1 L	

10x TBE

Tris	108 g
Boric acid	55 g
0.5 M EDTA (pH 8.0)	40 mL
dH_2O to 1 L	

Chapter 3

Isolation and biochemical characterisation of *Pseudomonas putida* ANR

3.0 Isolation and biochemical characterisation of *Pseudomonas putida* ANR

3.1 Introduction

Fumarate-Nitrate-Reduction (FNR) proteins are bacterial O_2-sensing transcription factors (Green *et al*., 2001, Sawers, 1999). Most bacteria that possess FNR proteins have only one. For example, *Escherichia coli* has a single *fnr* gene and the corresponding protein is the best-characterised FNR (Section 1.2.2; Spiro and Guest, 1990, Unden and Trageser, 1991). Like *E. coli*, *Pseudomonas aeruginosa* possesses a single *fnr* gene, designated *anr* for anaerobic nitrate regulator (Zimmermann *et al*., 1991). *Pseudomonas aeruginosa* ANR is active under low O_2 tensions and like *E. coli* FNR, possesses an O_2-sensitive [4Fe-4S] cluster that must be present to bind DNA and regulate gene expression (Yoon *et al*., 2007, Galimand *et al*., 1991, Ye *et al*., 1995). The *P. aeruginosa* ANR protein is 51% identical to *E. coli* FNR (Zimmermann *et al*., 1991). This includes conservation of the N-terminal cysteine-rich motif (Cys-20, 23, 29, 122; FNR numbering) that coordinates the iron-sulfur clusters and amino acids in the DNA-binding domain (Glu-209, Ser-212 and Arg-213; FNR numbering) that mediate sequence specific binding at an FNR box (TTGATNNNNATCAA) (Zimmermann *et al*., 1991, Winteler and Haas, 1996). The *P. aeruginosa* ANR protein plays an important role during adaptation to micro-aerobic growth, denitrification, induction of arginine deiminase, early stage biofilm development, synthesis of Type III secretion systems (T3SS) and fimbriae assembly factors (Vander Wauven *et al*., 1984, Vallet-Gely *et al*., 2007, Schreiber *et al*., 2007, Ugidos *et al*., 2008, O'Callaghan *et al*., 2011, Tribelli *et al*., 2013).

Unlike *E. coli* and *P. aeruginosa*, *P. putida* KT2440 possesses three FNR homologues (Jervis *et al*., 2009, Nelson *et al*., 2002). The three *P. putida* FNR proteins, ANR (PP_4265), PP_3233 and PP_3287 all retain the N-terminal cysteine cluster found in *E. coli* FNR and the three amino acids that interact with the FNR box with the exception of PP_3287, which has a Cys residue in place of Ser-212 (FNR numbering) (Figure 3.1). The *P. putida* ANR protein is 53% identical (76% similar over 226 amino acids) to *E. coli* FNR and 88% identical (94% similar over 244 amino acids) to *P. aeruginosa* ANR, but it has not previously been characterised. The work described in this chapter was undertaken to better understand the reasons why *P. putida* has three FNR proteins by initially determining the properties of the ANR protein to establish whether it operates as a *bona fide* O_2-sensitive regulatory protein like *E. coli* FNR and *P. aeruginosa* ANR.

3.2 Aerobic overproduction and purification of ANR

3.2.1 GST-ANR purification

ANR was overproduced aerobically with a Glutathione *S*-Transferase (GST) tag at the N-terminal and purified by affinity chromatography using Glutathione Sepharose™ 4B (GE Healthcare). Plasmid pGS2268 (Table 2.2; Figure 3.2) was purified and used to transform JRG5302 (Table 2.1). The cells were grown aerobically (1-5 L of broth culture) as described in Section 2.6.3. The cell pellets were resuspended in 10 mL of 25 mM HEPES containing 100 mM NaCl, 100 mM $NaNO_3$, 2.5 mM $CaCl_2$, pH 7.5 and sonicated according to Section 2.6.4. SDS-PAGE analysis (Section 2.6.2) showed a species at ~54 kDa corresponding to GST-ANR protein in the soluble fractions (Figure 3.3, lane 2), which suggested that the GST-ANR could be purified by affinity chromatography using Glutathione Sepharose 4B (GE Healthcare) and on column thrombin cleavage to release ANR (Section 2.6.5). Figure 3.3, lane 3 shows one species of purified ANR with molecular mass ~28 kDa. The purification provided 65-100 µM pure ANR. Glutathione (Sigma), 10 mM, (25 mM HEPES, 100 mM NaCl, 100 mM $NaNO_3$, 2.5 mM $CaCl_2$, pH 7.5) was used to strip the GST-tag (~26 kDa) from the column (Figure 3.3, lane 4).

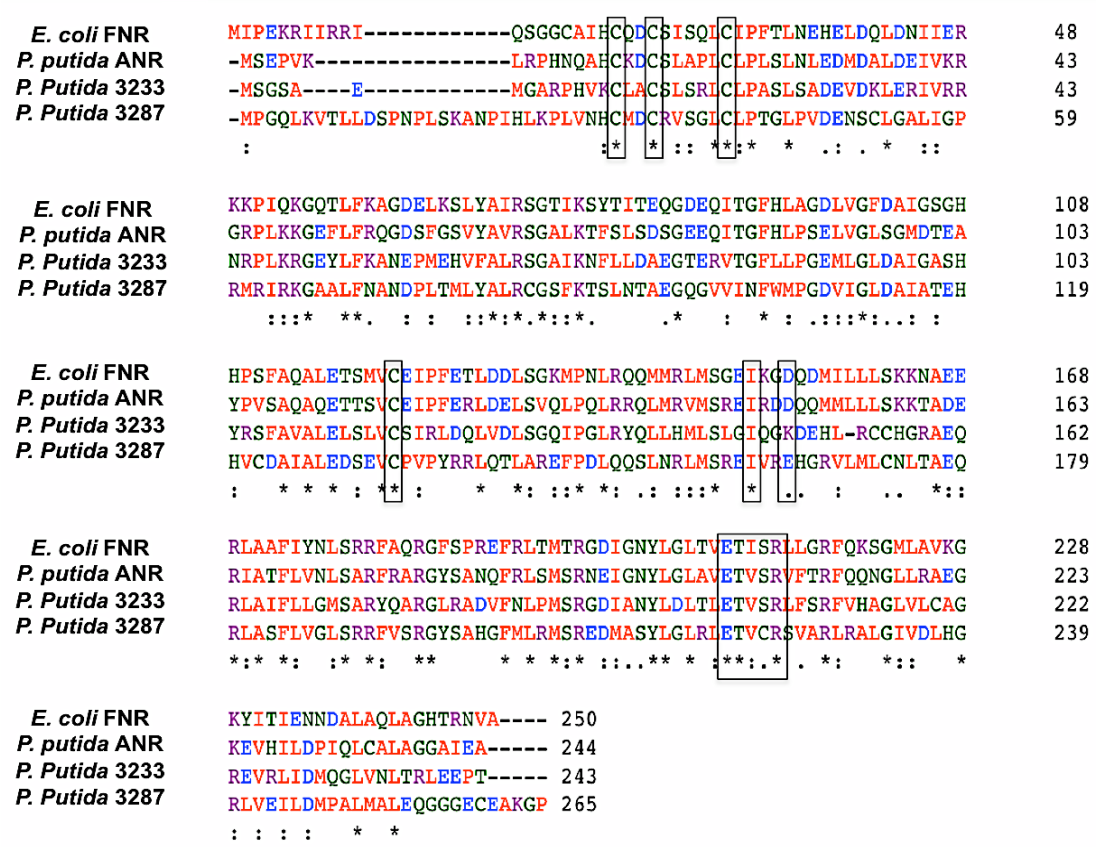

Figure 3.1: Sequences alignment of *P. putida* FNR proteins and the *E. coli* FNR protein. Alignment of *E. coli* FNR and *P. putida* ANR, PP_3233 and PP_3287 proteins by clustal Omega (Sievers *et al*., 2011). The four cysteine residues coordinate the FNR iron-sulfur cluster, Asp-154 and IIe-151 in dimerization helix, the DNA binding motive (black squares), residues that are identical in all four proteins (*), residues with strongly similar properties (:) and residues with weakly similar properties (.) are indicated.

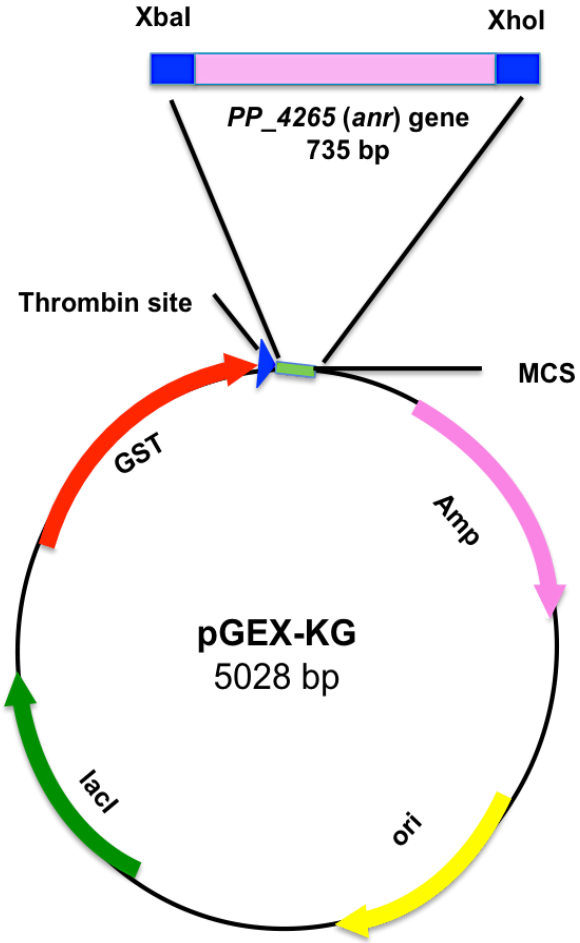

Figure 3.2: Schematic diagram of pGS2268 plasmid. The *anr* open reading frame (~ 700 bp) was amplified from *P. putida* genomic DNA with engineered flanking XbaI/XhoI restriction sites. The DNA fragment was ligated into p547 (pGEX-KG) to generate pGS2268, which encodes a GST-ANR fusion protein (Table 2.2).

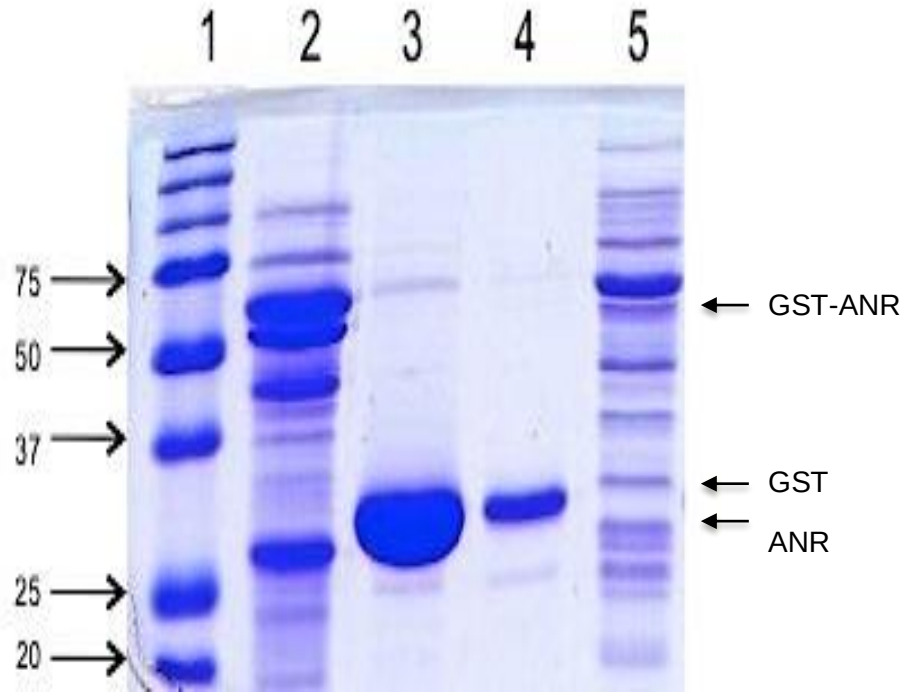

Figure 3.3: Aerobic purification of GST-ANR. Lane1, Precision plus protein standards (sizes in kDa are indicated); Lane 2, soluble protein; Lane 3, purified ANR ~28 kDa released from Glutathione Sepharose by incubation with thrombin (10 units; Section 2.6.5); Lane 4, GST ~26 kDa released by striping the Glutathione Sepharose column with 10 mM glutathione; Lane 5, unbound proteins.

3.2.2 ANR amino acid analysis

The concentration of purified ANR was measured using the Bradford assay as described in Section 2.6.1 (Bradford, 1976). Total amino acid analysis was used to obtain accurate measurement of ANR concentration allowing the calculation of a correction factor, which can be applied to all Bradford assays. A sample of ANR protein was purified as described (Section 2.6.3) and the concentration was measured by Bradford assay (Section 2.6.1). After that the same ANR sample was sent to Alta Biosciences, University of Birmingham for total amino acid analysis (Table S1). Results indicated that the Bradford assay was overestimating ANR concentration and a correction factor of 1.1 was applied to Bradford protein assays.

3.2.3 Gel filtration analysis

Gel filtration chromatography was used to determine the oligomeric state of apo-ANR (Section 2.6.10). The column was calibrated using a set of known molecular weight proteins (Figure 3.4A). Apo-ANR (250 μM) was purified as described in Section 2.6.5 and eluted with 25 mM Tris-HCl, 2 mM EDTA pH 7.5 containing 0.5 M NaCl from the heparin column (GE Healthcare). ANR (250 μM, 50 μl) was applied to the Superdex 200 column (Section 2.6.10), which was equilibrated with 25 mM Tris-HCl pH 7.5 containing 0.5 M NaCl, 2 mM EDTA pH 7.5 and 1 mM azide. Figure 3.5 shows a peak at ~29 min for apo-ANR. To determine the molecular mass of apo-ANR the standard curve was used (Figure 3.4B). An estimate of ~48 kDa was obtained, which corresponded to an apo-ANR dimer (subunit molecular weight is ~28.35 kDa).

A

Standard	MW (kDa)	Retention Time (min)
Blue Dextran	200	15
Haemoglobin	64.5	30
Ovalbumin	45	28
Cytchrome *c*	12.4	33
Aprotinin	6.5	36

B

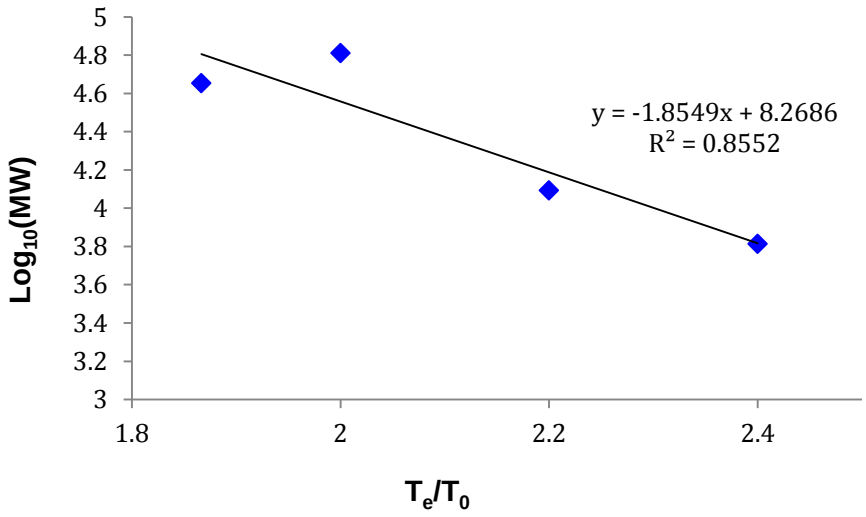

Figure 3.4: Gel filtration calibration curve. (A) Molecular weight of known proteins. List of proteins used to prepare the standard curve. **(B)** Standard curve. Log of molecular weight of known proteins was plotted against the elution time divided by retention time at 15 min.

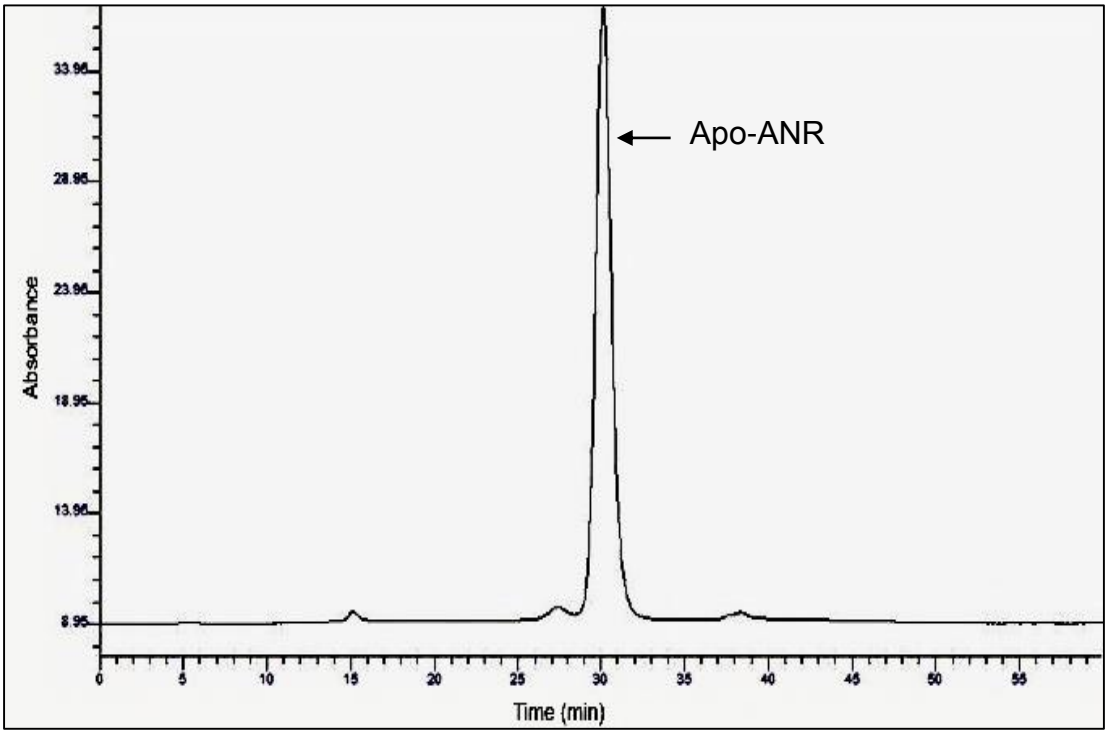

Figure 3.5: Gel filtration of apo-ANR. Apo-ANR (250 µM, 50 µl) was applied to the Superdex 200 column that was equilibrated with 25 mM Tris-HCl pH 7.5 containing 0.5 M NaCl, 2 mM EDTA pH 7.5 and 1 mM azide. The absorbance trace showed a peak corresponding to an ANR dimer.

3.3 Characterisation of the iron-sulfur cluster of ANR

3.3.1 Separation of [4Fe-4S] cluster ANR from reconstitution reaction components by heparin column chromatography

Upon incubation of apo-ANR (Figure 3.6A, blue line) with ferrous ions and L-cysteine and the cysteine desulfurase NifS in the presence of a reducing agent under anaerobic conditions (Section 2.7.1) the colourless protein solution became straw-brown in colour, which is typical of a [4Fe-4S] protein (Green *et al*., 1996a). Heparin chromatography was used to separate protein from other reconstitution reagents (Section 2.7.2). Figure 3.6 shows the UV-visible spectrum after purification of reconstituted ANR using a 1 mL HiTrap heparin column (GE Healthcare).

3.3.2 UV-visible spectrum of holo-ANR is consistent with the presence of a [4Fe-4S] cluster

The UV-visible spectrum of holo-ANR was similar to other [4Fe-4S] proteins (Figure 3.6A; Crack *et al*., 2004). The broad absorption band centred at ~420 nm resembled that of *E. coli* FNR (Crack *et al*., 2008b). The reaction of the iron-sulfur cluster with O_2 was investigated (Section 2.7.6). Spectra of holo-ANR (~6.2 µM) were recorded before (Figure 3.6B, red line) and after (Figure 3.6B, green line) exposure to 10-fold molar excess of air-saturated buffer leading to a decrease in absorbance at 420 nm and an increase at 450-650 nm. These changes are consistent with conversion of a [4Fe-4S] to [2Fe-2S] cluster (Crack *et al*., 2004). Prolonged exposure to air resulted in degradation of the [2Fe-2S] form, yielding apo-ANR that lacked absorption bands in the visible region (Figure 3.6B, black line). Thus, it was concluded that, similar to *E. coli* FNR, ANR is likely to possess an O_2-sensitive [4Fe-4S] cluster that degrades via a [2Fe-2S] cluster to ultimately yield apo-ANR in the presence of air (Crack *et al*., 2008a, Green *et al*., 1991).

3.3.3 Holo-ANR contains a [4Fe-4S] cluster

The straw-brown colour and UV-visible spectrum of holo-ANR were typical of a [4Fe-4S] protein. To validate this assignment, the total amount of iron in a holo-ANR was measured as described (Section 2.7.3). A calibration curve was made using a standard iron solution (Figure 3.7A). Reconstitution reactions for ANR were prepared in triplicate and purified by using heparin chromatography (Sections 2.7.1 and 2.7.2). Bradford assay was used to measure the concentration of the protein (Section 2.6.1) with the correction factor from total amino acid analysis applied and the samples were then subjected to total iron analysis. The ratio of iron to protein was calculated (Figure 3.7B). The average amount of iron in holo-ANR was 4.1 ± 0.3 iron atoms per cluster. Taken together with the spectral data (Figure 3.6A), it was concluded that ANR is likely to be a [4Fe-4S] cluster protein under anaerobic conditions.

The molar extinction coefficient for the protein bound iron-sulfur cluster at 405 nm (ε_{405}) could be estimated for the protein samples used in the iron assay as described in Section 2.7.8, yielding a value of ~18,000 $M^{-1}cm^{-1}$. Typical extinction coefficients for [4Fe-4S] proteins are ~16,000 $M^{-1}\,cm^{-1}$ (Sweeney and Rabinowitz, 1980).

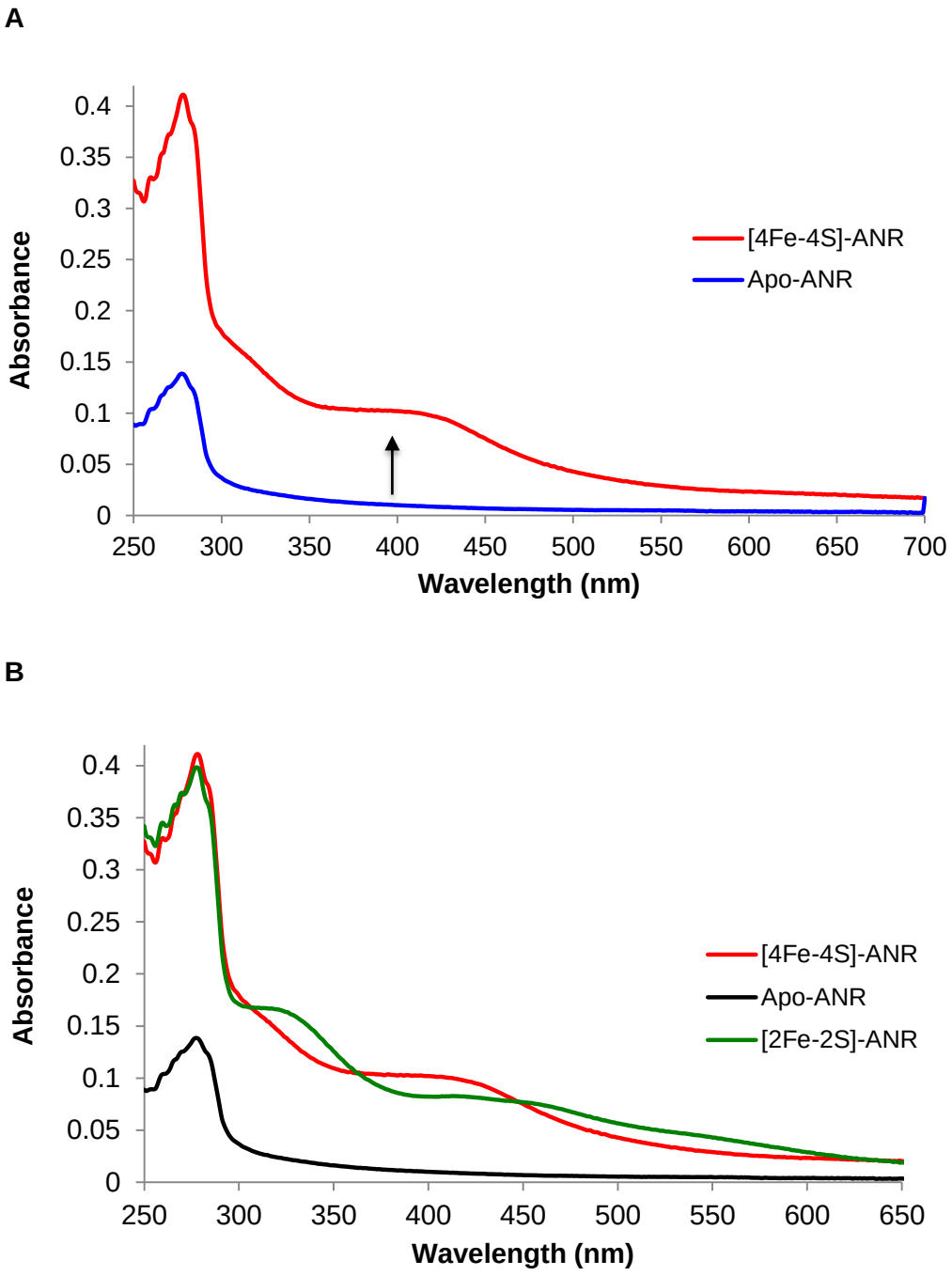

Figure 3.6: Spectral analysis of holo-ANR. (A) Holo-ANR (~6.2 µM cluster) under anaerobic conditions. The spectra are before (blue line) and after (red line) reconstitution. The arrow shows the enhancement in absorbance at 420 nm. **(B)** The [4Fe-4S] cluster of *P. putida* ANR reacts with O_2. Holo- ANR (~6.2 µM cluster, red line) after exposure to 10-fold molar excess of oxygen in air-saturated buffer (green line) and after 16 h exposure to air (black line).

A

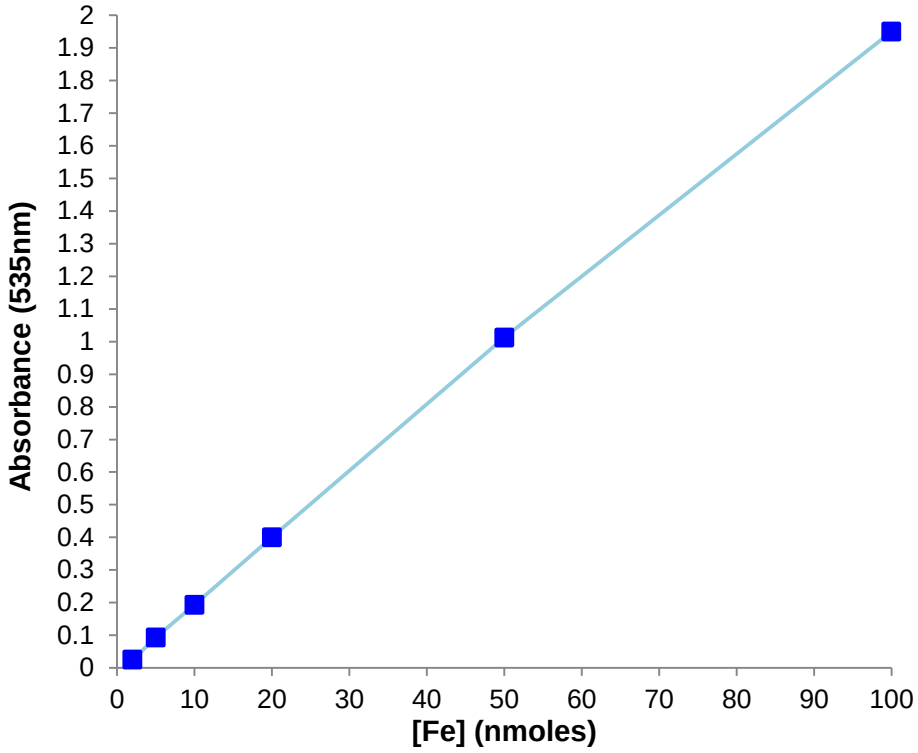

B

ANR (nmoles)	Fe (nmoles)	Ratio of iron to ANR
3.65	13.5	3.7
3.52	15	4.3
3.96	17	4.3

Figure 3.7: Iron content of reconstituted ANR protein. (A) Standard curve of iron measurement. Different concentrations of iron were tested using iron standard solution (iron standard solution, Alfa Aesar) (Section 2.7.3). **(B)** Ratio of iron to ANR. The spectroscopy measurements were used to calculate the iron concentration of the protein samples and the ratio was determined.

3.3.4 The [4Fe-4S] cluster of ANR reacts with two molecules of O_2

The [4Fe-4S] cluster of the *E. coli* FNR protein has been reported to react with between 0.5 and 3 O_2 molecules per cluster (Crack *et al*., 2004, Zhang *et al*., 2012). Reduction of O_2 to water is a 4 electron reaction and therefore 1 O_2 molecule could potentially convert 4[4Fe-4S] clusters to 4[2Fe-2S] clusters (Crack *et al*., 2007). The stoichiometry of the titration of holo-ANR with O_2 under anaerobic conditions at room temperature was achieved by sequential addition of air-saturated buffer (~220 µM O_2) into reconstituted samples as described in Section 2.7.9. The reaction was monitored using a Cary UV-visible spectrometer (Section 2.7.6). Holo-ANR (15.4 µM cluster) was held in a sealed quartz cuvette to maintain anaerobic conditions (Section 2.7.9) in reaction buffer (25 mM Tris-HCl pH 7.5 containing 500 mM NaCl). Air-saturated buffer was injected through the silicon seal of the cuvette in increasing amounts (0-124 µM final concentration). The sample was scanned 10 min after each successive addition. This led to a progressive decrease in the absorbance at 420 nm while values at 500-700 nm increased (Figure 3.8A), as previously described for FNR (Crack *et al*., 2004). The final spectrum indicated that the cluster had been converted to a $[2Fe\text{-}2S]^{2+}$ form. The progressive change at 405 nm as a response to addition of air-saturated buffer was calculated and plotted against the ratio $[O_2]$:[4Fe-4S]. The stoichiometry indicated two molecules of O_2 interacted with one $[4Fe\text{-}4S]^{2+}$ cluster of ANR (Figure 3.8B). These data suggest that the conversion of ANR [4Fe-4S] to the [2Fe-2S] cluster form occurred by the same mechanism as described for FNR (Crack *et al*., 2004).

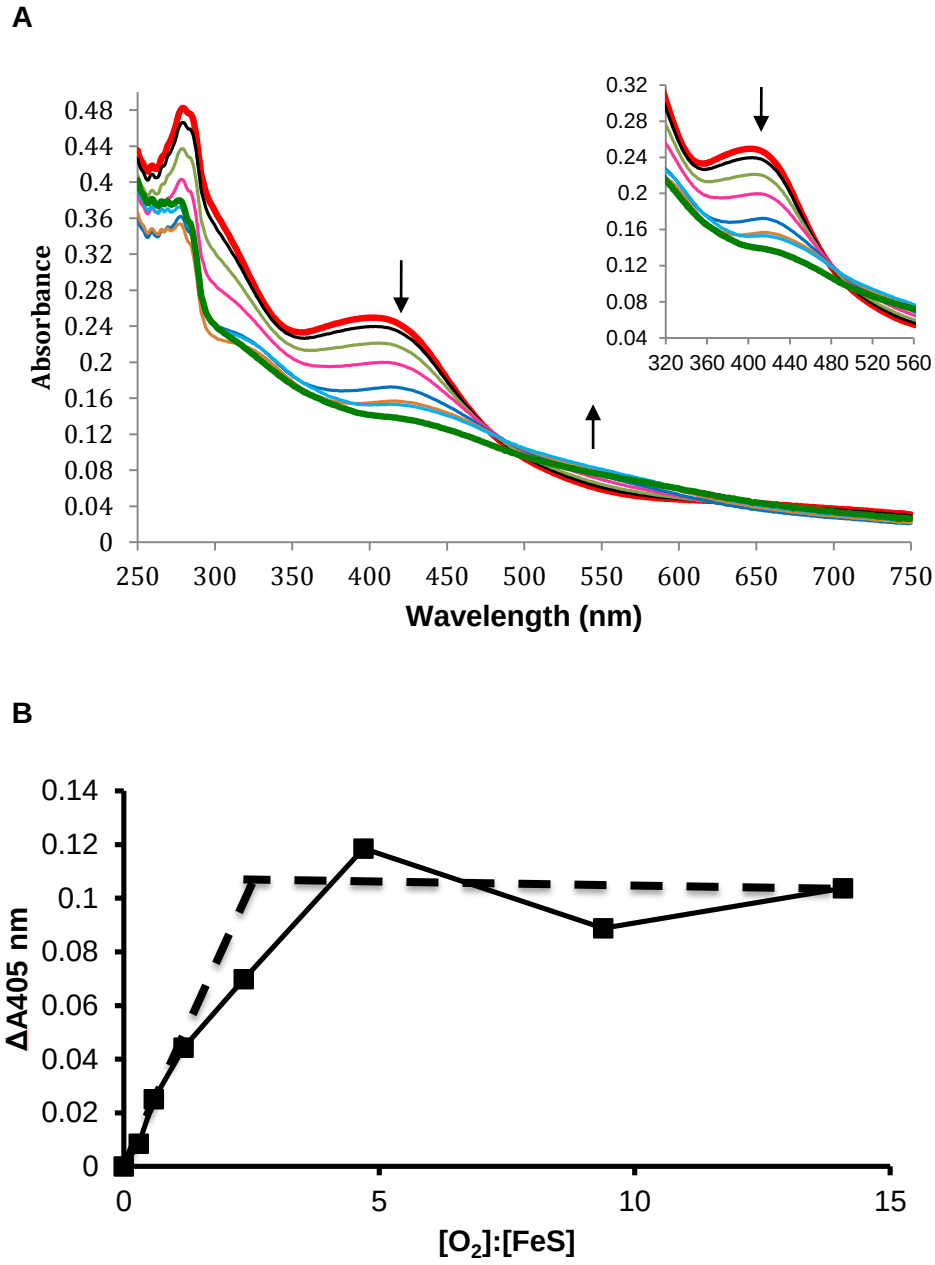

Figure 3.8: Titration of holo-ANR with O_2. (A) Holo-ANR (15.4 µM cluster) was exposed to increasing concentrations of O_2 in air-saturated buffer. The final concentrations were 0.0, 4.3, 8.5, 16.3, 30.3, 53.3, 85.85, 107.75, and 124 µM. The sample was incubated at room temperature for 10 min after each addition before measurement of the spectra. The arrows show the decreasing absorbance at 420 nm and increasing absorbance at 550 nm. **(B)** Changes in absorbance at 405 nm were plotted versus the total concentration of O_2 divided by the concentration of [4Fe-4S] cluster.

3.3.5 Circular dichroism (CD) spectroscopy

CD spectroscopy was used to monitor the reaction of ANR with O_2 as described in Section 2.7.4. The reaction was carried out on holo-ANR (29.8 μM cluster) in collaboration with Dr. Jason Crack, University of East Anglia (Section 2.7.4). Results showed that in the absence of O_2, the [4Fe-4S]-ANR CD spectrum displayed four positive bands at 296, 325, 375 and 420 nm (Figure 3.9A, solid line), which is similar to FNR from *E. coli* (Figure 3.9B; Crack *et al*., 2004). Following exposure to a 2-fold molar excess of O_2, supplied as air-saturated buffer, these bands for anaerobic holo-ANR were replaced by a broad spectrum with two positive bands at 325 nm and 450 nm, and one negative band at 375 nm (Figure 3.9A, dashed line). The observed changes are similar to those observed for the O_2-induced [4Fe-4S] to [2Fe-2S] transition in FNR (Figure 3.9B; Crack *et al*., 2004).

3.3.6 ANR $[4Fe\text{-}4S]^{2+}$ to $[3Fe\text{-}4S]^{1+}$ cluster conversion is an O_2-dependent oxidation

The reaction below was used as a model for the reaction of ANR $[4Fe\text{-}4S]^{2+}$ clusters with O_2 (Sutton *et al.,* 2004).

$$O_2 + \text{ANR} \underset{k_{-1}}{\overset{k_1}{\rightleftharpoons}} O_2 . \text{ANR} \xrightarrow{k_2} \text{Product}$$

The A_{420} decay for ANR fusion upon exposure to O_2 was measured using a Cary UV-visible spectrometer (Section 2.7.6). The reaction was initiated by injecting air-saturated buffer (~110 μM O_2) into sealed anaerobic cuvettes containing holo-ANR (~8.0 μM cluster) at 25°C (Section 2.7.9). The change at 420 nm was used to observe cluster conversion (Figure 3.10). The data were fitted by Dr. Jason Crack, University of East Anglia (Section 2.7.9). The data were best fitted to a double-exponential function. The observed rate constant (k_{obs}) for the first reaction was 0.034 ± 0.007 s^{-1} (Figure 3.10). Division of the observed rate constant by the O_2 concentration provided an estimate of the apparent second order rate constant for the reaction: 309 $M^{-1}s^{-1}$ for ANR. This value indicated that the [4Fe-4S] cluster of ANR displays similar sensitivity to that previously reported for *E. coli* FNR (278 $M^{-1}s^{-1}$) (Crack *et al*., 2007, Jervis *et al*., 2009).

The kinetic analysis suggested a two-step mechanism for the reaction of ANR [4Fe-4S]$^{2+}$ with O_2 *in vitro*. Based on work with *E. coli* FNR the initial step is the O_2-dependent oxidation of the [4Fe-4S]$^{2+}$ cluster followed by an O_2-independent slower conversion to a [2Fe-2S]$^{2+}$ cluster (Crack *et al*., 2007, Jervis *et al*., 2009).

Holo-ANR was exposed to various concentrations of O_2 as aliquots of air-saturated buffer to test this two-step reaction mechanism. The declines at 420 nm were measured (Figure 3.11A; Section 2.7.6) and the data were fitted to a double exponential function by Dr. Jason Crack, University of East Anglia (Section 2.7.9). A plot of k_{obs} against O_2 concentration was linear, which suggested that the conversion from [4Fe-4S]$^{2+}$ to the [3Fe-4S]$^{1+}$ intermediate is O_2-dependent (Figure 3.11B) with a second-order rate constant of k_1 ~309 $M^{-1}s^{-1}$ (Figure 3.10) compared to previously reported value of ~278 $M^{-1}s^{-1}$ for FNR (Jervis *et al*., 2009).

3.3.7 LCMS study of the [4Fe-4S]$^{2+}$ to [2Fe-2S]$^{2+}$ cluster conversion in ANR

Zhang *et al*. (2012) indicated that in response to O_2, [4Fe-4S] cluster of FNR converts to [2Fe-2S] cluster with the retention of bridging sulfide by formation of cysteine persulfide-liganded [2Fe-2S] cluster. LCMS was used to investigate ANR [4Fe-4S] cluster conversion to [2Fe-2S] cluster as a result of exposure to O_2 by Dr. Jason Crack, University of East Anglia (Section 2.7.5). In LCMS analysis, ANR was observed to have a molecular mass of 28,343 Da, indicative of the presence of two disulfide bonds (Figure 3.12, dashed line). A series of peaks at +32 mass units higher than apo-ANR, were indicative of S^0 adducts (+32 mass, 0.24 relative intensity). Upon exposure to a 2.8-fold molar excess of air-saturated buffer as described in Section 2.7.5, the relative intensity of these peaks increased (+32 mass, 0.65 relative intensity), implying cluster sulfide liberated during the [4Fe-4S] to [2Fe-2S] cluster conversion was retained by ANR in the form of persulfides (Figure 3.12, solid line). Thus, it was concluded that the reaction of the [4Fe-4S] cluster with O_2 proceeds via the same mechanism as that described for FNR, including the retention of cluster sulfide (Zhang *et al*., 2012).

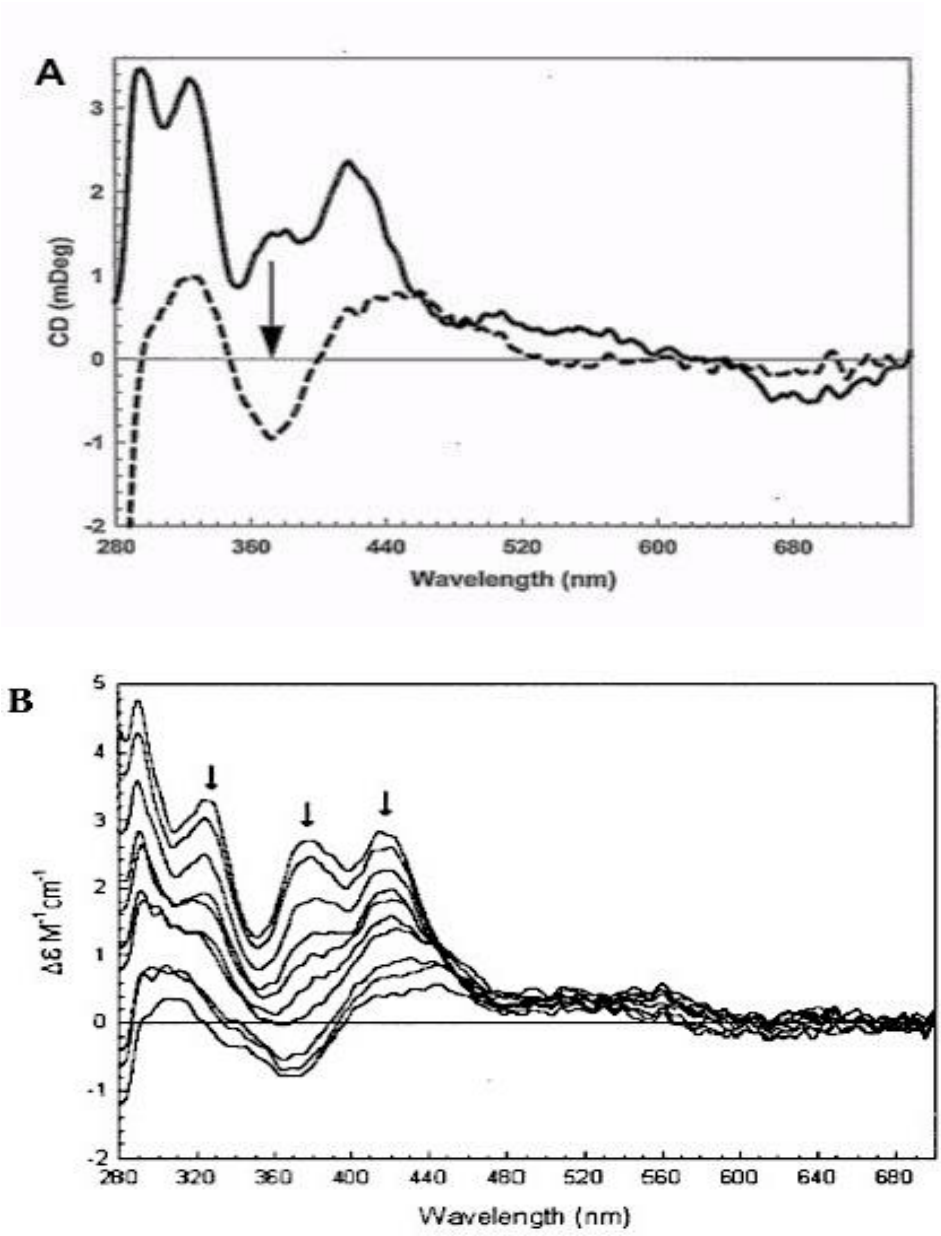

Figure 3.9: Analysis of $[4Fe\text{-}4S]^{2+}$ to $[2Fe\text{-}2S]^{2+}$ cluster conversion using CD spectroscopy. (A) CD spectra of [4Fe-4S]-ANR (29.8 μM cluster) before (solid line) and after (dashed line) exposure to O_2 (~2-fold molar excess). Arrow indicates the movement of spectral features in response to O_2. **(B)** CD spectra of [4Fe-4S]-FNR (30.8 μM cluster) from Crack *et al*. (2004), to show the similar features to ANR.

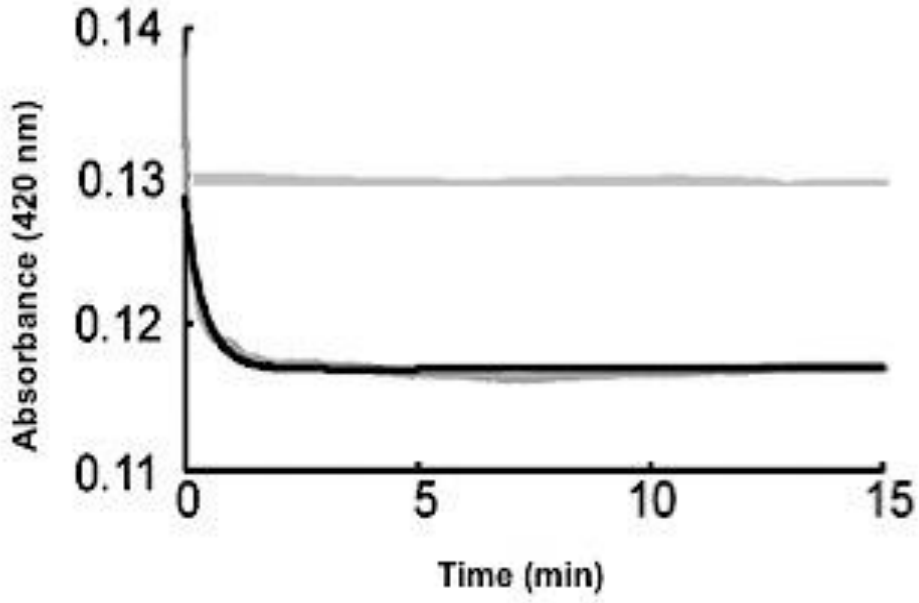

Figure 3.10: Reaction of holo-ANR with O_2. Holo-ANR (~8.0 µM cluster) was reacted with ~110 µM of air-saturated buffer at 25°C. The reaction buffer was 25 mM HEPES, 100 mM NaCl, 100 mM $NaNO_3$, pH 7.5. The data are shown as grey line and the fitting as black line. The upper data set (not fitted) shows the response when anaerobic buffer was used in place of aerobic buffer.

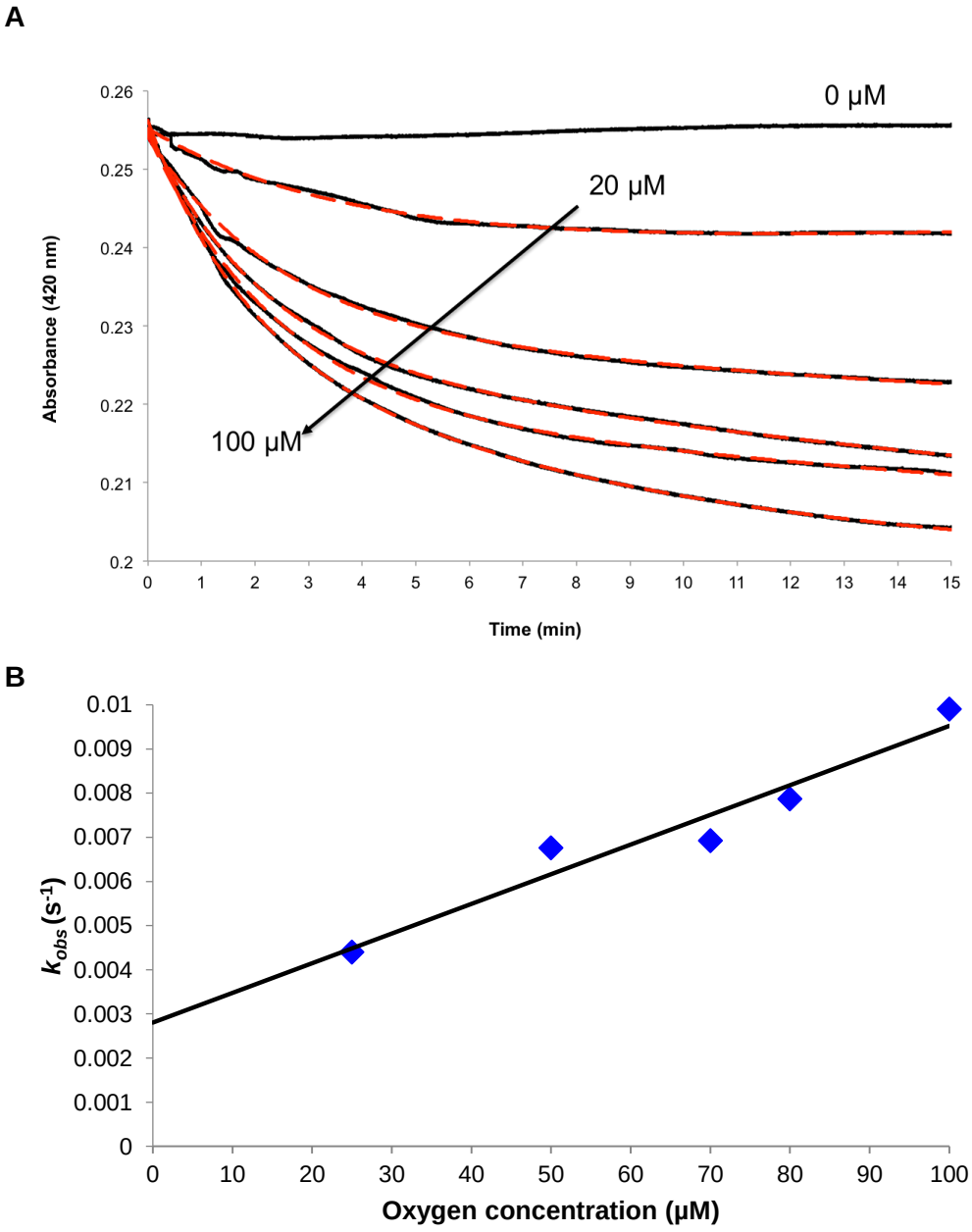

Figure 3.11: Kinetic reactions of [4Fe-4S]$^{2+}$ cluster of ANR. (A) Holo-ANR (~8.0 µM cluster) was mixed with various concentrations of air-saturated buffer (0, 25, 50, 70, 80 and 100 µM) at room temperature. The arrow indicates the increasing concentrations of O_2. The data are shown as black lines and double-exponential function fits are shown as red lines. **(B)** A plot of first order rate constants from A, as a function of the concentration of the O_2.

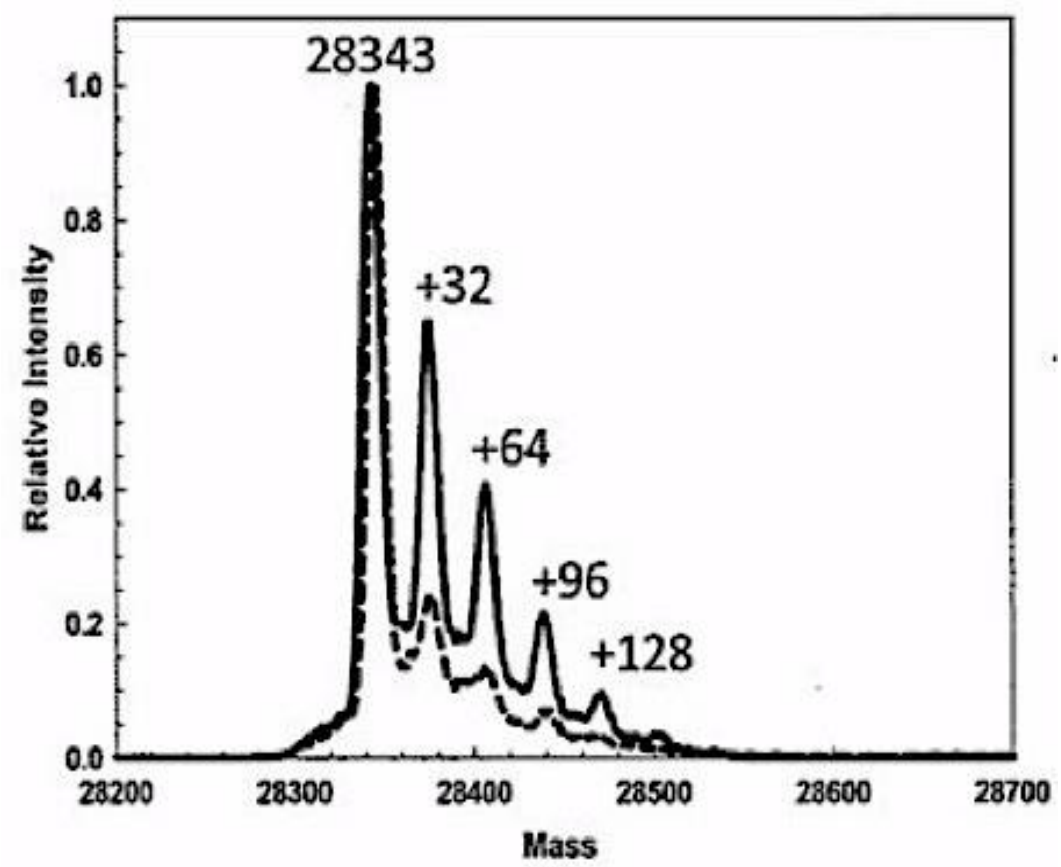

Figure 3.12: LCMS spectra of holo-ANR. Holo-ANR (20 µl, 80 µM cluster) before (dashed line) and after (solid line) exposure to air-saturated buffer (2.8-fold molar excess). The peak at 28343 Da corresponds to the monomer molecular ion peak of ANR, with two disulfide bonds, and the peaks at +32, +64, +96, +128 Da correspond to the addition of one, two, three and four covalently bound sulfur atoms, respectively. The predicted mass of ANR is 28,347 Da.

3.3.8 Repair of cysteine persulfide-ligated $[2Fe\text{-}2S]^{2+}$ ANR under anaerobic conditions

Zhang *et al.* (2012) showed that *E. coli* FNR has the ability to retain cluster sulfide after exposure to O_2 and form a cysteine persulfide-ligated [2Fe-2S] cluster. Here, ANR has also been shown to retain cluster sulfide after reaction with O_2 (Figure 3.12). This retention of cluster sulfide as S^0 has implications for the repair of [4Fe-4S] clusters under anaerobic conditions (Zhang *et al*., 2012). The $[2Fe\text{-}2S]^{2+}$ to $[4Fe\text{-}4S]^{2+}$ cluster conversion for ANR under anaerobic conditions was accomplished with a sample of $[2Fe\text{-}2S]^{2+}$ ANR (~60 µM cluster), which was prepared by exposing $[4Fe\text{-}4S]^{2+}$ cluster to air-saturated buffer (~220 µM O_2) for 30 min as described in Section 2.7.7. A heparin column was used to remove the degradation products as described in Section 2.7.2 to obtain [2Fe-2S] ANR (Figure 3.13, black line). Addition of 3 mM DTT and ferrous iron under anaerobic conditions showed ~64% yield of [4Fe-4S] cluster (Figure 3.13, red line) compared to the initial concentration of $[2Fe\text{-}2S]^{2+}$ cluster. These data show that the $[4Fe\text{-}4S]^{2+}$ to $[2Fe\text{-}2S]^{2+}$ cluster conversion is reversed by adding 4-fold molar excess of Fe^{2+} under reducing conditions without exogenous sulfide. This suggests that the cluster repair mechanism suggested for *E. coli* FNR is shared by other members of this family of transcription factors (Zhang *et al*., 2012).

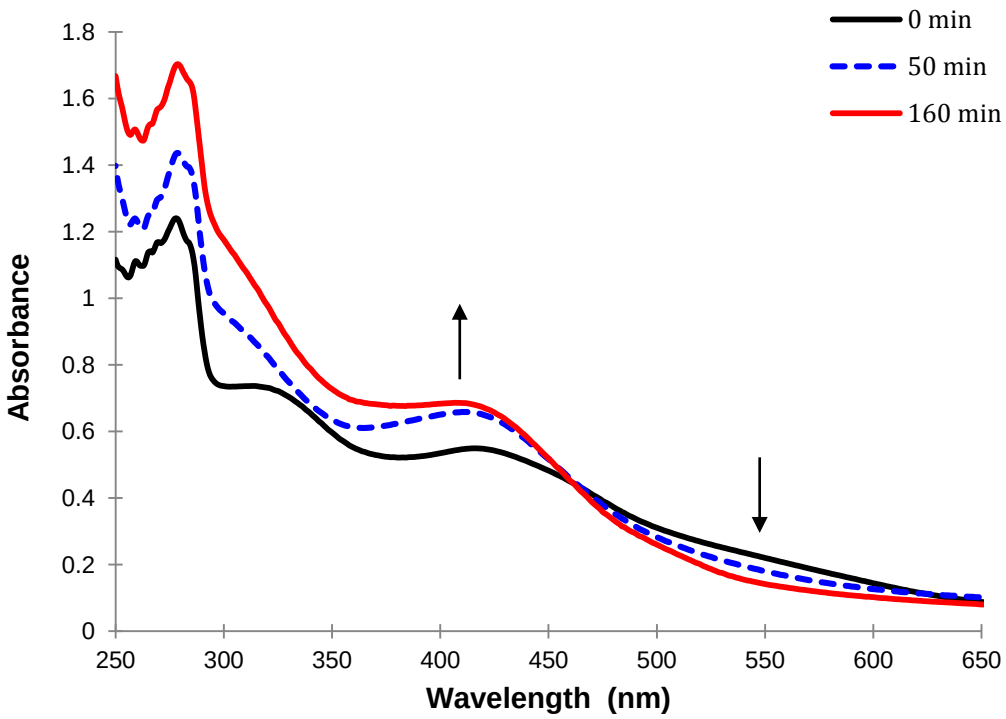

Figure 3.13: Repair of cysteine persulfide-ligated $[2Fe\text{-}2S]^{2+}$ ANR under anaerobic conditions. UV-visible spectra showing the $[4Fe\text{-}4S]^{2+}$ to $[2Fe\text{-}2S]^{2+}$ cluster conversion was reversed by adding 4-fold molar excess of Fe^{2+} under reducing conditions without exogenous sulfide. Blue line after 50 min, red line 160 min after iron addition.

3.4 The DNA binding properties of ANR

The conservation of amino acids in the DNA recognition helix of ANR suggested that it should bind at an FNR site (FF) (Figure 3.1). Electromobility shift assays (EMSAs) (Section 2.8.2) were used to investigate the ability of the ANR protein to recognise and bind to DNA sequences, which were the FF site (TTGAT - - - - ATCAA, FNR binding site), CC site (GTGAT - - - - ATCAC; CRP binding site), NN site (TCTGA - - - - ATCAG; FNR and CRP cannot recognise this site) (Figure 3.14; Green *et al*., 1996c), biotin-labelled DNA was amplified using PCR and biotin-labelled M13 primers as described in Section 2.8.1.

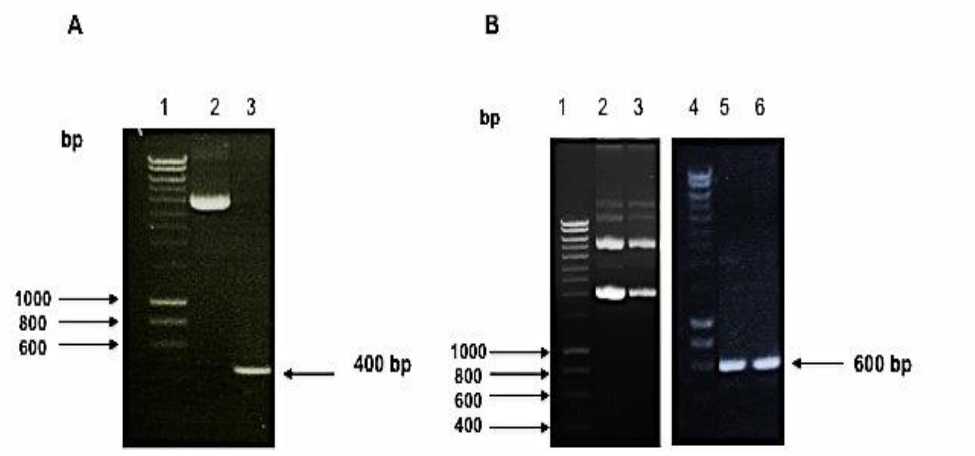

Figure 3.14: Agarose gel showing amplified DNA for EMSAs. (A) pGS422 plasmid (Table 2.2): Lane 1, Hyperladder I (1kb); Lane 2, uncut DNA plasmid; Lane 3, PCR product (FF site). **(B)** Plasmids pGS649 and pGS652 (Table 2.2): Lanes 1 and 4, Hyperladder I (1kb); Lanes 2 and 3 uncut DNA of pGS649 and pGS652 respectively. Lanes 5 and 6 PCR products, which are: CC site and NN site respectively.

PCR products of 400 bp for the FF site and 600 bp for CC site and NN site were produced. The concentration of PCR products were measured using the Nanodrop 1000 spectrophotometer (Section 2.5.4) and diluted to ~20 fmole for the EMSAs.

3.4.1 Holo-ANR binding to FF site is enhanced under anaerobic conditions

EMSAs were carried out to discover the binding capability of holo-ANR to different DNA sequences (Figure 3.14). Increasing concentrations of holo-ANR (0, 100, 200, 400, 800, 1000 and 1600 nM) were incubated with ~ 20 fmole of biotin-labelled DNA sequences (Figure 3.14; Section 2.8.2) under anaerobic conditions. The protein-DNA complexes were then separated from free DNA using 7.5% polyacrylamide Tris-glycine gels (Section 2.8.2). Figure 3.15A indicated that holo-ANR (800 nM) could recognise the FF site. However, holo-ANR appeared not to bind to the CC site (Figure 3.15B; Section 3.4) or the NN site (Figure 3.15C; Section 3.4). This is similar to *E. coli* FNR which specifically binds to the FF site (Lodge *et al*., 1990).

3.4.2 Apo-ANR does not bind to the FF site

Apo-ANR could not recognise the FF site (Figure 3.16) under anaerobic conditions. This result indicated that the ANR iron-sulfur cluster is required for DNA-binding, implying that under aerobic conditions ANR is inactive. This is similar to *E. coli* FNR, which is inactive under aerobic conditions, and cannot regulate target genes or bind to target DNA sequences (Green *et al*., 1996a, Khoroshilova *et al*., 1997).

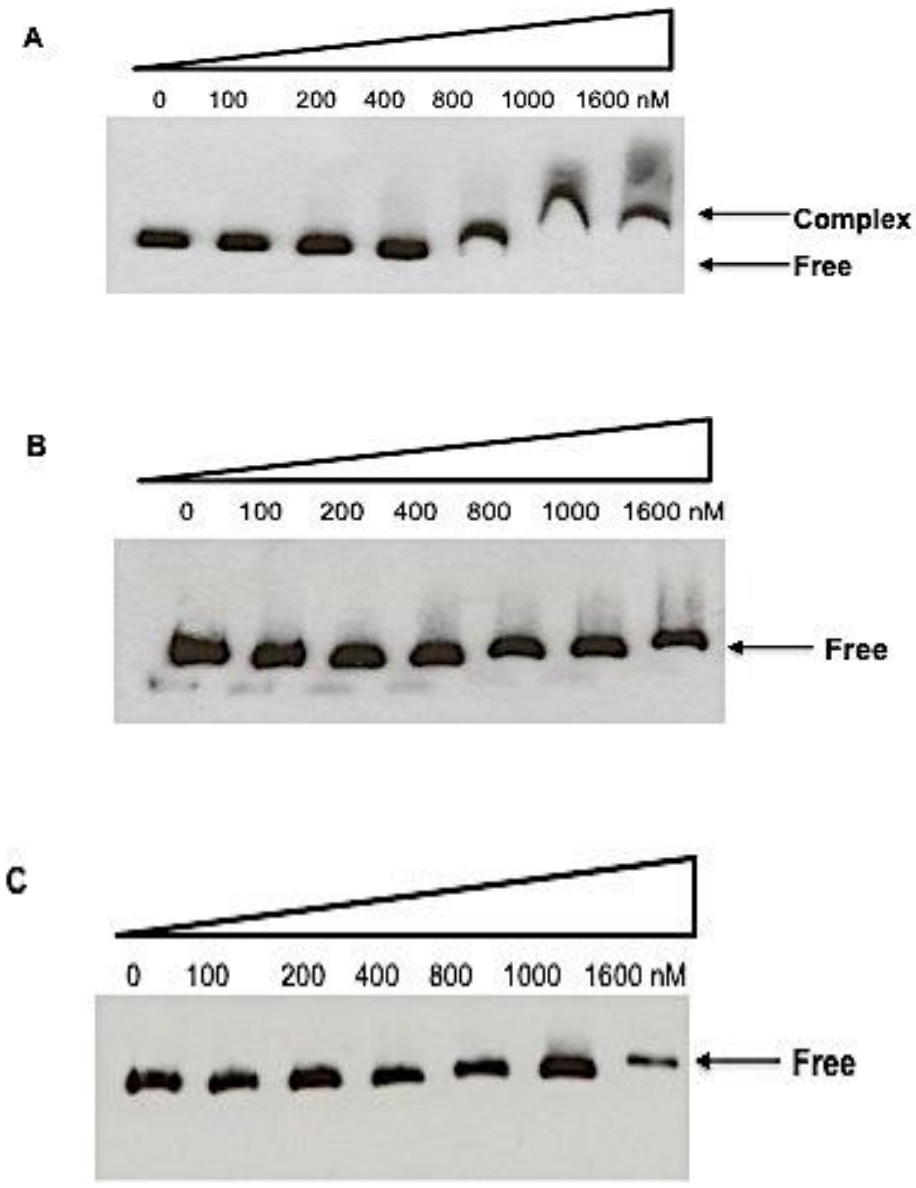

Figure 3.15: The binding of holo-ANR to different DNA sequences under anaerobic conditions. Increasing concentrations of holo-ANR (0, 100, 200, 400, 800, 1000 and 1600 nM) were incubated with ~20 fmol of biotin-labelled DNA that contained FF site (A), CC site (B), NN site (C) (Figure 3.14; Section 3.4) prior to gel electrophoresis to separate free and bound DNA fragments.

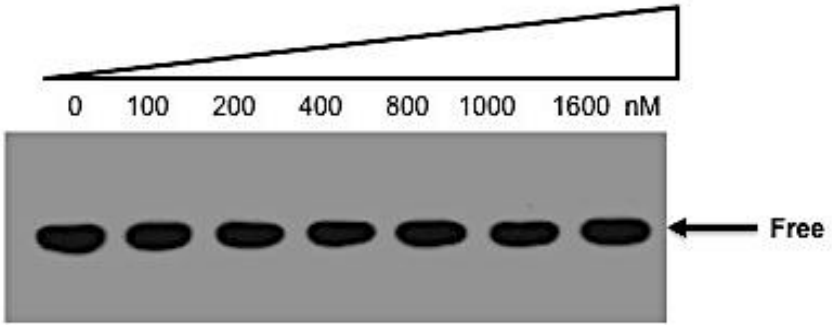

Figure 3.16: The binding of apo-ANR to the FF site under anaerobic conditions. Apo-ANR protein (0, 100, 200, 400, 800, 1000 and 1600 nM) was incubated with biotin-labelled DNA that contains the FF site ~20 fmol (Figure 3.14; Section 3.4) prior to gel electrophoresis.

3.5 Discussion

In vitro characterisation of *P. putida* ANR indicated that it acts as an O_2-sensitive DNA-binding protein. The reaction of the ANR [4Fe-4S] cluster with O_2 proceeded via a similar mechanism as that described for *E. coli* FNR (Crack *et al*., 2004, Crack *et al*., 2007). However, unlike apo-FNR, apo-ANR eluted from a gel filtration column as a dimer (Figure 3.5 and 3.17).

Apo-FNR is a monomer (~30 kDa; Figure 3.17) because no salt bridge could form. However, apo-ANR is a dimer similar to apo-CRP that is a dimer because of salt bridges interaction involving Arg-122, Glu-77 and Glu-78 according to CRP numbering (Popovych *et al*., 2009). The alignment results showed that Arg-122 and Glu-78 are conserved in ANR, but not in FNR suggesting that a salt bridge can from between Arg-122 and Glu-78 according to CRP numbering and affect the oligomeric state of ANR (Figure 3.18).

Like Apo-FNR, apo-ANR showed features at 280 nm only corresponding to aromatic amino acid absorbance (11 phenylalanine, 4 tyrosine, no tryptophan); (11 phenylalanine, 5 tyrosine, no tryptophan) for FNR (Section 3.3.2; Figure 3.6A). Similar to holo-FNR, ANR after reconstitution was straw-brown in colour with an absorbance band at 420 nm characteristic of [4Fe-4S] cluster. These data suggested that holo-ANR possesses one iron-sulfur cluster per monomer or two per dimer under anaerobic conditions, which is similar to FNR [4Fe-4S] cluster (Lazazzera *et al*., 1996). This observation was confirmed by iron assay indicating 4 Fe per ANR monomer (Section 3.3.3; Figure 3.7). The holo-ANR was exposed to 10-fold molar excess of O_2 as air-saturated buffer (Section 3.3.2; Figure 3.6B). After incubation at room temperature for 20 min, the spectrum showed clear change at 420 nm, indicating that the $[4Fe\text{-}4S]^{2+}$ cluster was converted to $[2Fe\text{-}2S]^{2+}$ cluster (Figure 3.6B). After prolonged exposure to O_2 at room temperature, the spectrum showed conversion of the $[2Fe\text{-}2S]^{2+}$ form to apo-ANR (Figure 3.6B). These data suggest that *P. putida* ANR possesses a [4Fe-4S] cluster under anaerobic conditions. In addition, ANR senses O_2 directly through its iron-sulfur cluster. Previous studies have shown that the FNR iron-sulfur cluster plays a crucial role in enhancing DNA binding under anaerobic conditions and replacement of amino acid residues adjacent to cluster coordinating cysteine residues can have profound effects on the reactivity of the *E. coli* FNR iron-sulfur cluster with O_2 (Bates *et al*., 2000, Ralph *et al*., 2001, Jervis *et al*., 2009).

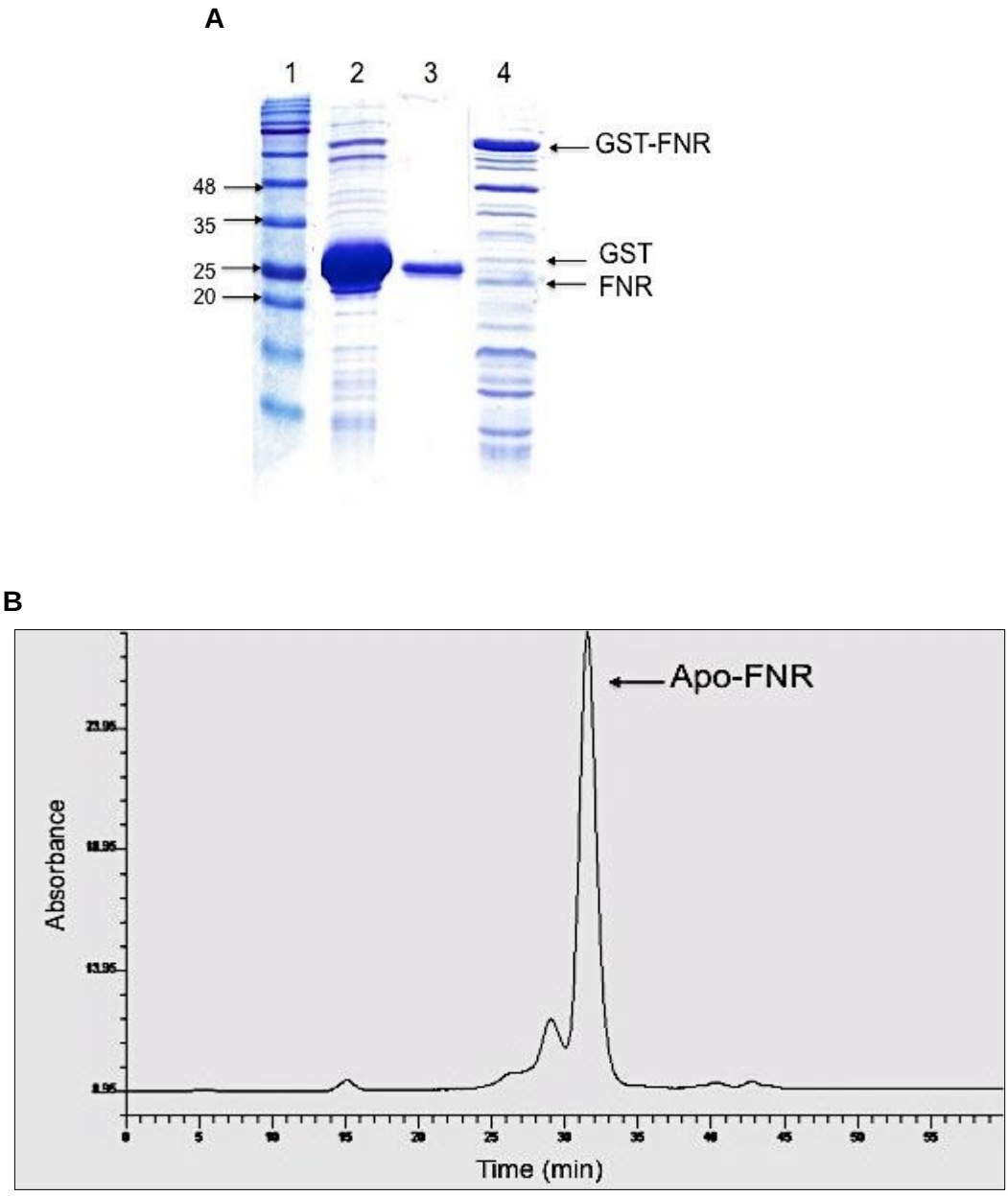

Figure 3.17: Apo-FNR protein. (A) Aerobic purification of GST-FNR. Lane1, Precision plus protein standards (sizes in kDa are indicated); Lane 2, purified FNR ~30 kDa released from Glutathione Sepharose by incubation with thrombin (10 units; Section 2.6.5); Lane 3, GST ~26 kDa released by striping the Glutathione Sepharose column with 10 mM glutathione; Lane 4, unbound proteins. **(B) Gel filtration of apo-FNR.** Apo-FNR (~159 µM, 50 µl) was applied to the Superdex 200 column that was equilibrated with 25 mM Tris-HCl pH 7.5 containing 0.5 M NaCl and 1 mM azide. The absorbance trace showed a peak corresponding to an FNR monomer.

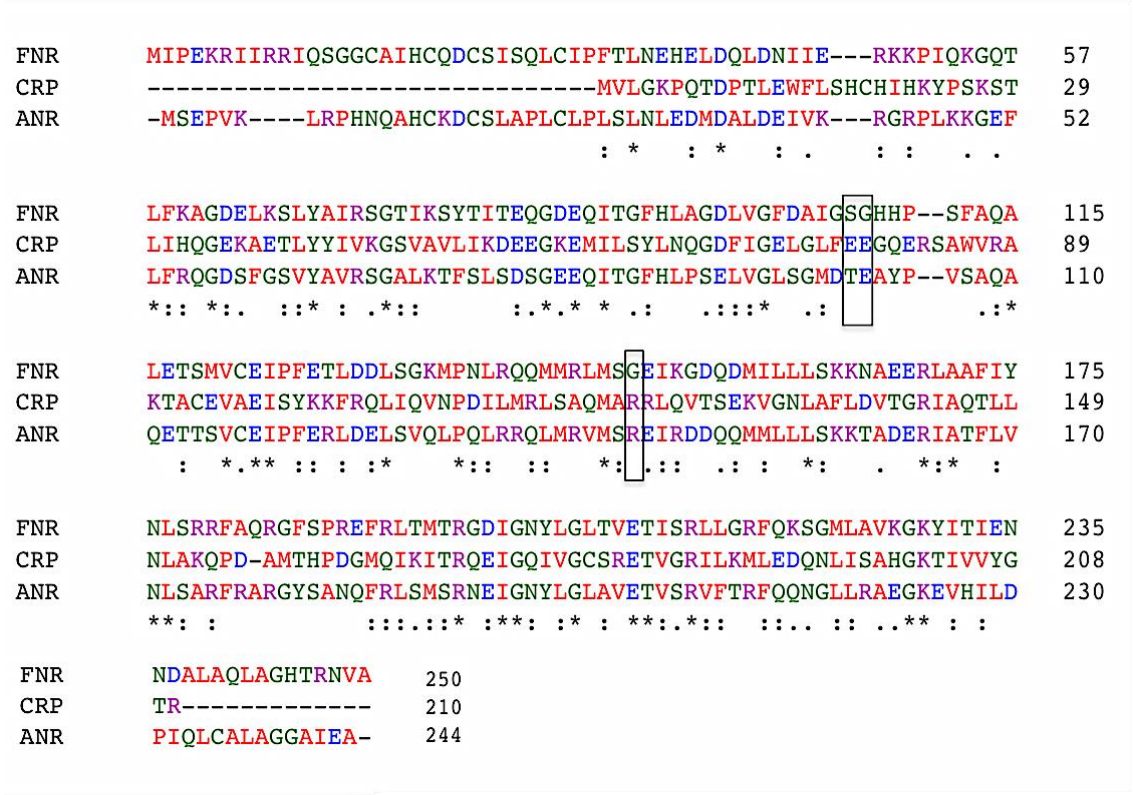

Figure 3.18: Sequences alignment of the *E. coli* FNR and CRP proteins and *P. putida* ANR protein. Alignment of *E. coli* FNR and CRP and *P. putida* ANR protein by clustal Omega (Sievers *et al*., 2011). The Glu-77, Glu-78 and Arg-122 according to CRP numbering are boxed. Residues that are identical in all three proteins (*), residues with strongly similar properties (:) and residues with weakly similar properties (.) are indicated.

The stoichiometric data showed that upon exposure to O_2, $[4Fe\text{-}4S]^{2+}$ cluster of ANR is converted to [2Fe-2S] cluster. This suggests that ANR is inactivated by O_2, which led to conversion of [4Fe-4S] cluster to [2Fe-2S] cluster as a result of oxidation. The results indicated that complete conversion of $[4Fe\text{-}4S]^{2+}$cluster requires two molecules of O_2. This observation is similar to O_2 sensing mechanism that reported previously for *E. coli* FNR (Green *et al*., 1996a, Lazazzera *et al*., 1996, Khoroshilova *et al*., 1997).

The CD spectrum of holo-ANR showed similar features to that previously reported for *E. coli* FNR (Crack *et al*., 2004). Upon exposure to O_2, the CD spectrum showed changes, that were similar to those observed for the O_2 induced [4Fe-4S] to [2Fe-2S] transition in *E. coli* FNR (Figure 3.9B; Crack *et al*., 2004). This suggested that the environment surrounding the [4Fe-4S] cluster of ANR is similar to that surrounding of [4Fe-4S] cluster of FNR.

Kinetic measurements indicated that the *P. putida* ANR showed similar sensitivity to O_2 to that of *E. coli* FNR (Crack *et al*., 2007). As discussed in Section 3.3.6, in response to O_2, the $[4Fe\text{-}4S]^{2+}$ to $[2Fe\text{-}2S]^{2+}$ conversion occurs in two steps via an intermediate species, $[3Fe\text{-}4S]^{1+}$. The first step is O_2-dependent oxidative conversion of [4Fe-4S] to result [3Fe-4S] cluster as intermediate product with one electron oxidation of Fe^{2+} and one electron reduction of O_2 to superoxide, but there is no sulfide oxidation in this step Eq. [3.1].

$$[4Fe\text{-}4S]^{2+} + O_2 \rightarrow [3Fe\text{-}4S]^{1+} + Fe^{2+} + O_2^{-} . \qquad [3.1]$$

The second step of this reaction is a slow O_2-independent step and includes the spontaneous conversion of [3Fe-4S] to [2Fe-2S] FNR and the release one iron and two sulfide ions per cluster Eq. [3.2].

$$[3Fe\text{-}4S]^{1+} \rightarrow [2Fe\text{-}2S]^{2+} + Fe^{3+} + 2S^{2-}. \qquad [3.2]$$

This step involves release of one Fe^{3+} because the $[2Fe\text{-}2S]^{2+}$ and $[3Fe\text{-}4S]^{1+}$ clusters contain two and three Fe^{3+} ions respectively. The sulfide can be retained by FNR via the formation of cysteine persulfide-ligated [2Fe-2S] clusters. The reaction can be written as Eq. [3.3].

$$[4Fe\text{-}4S]^{2+} + nO_2 \rightarrow [2Fe\text{-}2S]^{2+} + Fe^{2+} + Fe^{3+} + O_2^{-} . \qquad [3.3]$$

The [2Fe-2S] cluster is unstable and decays to yield apo-FNR Eq. [3.4].

$[2Fe\text{-}2S]^{2+} \rightarrow [apo] + 2S^{2-} + 2Fe^{3+}$. [3.4] (Figure 3.19; Crack *et al*., 2004, Crack *et al*., 2007, Crack *et al*., 2008a, Green *et al*., 2009, Zhang *et al*., 2012).

LCMS result showed clearly that during the treatment of ANR with air-saturated buffer the [4Fe-4S] cluster converted to [2Fe-2S] cluster with sulfide oxidation to reveal the presence of up to five sulfur adducts (Section 3.3.7; Figure 3.12). This suggested that the product was a [2Fe-2S] cluster with one or two cysteine persulfide ligands. Thus, it was concluded that the reaction of the ANR [4Fe-4S] cluster with O_2 proceeds via the same mechanism as described for FNR, including the retention of cluster sulfide as one (Eq. 3.5 and 3.6) or two (Eq. 3.5 and 3.7) cysteine persulfides (CysSS) (Zhang *et al*., 2012).

$[4Fe\text{-}4S(CysS)_4]^{2-} + O_2 \rightarrow [3Fe\text{-}4S(CysS)_3]^{2-} + CysS^- + O_2^- + Fe^{2+}$. [3.5]

$[3Fe\text{-}4S(CysS)_3]^{2-} + CysS^- + O_2 + 2H^+ \rightarrow [2Fe\text{-}2S(CysS)_3(CysSS)]^{2-} + Fe^{3+} + S^{2-} + H_2O_2$. [3.6]

$[3Fe\text{-}4S(CysS)_3]^{2-} + CysS^- + O_2 + 4H^+ \rightarrow [2Fe\text{-}2S(CysS)_2(CysSS)_2]^{2-} + Fe^{3+} + 2H_2O$. [3.7]

The retention of cluster sulfide as S^0 has implications for the repair of [4Fe-4S] clusters (Zhang *et al*., 2012).

Anaerobic incubation of [2Fe-2S]-ANR with ferrous ions in the presence of the reducing agent DTT regenerated the [4Fe-4S] form, indicated that the cysteine persulfide-ligands bound to [2Fe-2S] cluster were cleaved by DTT and in the presence of Fe^{2+} were re-incorporated into a [4Fe-4S] cluster (Eq. 3.8).

$$[Fe_2S_2(CysS)_2(CysSS)_2]^{2-} + 4e^- + 2Fe^{2+} \rightarrow [Fe_4S_4(CysS)_4]^{2-} \qquad [3.8]$$

This suggested that *P. putida* ANR could repair the [4Fe-4S] cluster in response to cellular O_2 level without need of the ISC pathway. Thus, the mechanism of [4Fe-4S] repair proposed for *E. coli* FNR is likely to be a common feature of this family of regulators and probably other iron-sulfur proteins (Zhang *et al*., 2012).

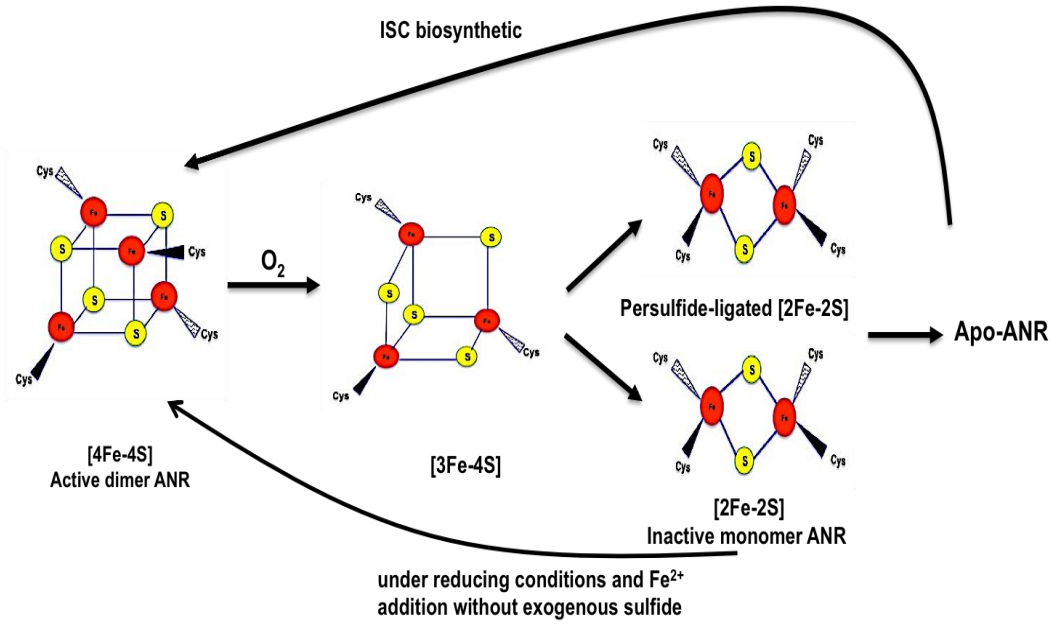

Figure 3.19: Scheme summarising the conversion [4Fe-4S] ANR to apo-ANR in response to O_2. In anoxic conditions, *P. putida* ANR acquires the [4Fe-4S] cluster (iron in red, sulfur of the cluster in yellow, cysteine sulfur). The [4Fe-4S] cluster is stable and is required for site-specific (consensus sequence: TTGAT[N4]ATCAA) DNA-binding. Under aerobic conditions (presence of O_2), the [4Fe-4S] cluster is converted to a [2Fe-2S] cluster via a [3Fe-4S] intermediate. This conversion leads to loss of DNA-binding and conversion to an inactive form. During this process, cluster sulfide is retained to form cysteine persulfide-ligated [2Fe-2S] clusters, which play a crucial role in cluster repair and restoration of the [4Fe-4S] in the presence of Fe^{2+} under reducing conditions without exogenous sulfide. Prolonged exposure to O_2 decomposes the [2Fe-2S] cluster to form apo-ANR. Apo-ANR can acquire a cubic [4Fe-4S] cluster via the iron-sulfur cluster biosynthetic machinery (ISC). Figure adapted from Green *et al*. (2013).

FNR residues Glu-209, Ser-212 and Arg-213 are conserved in *E. coli* FNR and *P. aeruginosa* ANR, which play important role in recognising and binding the FNR box (Lodge *et al*., 1990, Zimmermann *et al*., 1991). The amino acid analysis showed that *P. putida* ANR possesses those residues in C-terminal domain (Figure 3.1). This suggested that *P. putida* ANR protein would recognise and bind to FNR DNA sequence. Here, the EMSA results showed that holo-ANR was capable of specifically binding at an FNR box (FF site; TTGAT[N4]ATCAA) under anaerobic conditions (Figure 3.15A), whereas the apo-ANR was not (Figure 3.16). Thus, it was concluded that ANR is active under anaerobic conditions because it possesses [4Fe-4S] cluster. The iron-sulfur cluster plays important role in enhancement the DNA-binding activity under anaerobic conditions *in vitro* (Khoroshilova *et al*., 1995, Lazazzera *et al*., 1996, Beinert and Kiley, 1999).

On other hand, the holo-ANR could not recognise the CC site (Figure 3.15B), which is CRP protein recognition site and NN site (Figure 3.15C) that FNR and CRP bind very poorly. The EMSA results suggested that The *P. putida* ANR is similar to *E. coli* FNR rather than CRP (Lazazzera *et al*., 1996). Winteler and Hass (1996) have reported that *E. coli* FNR was capable of functionally replacing ANR of *P. aeruginosa* under anaerobic conditions on nitrate pathway (Winteler and Haas, 1996).

To conclude, *P. putida* KT2440 ANR is an O_2-responsive (via assembly and disassembly of its [4Fe-4S] cluster) DNA-binding protein, with similar properties to *E. coli* FNR.

Chapter 4

Isolation and biochemical characterisation of three *Pseudomonas putida* FNR proteins

4.0 Isolation and biochemical characterisation of three *Pseudomonas putida* FNR proteins

4.1 Introduction

Unlike many bacteria, *P. putida* possesses three FNR proteins (PP_4265 (ANR), PP_3233 and PP_3287) (Figure 3.1). As shown in Chapter three, ANR possesses an iron-sulfur cluster that responds to alterations in the concentration of cytoplasmic O_2 via assembly and disassembly of this cluster. In comparison with *E. coli* FNR, PP_3233 is 46% identical, 67% similar over 225 amino acid and PP_3287 is 41% identical, 58% similar over 224 amino acid residues. Moreover, PP_3233 is 44% identical, 65% similar over 223 amino acid residues and PP_3287 is 38% identical, 58% similar over 245 amino acid residues to *P. putida* ANR protein. In addition, PP_3287 is 41% identical, 57% similar over 227 amino acid residues to PP_3233.

The presence of three FNR proteins in *P. putida* suggested that they may have evolved to fulfil distinct but overlapping roles. For example, *P. putida* might use multiple FNR proteins to control gene expression in response to different but overlapping ranges of O_2 concentration. However, the functions and properties of PP_3233 and PP_3287 have not been studied. Here, for the first time PP_3233 and PP_3287 are shown to be iron-sulfur cluster proteins that bind DNA under anaerobic conditions. Although the [4Fe-4S] clusters of PP_3233 and PP_3287 respond to O_2 by disassembly to [2Fe-2S] clusters, these reactions are slower than that of ANR. Thus, it is possible that PP_3233 and PP_3287 extend the range of O_2-responsive gene expression in *P. putida*.

4.2 Aerobic overproduction and purification of *P. putida* ANR, PP_3233 and PP_3287

Several attempts were made to overproduce the *P. putida* PP_3233 and PP_3287 proteins, but they were consistently found as insoluble aggregates when expressed at high levels, except when fused to the C-terminus of the chaperone Trigger factor (Tig). Therefore, PP_3233 and PP_3287 were isolated as Tig fusions and a Tig fusion of ANR was also generated to permit direct comparisons (Section 2.6.8). His_6-Tig-ANR, -Tig-PP_3233 and -Tig-PP_3287 fusion proteins were overproduced aerobically in JRG5302 (Table 2.1) transformed with plasmids pGS2414, pGS2403 and pGS2413 respectively (Figure 4.1; Table 2.2; Section 2.6.6). The cell pellets were resuspended in 10 mL of binding buffer (Section 2.6.8). Lysozyme (200 µg/mL) was added and the suspension was incubated at room temperature for 30 min and then passed three times through a French pressure cell (Section 2.6.7). Tig-ANR, Tig-PP_3233 and Tig-PP_3287 fusions were purified by affinity chromatography as described (Section 2.6.8). Figures 4.2-4.4 show the polypeptide content of fractions eluted from HiTrap chelating columns (GE Healthcare). The fractions were analysed by SDS-PAGE (Section 2.6.2) to confirm the presence of Tig-ANR, Tig-PP_3233 and Tig-PP_3287 proteins with molecular weight ~82 kDa. The purified fractions were desalted into 25 mM HEPES, 100 mM NaCl, 100 mM $NaNO_3$ pH 7.5 (Section 2.6.8). The concentrations of the protein samples were estimated using the Bradford assay (Section 2.6.1).

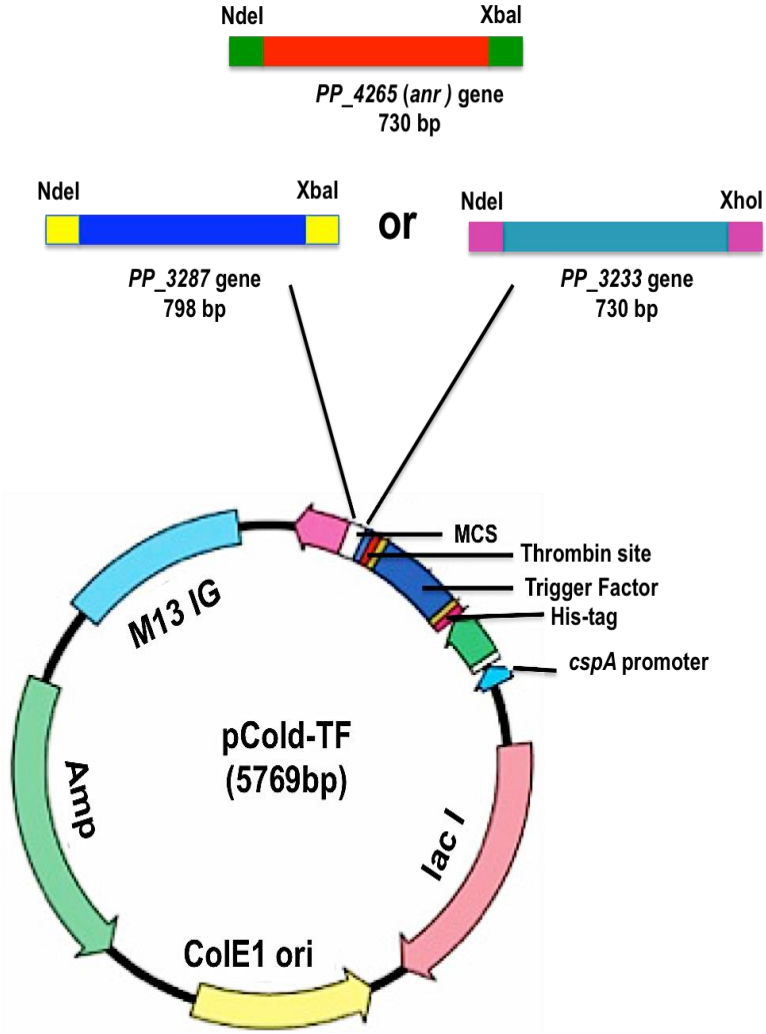

Figure 4.1: Plasmid construction. The *PP_4265* (*anr*), *PP-3233* and *PP-3287* genes were amplified from *P. putida* genomic DNA with flanking restriction sites for NdeI/XbaI, NdeI/XhoI and NdeI/XbaI respectively. The *anr*, *PP_3233* and *PP_3287* fragments were ligated into p2373 (Table 2.2) to generate pGS2414, pGS2403 and pGS2413, which encode a His_6-Tig-ANR, His_6-Tig-PP_3233 and His_6-Tig-PP_3287 fusion proteins (Table 2.2).

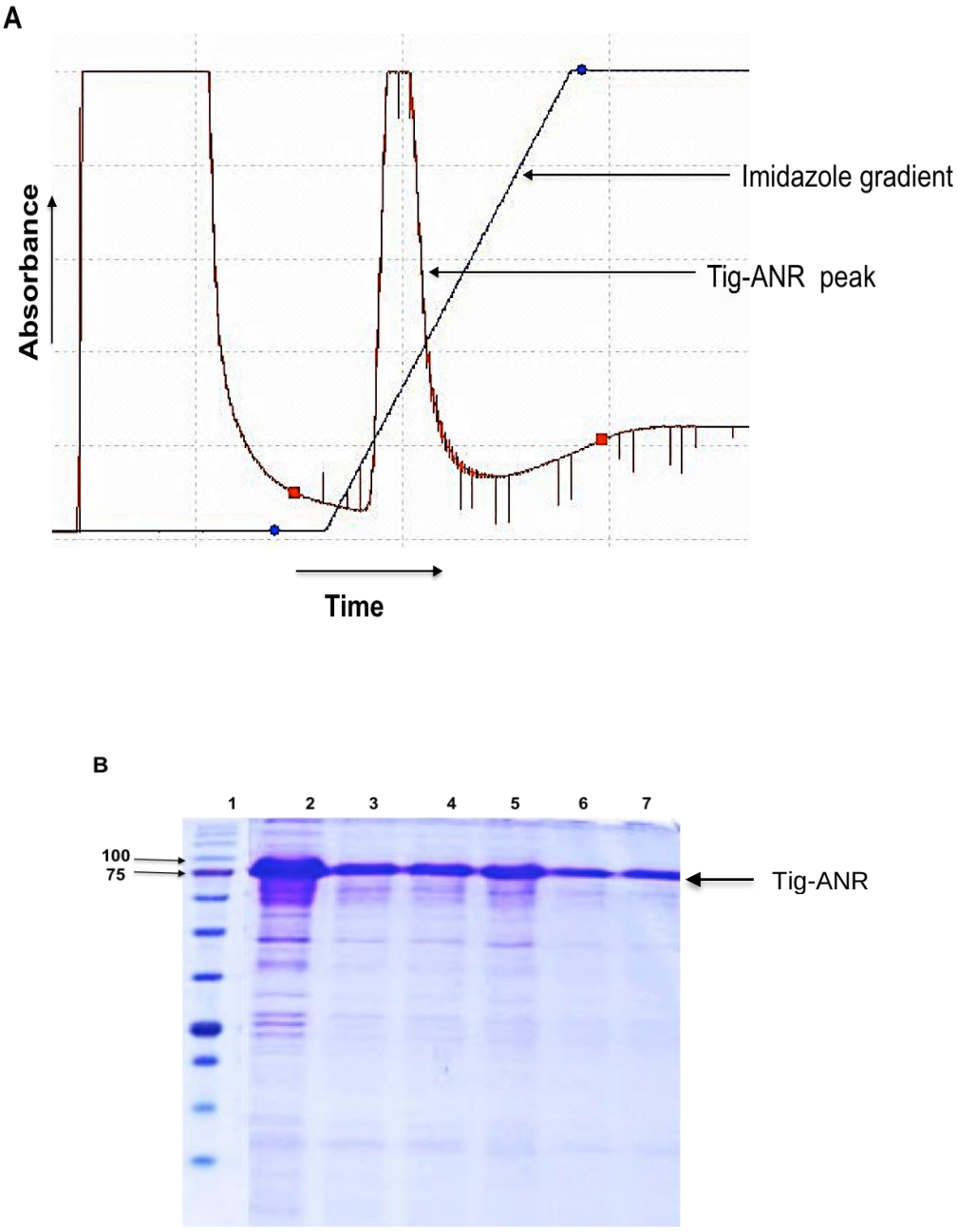

Figure 4.2: Aerobic purification of Tig-ANR using HiTrap chelating column. (A) The chromatograph for elution of Tig-ANR. Cell-free extract (10 mL) was injected on to the HiTrap chelating column (1 mL) and eluted (A_{280}: red line) with gradient imidazole (0-1 M) (blue line). **(B)** SDS-PAGE gel analysis of fractions eluted from the HiTrap chelating column. Lane 1, the CSL-BBL prestained protein ladder with relevant molecular weights indicated in kDa. Lanes 2-7, aliquots (10 µl) of Tig-ANR fractions corresponding to the A_{280} peak in Figure 4.2A.

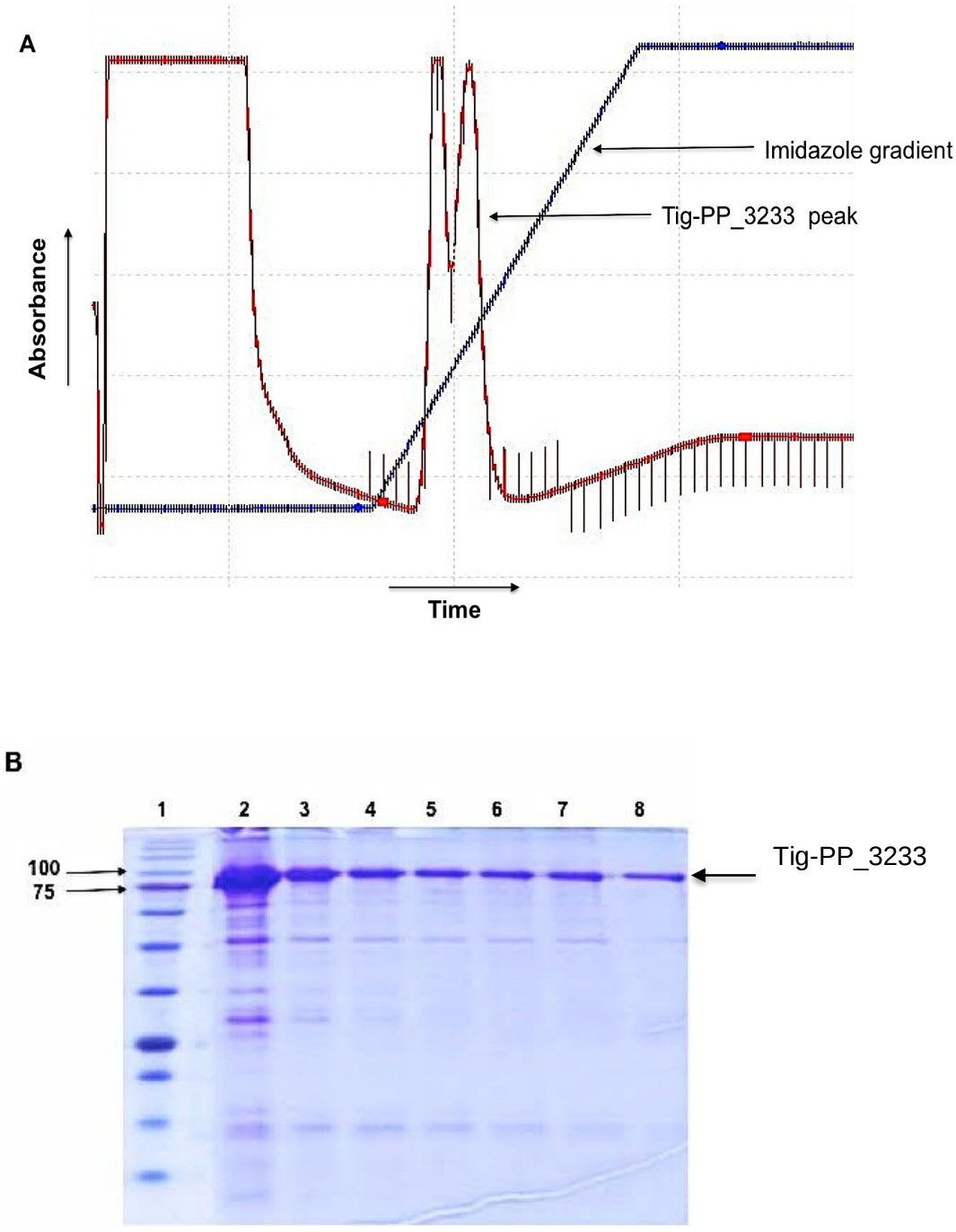

Figure 4.3: Aerobic purification of Tig-PP_3233 via Hi-Trap chelating column. (A) The chromatograph for elution of Tig-PP_3233. Cell-free extract (10 mL) was injected on to the HiTrap chelating column (1 mL) and eluted (A_{280}: red line) with gradient imidazole (0-1 M) (blue line). **(B)** SDS-PAGE gel analysis of fractions eluted from the HiTrap chelating column. Lane 1, the CSL-BBL prestained protein ladder with relevant molecular weights indicated in kDa. Lanes 2-8, aliquots (10 µl) of Tig-PP_3233 fractions corresponding to the A_{280} peak in Figure 4.3A.

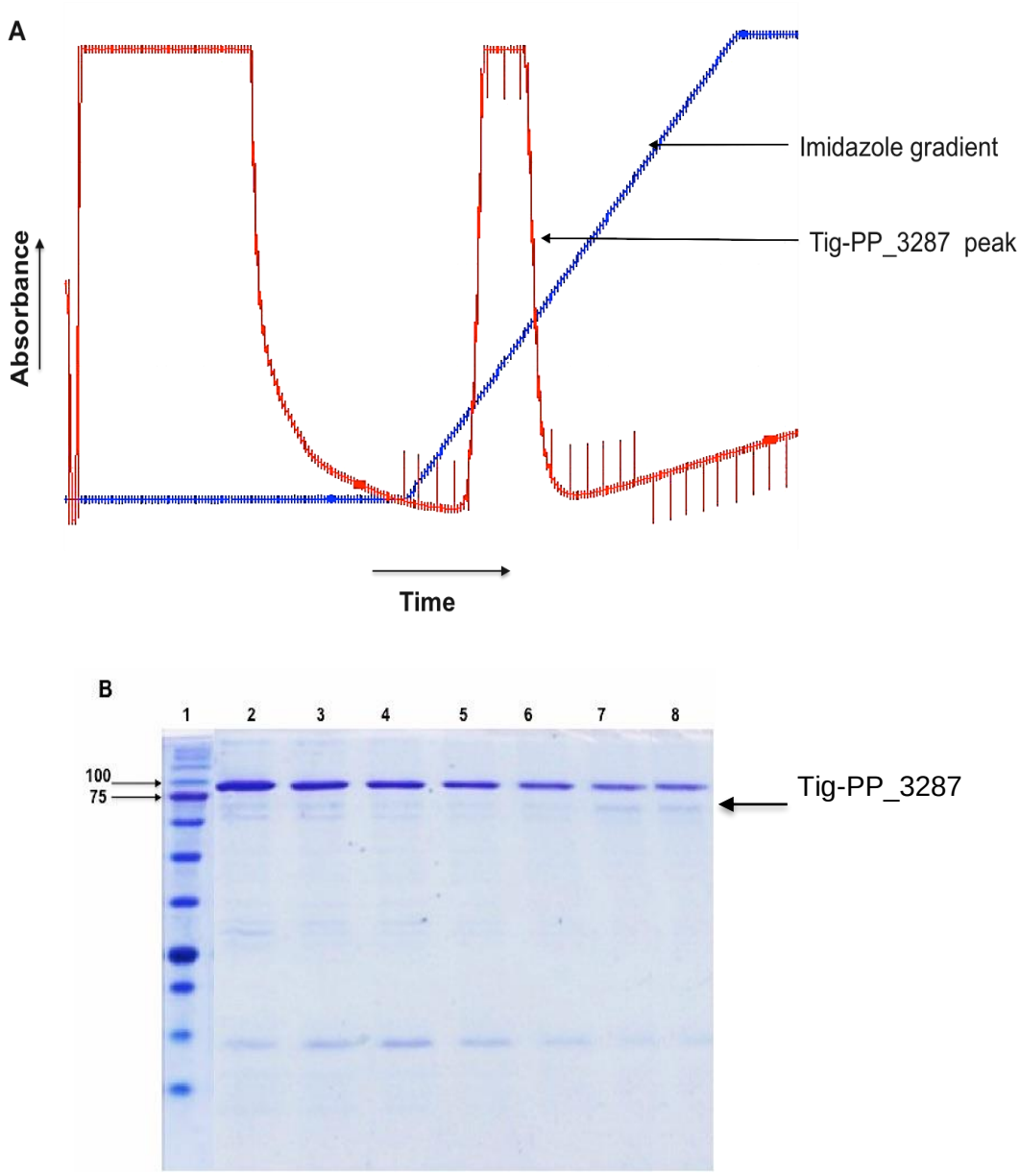

Figure 4.4: Aerobic purification of the Tig-PP_3287 by Hi-Trap chelating column. (A) The chromatograph for elution of Tig-PP_3287. Cell-free extract (10 mL) was injected on to the HiTrap chelating column (1 mL) and eluted (A_{280}: red line) with gradient imidazole (0-1 M) (blue line). **(B)** SDS-PAGE gel analysis of fractions eluted from the HiTrap chelating column. Lane 1, the CSL-BBL prestained protein ladder with relevant molecular weights indicated in kDa. Lanes 2-8, aliquots (10 µl) of Tig-PP_3287 fractions corresponding to the A_{280} peak in Figure 4.4A.

4.3 Characterisation of iron-sulfur clusters of Tig fusion proteins

4.3.1 UV-visible spectra of holo-Tig-ANR, holo-Tig-PP_3233 and holo-Tig-PP_3287 are consistent with presence of a [4Fe-4S] cluster

The reconstitution reactions were prepared by incubating apo-Tig-ANR, apo-Tig-PP_3233 and apo-Tig-PP_3287 with reconstitution reagents as described for ANR (Section 3.3.1; Section 2.7.1). After incubation, holo-Tig-ANR, holo-Tig-PP_3233 and holo-Tig-PP_3287 were purified from reconstituted reaction components using heparin chromatography (Section 2.7.2). Fractions (1 mL) were collected. The UV-visible spectra of the proteins showed a peak at ~420 nm for holo-Tig-ANR (Figure 4.5A), holo-Tig-PP_3233 (Figure 4.5B) and holo-Tig-PP_3287 (Figure 4.5C) similar to [4Fe-4S] cluster proteins (Crack *et al*., 2004). These observations suggest that Tig-ANR, Tig-PP_3233 and Tig-PP_3287 possess [4Fe-4S] clusters under anaerobic conditions similar to *E. coli* FNR protein (Green *et al*., 1996a, Crack *et al*., 2004).

4.3.2 Reactions of the [4Fe-4S] clusters of Tig-ANR, Tig-PP_3233 and Tig-PP_3287 with O_2 result in conversion to [2Fe-2S] forms

The UV-visible spectra and straw-brown colour of Tig-ANR, Tig-PP_3233 and Tig-PP_3287 were typical of [4Fe-4S] proteins. Therefore, the sensitivity of the iron-sulfur clusters of Tig fusion proteins to O_2 were investigated (Section 2.7.9). The stoichiometries of the reaction of holo-Tig-ANR (~8.6 μM cluster), holo-Tig-PP_3233 (~10.3 μM cluster) and holo-Tig-PP_3287 (~11.4 μM cluster) with O_2 were determined as described for ANR (Section 3.3.4; Section 2.7.9). Spectra obtained after successive additions of aerobic buffer showed a progressive decrease in absorbance at 420 nm while values at 500-700 nm increased for all three proteins (Figures 4.6-4.8). These observations were consistent with conversion of a [4Fe-4S] to [2Fe-2S] cluster. The changes in absorbance at 405 nm as result of addition of increasing concentrations of O_2 as air-saturated buffer were calculated and plotted against the ratio $[O_2]$:[4Fe-4S] (Section 2.7.9). The results indicated that two molecules of O_2 react with [4Fe-4S] cluster of Tig-ANR (Figure 4.6B) and Tig-PP_3233 (Figure 4.7B), but it appeared that four molecules of O_2 reacted with the [4Fe-4S] cluster of Tig-PP_3287 (Figure 4.8B). It should be noted that estimating the initial slope to obtain the intersection with the asymptote in these experiments is a potential source of error. The experiments were repeated twice more for each protein but unfortunately these additional experiments used higher concentrations of protein and thus it was not

possible to add sufficient aerobic buffer to reach saturation and so are not shown here. Nevertheless, all the data (including those shown in Figures 4.6-4.8) fitted to a one-site binding model [$y= B_{max} * x / (K_1+x)$] where K_1 gives the 'binding' stoichiometry. This analysis indicated that the O_2:[4Fe-4S] stoichiometries were: 1.9±0.2 for Tig-ANR; 1.8±0.3 for PP_3233; and 4.2±0.4 for PP_3287. These data suggested that the conversion of Tig-ANR, Tig-PP_3233 and Tig-PP_3287 [4Fe-4S] to [2Fe-2S] clusters occur via the same mechanism as described for FNR (Crack *et al*., 2004). These results also indicated that the ANR (Figure 3.7) and Tig-ANR proteins undergo the same reactions with O_2 and that the presence of the Tig-tag did not affect the properties of the iron-sulfur cluster.

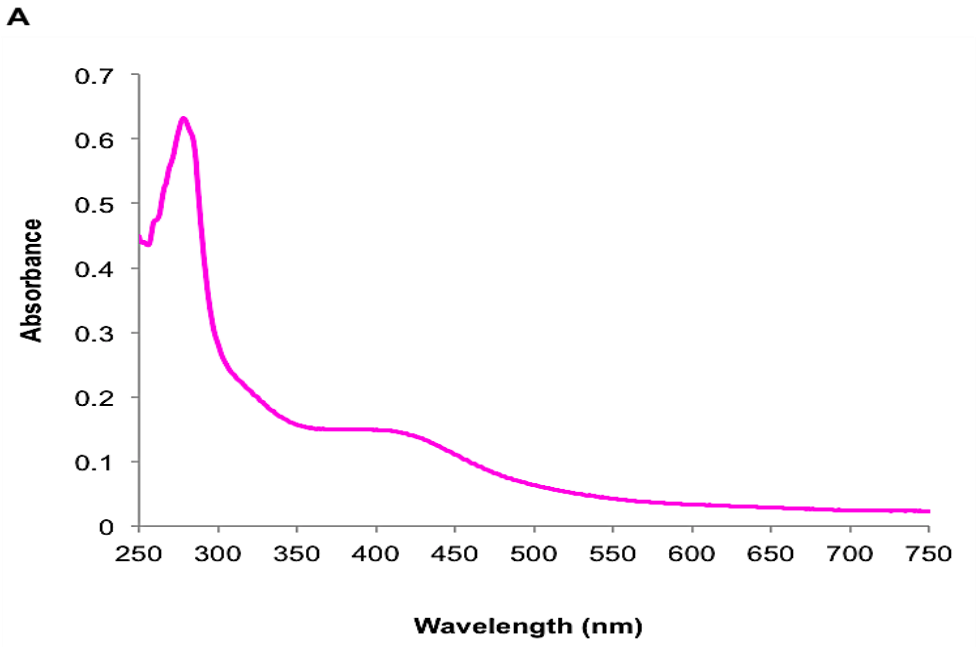

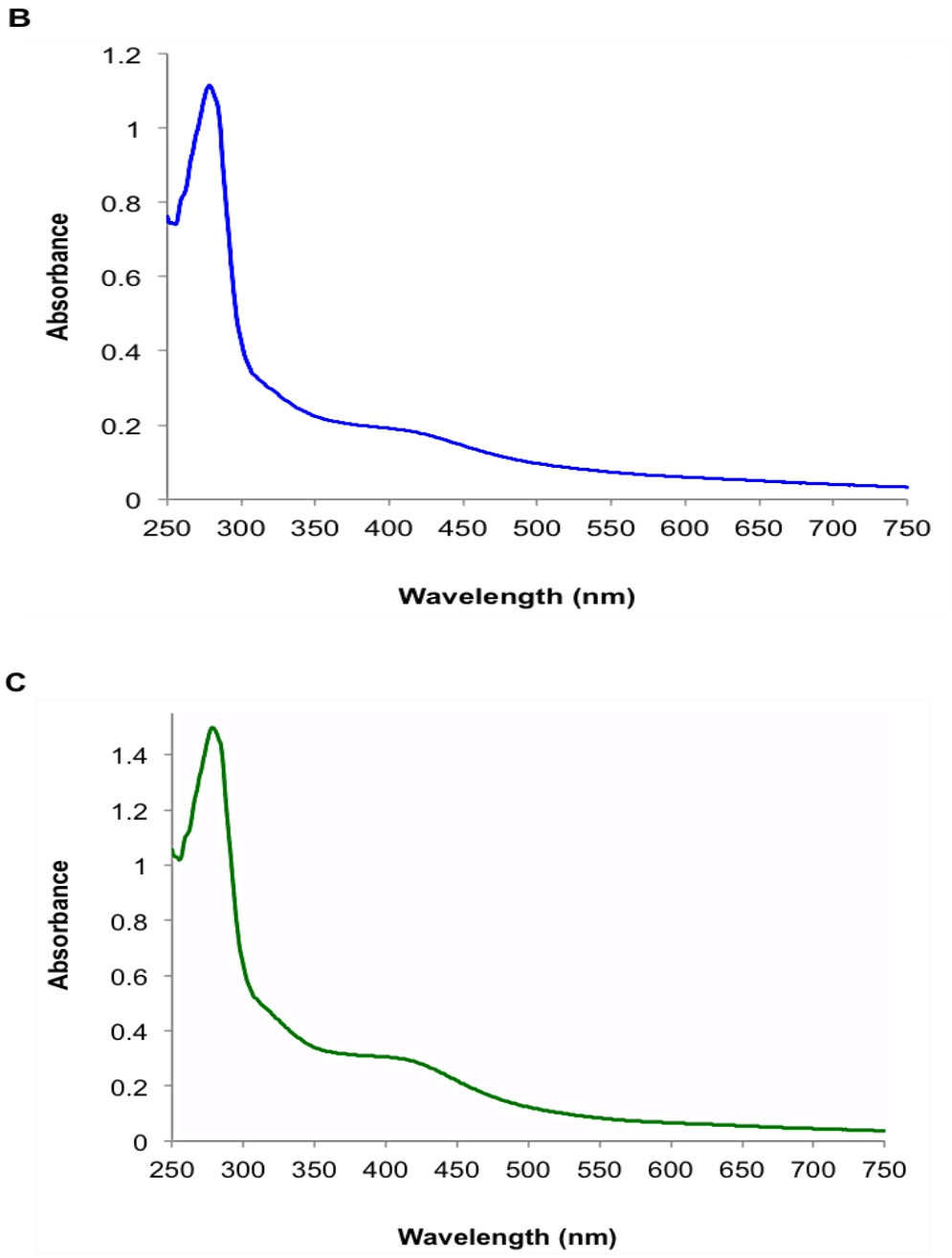

Figure 4.5: Spectra of holo-Tig-ANR, holo-Tig-PP_3233 and holo-Tig-PP_3287 proteins. Apo-Tig-ANR, apo-Tig-PP_3233 and apo-Tig-PP_3287 proteins were incubated anaerobically with L-cysteine, ammonium ferrous sulfate, dithiothreitol and the cysteine desulfurase NifS to reconstitute iron-sulfur cluster followed by removal of excess reagents by heparin chromatography (Section 2.7.2). UV-visible spectra were obtained using a Cary UV-visible spectrophotometer. **(A)** Holo-Tig-ANR (~7.5 µM cluster). **(B)** Holo-Tig-PP_3233 (~9.5 µM cluster). **(C)** Holo-Tig-PP_3287 (~15.2 µM cluster). The concentration of the cluster were determined using the extinction coefficient ~18,000 $M^{-1}cm^{-1}$ (Section 2.7.8).

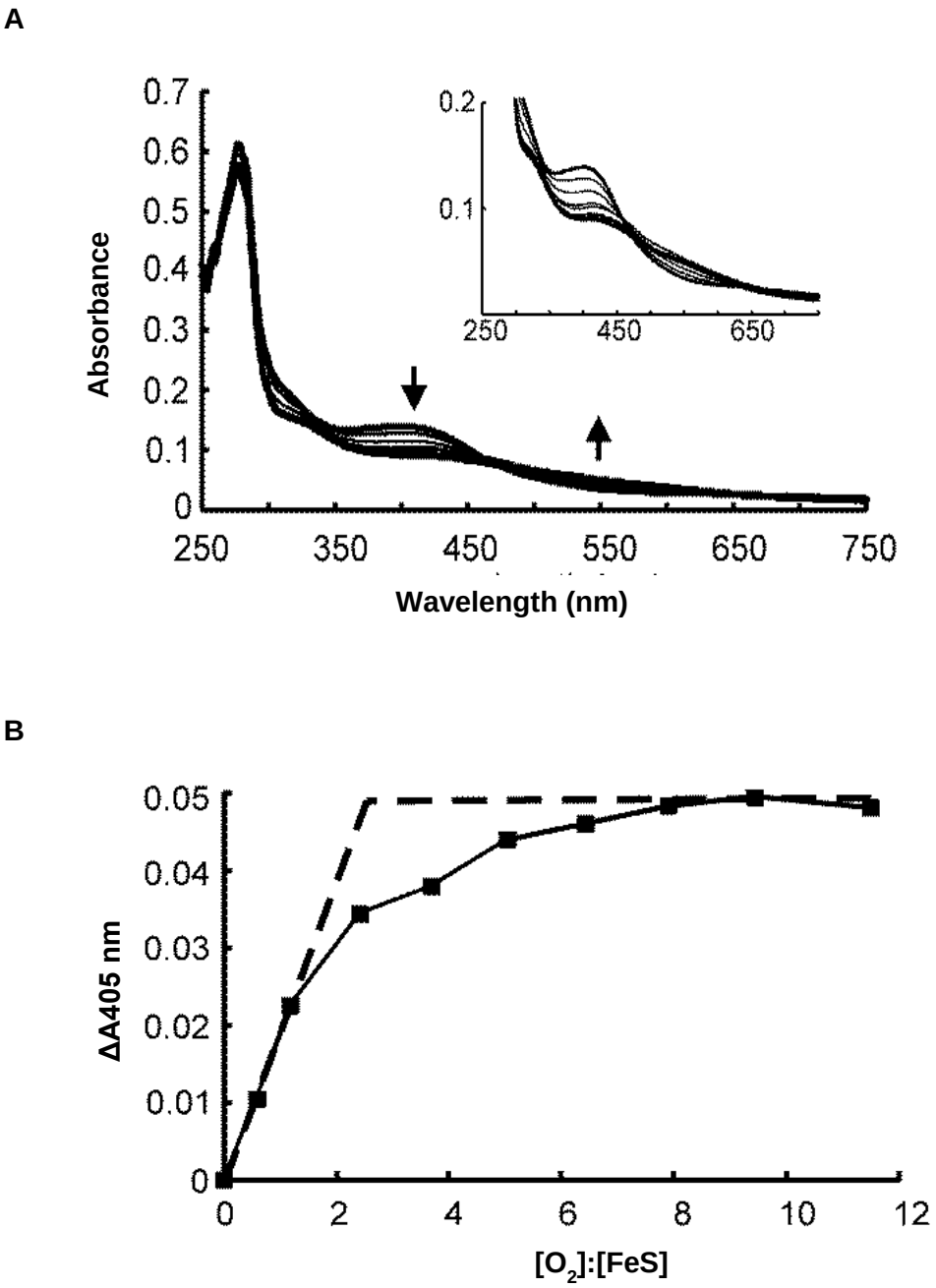

Figure 4.6: Titration of Tig-ANR with air- saturated buffer. (A) Holo-Tig-ANR (~8.6 µM cluster) was exposed to increasing amounts of air-saturated buffer. The sample was incubated at room temperature for 10 min after each addition before measurement of the spectra. The arrows show the decreasing absorbance at 420 nm and increasing absorbance at 550 nm. **(B)** Changes in absorbance at 405 nm were plotted versus the total concentration of O_2 divided by the concentration of [4Fe-4S] cluster (µM). The dashed lines show the initial slope and asymptote at high O_2 to estimate the binding stoichiometry. These experiments were carried out in collaboration with Dr. M. Stapleton (Ibrahim *et al*., 2015).

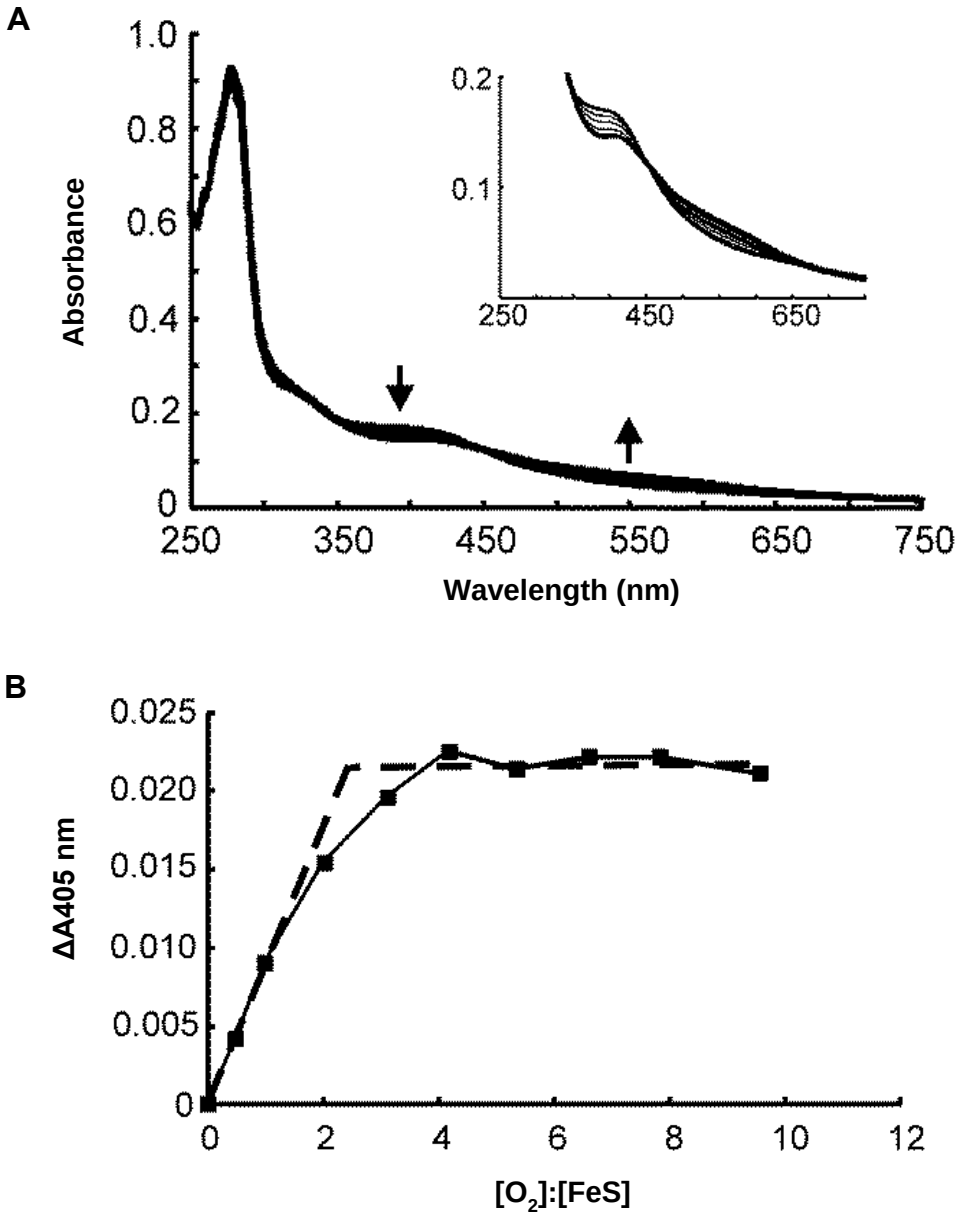

Figure 4.7: Titration of holo-Tig-PP_3233 with air-saturated buffer. (A) Holo-Tig-PP_3233 (~10.3 µM cluster) was exposed to increasing amounts of air-saturated buffer. The sample was incubated at room temperature for 10 min after each addition before obtaining the spectra. The arrows indicate the decreasing absorbance at 420 nm and increasing absorbance at 550 nm. **(B)** Changes in absorbance at 405 nm were plotted versus the total concentration of O_2 divided by the concentration of [4Fe-4S] cluster (µM). The dashed lines show the initial slope and asymptote at high O_2 to estimate the binding stoichiometry. These experiments were carried out in collaboration with Dr. M. Stapleton (Ibrahim *et al*., 2015).

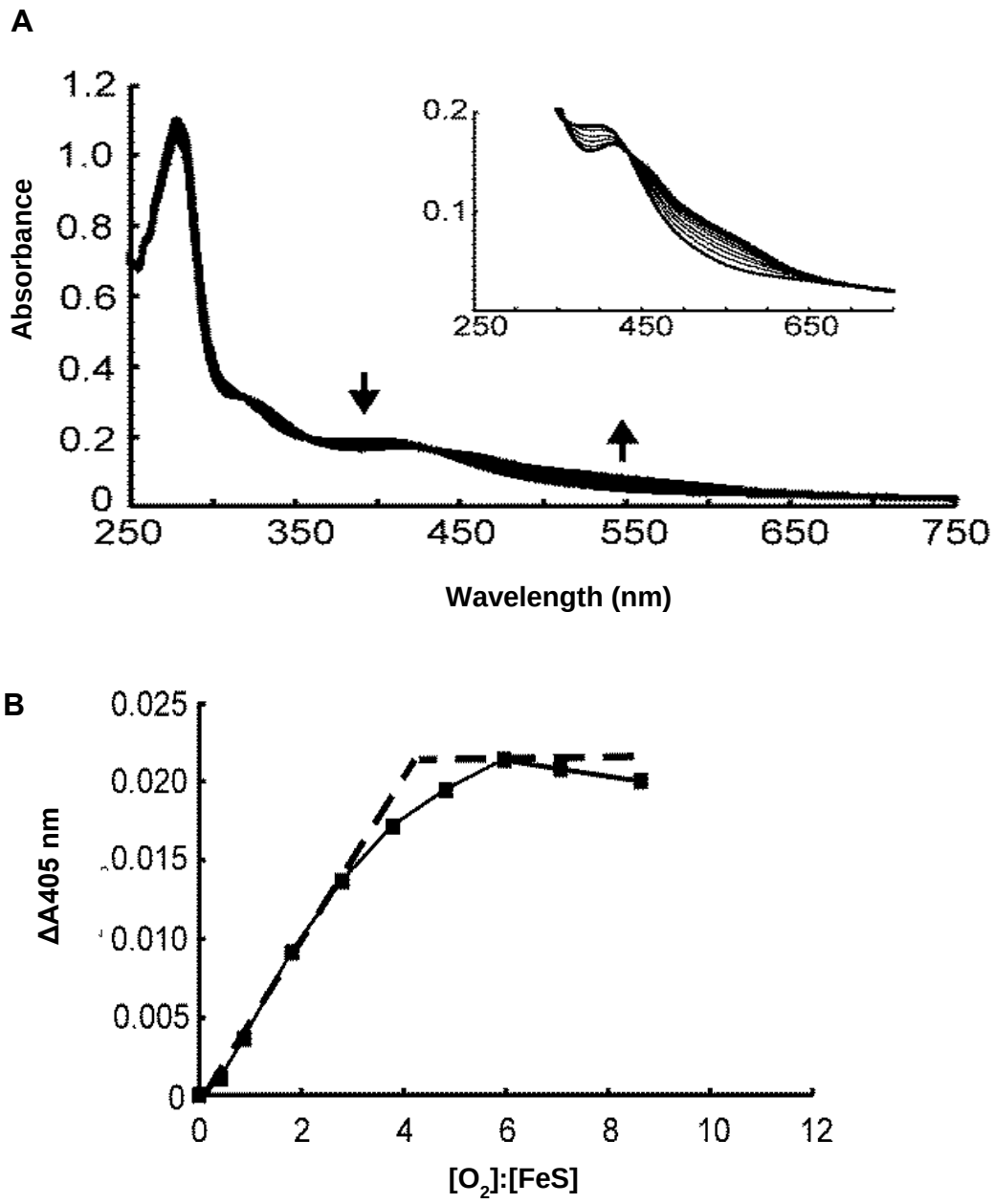

Figure 4.8: Titration of Tig-PP_3287 with air-saturated buffer. (A) Holo-Tig-PP_3287 (~11.4 µM cluster) was exposed to increasing amounts of air-saturated buffer. The sample was incubated at room temperature for 10 min after each addition before obtaining the spectra. The arrows show the decreasing absorbance at 420 nm and increasing absorbance at 550 nm. **(B)** Changes in absorbance at 405 nm were plotted versus the total concentration of O_2 divided by the concentration of [4Fe-4S] cluster (µM). The dashed lines show the initial slope and asymptote at high O_2 to estimate the binding stoichiometry. These experiments were carried out in collaboration with Dr. M. Stapleton (Ibrahim *et al.*, 2015).

4.3.3 PP_3233 and PP_3287 react more slowly than ANR with O_2 *in vitro*

Under pseudo-first-order reaction conditions the A_{420} decrease for Tig-ANR, Tig-PP_3233 and Tig-PP_3287 was measured. Reactions were modelled by using the same equation used for untagged-ANR (Section 3.3.6; Sutton *et al*. 2004). The reactions were carried out as described for ANR (Section 3.3.6). Holo-Tig-ANR, holo-Tig-PP_3233 and holo-Tig-PP_3287 were exposed to a 13-fold molar excess of O_2 (Figure 4.9). Changes in absorbance at 420 nm were monitored (Section 2.7.9). The rate constants are mean values with standard deviation from three experiments. The data were best fitted to a double- exponential function with observed rate constants (k_{obs}) 0.028 ± 0.0015 s^{-1} for the Tig-ANR (Figure 4.9A) and to a single-exponential function yielding (k_{obs}) values of 0.0038 ± 0.0002 s^{-1} for Tig-PP_3233 (Figure 4.9B) and 0.0055 ± 0.0001 s^{-1} for Tig-PP_3287 (Figure 4.9C). The fitting was carried out by Dr. Jason Crack, University of East Anglia (Section 2.7.9). Division of the observed rate constants by the O_2 concentration provides an estimate of the apparent second order rate constants for the fusion proteins: Tig-ANR, 280 $M^{-1}s^{-1}$; Tig-PP_3233, 38 $M^{-1}s^{-1}$ and Tig-PP_3287, 55 $M^{-1}s^{-1}$. These values indicate that the [4Fe-4S] cluster of Tig-ANR displays similar sensitivity to untagged-ANR (309 $M^{-1}s^{-1}$). Thus, it was concluded that the Tig-tag did not affect the properties the iron-sulfur cluster of ANR. This data of Tig-ANR (280 $M^{-1}s^{-1}$) is similar to that previously reported for *E. coli* FNR (278 $M^{-1}s^{-1}$) (Crack *et al*., 2007, Jervis *et al*., 2009). However, it appears that PP_3233 and PP_3287 are significantly less reactive with O_2 *in vitro*. The results show that they more closely resembled FNR-S24F (80 $M^{-1}s^{-1}$), which is less responsive to O_2 *in vivo* retaining significant aerobic activity (Jervis *et al*., 2009).

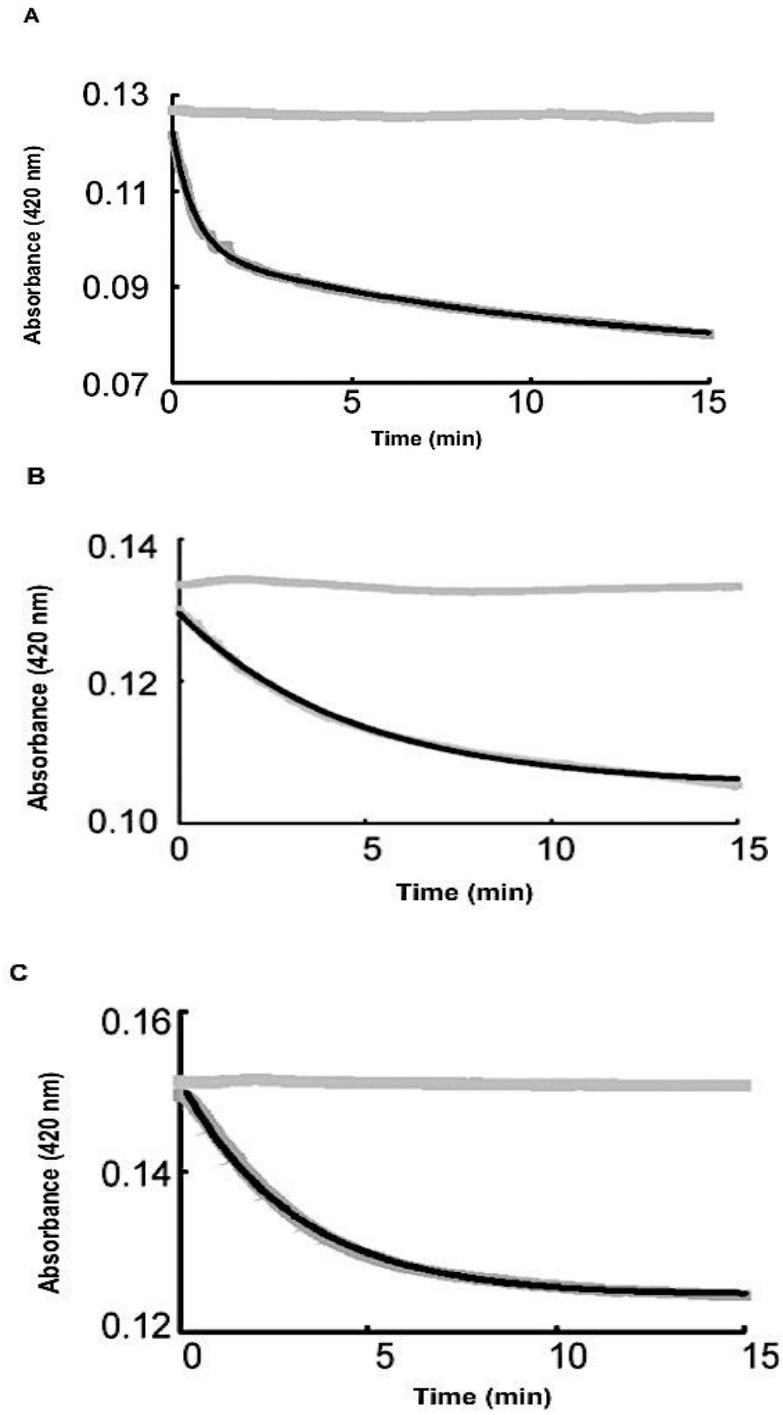

Figure 4.9: Reactions of holo-Tig-ANR, holo-Tig-PP_3233 and holo-Tig-PP_3287 with O_2. Samples of reconstituted **(A)** Tig-ANR (~8.0 µM cluster), **(B)** Tig-PP_3233 (~8.0 µM cluster) and **(C)** Tig-PP_3287 (~8.0 µM cluster) were mixed with a 13-fold molar excess of O_2 as aerobic buffer at 25ºC. The reaction buffer was 25 mM HEPES, 100 mM NaCl, 100 mM $NaNO_3$, pH 7.5. The data are shown as a grey lines and the fitting as black lines. The upper data set (not fitted) in each panel shows the response when anaerobic buffer was used in place of aerobic buffer. These reactions were carried out in collaboration with Dr. M. Stapleton and Dr. J. Crack (Ibrahim *et al*., 2015).

4.4 The DNA binding properties of PP_3233 and PP_3287

EMSAs (Section 2.8.2) were used to determine the effects of the PP_3233 and PP-3287 iron-sulfur clusters on the ability to bind to biotin-labelled DNA sequences: FF, CC and NN sites as previously described (Section 3.4; Figure 3.14). Purified fractions of Tig-PP_3233 and Tig-PP_3287 (1 mL, 100 µM) were incubated with thrombin (10 units, Sigma) at 4°C overnight to release ~28 kDa PP-3233 (Figure 4.10A, lanes 2) and ~30 kDa PP_3287 (Figure 4.11A, lane 2) from the ~54.4 kDa Trigger factor (Tig). Reconstituted reactions with mixtures of Tig and PP_3233 or PP_3287 (Figures 4.10B and 4.11B) were prepared under anaerobic conditions (Section 2.7.1) and purified via Heparin chromatography (Section 2.7.2) for use in EMSAs.

Trigger factor (Tig) was purified with PP_3233 and PP_3287 via Heparin column after reconstitution, which suggested that Tig bound to the Heparin column and might bind to DNA as well. Therefore, it was important to purify the Trigger factor (Tig) and establish its DNA-binding properties.

4.4.1 Trigger factor (Tig) can bind to FF site

Trigger factor (Tig) was overproduced aerobically in JRG5302 (Table 2.1) that contains plasmid p2373 (Table 2.2) as described for Tig fusion proteins (Section 4.2). Figure 4.12 shows the elution profile and polypeptides visible after SDS-PAGE separation of aliquots of fractions from the HiTrap chelating column (Section 2.6.8). The purified Tig was desalted into 25 mM HEPES, 100 mM NaCl, 100 mM $NaNO_3$ pH 7.5 and used in EMSAs.

The FF site (TTGAT----ATCAA) (Section 3.4; Figure 3.14) was used in the EMSAs to investigate the ability of Tig to bind to biotin-labelled DNA (Figure 4.13). The results of the EMSA indicated that Tig could bind to the DNA FF when Tig concentration was >2 µM (Figure 4.13). Therefore, high concentrations (>2 µM) of reconstituted PP_3233 and PP_3287 Tig mixtures were avoided in EMSAs.

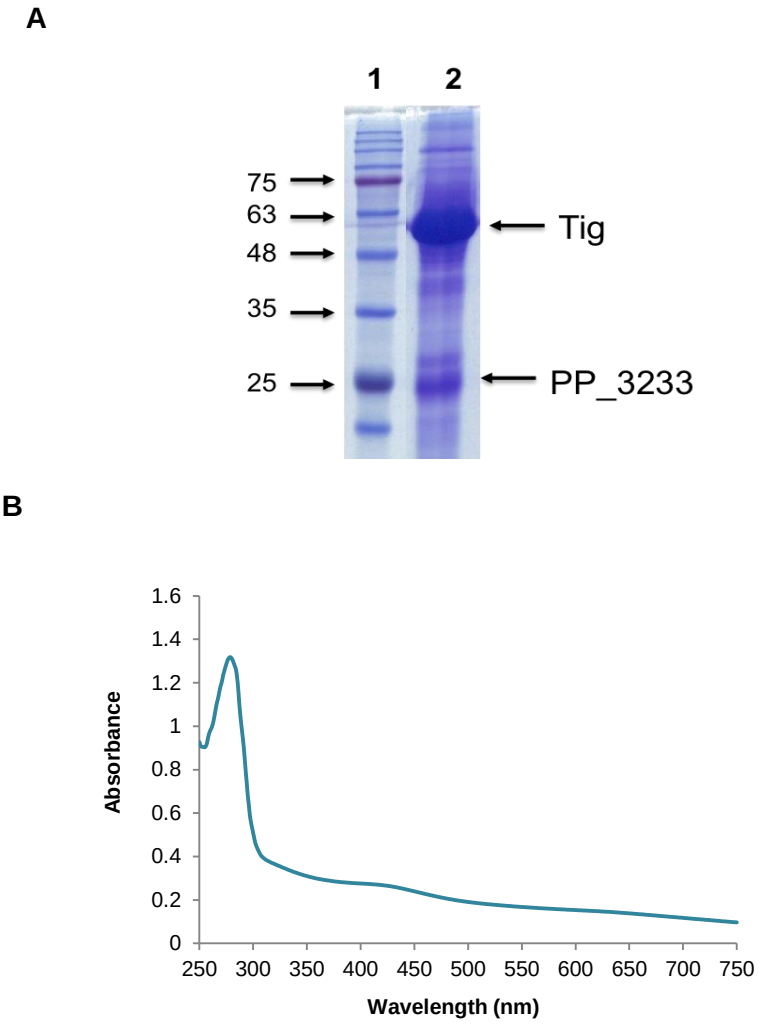

Figure 4.10: Treatment of Tig-PP_3233 with thrombin. (A) Coomassie blue-stained SDS-PAGE gel showing: lane 1, Precision plus protein standards (size in kDa are indicated); lane 2, Tig and PP_3233 after incubation with thrombin (10 units) at 4°C for 16 h. **(B)** Reconstituted mixture contained holo-PP_3233 (~12 μM cluster) under anaerobic conditions.

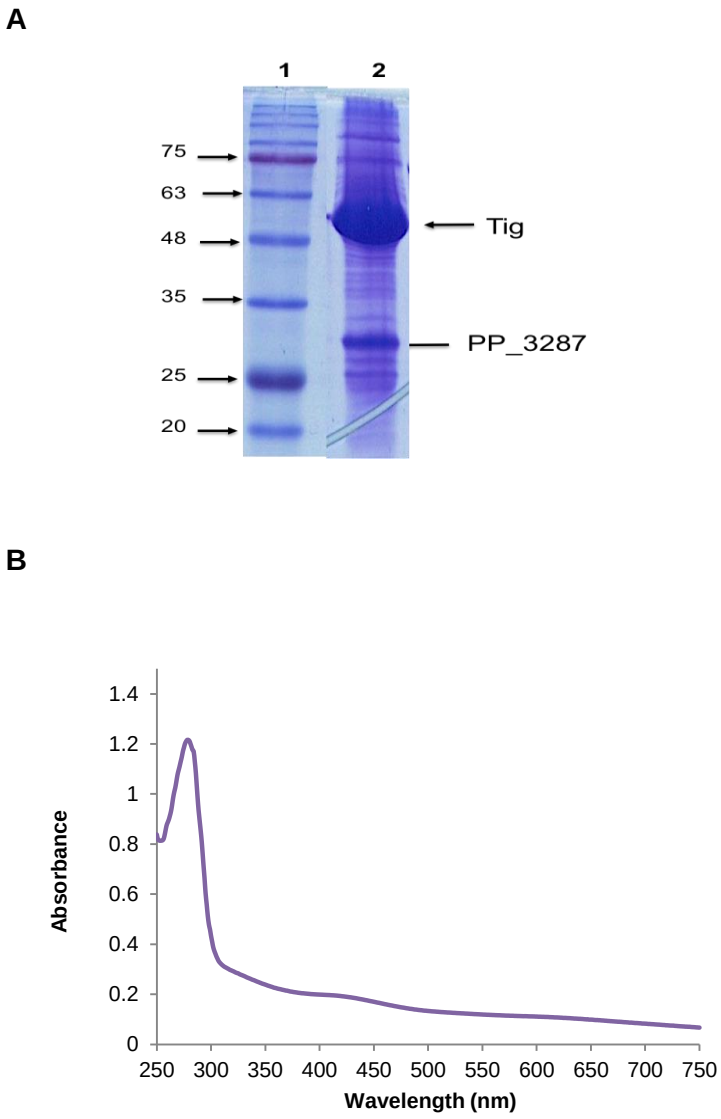

Figure 4.11: Treatment of Tig-PP_3287 with thrombin. (A) Coomassie blue-stained SDS-PAGE gel showing: lane 1, Precision plus protein standards (size in kDa are indicated); lane 2, Tig and holo-PP_3287 protein after incubation with thrombin (10 units) at 4°C for 16 h. **(B)** Reconstituted mixture contained holo-PP_3287 (~10 μM cluster) under anaerobic conditions.

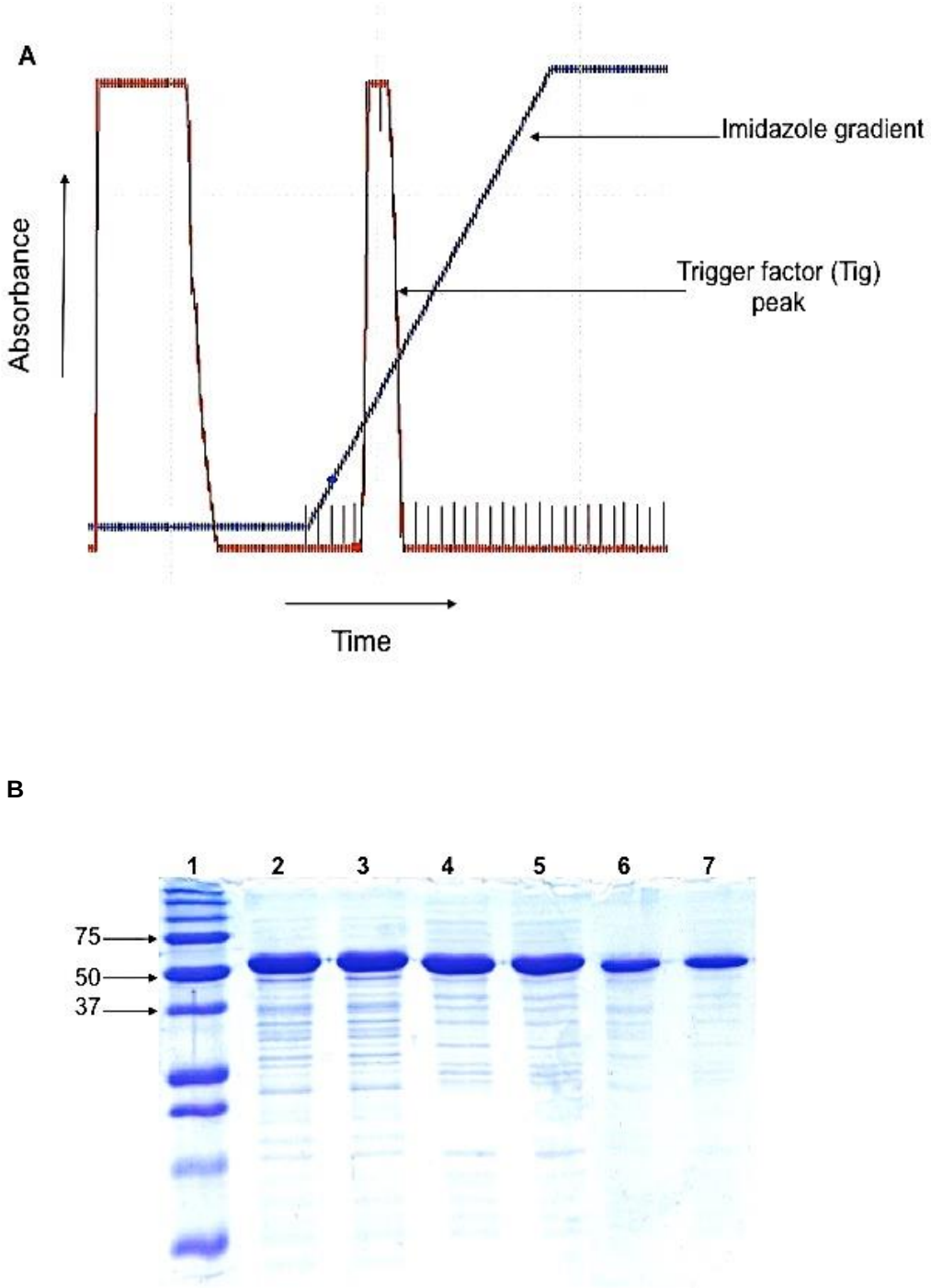

Figure 4.12: Purification of Trigger Factor (Tig). (A) The chromatograph for the elution of Trigger factor (Tig). Cell free extract (10 mL) was injected to HiTrap column (1 ml) and eluted (A_{280}: red line) with imidazole (0-1 M) (blue line). **(B)** SDS-PAGE gel analysis of fractions eluted from the HiTrap chelating column. Lane 1, protein markers with relevant molecular weights indicated in kDa. Lanes 2-5, Trigger Factor (Tig) purified via Hi-Trap chelating column; lanes 6 and 7, Trigger Factor (Tig) after desalting into 25 mM HEPES, 100 mM NaCl, 100 mM $NaNO_3$ pH 7.5.

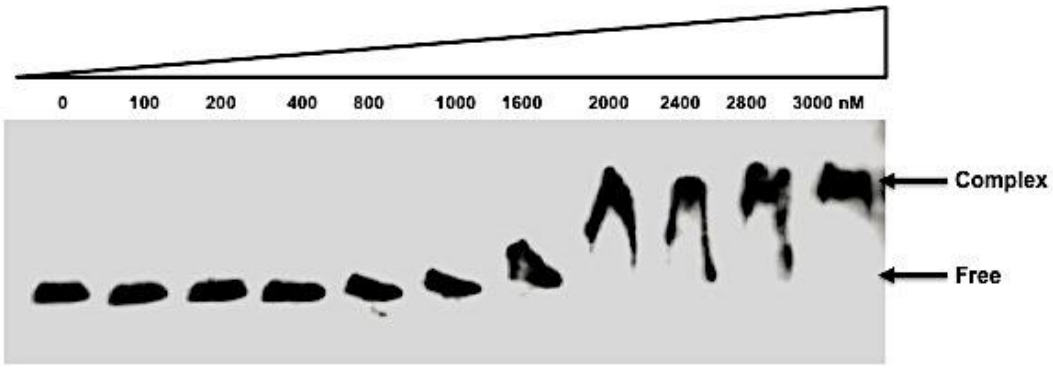

Figure 4.13: Binding of Tig to the FF site. Increasing concentrations of Trigger Factor (Tig) (0, 100, 200, 400, 800, 1000, 1600, 2000, 2400, 2800 and 3000 nM) were incubated with 20 fmole of biotin-labelled DNA that contained FF site (Figure 3.14; Section 3.4) prior to gel electrophoresis to separate free and bound DNA fragments. The concentration of Tig was estimated by Bradford assay (Section 2.6.1).

4.4.2 PP_3233 binds to FF site under anaerobic conditions

To investigate the capability of holo-PP_3233 to bind to DNA sequences, EMSAs were used (Section 2.8.2). Apo-Tig-PP_3233 fraction (1 mL, 100 μM) was treated with thrombin (Section 4.4; Figure 4.10, lane 2). This was reconstituted under anaerobic conditions (Section 2.7.1) and purified by Heparin column chromatography (Section 2.7.2) to yield a mixture containing Tig and holo-PP_3233 for EMSA (Figure 4.10B). Increasing concentrations of the holo-PP_3233 Tig mixture (0, 100, 200, 400, 800, 1000 and 1600 nM, estimating by Bradford assay using Tig-PP_3233 molecular weight) were incubated with ~20 fmol of biotin-labelled DNA that contained FF, CC or NN sites (Section 3.4; Figure 3.14) under anaerobic conditions (Section 2.8.2). The bound DNA was separated from free DNA by 7.5% polyacrylamide Tris-glycine gels (Section 2.8.2). This showed that holo-PP_3233 (200 nM) bound tightly with FF site (TTGAT----ATCAA) (Figure 4.14A). Moreover, the holo-PP_3233 (400 nM) could recognise the CC site (GTGAT----ATCAC) (Figure 4.14B). However, holo-PP_3233 appeared not to bind to the NN site (TCTGA----ATCAG) (Figure 4.14C). In contrast, apo-PP_3233 could not recognise the FF site under anaerobic conditions (Figure 4.15). This is similar to *E. coli* FNR, which binds specifically to the FF site (Lodge *et al*., 1990, Bell *et al*., 1989). These data suggested that the [4Fe-4S] cluster of PP_3233 is important to enhance DNA-binding under anaerobic conditions.

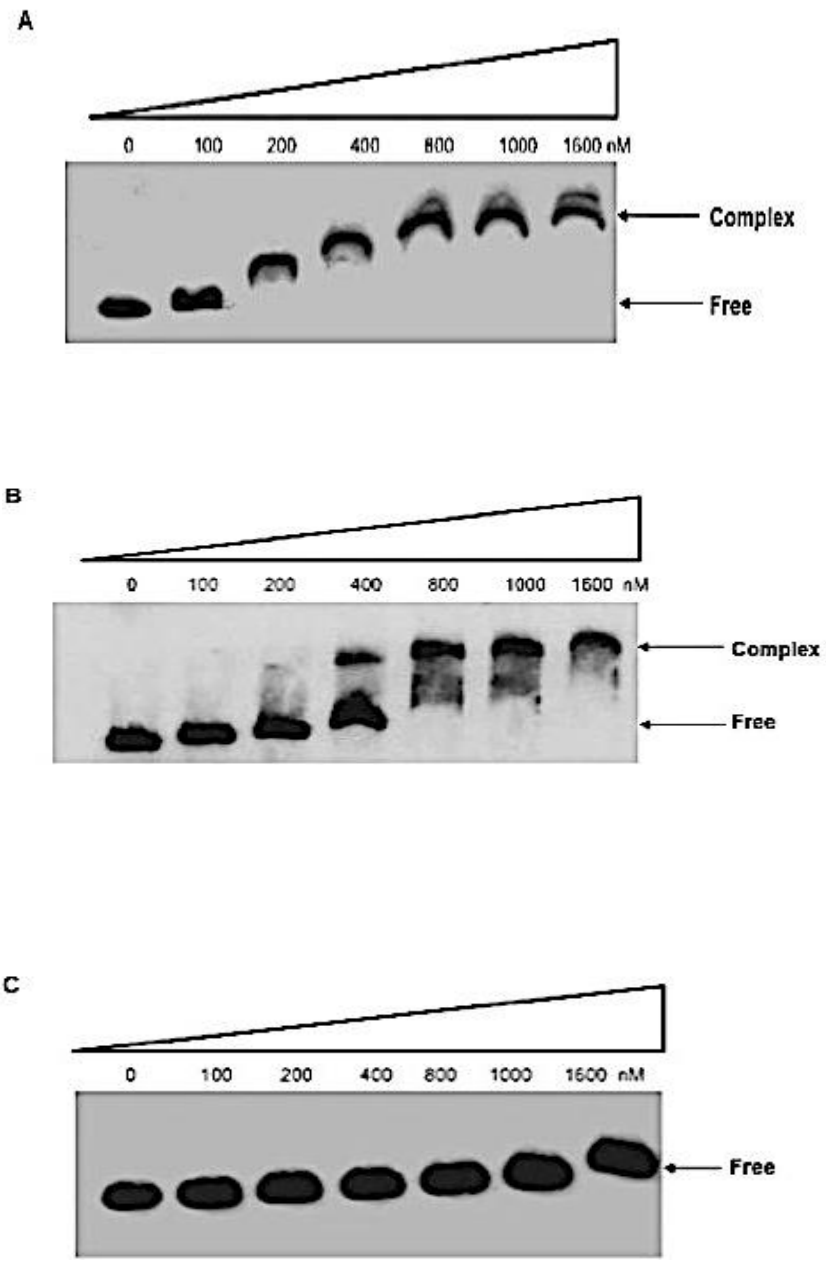

Figure 4.14: Binding of holo-PP_3233 to different DNA sequences under anaerobic conditions. Increasing concentrations of holo-PP_3233 Tig mixtures (0, 100, 200, 400, 800, 1000 and 1600 nM, estimated by Bradford assay using Tig-PP_3233 molecular weight) (Section 2.6.1) were incubated with ~20 fmol of biotin-labelled DNA fragments: FF site **(A)**, CC site **(B)** and NN site **(C)** before electrophoresis to separate bound and free DNA fragments.

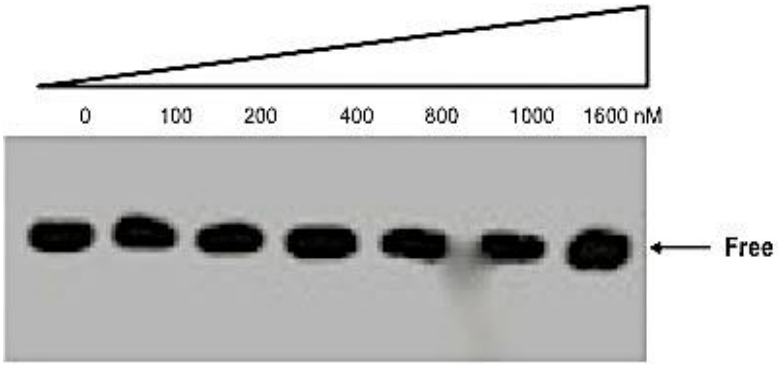

Figure 4.15: Binding of apo-PP_3233 to the FF site under anaerobic conditions. Apo-Tig-PP_3233 (0, 100, 200, 400, 800, 1000 and 1600 nM, estimated by Bradford assay using Tig fusion molecular weight) (Section 2.6.1) was incubated with biotin-labelled DNA that contained FF site (~20 fmol) prior to electrophoresis.

4.4.3 Binding of PP_3287 to FF site under anaerobic conditions

The capability of holo-PP_3287 to bind to different DNA sequences was investigated using EMSAs (Section 2.8.2) assessed as described for PP_3233 (Section 4.4.2). Increasing concentrations of holo-PP_3287 (0, 100, 200, 400, 800, 1000 and 1600 nM, estimated by Bradford assay using Tig-PP_3287 molecular weight) were incubated with ~20 fmol of biotin-labelled DNA, which contained the FF, CC or NN sites (Section 3.4; Figure 3.14) under anaerobic conditions. The EMSAs indicated that holo-PP_3287 (100 nM) was capable of binding at the FF site (Figure 4.16A), with weaker binding at the CC site (800 nM) (Figure 4.16B). Holo-PP_3287 could not bind to NN site (Figure 4.16C). Furthermore, apo-PP_3287 could not recognise the FF site under anaerobic conditions (Figure 4.17). These data showed that the [4Fe-4S] cluster of PP_3287 plays a crucial role in enhancing the DNA-binding under anaerobic conditions, indicating that PP_3287 is inactive aerobically.

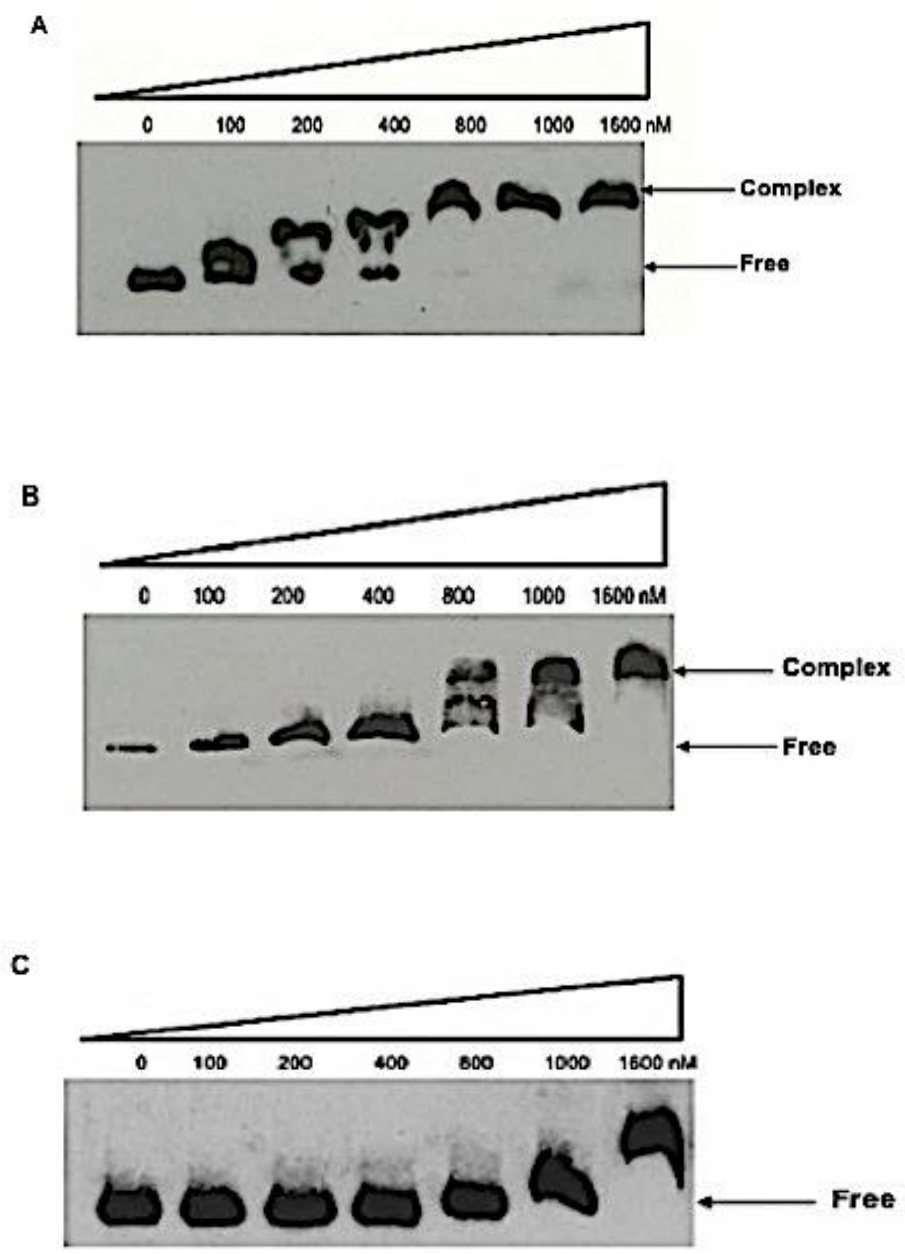

Figure 4.16: Anaerobic binding of holo-PP_3287 to different biotin-labelled DNA. Increasing concentrations of reconstituted PP_3287 (0, 100, 200, 400, 800, 1000 and 1600 nM, estimated by Bradford assay using Tig-PP_3287 molecular weight) (Section 2.6.1) were incubated with biotin-labelled DNA ~20 fmol: FF site **(A)**, CC site **(B)** and NN site **(C)** prior to electrophoresis to separate free and bound DNA fragments.

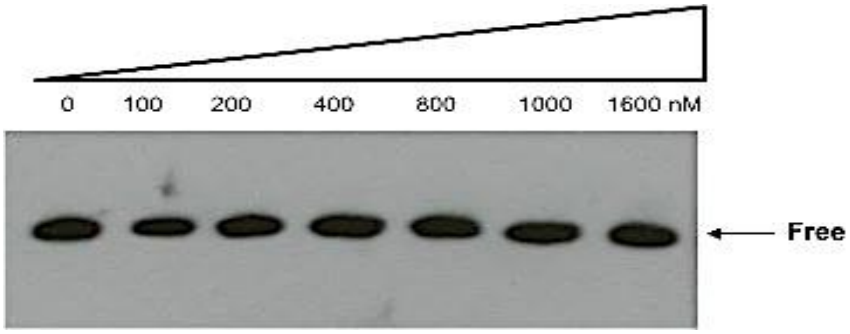

Figure 4.17: Binding of apo-PP_3287 to the FF site under anaerobic conditions. Apo-Tig-PP_3287 (0, 100, 200, 400, 800, 1000 and 1600 nM, estimated by Bradford assay using Tig-PP_3287 molecular weight) (Section 2.6.1) was incubated with ~20 fmol of biotin-labelled DNA that contained FF site prior to electrophoresis.

4.5 Sensitivity of [4Fe-4S] ANR and [4Fe-4S] PP_3287 to nitric oxide *in vitro*

Crack *et al.* (2011; 2013) reported that the [4Fe-4S] cluster of *E. coli* FNR and the [4Fe-4S] cluster of WhiB-like proteins react with eight molecules of nitric oxide per [4Fe-4S] cluster to produce nitrosylated clusters. Therefore, the sensitivity of ANR, PP_3233 and PP_3287 to nitric oxide was analysed using Proli NONOate (Cayman Chemicals) (Section 2.7.11). Holo-Tig-ANR (~7.9 μM cluster); holo-Tig-PP_3287 (~7.6 μM cluster) and holo-Tig-PP_3233 (~9.4 μM cluster) were exposed to 108 μM of Proli NONOate (equivalent to 216 μM of nitric oxide) for 2 h under anaerobic conditions (Section 2.7.11). The UV-visible spectrum before addition of nitric oxide showed the expected absorbance band centred at ~420 nm for Tig-ANR (Figure 4.18, black line); Tig-PP_3287 (Figure 4.19, blue line) and Tig-PP_3233 (Figure 4.20, pink line). After incubation with nitric oxide an increase in absorbance at ~350-360 nm and combined with decreased absorbance at 420 nm were observed with an isobestic point at ~400 nm for Tig-ANR (Figures 4.18) and Tig-PP_3287 (Figure 4.19). These changes are indicative of the formation of a dimeric dinitrosyl-iron-cysteine complex (Figure 4.21; Cruz-Ramos *et al*., 2002). However, the [4Fe-4S] cluster of PP_3233 showed only a minor increase in absorbance at 360 nm after incubation for 2 h with nitric oxide (Figure 4.20). This suggests that the [4Fe-4S] cluster of PP_3233 might be stable in the presence of nitric oxide *in vitro*.

4.5.1 The [4Fe-4S] cluster of ANR and PP_3287 react with eight molecules of nitric oxide

Reactions of holo-Tig-ANR and holo-Tig-PP_3287 with Proli NONOate under anaerobic conditions were monitored using a Cary UV-visible spectrophotometer (Section 2.7.6; Section 2.7.10). Holo-Tig-ANR (~7.0 μM cluster) and holo-Tig-PP_3287 (~7.6 μM cluster) were incubated with increasing concentrations of Proli NONOate in a quartz cuvette whilst maintaining anaerobic conditions (Section 2.7.11). Increasing amounts of nitric oxide (5-216 μM) from Proli NONOate (500 μM, equivalent to 1 mM of nitric oxide) were injected through the silica seal of the cuvette. The reaction buffer was 25 mM Tris-HCl pH 7.5 containing 500 mM NaCl. Samples were scanned after incubation for 10 min at room temperature after each addition (Figure 4.22A) for Tig-ANR and (Figure 4.23A) for Tig-PP_3287. The spectra showed increasing absorbance at 360 nm and decreasing absorbance at 420 nm, which suggested formation of nitrosylated iron-sulfur clusters (Figure 4.21; Cruz-Ramos *et al*., 2002). The changes in absorbance at 360 nm were measured for each addition of

nitric oxide and plotted against the ratio of [nitric oxide]:[4Fe-4S]. Between eight and nine molecules of nitric oxide interacted with one [4Fe-4S] cluster suggesting the formation of octa-nirosylated iron clusters (Figure 4.22B) for Tig-ANR and (Figure 4.23B) for Tig-PP_3287.

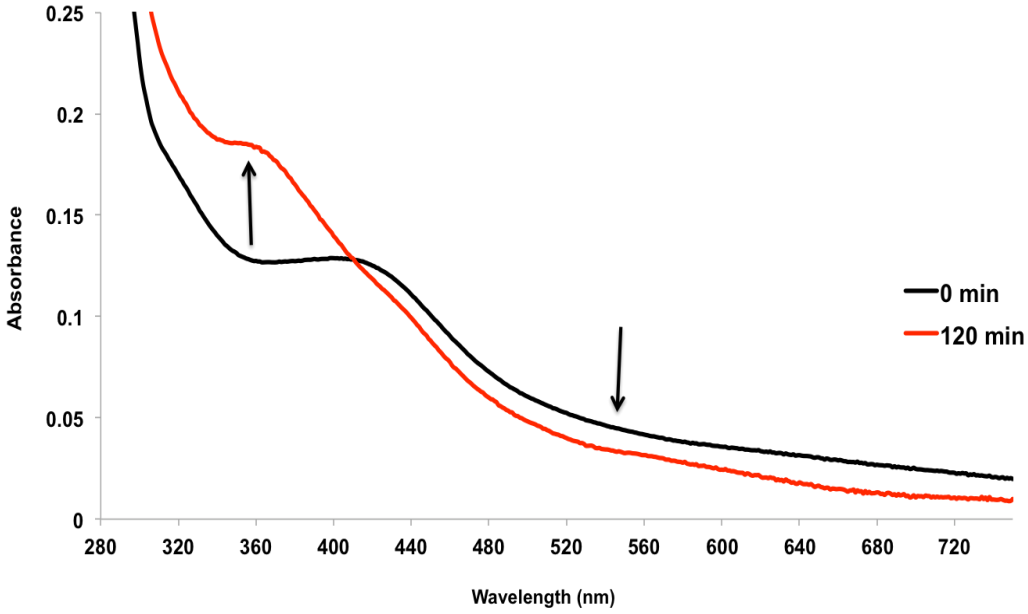

Figure 4.18: UV-visible spectra of the reaction of Tig-ANR with nitric oxide. The spectra of holo-Tig-ANR (~7.9 µM cluster), before (black line) and after (red line) adding 108 µM of Proli NONOate (equivalent to 216 µM of nitric oxide) for 2 h were recorded. The arrows show the increased absorbance at 360 nm and decreased absorbance at 550 nm as a result the formation of nitrosylated clusters.

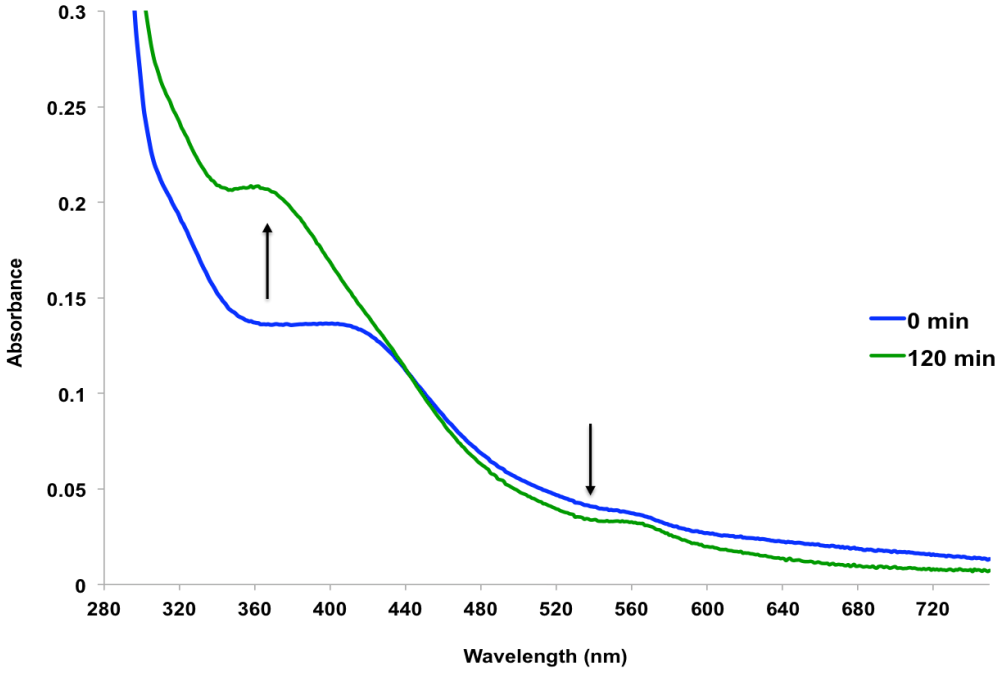

Figure 4.19: UV-visible spectra of the reaction of Tig-PP_3287 with nitric oxide. The spectra of holo-Tig-PP_3287 (~7.6 μM cluster) before (blue line) and after (green line) adding 108 μM of Proli NONOate (equivalent to 216 μM of nitric oxide) for 2 h were recorded. The arrows show the increased absorbance at 360 nm and decreased absorbance at 550 nm as a result the formation of nitrosylated clusters.

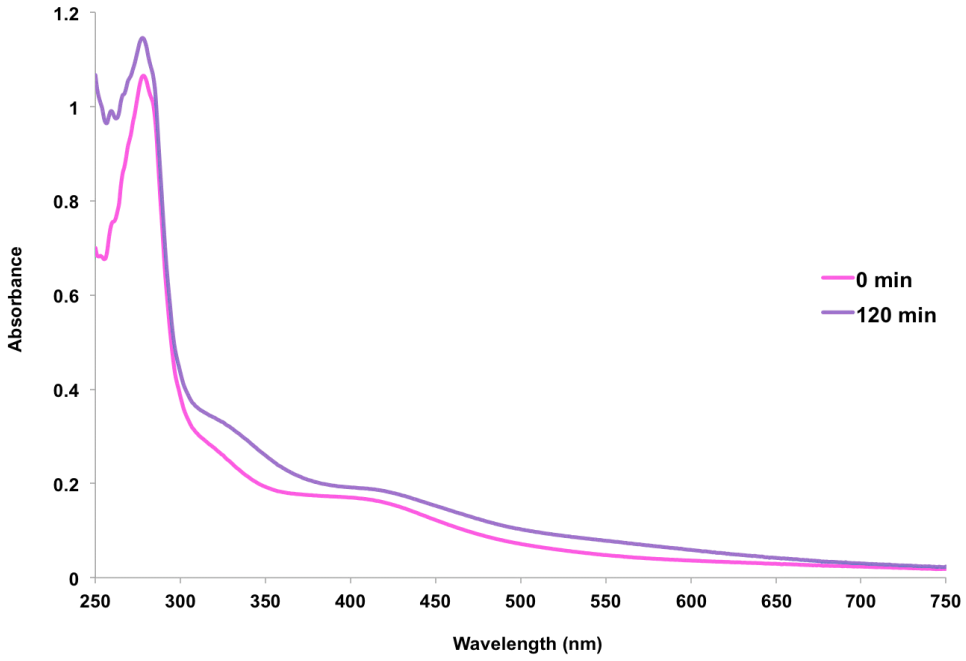

Figure 4.20: UV-visible spectra of the reaction of Tig-PP_3233 with nitric oxide. The spectra of holo-Tig-PP_3233 (~9.4 μM cluster) before (pink line) and after (purple line) adding 108 μM of Proli NONOate (equivalent to 216 μM of nitric oxide) for 2 h were recorded.

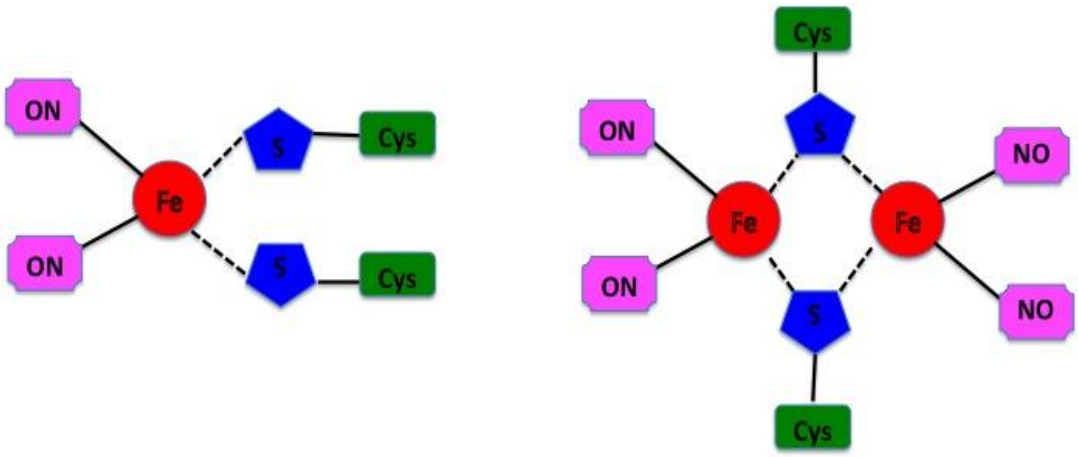

Monomeric dinitrosyl-iron-cysteine complex

Dimeric dinitrosyl-iron-cysteine complex

Figure 4.21: Graphic shows dinitrosyl-iron-cysteine (DNIC) complexes.

A

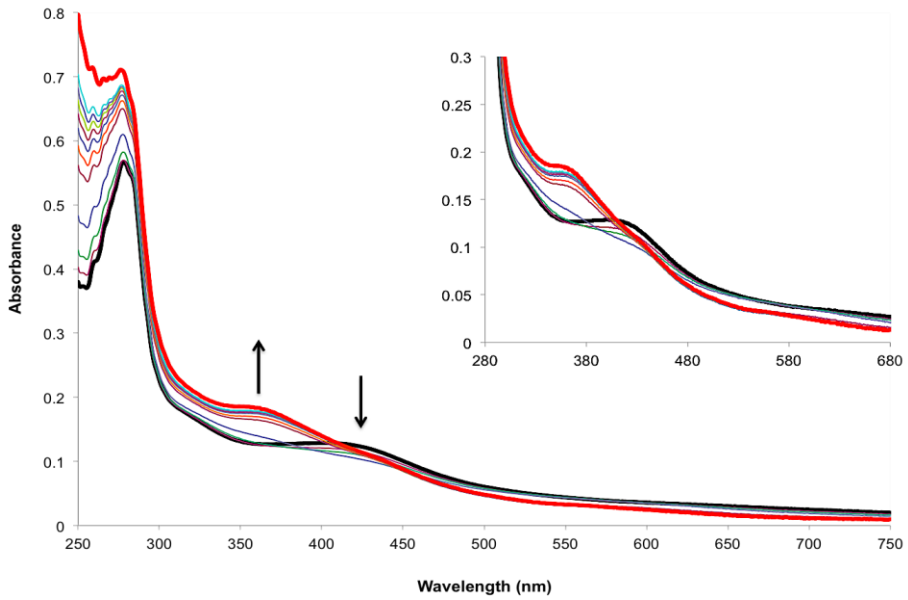

B

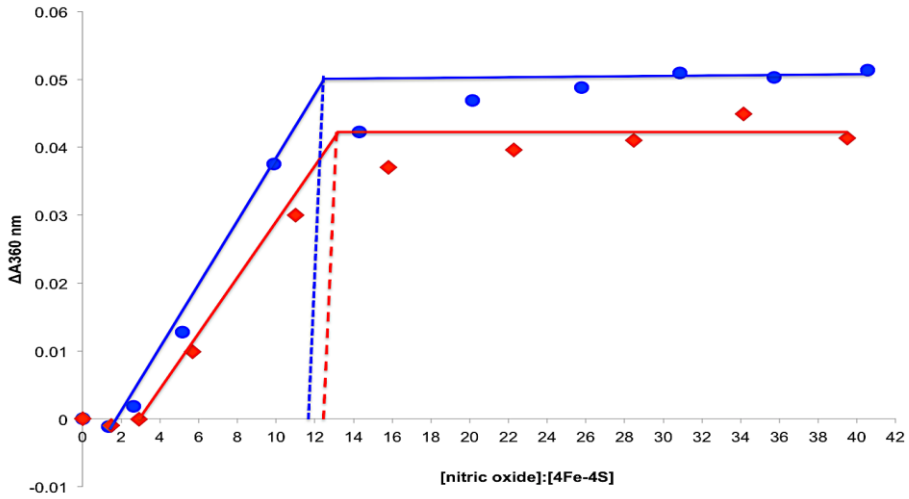

Figure 4.22: UV-visible spectroscopy of the reaction of [4Fe-4S] cluster of Tig-ANR with nitric oxide. (A) The spectra of holo-Tig-ANR (~7.0 μM cluster) with increasing concentrations of nitric oxide from Proli NONOate (5.2, 10.3, 20.2, 39, 56, 79, 101, 121, 140, 159 and 216 μM) under anaerobic conditions. The arrows show the increase in absorbance at 360 nm and decrease in absorbance at 420 nm as a result of the formation of a nitrosylated cluster. **(B)** Changes in absorbance at 360 nm for two repeated experiments were plotted against the ratio of [nitric oxide]:[4Fe-4S]. These reactions were carried out in collaboration with Dr. M. Stapleton.

A

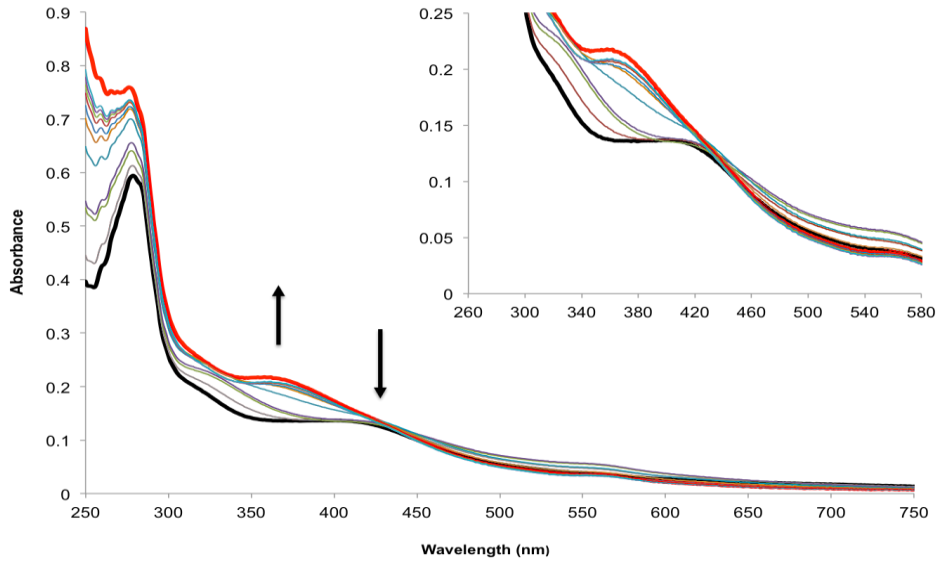

B

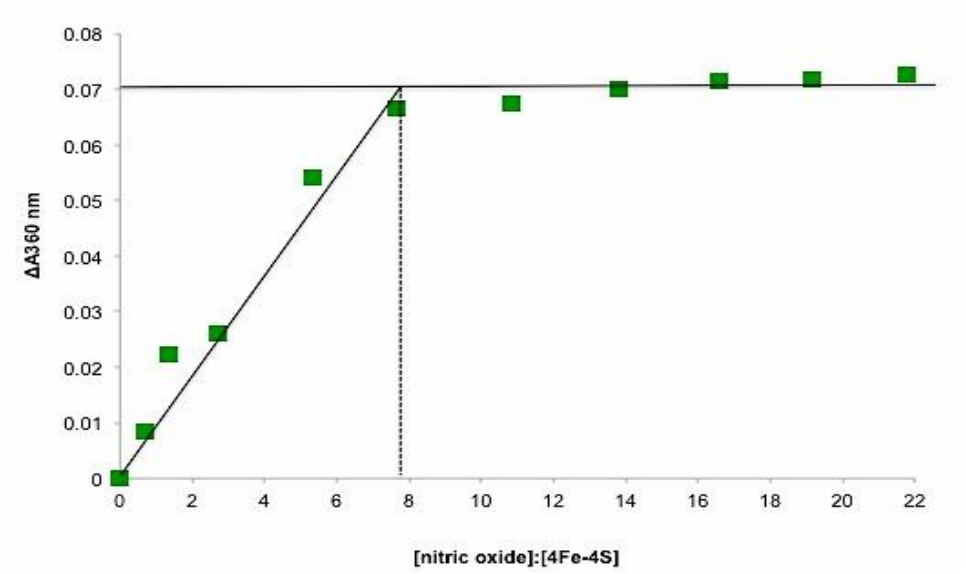

Figure 4.23: UV-visible spectroscopy of the reaction of [4Fe-4S] cluster of Tig-PP_3287 with nitric oxide. **(A)** The spectra of holo-Tig-PP_3287 (~7.6 μM cluster) with increasing concentrations of nitric oxide from Proli NONOate (5.2, 10.3, 20.2, 39, 56, 79, 101, 121, 140, 159 and 216 μM) under anaerobic conditions. The arrows show the increase in absorbance at 360 nm and decrease in absorbance at 420 nm as a result of formation of a nitrosylated cluster. **(B)** Changes in absorbance at 360 nm were plotted against the ratio of [nitric oxide]:[4Fe-4S]. These reactions were carried out in collaboration with Dr. M. Stapleton.

4.5.2 Kinetics of Tig-ANR and Tig-PP_3287 [4Fe-4S] clusters reacting with nitric oxide

Reactions of the [4Fe-4S] clusters of Tig-ANR and Tig-PP_3287 with nitric oxide were measured by detecting the changes in absorbance at 350 nm. Reactions were modelled according to Sutton *et al*., (2004) for the FNR O_2 reaction (Section 3.3.6). Reactions were initiated by injecting nitric oxide from Proli NONOate (final concentration ~100 µM nitric oxide) through the seal into anaerobic cuvettes containing holo-Tig-ANR (~8.3 µM cluster) and holo-Tig-PP_3287 (~9.3 µM cluster) at 25°C (Sections 2.7.10; 2.7.11). Changes in absorbance at 350 nm were measured and monitored to record the conversion of the [4Fe-4S] cluster of Tig-ANR (Figures 4.24A) and Tig-PP_3287 (Figure 4.25A). Three phases were detected at 350 nm that suggested three reaction steps A → B → C → D.The data were best fitted to a series of single or double exponential functions (as appropriate) by Dr. Jason Crack, University of East Anglia (Section 2.7.11) with observed rate constants (k_{obs}) as shown below for Tig-ANR (Figures 4.24B) and Tig-PP_3287 (Figure 4.25B):

Tig-ANR

Reaction steps	**Observed rate constants (k_{obs})**
A → B (Phase 1)	0.182 ± 0.003 s^{-1}
B →C (Phase 2)	0.033 ± 0.0008 s^{-1}
C →D (Phase 3)	0.005 ± 0.000008 s^{-1}

Tig-PP_3287

Reaction steps	**Observed rate constants (k_{obs})**
A → B (Phase 1)	0.123 ± 0.001 s^{-1}
B → C (Phase 2)	0.021 ± 0.00006 s^{-1}
C → D (Phase 3)	0.0002 ± 0.000097 s^{-1}

Division of the observed rate constants by the nitric oxide concentration provides an estimate of the apparent second order rate constants ($M^{-1}s^{-1}$) for the three phases for Tig-ANR and Tig-PP_3287 respectively:

Tig-ANR

Reaction steps	**Rate constants ($M^{-1}s^{-1}$)**
A → B (Phase 1)	1.82 x10^3
B → C (Phase 2)	3.3 x10^2
C → D (Phase 3)	50

Tig-PP_3287

Reaction steps	**Rate constants ($M^{-1}s^{-1}$)**
A → B (Phase 1)	1.23 x10^3
B → C (Phase 2)	2.1 x10^2
C → D (Phase 3)	2.0

The observation of three phases reactions of Tig-ANR and Tig-PP_3287 with nitric oxide are similar that reported for *E. coli* FNR and WbiB-like protein reactions with nitric oxide (Crack *et al*., 2011, Crack *et al*., 2013). The responses of Tig-ANR and Tig-PP_3287 to nitric oxide were apparently much slower than that previously reported for *E. coli* FNR (A → B 2.81 x10^5 $M^{-1}s^{-1}$; B →C 1.89 x10^4 $M^{-1}s^{-1}$; C → D 0.75 x10^3 $M^{-1}s^{-1}$; Crack *et al*., 2013). In addition, the response of Tig-PP_3287 was slower than Tig-ANR. This suggested that proteins possess different solvent accessibility and not all [4Fe-4S] cluster proteins possess the same reactivity with nitric oxide (Varghese *et al*., 2003, Duan *et al*., 2009).

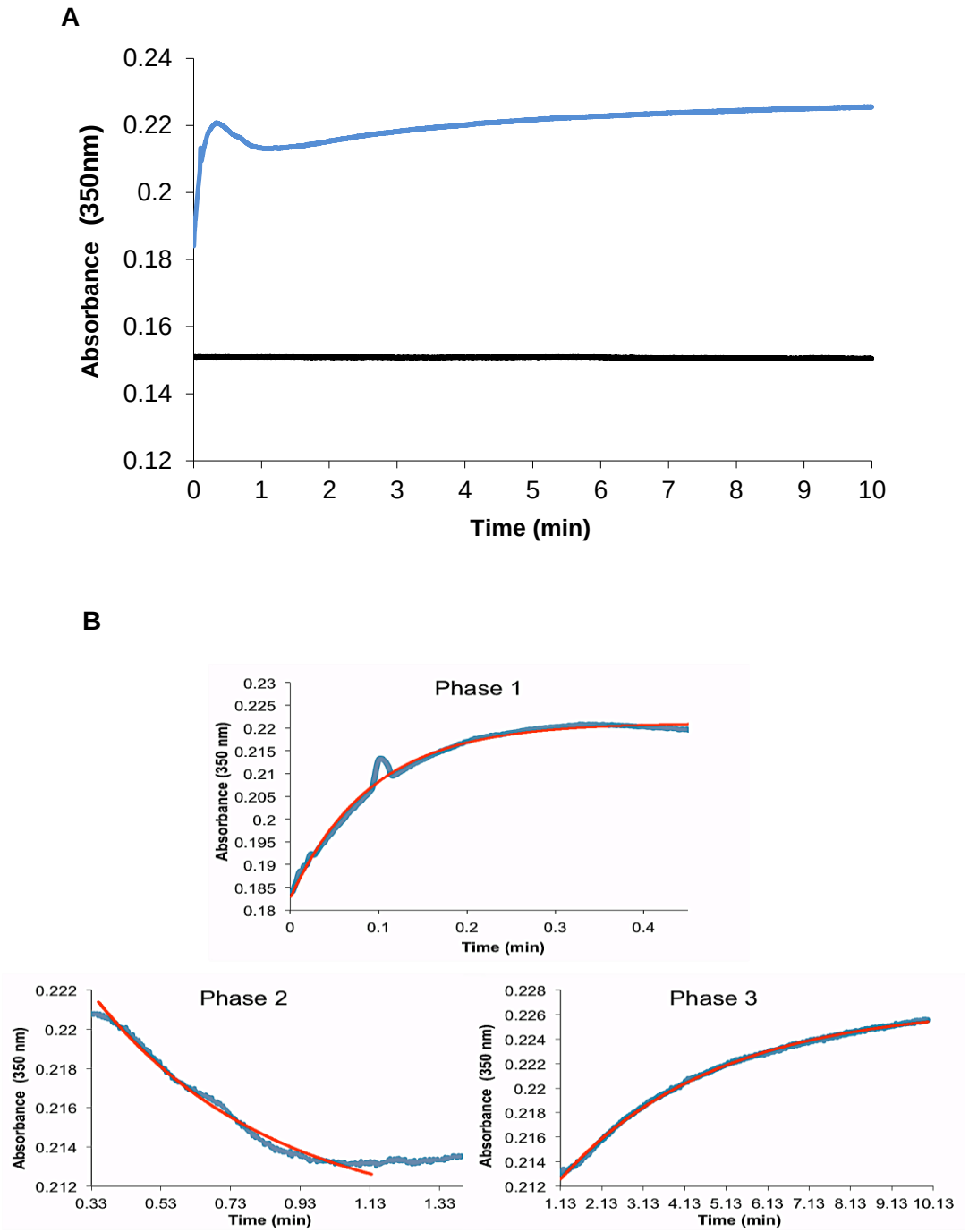

Figure 4.24: Reaction of [4Fe-4S] cluster of Tig-ANR with nitric oxide. (A) Holo-Tig-ANR (~8.3 μM cluster) interacted with ~100 μM nitric oxide from Proli NONOate. The change in absorbance at 350 nm was recorded. **(B)** Fitting data for three phases are showed in red lines. These data were fitted by Dr. Jason Crack, University of East Anglia. This reaction was average of three replicates and was carried out with collaboration with Dr. M. Stapleton.

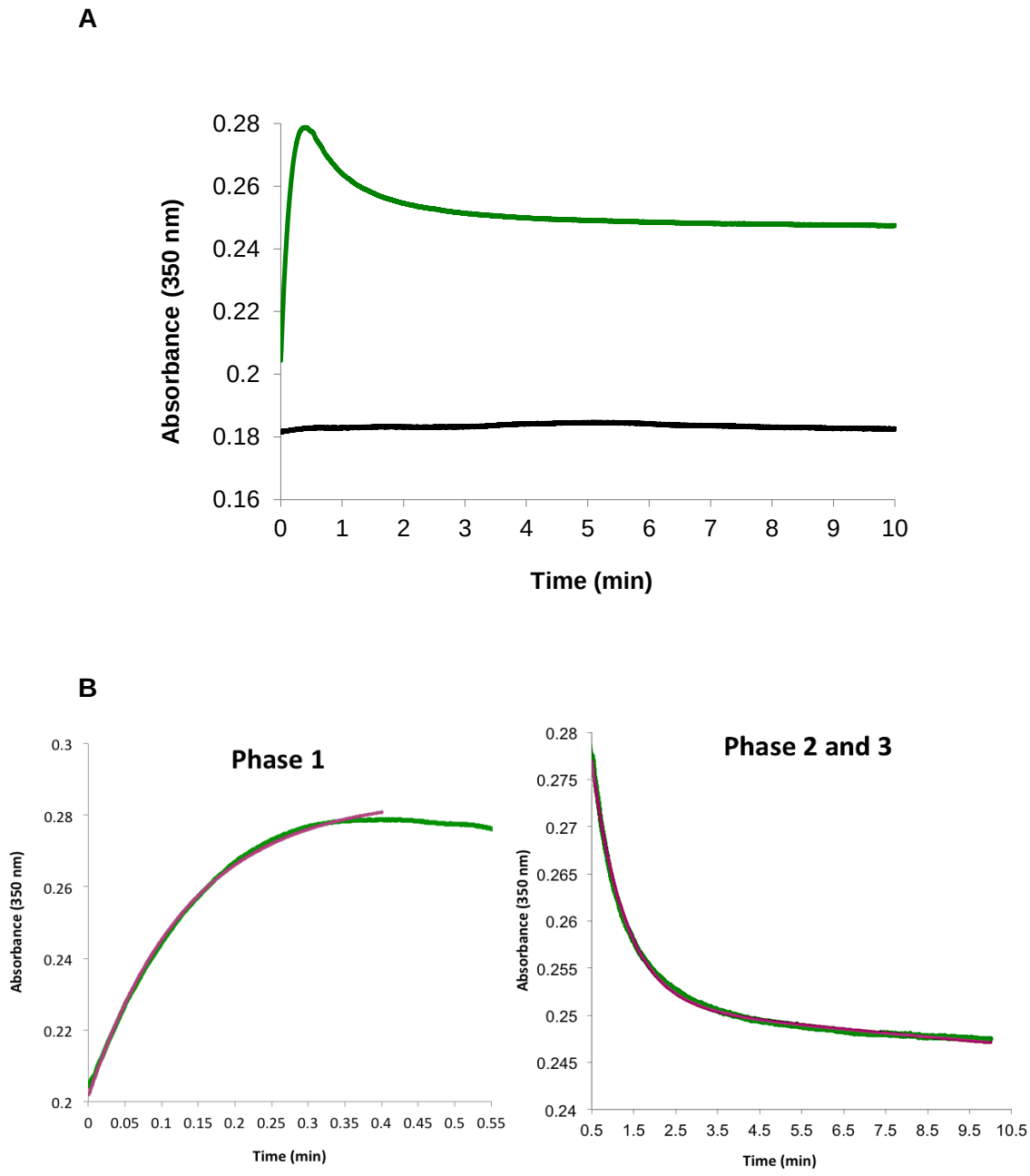

Figure 4.25: Reaction of [4Fe-4S] cluster of holo-PP_3287 with nitric oxide. (A) Holo-PP_3287 (~9.3 µM cluster) interacted with ~100 µM nitric oxide from Proli NONOate. The change in absorbance at 350 nm was recorded. **(B)** Fitting data for three phases are showed in red lines. These data were fitted by Dr. Jason Crack, University of East Anglia. This reaction was average of three replicates and was carried out in collaboration with Dr. M. Stapleton.

4.6 Discussion

Characterisation of *P. putida* FNR proteins: ANR, PP_3233 and PP_3287 showed that they act as O_2-sensitive transcription factors. All three regulators, ANR, PP_3233 and PP_3287 acquired [4Fe-4S] clusters under anaerobic conditions. Reactions of the [4Fe-4S] cluster of ANR, PP_3233 and PP_3287 with O_2 proceeded via a similar mechanism as that described for *E. coli* FNR (Figure 3.18; Crack *et al*., 2004, Crack *et al*., 2007). The spectroscopic data indicated that Tig-ANR and untagged-ANR proteins undergo similar reaction with O_2, which suggested that Tig-tag did not affect the properties of the iron-sulfur cluster or impair O_2-mediated cluster conversion.

The kinetic data showed that the reaction of Tig-ANR [4Fe-4S] cluster was similar to untagged-ANR (Figure 3.9) indicating that the Tig-tag did not influence the iron-sulfur cluster activity. Holo-ANR showed similar sensitivity to O_2 as *E. coli* FNR (Figure 4.9A; Crack *et al*., 2007). However, the [4Fe-4S] clusters of PP_3233 and PP_3287 showed slower reactions with O_2. The kinetic data for reactions of the PP_3233 and PP_3287 [4Fe-4S] clusters with O_2 fitted well to a single-, rather than double-, exponential function, implying that, unlike FNR and ANR, the initial cluster oxidation step to generate the $[3Fe\text{-}4S]^{1+}$ intermediate (Section 3.5, Eq. 3.1) was much slower than the subsequent decay of the $[3Fe\text{-}4S]^{1+}$ to the $[2Fe\text{-}2S]^{2+}$ form (Section 3.5, Eq. 3.2 and 3.3; Figure 4.9B and 4.9C). Thus, it is suggested that the mechanism for [4Fe-4S] to [2Fe-2S] cluster conversion in PP_3233 and PP_3287 was similar to that described for FNR (Crack *et al*., 2007) and ANR, but the PP_3233 and PP_3287 [4Fe-4S] clusters appear to be more stable when exposed to air. The relative rates of ANR, PP_3233 and PP_3287 cluster reactions with O_2 could therefore result in differential responses to O_2 availability.

Transcription factors that utilize iron-sulfur clusters as sensory modules have been shown to respond to O_2 (e.g. FNR), redox state (e.g. SoxR), nitric oxide (e.g. NsrR) and iron-sulfur cluster/iron homeostasis (e.g. IscR) (Crack *et al*., 2012b). Some of these transcription factors respond to more than one of these signals. Hence, the *E. coli* FNR and SoxR proteins respond to nitric oxide in addition to their primary signals, O_2 and redox cycling, respectively. *In vitro* kinetic measurements with the [4Fe-4S] form of FNR indicated that it is much more sensitive to nitric oxide than it is to O_2. However, *in vivo*, FNR is only nitrosylated when the major nitric oxide sensors (e.g. NsrR and NorR) and detoxification systems (e.g. NorVW, NrfA and Hmp) are overwhelmed. Thus, FNR serves primarily as an O_2 sensor with a

secondary nitric oxide sensing role (Crack *et al*., 2013). By contrast, the iron-sulfur clusters of regulators that are primarily nitric oxide sensors (e.g. NsrR and Wbl proteins) or redox sensors (e.g. SoxR) are generally stable for several hours in the presence of O_2 (Bodenmiller and Spiro, 2006, Filenko *et al*., 2007, Smith *et al*., 2010, Crack *et al*., 2011, Singh *et al*., 2013).

Reactions of ANR and PP_3287 with nitric oxide showed slow reactions compared with *E. coli* FNR (Crack *et al*., 2013). However, the reaction of PP_3233 with nitric oxide showed a minor change in spectra at 360 nm and 420 nm indicating that the [4Fe-4S] cluster of PP_3233 was not sensitive to nitric oxide (Figure 4.20).

Titration ANR and PP_3287 with increasing concentrations of nitric oxide indicated that iron-sulfur clusters were nitrosylated. In addition, the results showed that ~8-10 molecules of nitric oxide were required to nitrosylate one [4Fe-4S] cluster of ANR (Figure 4.22B) and PP_3287 (Figure 4.23B). These observations are similar to that described previously for the [4Fe-4S] cluster of FNR which exhibited a fast and multi-step reaction, which required eight molecules of nitric oxide per cluster to complete the reaction (Cruz-Ramos *et al*., 2002, Crack *et al*., 2013). Furthermore, Crack *et al*., (2001) reported that the [4Fe-4S] cluster of *Streptomyces coelicolor* WhiD and *Mycobacterium tuberculosis* WhiBI respond to nitric oxide by a similar rapid and multi-phasic reaction that involves eight molecules of nitric oxide per cluster (Crack *et al*., 2011).

As shown in Section 4.5.2, Figure 4.24 and Figure 4.25, reactions of ANR and PP_3287 with nitric oxide occurred in a three-step reaction. The first step A → B is suggested to consist of binding of one nitric oxide molecule to the [4Fe-4S] cluster, which is fastest step. This leads to further binding of nitric oxide in steps B → C and C → D. For FNR, and Wb1 proteins three steps are first order with respect to nitric oxide, which indicates that either one nitric oxide is included in each or the nitric oxide binding to each iron of the cluster happens independently. Overall, it is likely that nitrosylation of [4Fe-4S] cluster of ANR and PP_3287 resulted in formation of octa-nitrosylated clusters. Similar observations were seen for [4Fe-4S] clusters of FNR and WhiBI in response to nitric oxide (Figure 4.26).

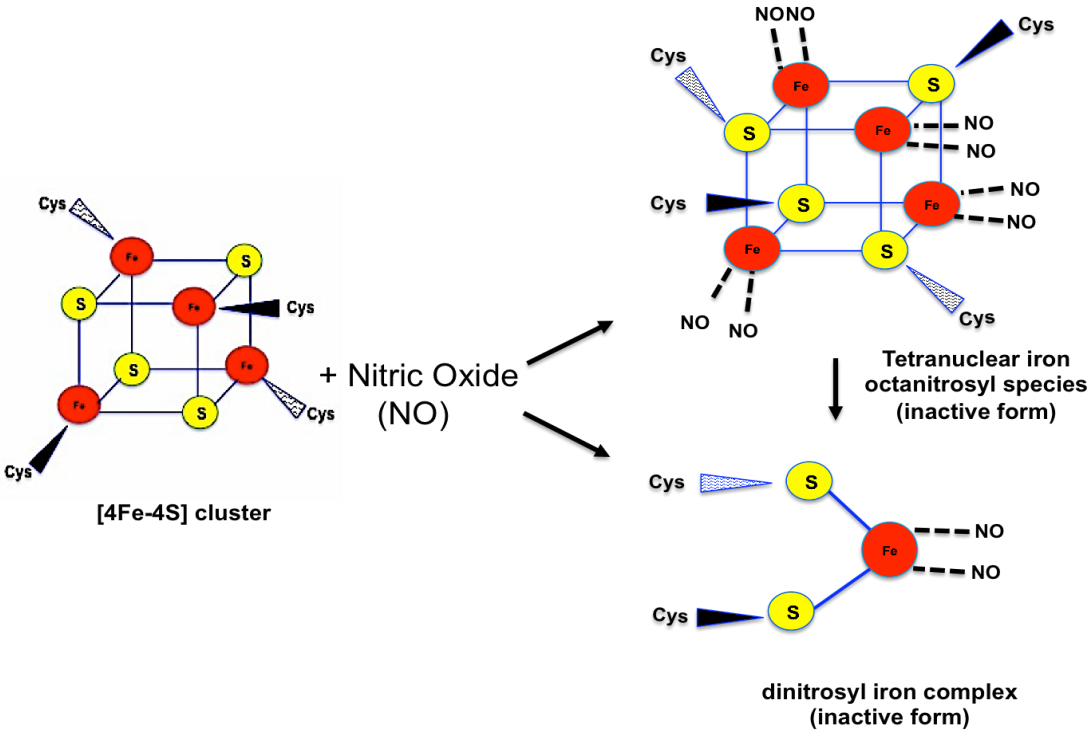

Figure 4.26: Figure illustrates the reaction of *P. putida* FNR proteins with nitric oxide under anaerobic conditions. ANR and PP_3287 respond to nitric oxide similar to O_2 resulting an inactive form. The reaction of [4Fe-4S] cluster with nitric oxide leads to nitrosylation and yields an octa-nitrosylated form and dinitrosyl iron complexes. Figure adapted from Crack *et al*. (2012a) and Green *et al*. (2013).

The *E. coli* FNR residues Glu-209, Ser-212 and Arg-213 in the DNA-binding domain play a major role in the interactions with the FNR box (TTGAT----ATCAA; FF site) (Lodge *et al*., 1990, Zimmermann *et al*., 1991). Amino acid analysis of *P. putida* FNR proteins showed similar sequences to FNR except PP_3287 possesses Cys in place of Ser (Figure 3.1), indicating that PP_3233 and PP_3287 could bind the FF site. EMSAs indicated that holo-PP_3233 and holo-PP_3287 could recognise the FF site under anaerobic conditions (Figure 4.14A; Figure 4.16A), but apo-PP_3233 and apo-3287 could not (Figure 4.15; Figure 4.17). These data suggest that PP_3233 and PP_3287 are active anaerobically because of the [4Fe-4S] clusters that enhance DNA-binding under anaerobic conditions like *E. coli* FNR and *P. putida* ANR (Section 3.4.1; Figure 3.15). Furthermore, holo-PP_3233 and holo-PP_3287 could recognise the CC site under anaerobic conditions (Figure 4.14B; Figure 4.16B) and in that regard resemble *E. coli* FNR, which binds to CC site (GTGAT - - - - ATCAC; CRP binding site) *in vivo* (Sawers *et al*., 1997).

To conclude, *P. putida* ANR, PP_3233 and PP_3287 are O_2-responsive DNA-binding protein, which respond to alteration in O_2 concentration via assembly and disassembly of their iron-sulfur clusters. ANR resembles *E. coli* FNR and responds to low concentration of O_2, while PP_3233 and PP_3287 appear to be less sensitive to O_2.

Chapter 5

Activities of *Pseudomonas putida* KT2440 FNR proteins *in vivo*

5.0 Activities of *Pseudomonas putida* KT2440 FNR proteins *in vivo*

5.1 Introduction

Pseudomonas putida KT2440 possesses three FNR proteins: PP_4265 (ANR), PP_3233 and PP_3287. As shown in Chapters three and four, all three proteins are O_2-responsive DNA-binding proteins *in vitro*. EMSAs showed that all three *P. putida* FNR proteins could bind at an FF site (FNR box) in a [4Fe-4S] cluster dependent manner under anaerobic conditions.

To investigate the roles of the FNR proteins *in vivo* our collaborators in Germany created three double mutant strains in which two of three encoding genes of FNR proteins were deleted: JRG6723 (*P. putida* KT2440 Δ*3233*Δ*3287* (ANR^+)), JRG6722 (*P. putida* KT2440 Δ*anr*Δ*3287* (PP_3233^+)) and JRG6721 (*P. putida* KT2440 Δ*anr*Δ*3233* (PP_3287^+)) (Table 2.1; Section 2.6.11). Here, this shown that the properties of *P. putida* FNR proteins *in vivo* were consistent with those *in vitro*. Hence, *P. putida* PP_3233 and PP_3287 are sensitive to O_2, but they are less responsive than ANR, potentially extending the range of O_2-responsive gene regulation in this bacterium.

5.2 *Pseudomonas putida* strains lacking either PP_3233 or PP_3287 exhibit an aerobic growth defect; strains lacking ANR are impaired in low O_2 environments

The primary and secondary cultures of *P. putida* KT2440 strains (wild type and mutants) were prepared (Section 2.4.2; Section 2.4.10). Cultures were grown under O_2-limited conditions (40 mL of LB medium in 50 mL shaking conical flask) and aerobic conditions (10 mL of LB medium in 50 mL shaking conical flask) at 30°C/200 rpm. The OD_{600} was taken to measure the growth for all strains and plotted against time (Figure 5.1). The results showed that cultures that express only ANR^+, PP_3233^+ or PP_3287^+ (Table 2.1) were impaired under aerobic conditions (Figure 5.1A). In contrast, under low O_2 conditions the cultures of that expresses only ANR was enhanced while, the strains that lack ANR (*P. putida* JRG6722, expresses only PP_3233^+; and *P. putida* JRG6721, expresses only PP_3287^+) were impaired (Figure 5.1B). These results are consistent with responses of the iron-sulfur clusters of the ANR, PP_3233 and PP_3287 to O_2 *in vitro* (Chapter four).

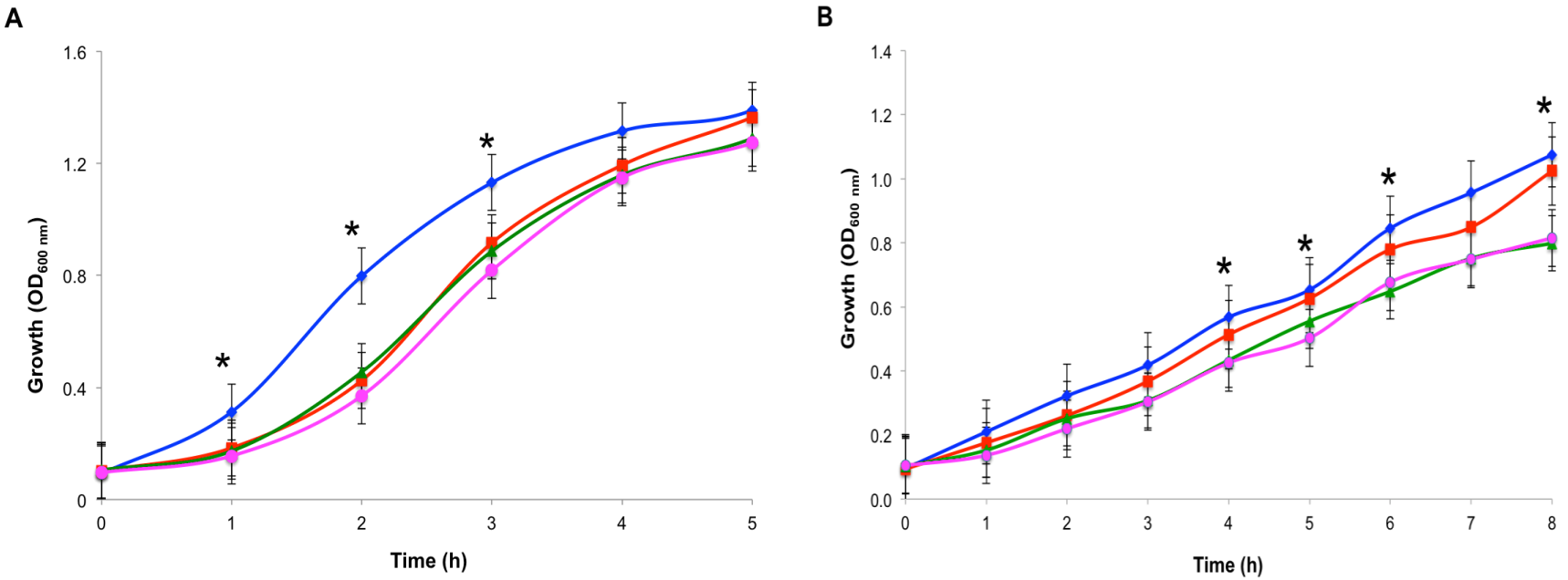

Figure 5.1: Growth of *P. putida* KT2440 under aerobic and O_2-limited conditions. *Pseudomonas putida* mutants that lack two of three *fnr* genes present in the wild-type strain were grown under **(A)** aerobic conditions (10 mL of medium in 50 mL conical flask with shaking at 200 rpm at 30°C) or **(B)** O_2-limited conditions (40 mL of medium in 50 mL flasks with shaking at 200 rpm at 30°C). Growth was monitored by measuring the optical density of the cultures (OD_{600} nm). Wild-type (ANR^+, PP_3233^+ and PP_3287^+; filled diamonds); JRG6723 (ANR^+; filled squares); JRG6722 (PP_3233^+; filled triangles); JRG6721 (PP_3287^+; filled circles). The data-points show the means and standard deviations (n=6). * Indicates a significant difference between: (A) wild type and all the mutant strains (B) strains possessing the *anr* gene (wild type and JRG6723) and those lacking *anr* (JRG6721 and JRG6722) ($P \leq 0.05$).

5.3 *Pseudomonas putida* KT2440 strains transformed with reporter plasmid (pGS810)

Reporter plasmid pGS810 (FF-41.5-*lac*Z) was used to transform *P. putida* KT2440 strains (wild-type and mutants) (Section 2.4.9). The resultant colonies were blue on LB/tetracycline 35 µg/mL/X-gal/IPTG plates (Figure 5.2A). For comparison, the *P. putida* KT2440 strains (wild-type and mutants) without the reporter plasmid yielded white colonies on LB-X-gal /IPTG plates (Figure 5.2B)

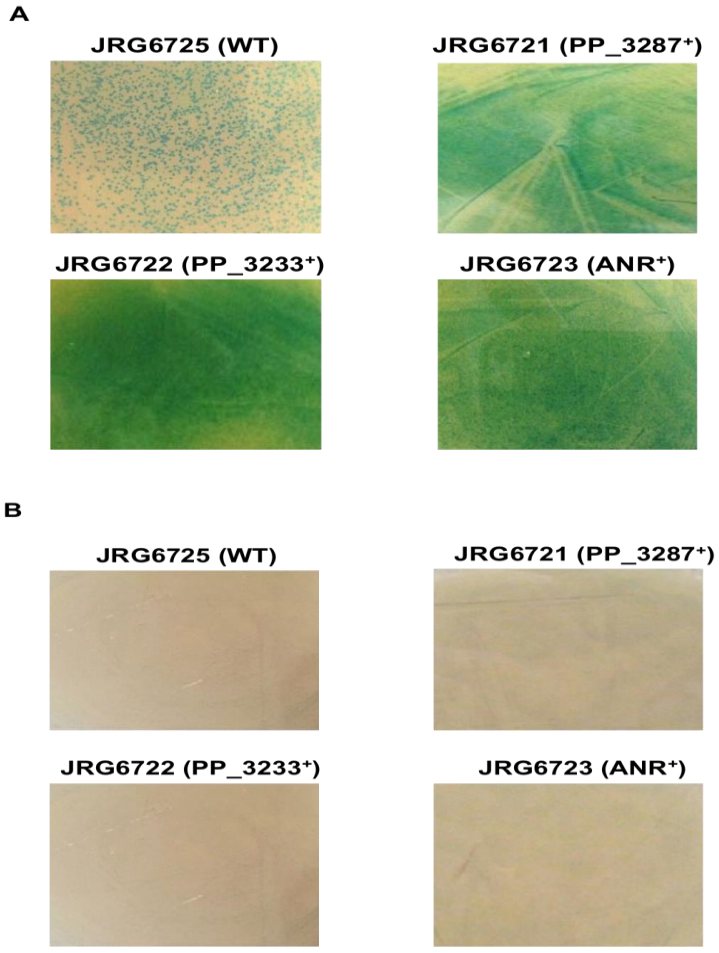

Figure 5.2: *Pseudomonas putida* KT2440 strains transformed with reporter plasmid (pGS810). (A) Transformed *P. putida* KT2440 strains (JRG6725 (wild type), JRG6723 (ANR$^+$), JRG6722 (PP_3233$^+$) and JRG6721 (PP_3287$^+$); Table 2.1) with pGS810 (FF-41.5-*lac*Z; Table 2.2) on LB plates containing tetracycline 35 µg/mL and X-gal/IPTG. **(B)** *Pseudomonas putida* KT2440 strains (JRG6725 (wild type), JRG6723 (ANR$^+$), JRG6722 (PP_3233$^+$) and JRG6721 (PP_3287$^+$)) with out plasmid on LB plates containing X-gal/IPTG. All plates were incubated at 30°C for 16 h.

5.4 ANR-dependent gene expression is enhanced ~5-fold under O_2-limited conditions *in vivo*

Measurement of ANR-dependent expression from the FF-41.5-*lac*Z promoter was carried out by measuring β-galactosidase activity according to Miller (1992) (Section 2.7.12). Cultures were grown in 50 mL shaking flasks containing 10, or 50 mL LB medium with tetracycline 35 µg/mL resulting in decreasing O_2 transfer rate as the volume of medium increased. Cultures were incubated at 30°C/200 rpm for 3 h. Growth was measured by recording the OD_{600} (Section 2.4.3).

Under O_2-limited conditions, the β-galactosidase assay for *P. putida* JRG6723 (ANR^+; Table 2.1) showed that ANR activity was enhanced ~5-fold in response to decrease aeration (Figure 5.3). This suggests that ANR is active under O_2-limited conditions, which is consistent with *in vitro* results (Chapter three). Thus, it was concluded that ANR has properties similar to *E. coli* FNR.

5.5 Cytoplasmic ANR concentration is similar under different aeration conditions

The concentration of *E. coli* FNR is similar under aerobic and anaerobic conditions. Changes in activity are not mediated by changes in protein concentration but by assembly and disassembly of the [4Fe-4S] clusters in response to O_2 concentration thus FNR can continuously monitor O_2 availability (Dibden and Green, 2005, Sutton *et al*., 2004, Unden and Duchene, 1987). *Pseudomonas putida* JRG6723, JRG6722 or JRG6721 that express only ANR^+, PP_3233^+ or PP_3287^+ were grown in 50 mL shaking conical flask containing 10, 20, 30, 40 or 50 mL of LB medium containing tetracycline 35 µg/mL at 30°C /200 rpm.

Antibodies raised against *E. coli* FNR protein only cross-reacted with ANR (Figure 5.4). The Western blots showed that the amount of ANR was similar in all the cultures grown under different aeration conditions (Figure 5.4), but increased aeration progressively lowered FF-41.5 promoter activity (Figure 5.4). Thus, it was concluded that ANR has properties similar to *E. coli* FNR and is a *bona fide* O_2-responsive gene regulator in *P. putida*.

Similar experiments with *P. putida* strains lacking the *anr* gene (*P. putida* JRG6722, expresses only PP_3233^+; and *P. putida* JRG6721, expresses only

PP_3287^{+}) showed only a small response to decreased aeration and low levels of β-galactosidase activities (128 ± 6 and 184 ± 3 Miller units respectively under O_2-limited conditions compared to ANR (8550 ± 54 Miller units; Figure 5.3). This could be a result of poor expression of these proteins under the conditions tested. Therefore, qRT-PCR was used to determine whether *PP_3233* and *PP_3287* were expressed in JRG6722 and JRG6721 respectively under the conditions tested.

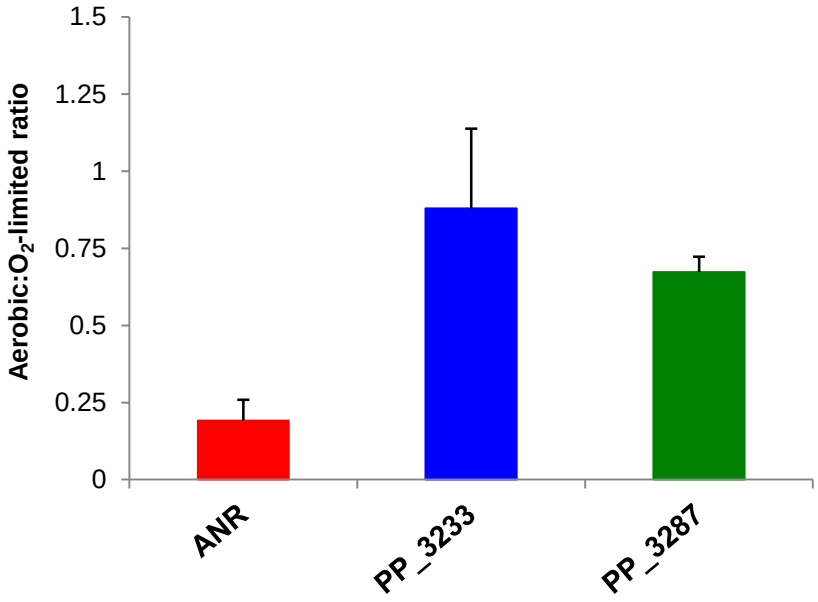

Figure 5.3: Responses of *P. putida* FNR proteins to O_2 *in vivo*. The output from an FNR-dependent promoter in response to enhanced aeration of *P. putida* JRG6723, JRG6722 and JRG6721 that express only ANR^{+}, PP_3233^{+} and PP_3287^{+} (Table 2.1) and transformed with the FF-41.5-*lac*Z reporter plasmid pGS810 (Table 2.2). The rate of culture aeration was increased by decreasing the volume of medium in shaking conical flasks (50 mL of medium for O_2-limited cultures, 10 mL for aerobic cultures). Cultures were grown at 30°C/200 rpm for 3 h, at which point samples were taken for measurement of β-galactosidase activity. The β-galactosidase activities of the aerobic cultures were divided by those of the O_2-limited cultures. The error bars are the standard deviation from the mean values of the aerobic:O_2-limited ratios (n=4). ANR, PP_3233 and PP_3287 indicate chromosomal expression of the corresponding genes.

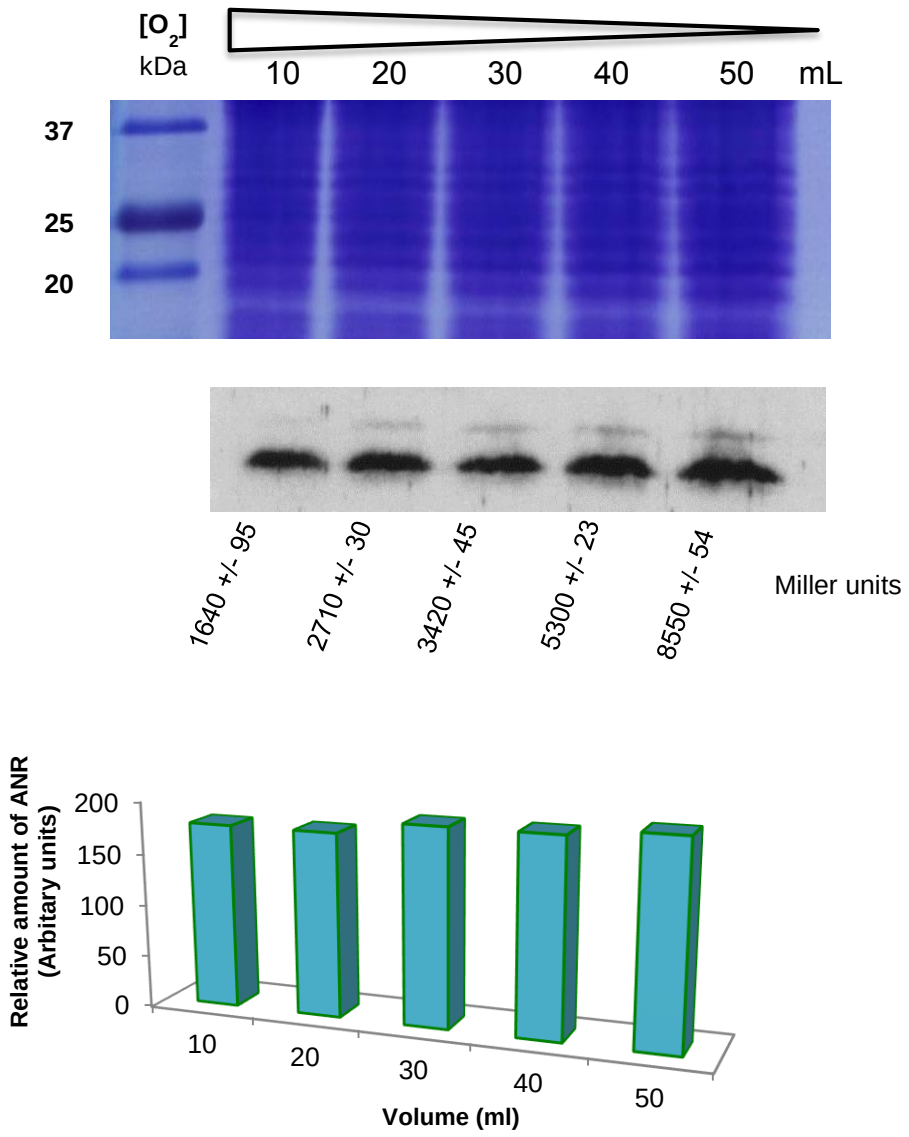

Figure 5.4: Concentration of cytoplasmic ANR does not respond to changes in culture aeration. Western blot developed with anti-serum raised against *E. coli* FNR for cell samples from *P. putida* JRG6723 cultures that express only ANR$^+$ grown in 50 mL shaking conical flasks containing 10, 20, 30, 40 or 50 mL medium to impose an increasing degree of O_2-limitation on the cultures. The equivalent region of a Coomassie blue stained gel is shown as a loading control. The outputs from the pFF-41.5 reporter (pGS810) for cultures grown as described (Section 5.4) are shown below each lane (mean values □ standard deviation, n=3). ImageJ software was used to determine the amount of ANR under different O_2 rate in blotting.

5.6 Expression of *PP_3233* is ~10-fold lower and *PP_3287* is ~5-fold lower than *anr*

Pseudomonas putida strains JRG6723, JRG6722 and JRG6721, which express ANR^+, PP_3233^+ or PP_3287^+ respectively (Table 2.1), were exposed to different O_2 transfer rates (Section 2.5.10A) and RNA samples were purified (Section 2.5.10B). The concentration of RNA samples were measured by Nanodrop and diluted to 20 ng/µl (Section 2.5.9B).

Levels of expression of four housekeeping genes: *gryB*, *gyrA*, *rpoD* and *gap-1* under different aeration conditions were studied using qRT-PCR (Section 2.5.10). The *gryB* and *gyrA* transcripts were chosen because the products of these genes are: the A and B subunits of the tetrameric holoenzyme gyrase. Gyrase is a DNA topoisomerase II and plays a crucial role in DNA replication, recombination and transcriptional regulation. DNA double strand break and re-joining is controlled by GyrA, while GyrB is the site of ATP hydrolysis and plays an important role in DNA supercoiling during replication (Kureishi *et al*., 1994). In addition, *rpoD* and *gap-1* were chosen because *rpoD* encodes the housekeeping sigma factor σ^{70} (Schnider *et al*., 1995) and *gap-1* encodes glyceraldehyde-3-phosphate dehydrogenase, which has important role in glycolysis (Daddaoua *et al*., 2014). Figure S1 (A, B, C and D) shows the expression of *gryB*, *gyrA*, *rpoD* and *gap-1* for the three *P. putida* mutant strains exposed to different O_2 transfer rates. The levels of expression of *anr*, *PP_3233* and *PP_3287* were compared. The data in Figure 5.5 were normalized to the *gyrB* level because *gyrB* expression was consistent in all strains under the tested conditions. The results were similar in all tested conditions and indicated that the level of expression of *PP_3233* was ~10-fold lower and *PP_3287* was ~5-fold lower than *anr*. Low levels of *PP_3233* and *PP_3287* mRNA were consistent with the hypothesis that expression of the three *P. putida* FNR proteins is likely to be temporally and/or spatially distinct because they recognise a common DNA sequence as discussed (Chapters three and four). Therefore, the expression of *PP_3233* and *PP_3287* genes was increased using p2490 (Table 2.2).

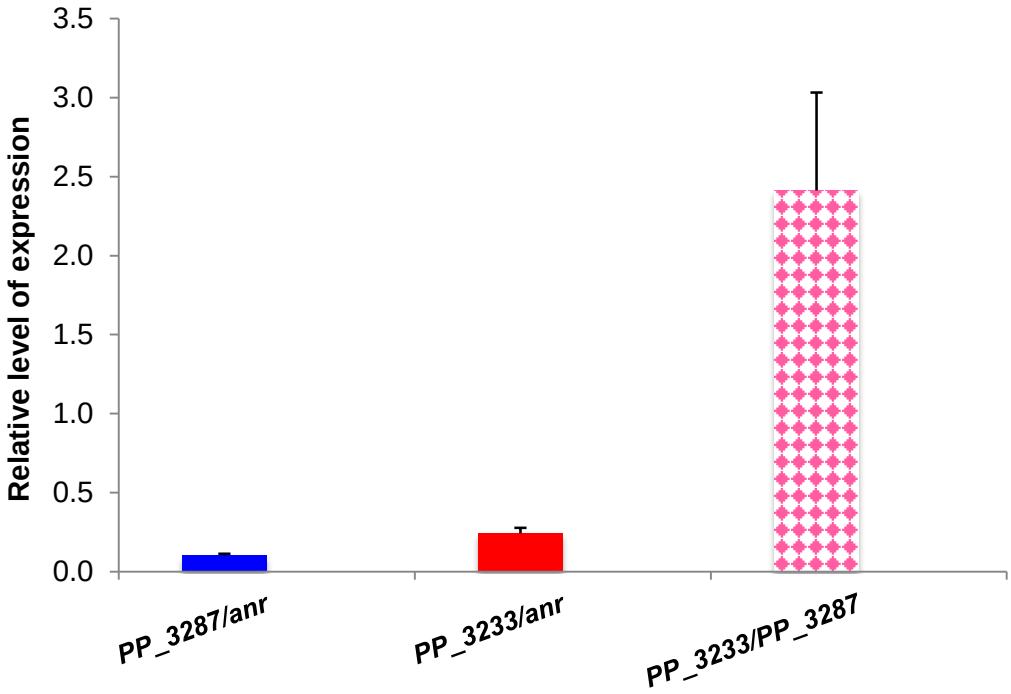

Figure 5.5: Expression of *anr*, *PP_3233* and *PP_3287* exposed to different O_2 transfer rate. Cultures of *P. putida* JRG6723, JRG6722 or JRG6721, which express ANR$^+$, PP_3233$^+$ or PP_3287$^+$ (Table 2.1) were grown in 50 mL shaking flasks containing increasing volume of LB medium (10, 20, 30, 40 or 50 mL) containing tetracycline 35 µg/mL at 30°C/200 rpm resulting in a decrease in O_2 concentration. The results were similar under all conditions tested. RNA samples were purified and diluted to 20 ng/µl after measuring the concentration (Section 2.5.9B). The expression level of *gyrB* was used to normalize expression levels of *anr*, *PP_3233* and *PP_3287*. Relative expression level of *PP_3233* and *PP_3287* RNA compared to *anr* are shown. Error bars are the standard division from the mean (n=4).

5.7 Activities of *PP_3233* and *PP_3287* are enhanced ~5-fold and ~2-fold respectively under O_2-limited conditions

The *PP_3233* and *PP_3287* open reading frames along with their own promoters were amplified from *P. putida* KT2440 genomic DNA and ligated into p2490 (Table 2.2) to give pGS2508 and pGS2509 respectively (Table 2.2; Section 2.6.12). The constructs were checked by double digestion using EcoRI and XhoI and DNA sequencing.

Plasmids pGS2508 and pGS810 were used to transform *P. putida* JRG6722. In addition, pGS2509 and pGS810 were used to transform *P. putida* JRG6721 (Table 2.1; Section 2.4.9). These *P. putida* strains that were capable of expressing only *PP_3233* from a multi-copy plasmid (PP_3233^{++}) or only *PP_3287* from a plasmid (PP_3287^{++}) were grown at 30°C/200 rpm (Section 5.4; Section 5.5). FNR-dependent expression from the FF-41.5-*lac*Z promoter was measured by determining the β-galacosidase activities of cultures expressing PP_3233^{++} and PP_3287^{++} (Section 2.7.12). The results indicated that PP_3233^{++} and PP_3287^{++} showed increasing activity in response to decreased aeration (Figure 5.6). qRT-PCR indicated that the expression of *PP_3233* and *PP_3287* was ~10-fold and ~5-fold respectively higher than that of chromosomal *anr* (Figure 5.7). Moreover, the *PP_3233* expression was ~2-fold higher than *PP_3287* (Figure 5.7). The results confirmed that *P. putida* PP_3233 and PP_3287 proteins are O_2-responsive transcription factors *in vivo*, consistent with their *in vitro* responses to O_2 (Chapter four).

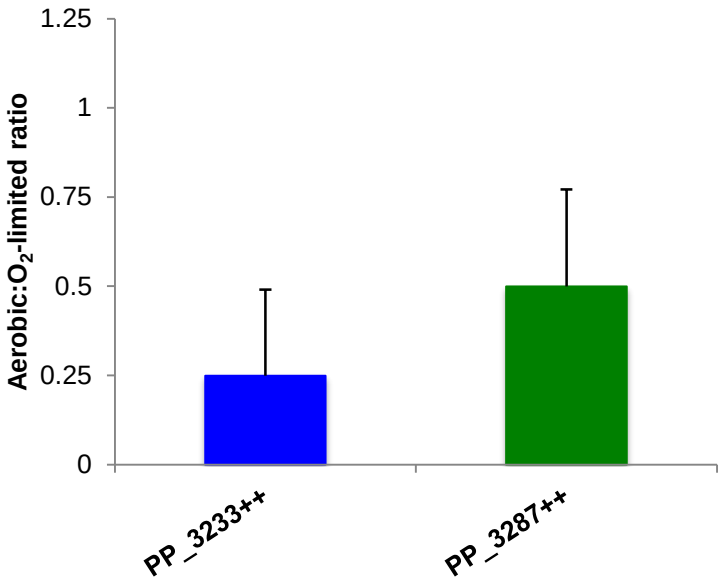

Figure 5.6: Responses of *P. putida* PP_3233 and PP_3287 proteins to O_2 *in vivo*. The output from an FNR-dependent promoter in response to enhanced aeration of *P. putida* JRG6722 and JRG6721 that express only *PP_3233* from multi-copy plasmid (PP_3233^{++}) and JRG6722 that expresses only *PP_3287* from multi-copy plasmid (PP_3287^{++}) (Table 2.1) and transformed with the FF-41.5-*lac*Z reporter plasmid pGS810 (Table 2.2). The rate of culture aeration was increased by decreasing the volume of medium in shaking conical flasks (50 mL of medium for O_2-limited cultures, 10 mL for aerobic cultures). Cultures were grown at 30°C/200 rpm for 3 h, at which point samples were taken for measurement of β-galactosidase activity. The β-galactosidase activities of the aerobic cultures were divided by those of the O_2-limited cultures. The error bars are the standard deviation from the mean values of the aerobic:O_2-limited ratios (n=4). PP_3233^{++} and PP_3287^{++} indicate expression of corresponding genes from a multi-copy plasmid.

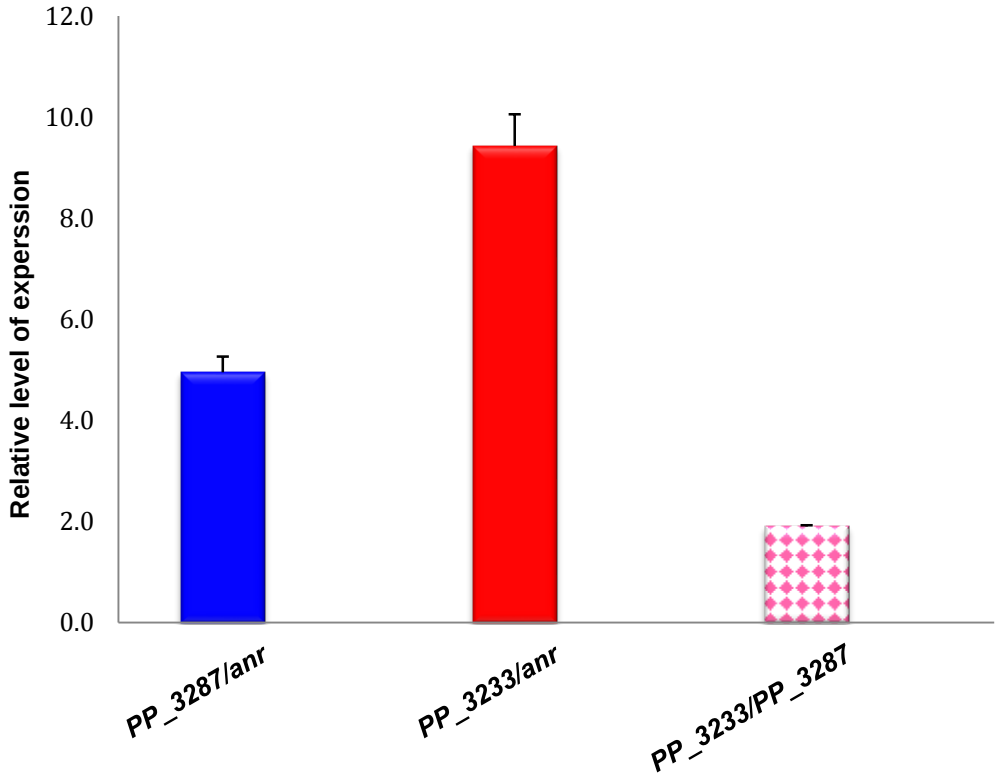

Figure 5.7: Expression of *PP_3233* and *PP_3287* under O_2-limited conditions. Cultures of *PP_3233* from multi-copy plasmid (PP_3233^{++}) and *PP_3287* from multi-copy plasmid (PP_3287^{++}) were grown in 50 mL shaking flasks containing increasing volume of LB medium (10, 20, 30, 40 or 50 mL) with tetracycline 35 µg/mL and gentamycin 20 µg/mL resulting in a decrease in O_2 transfer rate. The results were similar in all conditions tested. RNA samples were purified and diluted to 20 ng/µl after measuring the concentration (Section 2.5.9B). Results were normalized to *gyrB*. Relative expression levels of *PP_3233* and *PP_3287* RNA compared to chromosomal *anr* are shown. The error bars are the standard deviation from the mean (n=4).

To confirm the *in vivo* O_2-responsiveness of the *P. putida* FNR proteins, a heterologous reporter system, consisting of an *E. coli fnr*, *lac* double mutant (JRG6348; Table 2.1) with a chromosomal copy of the FNR-dependent FF-41.5 promoter fused to *lac*Z was transformed with pBAD-His-derviatives pGS2350, pGS2351, pGS2352 and pGS2353 (Table 2.2) that express *E. coli* FNR, *P. putida* ANR, PP_3233 or PP_3287 under the control of the pBAD promoter (Section 2.6.12). Cultures of JRG6348 expressing either vector (p2236; Table 2.2), *E. coli* FNR, *P. putida* ANR, PP_3233 or PP_3287 (Table 2.1) were grown in sealed tubes filled to neck in M9 medium under anaerobic conditions (Section 2.4.1). RNA samples were purified (Section 2.5.9). The decrease in *lac*Z transcript abundance was measured by qRT-PCR after exposure of the anaerobic cultures to O_2 for 20 min. This showed that the activities of *E. coli* FNR and all three *P. putida* regulators decreased, with FNR- and ANR- dependent transcription showing the greatest responses. PP_3233 and PP_3287 were less responsive (Figure 5.8). The lesser responses of PP_3233 and PP_3287 suggested that these proteins were less sensitive to O_2 compared to FNR and ANR, consistent with the *in vitro* data presented in Chapters three and four.

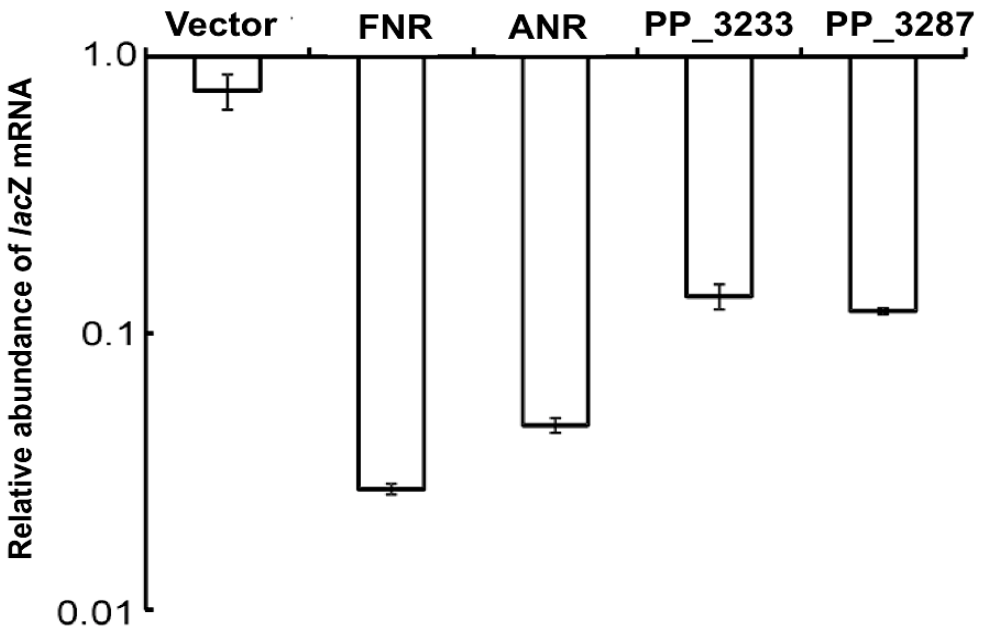

Figure 5.8: Inactivation of FNR proteins upon exposure of anaerobic cultures to O_2. Cultures of *E. coli* JRG6348 expressing either no FNR (vector), *E. coli* FNR, *P. putida* ANR, PP_3233 or PP_3287, as indicated, were grown under anaerobic conditions and the abundance of FNR-protein-dependent *lac*Z transcription was measured by qRT-PCR. The cultures were exposed to air for 20 min and then the abundance of the *lac*Z transcript was measured again. The relative abundances of *lac*Z RNA before and after transfer to aerobic conditions is shown. The error bars are the standard deviation from the mean (n=3). This experiment was carried out in collaboration with Dr. M. Stapleton (Ibrahim *et al*., 2015).

5.8 ANR responds to nitric oxide *in vivo*

The exposure of *E. coli* FNR to nitric oxide from exogenous donors at micromolar concentrations led to nitrosylation of the iron-sulfur cluster and altered the expression of FNR-regulated genes (Cruz-Ramos *et al*., 2002, Pullan *et al*., 2007, Crack *et al*., 2013). To investigate the response of ANR to nitric oxide and redox stress *in vivo*, *P. putida* JRG6723 (Table 2.1) transformed with pGS810 (Table 2.2) was exposed to anaerobic conditions and exogenous nitric oxide using NOC-7 (Section 2.7.10). At the same time, the strain was grown under aerobic conditions in the presence of the redox agent paraquat (PQ). LB medium was used for aerobic cultures and medium 154 supplemented with 0.4% yeast extract and 30 mM L-arginine was for anaerobic cultures, both were supplemented with tetracycline (35 µg/mL) (Section 2.4.1 and 2.7.14). The responses of ANR-dependent expression from the FF-41.5 promoter were determined by measuring β-galactosidase activity (Section 2.7.12) for aerobic, aerobic plus PQ (200 µM), anaerobic, anaerobic plus NOC-7 (20 µM) for 3 h at 30°C/200 rpm (Figure 5.9). This experiment showed that ANR activity was lowered under aerobic conditions as well as in the presence of nitric oxide donors (Figure 5.9). However, the ANR activity did not change in response to PQ (200 µM, blue bar) compared to aerobic growth (Figure 5.9). Thus, it was concluded that *in vivo* ANR has a similar response to anaerobic conditions and nitric oxide to that of *E. coli* FNR. This suggested that ANR is a potential nitric oxide sensor in addition to its O_2- sensing role.

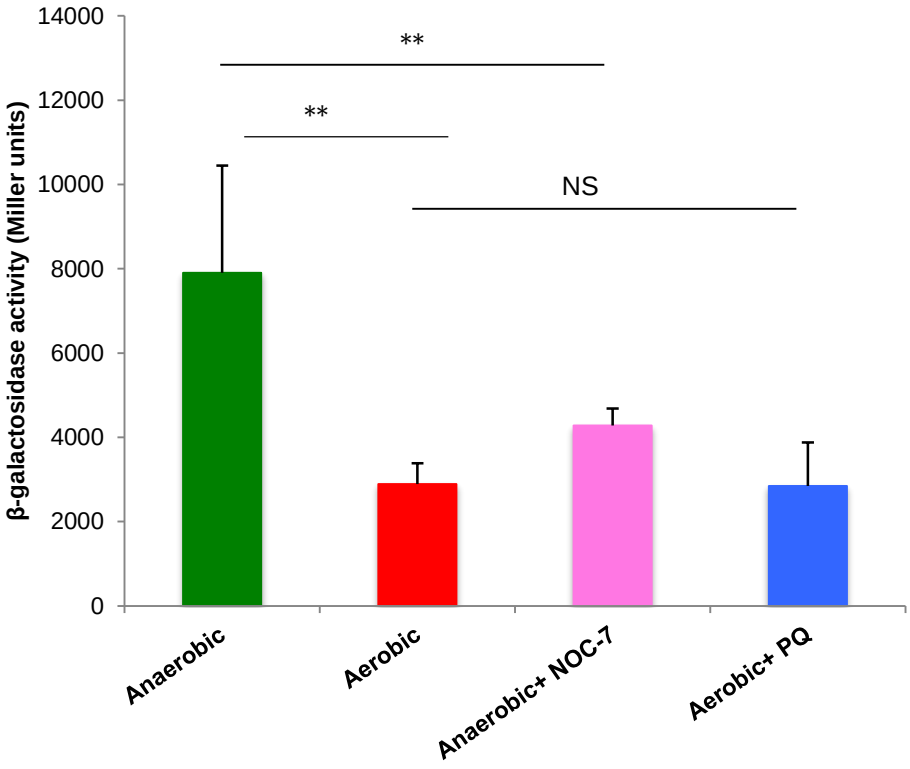

Figure 5.9: *In vivo* ANR transcription in response to nitric oxide and oxidative stress. Cultures of JRG6723 (Table 2.1) that express *anr* from chromosome (ANR^+) only with pGS810 (Table 2.2) were grown in LB medium for aerobic growth and medium 154 for anaerobic growth (Section 2.4.1). The cultures were exposed to aerobic (50 mL flask containing 10 mL medium, red bar), aerobic plus PQ (200 µM, blue bar), anaerobic conditions (sealed 50 mL flasks filled with 50 mL medium, green bar), anaerobic plus NOC-7 as a nitric oxide exogenous donor (20 µM, pink bar) for 3 h at 30°C/200 rpm. Culture supplemented with NOC-7 was incubated in the anaerobic cabinet and the reagent was injected with a Hamilton syringe through a seal into the cultures and mixed. After incubation, the β-galactosidase activities were measured in triplicate. The error bars are the standard deviation from the mean (n=3). *P* values were determined *t* test. **, *P* <0.01; NS, *P* >0.5.

5.9 PP-3287 and PP_3233 do not respond to nitric oxide *in vivo*

The responses of PP_3287 and PP_3233 to nitric oxide and oxidative stress *in vivo* were investigated. The strains JRG6721 and JRG6722 (Table 2.1) expressed only *PP-3287* from a multi-copy plasmid (PP_3287^{++}) (pGS2509, Table 2.2) and only *PP_3233* from a multi-copy plasmid (PP_3233^{++}) (pGS2508, Table 2.2) were transformed with pGS810 (Table 2.2). *Pseudomonas putida* JRG6721 and JRG6722 were exposed to nitric oxide and oxidative stress as described for *P. putida* JRG6723 (Section 5.8). The cultures were grown aerobically in LB medium and anaerobically in medium 154 supplemented tetracycline (35 µg/mL) and gentamicin (20 µg/mL) at 30°C/200 rpm for 3 h (Section 3.3.9; Section 2.4.1 and Section 2.7.14). After incubation, the β-galactosidase activities were measured (Section 2.7.12). This experiment showed that PP_3287 and PP_3233 activity was higher under anaerobic conditions than aerobic conditions (Figure 5.10, green bar; Figure 5.11, green bar). However, nitric oxide had little or no effect on the activity of PP_3287 and PP_3233 under anaerobic conditions. In addition, paraquat had no effect under aerobic conditions (Figures 5.10; Figure 5.11). Thus, it was concluded that PP_3287 and PP_3233 are O_2 sensors. Although PP_3287 and PP_3233 showed similar response to O_2 under anaerobic conditions, they were less responsive to O_2 than ANR *in vivo* (Figure 5.9).

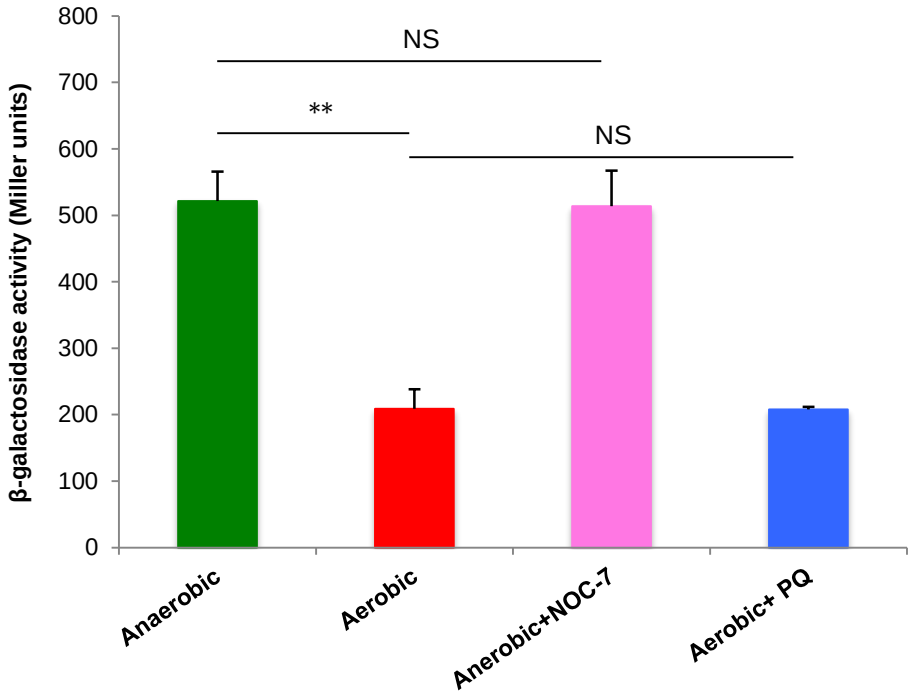

Figure 5.10: *In vivo* PP_3287 transcription in response to nitric oxide and oxidative stress. The cultures of JRG6721 (Table 2.1) that express *PP_3287* from multi-copy plasmid (PP_3287^{++}) only and transformed with pGS810 (Table 2.2) were grown in LB medium for aerobic growth and medium 154 for anaerobic growth (Section 2.4.1). The cultures were exposed to aerobic (50 mL flask containing 10 mL medium, red bar), aerobic plus PQ (200 µM, blue bar), anaerobic conditions (sealed 50 mL flasks filled with 50 mL medium, green bar), anaerobic plus NOC-7 as a nitric oxide exogenous donor (20 µM, pink bar) for 3 h at 30°C/200 rpm. Culture supplemented with NOC-7 was incubated in the anaerobic cabinet and the reagent was injected with a Hamilton syringe through a seal into the culture and mixed. After incubation, the β-galactosidase activities were measured in triplicate. The error bars are the standard deviation from the mean (n=3). *P* values were determined *t* test. **, *P* <0.01; NS, *P* >0.5.

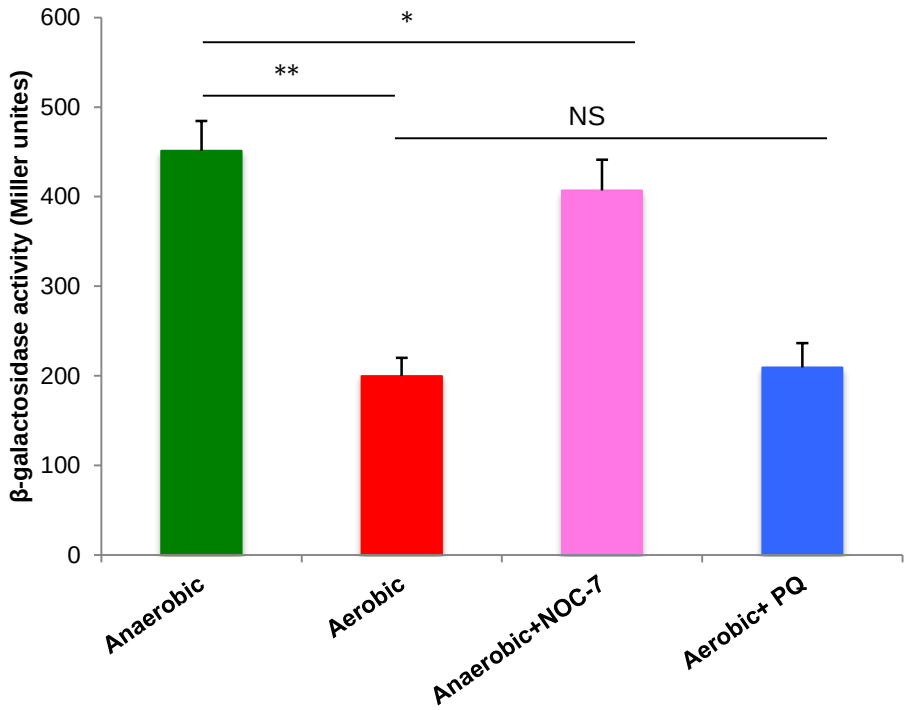

Figure 5.11: *In vivo* PP_3233 transcription in response to nitric oxide and oxidative stress. The cultures of JRG6722 (Table 2.1) that express *PP_3233* from multi-copy plasmid (PP_3233^{++}) only and transformed with pGS810 (Table 2.2) were grown in LB medium for aerobic growth and medium 154 for anaerobic growth (Section 2.4.1). The cultures were exposed to aerobic (50 mL flask containing 10 mL medium, red bar), aerobic plus PQ (200 µM, blue bar), anaerobic conditions (sealed 50 mL flasks filled with 50 mL medium, green bar), anaerobic plus NOC-7 as a nitric oxide exogenous donor (20 µM, pink bar) for 3 h at 30°C/200 rpm. Culture supplemented with NOC-7 was incubated in the anaerobic cabinet and the reagent was injected with a Hamilton syringe through a seal into the cultures and mixed. After incubation, the β-galactosidase activities were measured in triplicate. The error bars are the standard deviation from the mean (n=3). *P* values were determined *t* test. **, *P* <0.01; *, *P*<0.1; NS, *P* >0.5.

5.10 Discussion

The *in vivo* properties of ANR, PP_3233 and PP_3287 were consistent with the observed activities of the [4Fe-4S] clusters with O_2 *in vitro*. *Pseudomonas putida* ANR plays important role to switch the growth from aerobic to O_2-limited conditions and its activity related to assembly and disassembly of the iron-sulfur cluster similar to *E. coli* FNR (Jervis and Green, 2007).

Responses of PP_3233 and PP_3287 to O_2 were less pronounced than for ANR. However, nitric oxide had a minor or no effect on a PP_3233/PP_3287 dependent reporter gene *in vivo*. These observations confirmed that PP_3233 and PP_3287 proteins are O_2 sensors via assembly and disassembly of their iron-sulfur clusters like, *E. coli* FNR and ANR, but they were less responsive. Previous work with *E. coli* FNR showed that replacement of Ser-24, which is located immediately adjacent to the cluster ligand Cys-23, by Arg resulted in hindering flexibility of the Cys23-Cys29 loop that is important for conversion of [3Fe-4S] to [2Fe-2S] clusters making FNR-S24R iron-sulfur cluster more stable (Jervis *et al*., 2009, Volbeda *et al*., 2015). Interestingly, PP_3287 has Arg in the position equivalent to Ser-24 in FNR (Figure 3.1; Figure 5.12) and thus this amino acid substitution could, at least partially, account for the lower reactivity of PP_3287 with O_2. On the other hand, PP_3233 resembles *E. coli* FNR by retaining a Ser residue at the equivalent of position 24 (Figure 3.1; Figure 5.12); however, amino acid substitutions in other locations are known to influence the reactivity of the *E. coli* FNR iron-sulfur cluster with O_2 (Kiley and Reznikoff, 1991, Bates *et al*., 2000). Like Ser24Arg, another amino acid substitution that promoted aerobic FNR activity was also located immediately adjacent to Cys23, but this time on the other flank (D22G) (Kiley and Reznikoff, 1991). The equivalent position in PP_3233 is occupied by Ala (Figure 3.1; Figure 5.12), and thus by analogy, replacement of the acidic Asp residue might alter the redox properties of the PP_3233 iron-sulfur cluster, such that it is less O_2 reactive.

The response of ANR to nitric oxide *in vitro* was confirmed *in vivo*. Thus, it was concluded that *P. putida* ANR is essentially an O_2-sensing transcription regulator. Like *E. coli* FNR and *P. aeruginosa* ANR, *P. putida* ANR was also inhibited by nitric oxide (Crack *et al*., 2013, Kuroki *et al*., 2014). These data confirmed the similarities between ANR and FNR proteins. Response of PP_3233 and PP_3287 to nitric oxide showed a minor or no effect, which confirmed that PP_3233 and PP_3287 proteins are O_2 sensors via assembly and disassembly of their iron-sulfur clusters like, *E. coli* FNR and ANR, but they were less responsive.

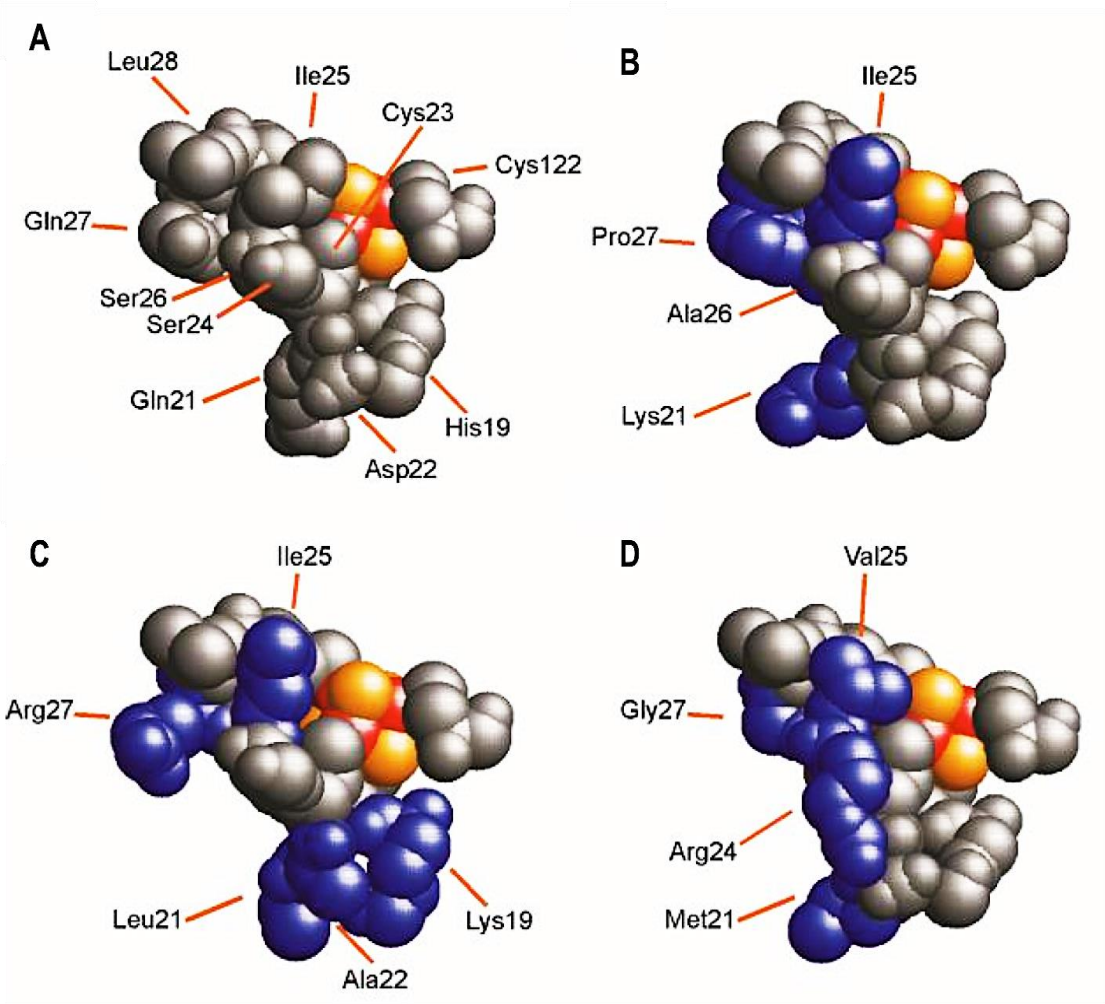

Figure 5.12: Models of N-terminal [4Fe-4S] cluster binding regions of four FNR proteins.

The models were constructed in SWISS-Model (Bordoli *et al*., 2009) using endonuclease III (PDB code 2abk) as the template as described by Jervis *et al.* (2009). The images were produced as space filled representations in RasMol (Sayle and Milner-White, 1995). The iron (red) and sulfide (gold) atoms of the [4Fe-4S] cluster are shown. Amino acids are labelled and numbered according to *E. coli* FNR. Conserved amino acids are colored grey; those of the *P. putida* FNR proteins that differ from those present in *E. coli* FNR are colored blue. (A) *E. coli* FNR; (B) *P. putida* ANR; (C) *P. putida* 3233 and (D) *P. putida* 3287.

Chapter 6

Biochemical characterisation of *Desulfovibrio desulfuricans* HcpR2 protein

6.0 Biochemical characterisation of *Desulfovibrio desulfuricans* HcpR2 protein

6.1 Introduction

The sulfate reducing bacteria (SRB) are obligate anaerobic bacteria, ubiquitous in diverse anaerobic habitats such as soil, water, sediments and the digestive system (the mouth and gut) of humans and animals. SRB play a crucial role in sulfur and carbon global cycles in anaerobic environments, especially marine environments because of the higher sulfate concentrations that are found there. Under anoxic conditions, SRB have the ability to use sulfate as an electron acceptor (Pires *et al*., 2006, Muyzer and Stams, 2008, Sun *et al*., 2010). Much of the biochemical information about these bacteria has come from studies of three species of *Desulfovibrio*: *D. vulgaris*, especially strain Hildenborough; *Desulfovibrio* strain G20; and *D. desulfuricans*, especially strain ATCC27774. Despite well-developed genetic systems to study *D. vulgaris* there are no similar systems for *D. desulfuricans*. Therefore, most gene functions and regulation have been studied using *D. vulgaris* rather than *D. desulfuricans* (Cadby, 2014).

Desulfovibrio desulfuricans ATCC27774 has the ability to utilize nitrate and sulfate as electron acceptors (Steenkamp and Peck, 1980, Lobo *et al*., 2007). During anaerobic growth sulfate is utilized first and then nitrate. However, the energy conserved from nitrate reduction is greater and growth yields are higher than those supported by sulfate respiration. This metabolic choice goes against the dogma that bacteria will select the thermodynamically most favorable metabolic mode when more than one resource is available (Thauer *et al*., 1977, Odom and Peck, 1981, Mitchell *et al*., 1986, Greene *et al*., 2003, Marietou *et al*., 2009; Figure 6.1 and 6.2; Eq. 6.1 and 6.2):

$SO_4^{2-} + 4H_2 \rightarrow S^{2-} + 4H_2O$ ΔG= -152 kJ/mol [6.1]

$NO^{3-} + 4H_2 + 2H^+ \rightarrow 3H_2O + NH_4^+$ ΔG= -599 kJ/mol [6.2]

As illustrated in Figure 6.1, sulfate is reduced in the cytoplasm, unlike nitrate, which is reduced in the periplasm (Figure 6.2). Consequently, sulfate, but not nitrate, has to be transported into the cell and this requires energy. It has been suggested that sulfate uptake is achieved by a symport system driven by the proton gradient ($2H^+$ per SO_4^{2-}; Figure 6.1). Furthermore, the export of the product of sulfate reduction, hydrogen sulfide, is thought to mitigate the energetic cost of sulfate uptake, by being equivalent to the export of two protons. Nevertheless, unlike nitrate, sulfate must be activated to act as an electron acceptor. This involves conversion to adenosinephosphosulfate

(APS) by the enzyme sulfate adenyltransferase, a process that consumes two ATP molecules. As shown in Figure 6.1, where hydrogen gas acts as the electron donor for sulfate reduction, net proton translocation is $8H^+$ per SO_4^{2-} and assuming that ~$3H^+$ are required to convert ADP to ATP then 2.7 ATP can be generated by the ATPase; however 2 ATP are used to make APS and therefore the net ATP yield is only 0.7 ATP/SO_4^{2-}. In contrast, because nitrate does not require activating to act as an electron acceptor and is reduced in the periplasm, the six protons (net) that are translocated can be used to generate 2 ATP molecules and thus nitrate respiration should be more energetically favourable than sulfate respiration (Figure 6.2). The fact that sulfate respiration is preferred to nitrate respiration indicates that there is a regulatory process controlling this choice. In *E. coli*, the FNR protein acts as the master regulator that determines the choice of electron acceptor. Bioinformatic analysis identified five FNR-CRP family proteins in *D. desulfuricans*. Two of these: HcpR1 (Ddes_0528) and HcpR2 (Ddes_1827) were predicted effect the transcription of *nap* ecoding nitrate reductase, *sat* encoding sulfate adenyltransferase, *aps* encoding adenosine-5'-phosphosulfate and *hcp* encoding hybrid cluster protein suggesting that they could be the transcription factors that control the preference for sulfate reduction over nitrate reduction (Zhou *et al*., 2012, Cadby, 2014; Figure 6.3).

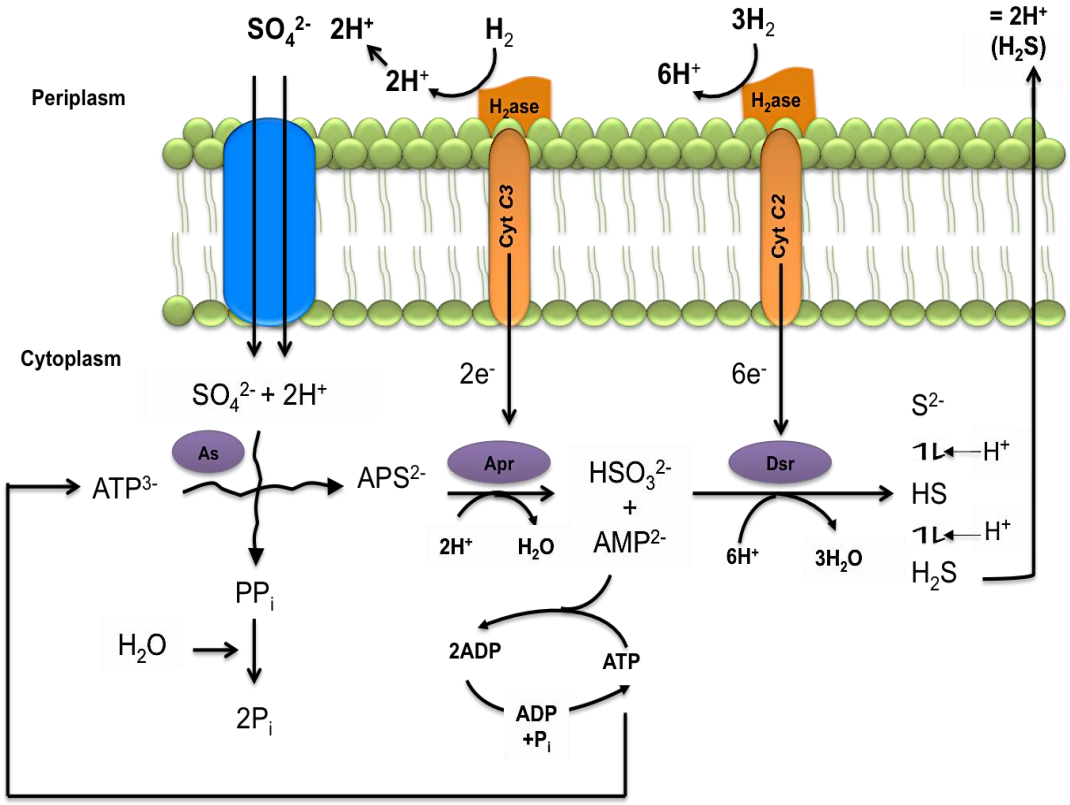

Figure 6.1: Sulfate reduction model by *Desulfovibrio desulfuricans* ATCC27774. Electrons (e^-) are believed to migrate from periplasm via cytochrome *c*3 to Apr and Dsr in the cytoplasm for sulfate reduction. APS: adenosine-5'-phosphosulfate, Apr: APS reductase, Dsr: dissimilatory sulfite reductase, PP_i: inorganic pyrophosphate, As: ATP sulfurylases, H_2ase: hydrogenase and blue oval: SO_4^{2-} - symporter are shown

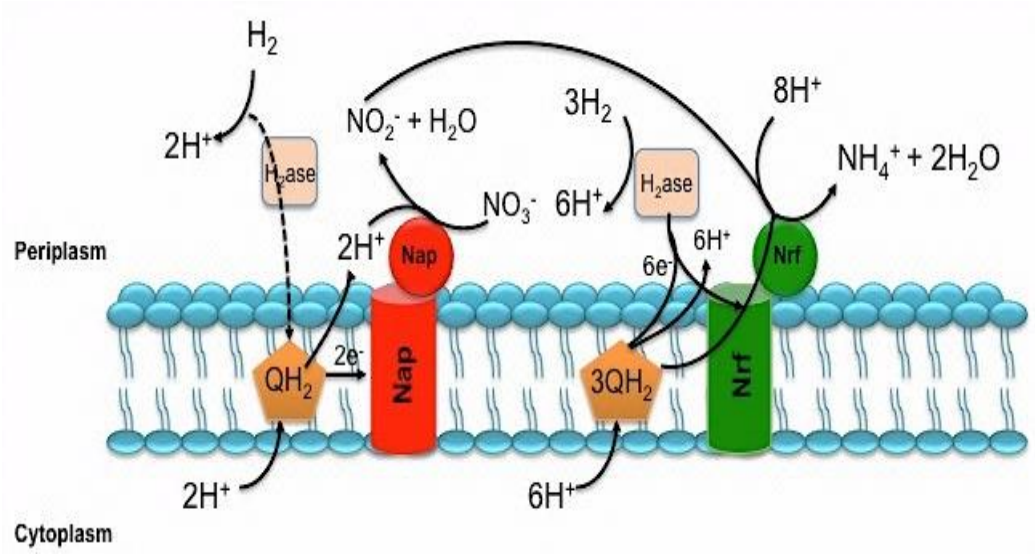

Figure 6.2: Nitrate reduction model in *Desulfovibrio desulfuricans* ATCC27774. Nitrate reduction in periplasm. QH_2: electrons transport "quinol pool", Nap: periplasmic nitrate reductase, Nrf: nitrite reductase and H_2ase: hydrogenase are indicated.

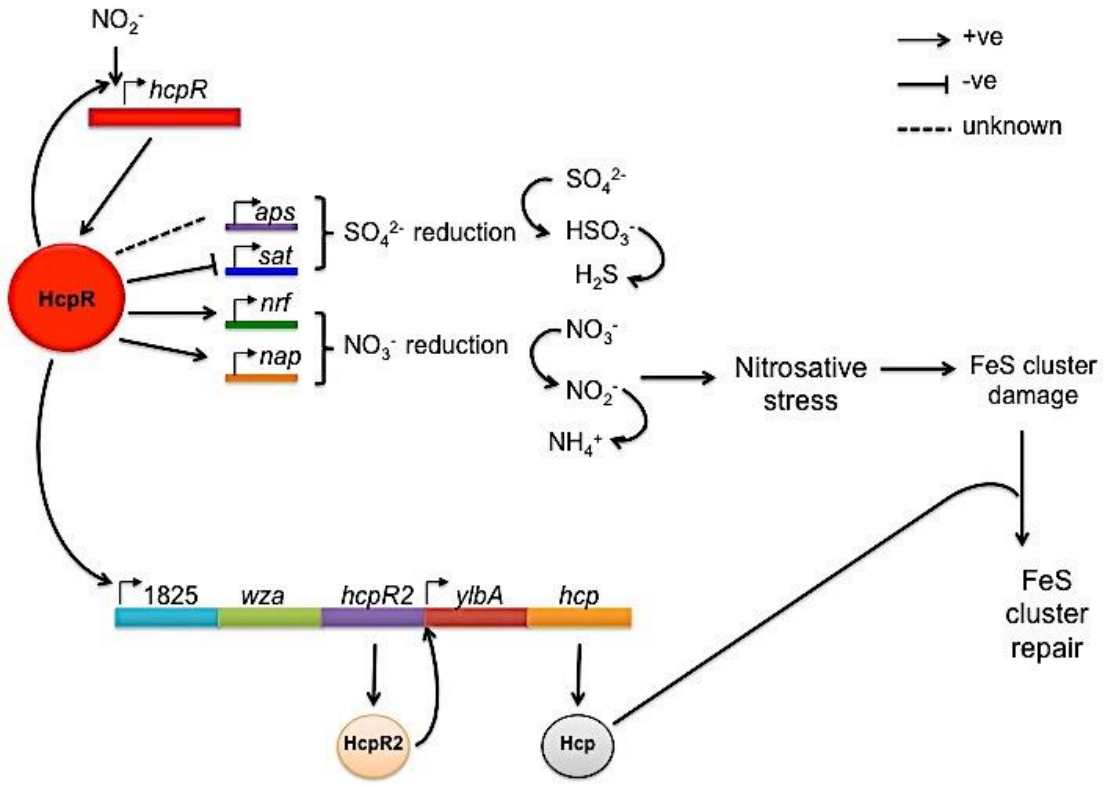

Figure 6.3: Regulation model of HcpR and HcpR2 in *Desulfovibrio desulfuricans* ATCC27774. The predicted model of transcription regulation by HcpR and HcpR2 under anaerobic conditions. Figure adapted from Cadby (2014).

Alignment of 12 HcpR2 family proteins (Figure 6.4) revealed the presence of three conserved cysteine residues (Cys-25, 117 and 121) and a conserved histidine residue (His-124). HcpR2 also possesses four other less well-conserved cysteine residues (Cys-8, 22, 41 and 95). Analysis of the primary structure of HcpR2 using SWISS-Model (Bordoli *et al*., 2009) predicted that the four fully conserved residues are located close together at the opposite end of the protein to the DNA-binding helix and that the less conserved Cys-22 is located in the same region (Figure 6.5). This raised the possibility that these amino acid residues could be involved in redox sensing and/or binding a sensory co-factor. Here it is shown that HcpR2 can incorporate an oxygen and nitric oxide sensitive iron-sulfur cluster that enhances DNA-binding under anaerobic conditions.

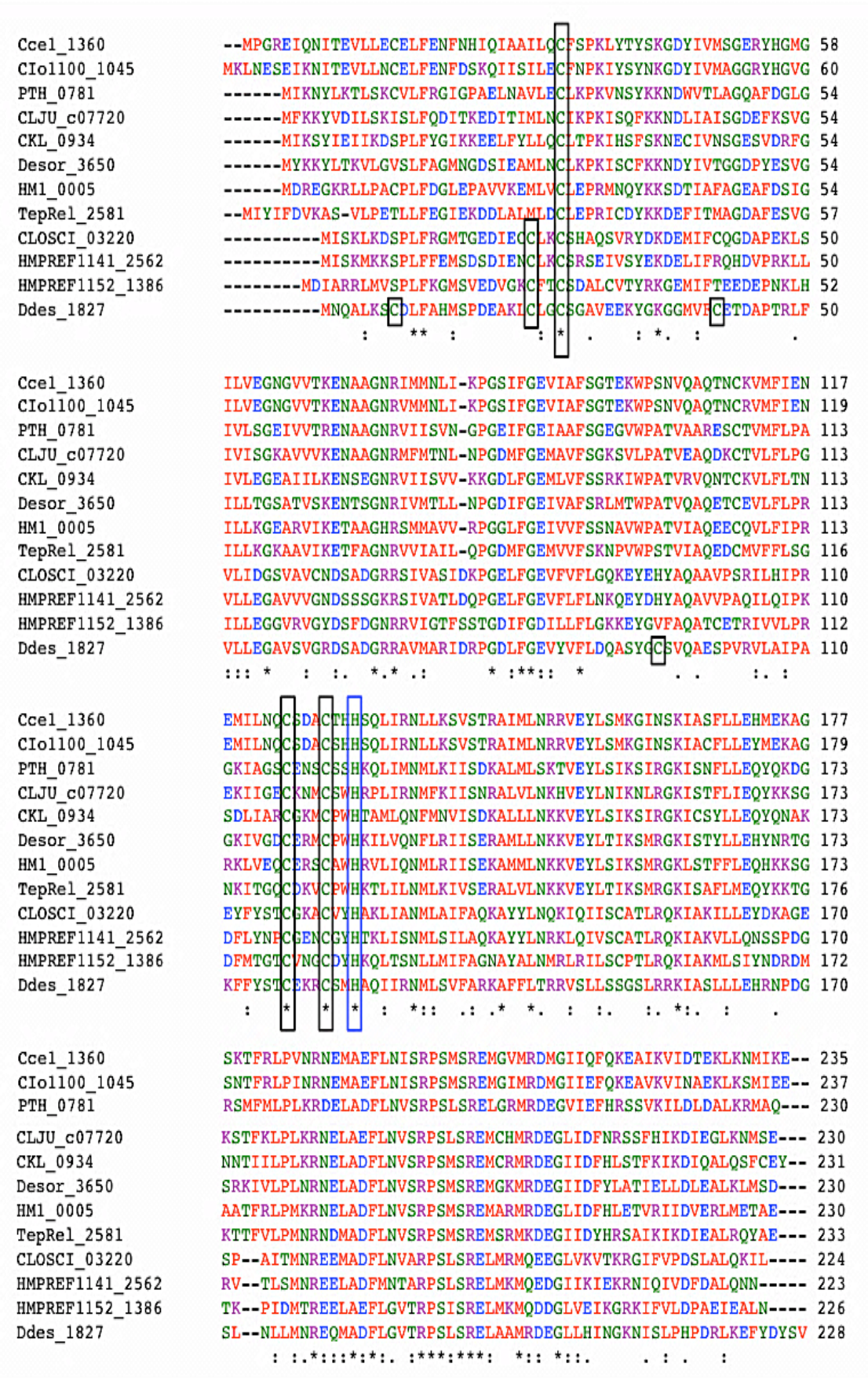
Ccel_1360 --MPGREIQNITEVLLECELFENFNHIQIAAILQCFSPKLYTYSKGDYIVMSGERYHGMG 58
CIol100_1045 MKLNESEIKNITEVLLNCELFENFDSKQIISILECFNPKIYSYNKGDYIVMAGGRYHGVG 60
PTH_0781 ------MIKNYLKTLSKCVLFRGIGPAELNAVLECLKPKVNSYKKNDWVTLAGQAFDGLG 54
CLJU_c07720 ------MFKKYVDILSKISLFQDITKEDITIMLNCIKPKISQFKKNDLIAISGDEFKSVG 54
CKL_0934 ------MIKSYIEIIKDSPLFYGIKKEELFYLLQCLTPKIHSFSKNECIVNSGESVDRFG 54
Desor_3650 ------MYKKYLTKVLGVSLFAGMNGDSIEAMLNCLKPKISCFKKNDYIVTGGDPYESVG 54
HM1_0005 ------MDREGKRLLPACPLFDGLEPAVVKEMLVCLEPRMNQYKKSDTIAFAGEAFDSIG 54
TepRel_2581 --MIYIFDVKAS-VLPETLLFEGIEKDDLALMLDCLEPRICDYKKDEFITMAGDAFESVG 57
CLOSCI_03220 ----------MISKLKDSPLFRGMTGEDIECCLKCSHAQSVRYDKDEMIFCQGDAPEKLS 50
HMPREF1141_2562 ----------MISKMKKSPLFFEMSDSDIENCLKCSRSEIVSYEKDELIFRQHDVPRKLL 50
HMPREF1152_1386 --------MDIARRLMVSPLFKGMSVEDVGKCFTCSDALCVTYRKGEMIFTEEDEPNKLH 52
Ddes_1827 ----------MNQALKSCDLFAHMSPDEAKLCLGCSGAVEEKYGKGGMVRCETDAPTRLF 50
ILVEGNGVVTKENAAGNRIMMNLI-KPGSIFGEVIAFSGTEKWPSNVQAQTNCKVMFIEN 117
ILVEGNGVVTKENAAGNRVMMNLI-KPGSIFGEVIAFSGTEKWPSNVQAQTNCRVMFIEN 119
IVLSGEIVVTRENAAGNRVIISVN-GPGEIFGEIAAFSGEGVWPATVAARESCTVMFLPA 113
IVISGKAVVVKENAAGNRMFMTNL-NPGDMFGEMAVFSGKSVLPATVEAQDKCTVLFLPG 113
IVLEGEAIILKENSEGNRVIISVV-KKGDLFGEMLVFSSRKIWPATVRVQNTCKVLFLTN 113
ILLTGSATVSKENTSGNRIVMTLL-NPGDIFGEIVAFSRLMTWPATVQAQETCEVLFLPR 113
ILLKGEARVIKETAAGHRSMMAVV-RPGGLFGEIVVFSSNAVWPATVIAQEECQVLFIPR 113
ILLKGKAAVIKETFAGNRVVIAIL-QPGDMFGEMVVFSKNPVWPSTVIAQEDCMVFFLSG 116
VLIDGSVAVCNDSADGRRSIVASIDKPGELFGEVFVFLGQKEYEHYAQAAVPSRILHIPR 110
VLLEGAVVVGNDSSSGKRSIVATLDQPGELFGEVFLFLNKQEYDHYAQAVVPAQILQIPK 110
ILLEGGVRVGYDSFDGNRRVIGTFSSTGDIFGDILLFLGKKEYGVFAQATCETRIVVLPR 112
VLLEGAVSVGRDSADGRRAVMARIDRPGDLFGEVYVFLDQASYGCSVQAESPVRVLAIPA 110
EMILNQCSDACTHHSQLIRNLLKSVSTRAIMLNRRVEYLSMKGINSKIASFLLEHMEKAG 177
EMILNQCSDACSHHSQLIRNLLKSVSTRAIMLNRRVEYLSMKGINSKIACFLLEYMEKAG 179
GKIAGSCENSCSSHKQLIMNMLKIISDKALMLSKTVEYLSIKSIRGKISNFLLEQYQKDG 173
EKIIGECKNMCSWHRPLIRNMFKIISNRALVLNKHVEYLNIKNLRGKISTFLIEQYKKSG 173
SDLIARCGKMCPWHTAMLQNFMNVISDKALLLNKKVEYLSIKSIRGKICSYLLEQYQNAK 173
GKIVGDCERMCPWHKILVQNFLRIISERAMLLNKKVEYLTIKSMRGKISTYLLEHYNRTG 173
RKLVEQCERSCAWHRVLIQNMLRIISEKAMMLNKKVEYLSIKSMRGKLSTFFLEQHKKSG 173
NKITGQCDKVCPWHKTLILNMLKIVSERALVLNKKVEYLTIKSMRGKISAFLMEQYKKTG 176
EYFYSTCGKACVYHAKLIANMLAIFAQKAYYLNQKIQIISCATLRQKIAKILLEYDKAGE 170
DFLYNRCGENCGYHTKLISNMLSILAQKAYYLNRKLQIVSCATLRQKIAKVLLQNSSPDG 170
DFMTGTCVNGCDYHKQLTSNLLMIFAGNAYALNMRLRILSCPTLRQKIAKMLSIYNDRDM 172
KFFYSTCEKRCSMHAQIIRNMLSVFARKAFFLTRRVSLLSSGSLRRKIASLLLEHRNPDG 170
SKTFRLPVNRNEMAEFLNISRPSMSREMGVMRDMGIIQFQKEAIKVIDTEKLKNMIKE-- 235
SNTFRLPINRNEMAEFLNISRPSMSREMGIMRDMGIIEFQKEAVKVINAEKLKSMIEE-- 237
RSMFMLPLKRDELADFLNVSRPSLSRELGRMRDEGVIEFHRSSVKILDLDALKRMAQ--- 230
KSTFKLPLKRNELAEFLNVSRPSLSREMCHMRDEGLIDFNRSSFHIKDIEGLKNMSE--- 230
NNTIILPLKRNELADFLNVSRPSMSREMCRMRDEGIIDFHLSTFKIKDIQALQSFCEY-- 231
SRKIVLPLNRNELADFLNVSRPSMSREMGKMRDEGIIDFYLATIELLDLEALKLMSD--- 230
AATFRLPMKRNELADFLNVSRPSMSREMARMRDEGLIDFHLETVRIIDVERLMETAE--- 230
KTTFVLPMNRNDMADFLNVSRPSMSREMSRMKDEGIIDYHRSAIKIKDIEALRQYAE--- 233
SP--AITMNREEMADFLNVARPSLSRELMRMQEEGLVKVTKRGIFVPDSLALQKIL---- 224
RV--TLSMNREELADFMNTARPSLSRELMKMQEDGIIKIEKRNIQIVDFDALQNN----- 223
TK--PIDMTREELAEFLGVTRPSISRELMKMQDDGLVEIKGRKIFVLDPAEIEALN---- 226
SL--NLLMNREQMADFLGVTRPSLSRELAAMRDEGLLHINGKNISLPHPDRLKEFYDYSV 228

Figure 6.4: Alignment of HcpR2 family proteins. Alignment of HcpR2 family proteins by clustal Omega (Sievers *et al*., 2011). The residues that are identical in all proteins (*), residues with strongly similar properties (:) and residues with weakly similar properties (.) are indicated. The conserved cysteine and histidine residues are highlighted in black and blue. Protein sequences used for the analysis came from the following bacteria: *Clostridium cellulolyticum* H10 (Ccel_1360); *Clostridium* sp. BNL1100 (Clo1100_1045); *Pelotomaculum thermopropionicum* SI (PTH_0781); *Clostridium ljungdahlii* DSM13528 (CLJU_c07720); *Clostridium kluyveri* DSM555 (CKL_0934); *Desulfosporosinus orientis* DSM765 (Desor_3650); *Heliobacterium modesticaldum* Ice1 (HM1_0005); *Tepidanaerobacter* sp. Re1 (TepRe1_2581); *Clostridium scindens* ATCC35704 (CLOSCI_03220); *Clostridium* sp. MSTE9 (HMPREF1141_2562); *Mogibacterium* sp. CM50 (HMPREF1152_1386) and *Desulfovibrio desulfuricans* (Ddes_1827).

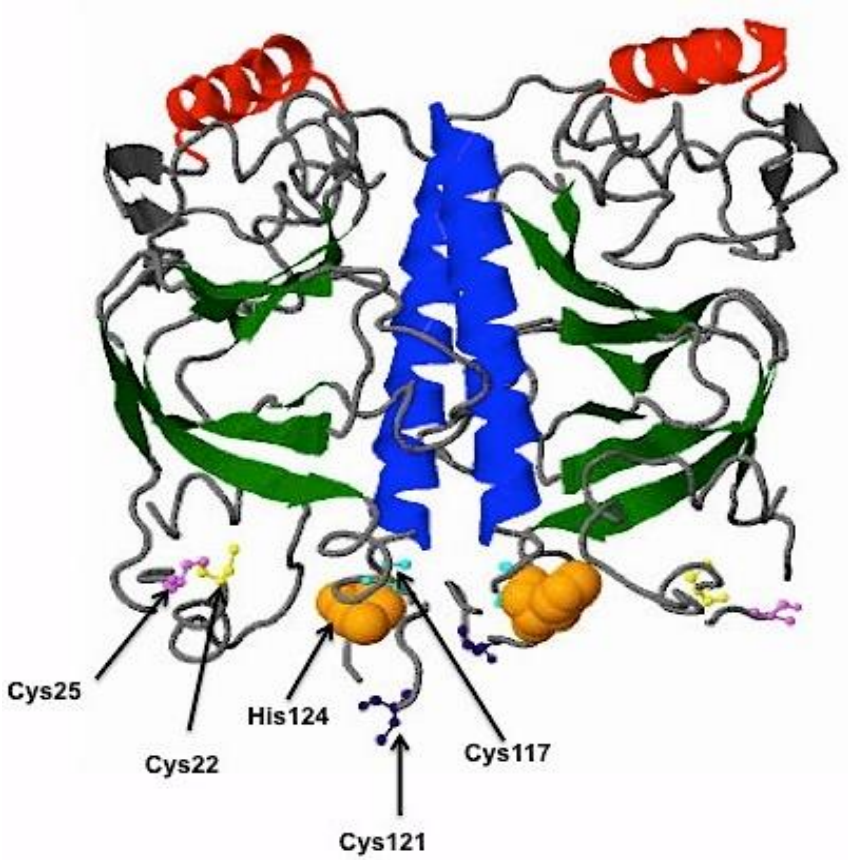

Figure 6.5: Model of the structure of HcpR2 (Ddes-1827). The model was constructed in SWISS-Model (Bordoli *et al*., 2009). The DNA binding helix (red), the β-roll motif (green) and dimerization helix (blue), conserved cysteine residues (Cys-25, 117, 121), less conserved Cys-22 and His-124 of each monomer are shown. The template was *Mtb*CRP (PDB: 3i54.2).

6.2 HcpR2 is a dimer

Oligomeric state of apo-HcpR2 was investigated using gel filtration chromatography (Section 2.6.10). Apo-HcpR2 (~69 µM; Figure 6.6, lane 2) was eluted from heparin column (GE Healthcare) with 20 mM sodium phosphate pH 7.4 containing 100 mM NaCl (Figure 6.6, lane 3) and applied to a Superdex 200 column equilibrated with 20 mM sodium phosphate pH 7.4 containing 100 mM NaCl. The column was calibrated with a set of known molecular weight proteins as described for ANR (Section 3.2.3; Figure 3.4A). Figure 6.7 shows a peak at ~28 min for apo-HcpR2. An estimate of ~45 kDa was obtained, which corresponded to an apo-HcpR2 dimer (subunit molecular weight is 26.74 kDa).

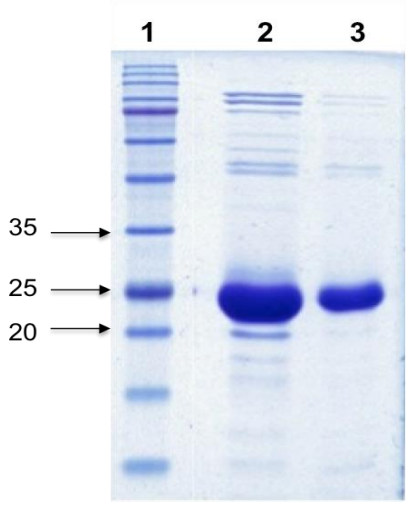

Figure 6.6: SDS-PAGE gel of purified HcpR2. Lane 1, Precision plus protein standards (sizes in kDa are indicated); lane 2, purified HcpR2 (~26 kDa); lane 3, apo-HcpR2 purified by heparin column under aerobic conditions.

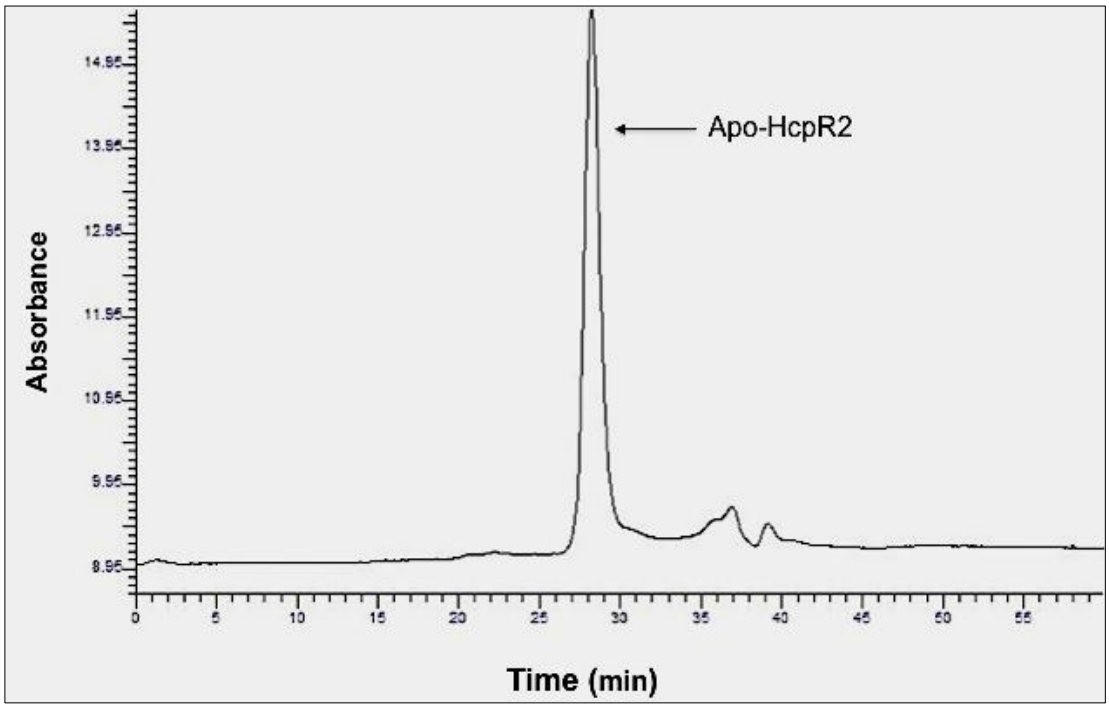

Figure 6.7: Gel filtration for apo-HcpR2. Apo-HcpR2 (~69 µM, 50 µl) was applied to the Superdex 200 column, which was equilibrated with 20 mM sodium phosphate pH 7.4 containing 100 mM NaCl and 1 mM azide. The absorbance trace showed a peak corresponding to an HcpR2 dimer.

6.3 HcpR2 can incorporate a [4Fe-4S] cluster

6.3.1 UV-visible spectrum of reconstituted HcpR2 is consistent with the presence of a [4Fe-4S] cluster

The reconstitution reactions were prepared by incubating apo-HcpR2 with reconstitution reagents under anaerobic reaction as described (Section 3.3.1; Section 2.7.1). Upon incubation, the colourless protein solution became straw-brown in colour, which is typical of a [4Fe-4S] protein (Figure 6.8, Inset; Green *et al*., 1996a). Heparin chromatography was used to separate HcpR2 from other reconstitution reagents (Section 2.7.2). Figure 6.8 shows the UV-visible spectrum after purification of reconstituted HcpR2 using 1 mL HiTrap heparin column (GE Healthcare). The UV-visible spectrum of the reconstituted protein was similar to other [4Fe-4S] proteins (Figure 6.8; Crack *et al*., 2004). The broad absorption band centred at ~420 nm resembled that of *E. coli* FNR (Crack *et al*., 2008b).

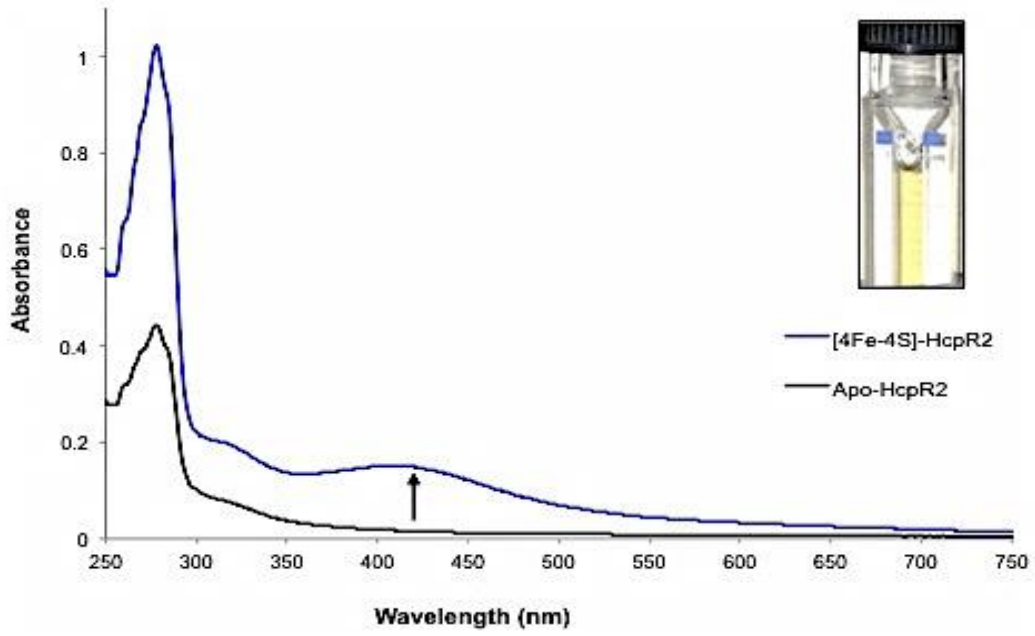

Figure 6.8: Spectral analysis of holo-HcpR2. Holo-HcpR2 (~9.0 µM cluster) under anaerobic conditions. The UV-visible spectra are before (black line) and after (blue line) reconstitution. The arrow shows the enhancement in absorbance at 420 nm. (Inset) Straw-brown colour developed after reconstitution.

6.3.2 Iron content of holo-HcpR2

The straw-brown colour and UV-visible spectrum of reconstituted HcpR2 were typical of a [4Fe-4S] protein. To validate this assignment, the total amount of iron in a reconstituted sample of HcpR2 was measured (Section 2.7.3). A calibration curve was made using a standard iron solution as described for ANR (Figure 3.7A; Chapter 3). Reconstitution reactions for HcpR2 protein were prepared four times and purified by using heparin chromatography as described for ANR (Sections 3.3.1; 2.7.1 and 2.7.2). The Bradford protein assay was then used to measure the concentration of the protein and the same samples were then subjected to total iron analysis (Section 2.6.1). The ratio of iron to protein was calculated as described for ANR (Section 3.3.3; Table 6.1). The average amount of iron in reconstituted HcpR2 was 3.2 moles of iron per mole of HcpR2 monomer. Taken together with the spectral data (Figure 6.8), it was concluded that HcpR2 is likely to be a [4Fe-4S] cluster protein under anaerobic conditions, but the possibility that HcpR2 possesses a [3Fe-4S] or a mixture of [4Fe-4S] and [2Fe-2S] clusters cannot be dismissed.

HcpR2 (nmoles)	Fe (nmoles)	Ratio of iron to HcpR2
1.4	4.2	3.1
1.2	3.9	3.3
1.4	4.2	3.1
1.3	4.0	3.2

Table 6.1: Iron content of reconstituted HcpR2. Ratio of iron to HcpR2 monomers. The results of the iron and protein concentration measurements were used to calculate the number of iron molecules associated with each HcpR2 monomer.

6.3.3 Reaction of the [4Fe-4S] cluster of HcpR2 with O_2 results in conversion to [2Fe-2S] form

The sensitivity of iron-sulfur cluster of HcpR2 to O_2 was investigated (Section 2.7.6). The stoichiometry of holo-HcpR2 reaction (~9.4 μM cluster using a typical extinction coefficient of ~16,000 $M^{-1}cm^{-1}$) with O_2 was determined as described for ANR (Section 3.3.4; Section 2.7.9). UV-visible spectra obtained after successive additions of aerobic air-saturated buffer showed a progressive decrease in absorbance at 420 nm accompanied by an increase in absorbance around 550 nm (Figure 6.9A).

Plotting the changes in absorbance at 550 nm (ΔA_{550}) against the ratio of [O_2]:[4Fe-4S] and obtaining the intersection of the tangent to the initial slope and the asymptote showed that conversion of the [4Fe-4S] cluster was complete after the addition of 2-3 molecules of O_2 per [4Fe-4S] cluster (Figure 6.9B). This stoichiometry is similar to that obtained for the reaction of the [4Fe-4S] cluster of *E. coli* FNR, which was ~87% complete at a cluster:O_2 ratio of 2 (Crack *et al*., 2008b). Thus, it was concluded that like *E. coli* FNR, HcpR2 could acquire an oxygen-sensitive [4Fe-4S] cluster that degrades via a [2Fe-2S] cluster in the presence of air to ultimately yield apo-HcpR2 (Green *et al*., 2009)

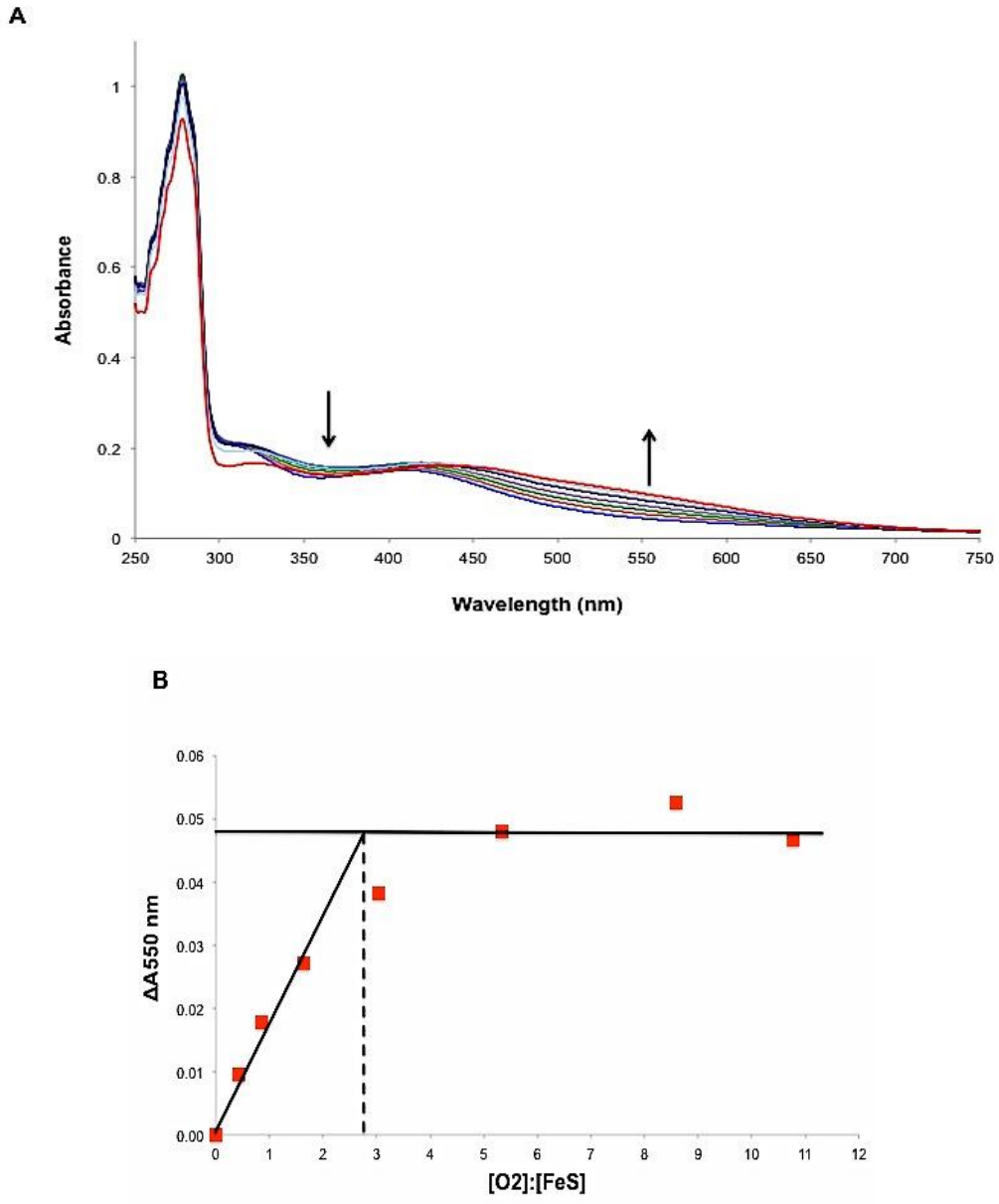

Figure 6.9: Titration of holo-HcpR2 with air-saturated buffer. (A) Holo-HcpR2 (~9.4 µM cluster) was exposed to increasing concentrations of air-saturated buffer. The final concentrations were 0.0, 4.3, 8.5, 16.3, 30.3, 53.3 and 85.9 µM. The sample was incubated at room temperature for 10 min after each addition before measurement of the spectra. The arrows show the decreasing absorbance at 420 nm and increasing absorbance at 550 nm. **(B)** Changes in absorbance at 550 nm (ΔA_{550}), representing the appearance of the [2Fe-2S] cluster were plotted at versus the ratio of [O_2] from the spectra shown in Figure 6.9A. The dashed lines represent the tangent to the initial slope and the asymptote of the curve.

6.4 The DNA binding properties of HcpR2

EMSAs (Section 2.8.2) were used to determine the ability of the iron-sulfur cluster of HcpR2 to bind to the biotin-labelled DNA sequence (GTAAC ---- GTTAC, predicted HcpR2 binding site). Biotin-labelled DNA was amplified using PCR and biotin-labelled primers: p1827cTERM-F 5´-CAACGGAAAAAACATCTCCC-3´ and p1827cTERM-R 5´-GGGCAGCGCGGTGGCGTAATCC-3´ as described (Section 2.8.1). The gDNA template was provided by Dr. Ian Cadby, Birmingham University. A PCR product of ~200 bp was produced and the concentration measured using Nanodrop 1000 spectrophotometer (Section 2.5.4) and diluted to ~20 fmol for the EMSAs (Figure 6.10).

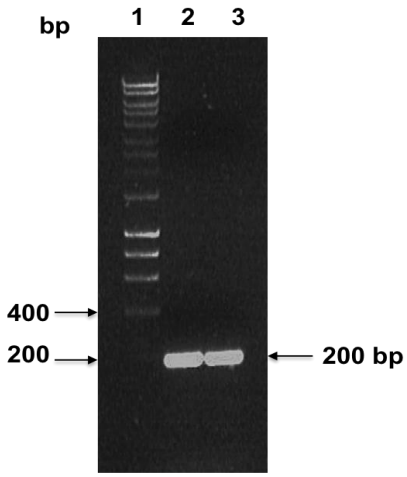

Figure 6.10: Agarose gel showing amplified DNA for EMSAs. Lane 1, Hyperladder I (1kb); lanes 2 and 3, PCR product containing HcpR2 binding site (Biotin-labelled DNA).

6.4.1 The DNA binding of HcpR2 is enhanced by the presence of its iron-sulfur cluster

EMSAs were used to investigate the ability of apo-HcpR2 or holo-HcpR2 to recognise and bind to DNA containing the predicted HcpR2 binding site. Increasing concentrations of apo- or holo-HcpR2 (0, 100, 200, 400, 800, 1000, 1600, 2000, 2400, 2800 and 3000 nM) were incubated with biotin-labelled DNA (~20 fmol) under anaerobic conditions (Figure 6.10; Section 6.4). The binding buffer was KG buffer (2x buffer recipe is: 200 mM potassium glutamate, 50 M Tris-acetate (pH 7.6), 20 mM magnesium acetate, 100 µg/ml BSA, 20 mM DTT). The protein-DNA complexes were separated from the free DNA using 7.5% acrylamide gels that were prepared with 0.25% TBE. The running buffer was 0.25% TBE and 5% glycerol.

The EMSAs showed that, whereas maximal DNA-binding was obtained with 1.6 µM reconstituted HcpR2; higher concentrations of the unreconstituted protein were required to approach a similar level of HcpR2-DNA complex formation (Figures 6.11 - 6.13).

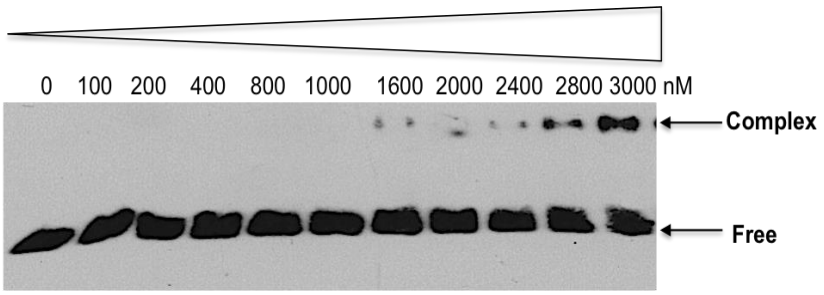

Figure 6.11: The binding of apo-HcpR2 under anaerobic conditions. Apo-HcpR2 protein (0, 100, 200, 400, 800, 1000, 1600, 2000, 2400, 2800 and 3000 nM) was incubated with biotin-labelled DNA that contains the HcpR2 binding site ~20 fmol (Figure 6.10, Section 6.4) prior to gel electrophoresis.

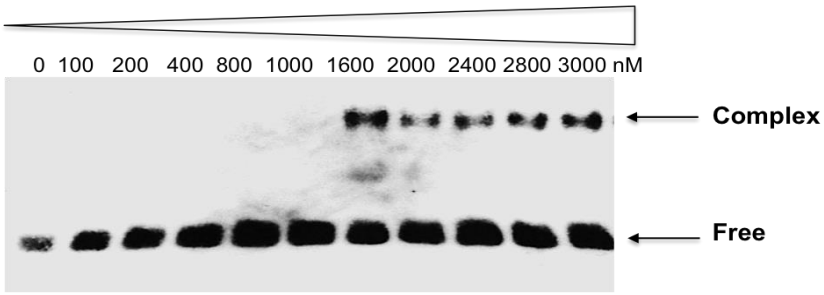

Figure 6.12: The binding of holo-HcpR2 under anaerobic conditions. Increasing concentrations of holo-HcpR2 (0, 100, 200, 400, 800, 1000, 1600, 2000, 2400, 2800 and 3000 nM) were incubated with ~20 fmol of biotin-labelled DNA that contained HcpR2 binding site (Figure 6.10; Section 6.4) prior to gel electrophoresis to separate free and bound DNA fragments.

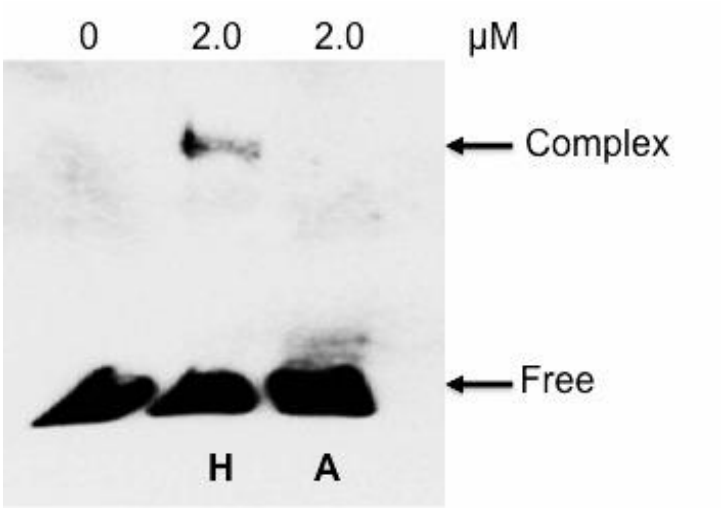

Figure 6.13: Iron-sulfur cluster enhanced HcpR2 DNA binding. Holo-HcpR2 (**H**) and apo-HcpR2 (**A**) (~2.0 μM) were incubated with ~20 fmol biotin-labelled DNA containing HcpR2 binding site (Figure 6.10; Section 6.4) prior to gel electrophoresis to separate free and bound DNA fragments.

6.5 HcpR2 reacts with nitric oxide

Several transcription factors that possess iron-sulfur clusters are known to respond to nitric oxide as well as to O_2 and HcpR2 is implicated in the regulation of *hcp*, which encodes a protein involved in the response to nitrosative stress (Figure 6.3; Crack *et al*., 2012; Green *et al*., 2013). The UV-visible spectrum of holo-HcpR2 (~10 μM) before addition of nitric oxide showed the expected absorbance band at ~420 nm (Figure 6.14A, black line). After exposure of holo-HcpR2 to nitric oxide released from the donor molecule Proli NONOate (Cayman Chemical) at room temperature, the spectrum showed increasing absorbance between 300-425 nm and decreasing between 500-700 nm with isobestic point at ~425 nm (Figure 6.14A). This spectrum was unlike those reported for FNR, WbI and WhiD proteins that showed increased in absorbance at ~355 nm and decreased at 420 nm and 500-700 nm with isobestic point at ~395 nm (Cruz-Ramos *et al*., 2002, Smith *et al*., 2010, Crack *et al*., 2011, Crack *et al*., 2013; Figure 6.14B).

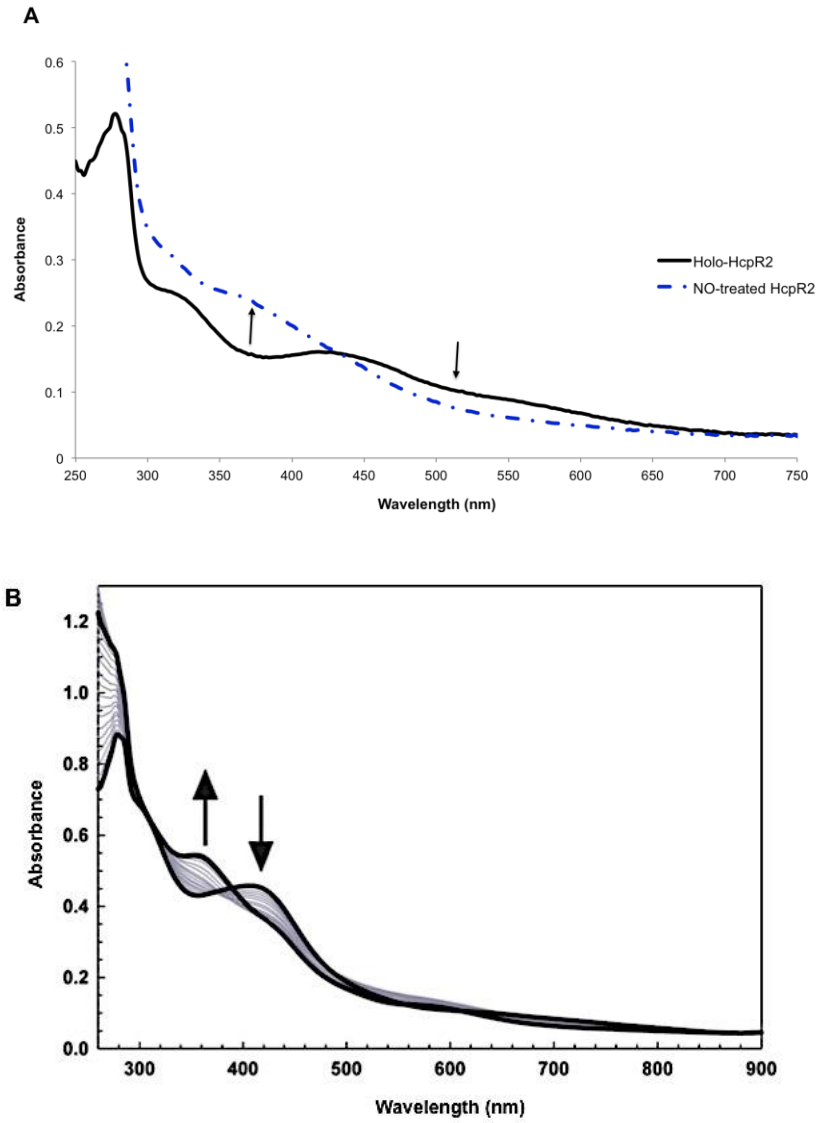

Figure 6.14: UV-visible spectra showing the reaction of holo-HcpR2 with nitric oxide. (A) Spectra of holo-HcpR2 (~10 μM) before (solid black line) and after (dash blue line) addition of nitric oxide from Proli NONOate at room temperature are shown. The arrows show the enhancement in absorbance at ~360 nm and decreased absorbance at 550 nm. **(B)** Spectra of holo-FNR (28.2 μM) after adding increasing concentration of nitric oxide. Figure adapted from Crack *et al*. (2013) to show the difference in isobestic point.

6.6 DNA-binding of NO-treated HcpR2 shows low affinity under anaerobic conditions

EMSAs (Section 2.8.2) were used to investigate the ability of NO-treated holo-HcpR2 to bind to DNA containing the predicted HcpR2 binding site (Figure 6.10; Section 6.4). Reconstituted HcpR2 (~8 μM cluster) was exposed to nitric oxide released from the donor molecule Proli NONOate for 1 min at room temperature under anaerobic conditions (Section 2.7.11). After that the NO-treated holo-HcpR2 sample was used in EMSAs. The results indicated that binding of NO-treated holo-HcpR2 showed lower affinity at (~2.0 and 2.4 μM) compared with the same concentrations of holo-HcpR2 under anaerobic conditions (Figure 6.15).

A

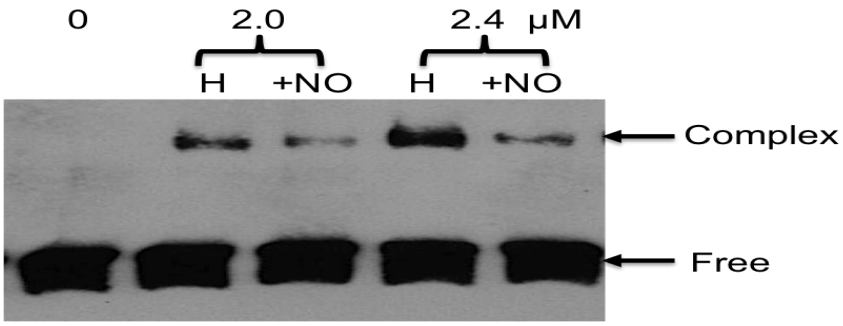

B

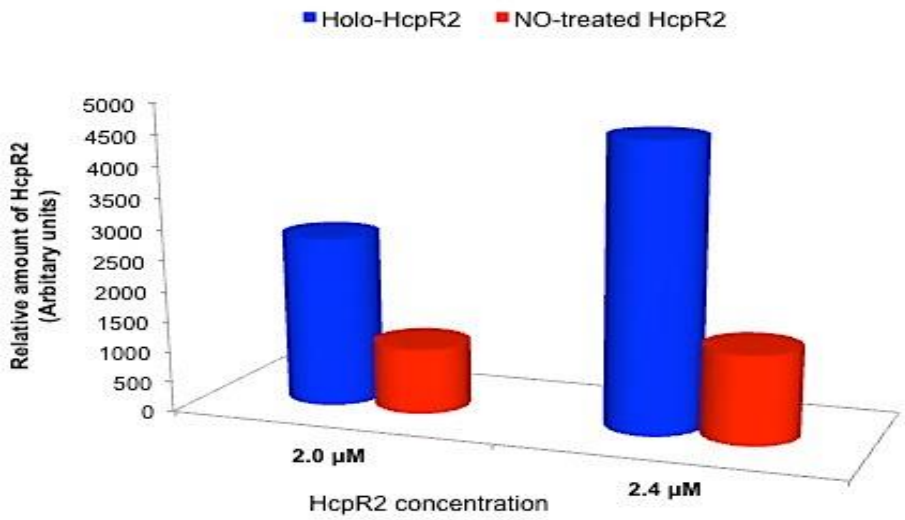

Figure 6.15: DNA-binding by NO-treated HcpR2. (A) Increasing concentrations of holo-HcpR2 (**H**) and NO-treated reconstituted HcpR2 **(+NO**) (~2.0 and 2.4 µM) were incubated with ~20 fmol biotin-labelled DNA containing HcpR2 binding site (Figure 6.10; Section 6.4) prior to gel electrophoresis to separate free and bound DNA fragments. **(B)** ImageJ software was used to determine the amounts of DNA-HcpR2 complexes under the indicated conditions.

6.7 Discussion

Characterisation of *D. desulfuricans* HcpR2 *in vitro* showed that it likely acts as O_2/NO sensing DNA-binding protein. Apo-HcpR2 eluted from a gel filtration column as a dimer similar to *P. putida* apo-ANR (Figure 3.5), but unlike *E. coli* apo-FNR, which is a monomer (Figure 3.17). Holo-HcpR2 showed absorbance at 420 nm and was straw-brown in colour indicating the presence of a [4Fe-4S] cluster (Figure 6.8). Iron assays confirmed this, indicating ~3 Fe per HcpR2 monomer (Section 6.3.2; Table 6.1). These results suggested that holo-HcpR2 possesses one iron-sulfur cluster per monomer similar to ANR and FNR (Figure 3.6; Lazazzera *et al*., 1996).

The O_2 titration experiment showed that [4Fe-4S] cluster of HcpR2 is converted to [2Fe-2S] cluster in response to increasing concentrations of O_2 as air-saturated buffer. The data showed that complete conversion reaction from [4Fe-4S] to [2Fe-2S] required 2-3 molecules of O_2 similar to *P. putida* ANR (Section 3.3.4; Figure 3.8) and *E. coli* FNR (Green *et al*., 1996a, Lazazzera *et al*., 1996, Khoroshilova *et al*., 1997).

EMSAs results showed that holo-HcpR2 (~2 μM) binds to its DNA site (Figure 6.12). However, apo-HcpR2 (~2 μM) could not recognise the same binding site under anaerobic conditions (Figure 6.11), indicating that the HcpR2 is active anaerobically and that the iron-sulfur cluster enhanced the DNA-binding of HcpR2 similar to *P. putida* ANR (Section 3.4.1; Figure 3.15) and *E. coli* FNR (Lazazzera *et al*., 1996).

Incubation of holo-HcpR2 with nitric oxide suggested nitrosylation of the cluster (Figure 6.14). EMSAs indicated that DNA binding of NO treated holo-HcpR2 showed low affinity compared with holo-HcpR2 suggesting that NO impaired the DNA binding activity (Figure 6.15).

To summarize, *D. desulfuricans* HcpR2 is likely to respond to O_2 and nitric oxide via assembly and disassembly of iron-sulfur cluster similar to *P. putida* ANR (Chapter 3) and *E. coli* FNR.

Chapter 7

General discussion

7.0 General discussion

7.1 *Pseudomonas putida* KT2440 FNR proteins

Pseudomonas putida is a Gram-negative bacterium that is found in soils and freshwater environments that contain O_2. It has flexible a catabolism with a branched aerobic respiratory chain terminating in several alternative oxidases (Ugidos *et al*., 2008). However, unlike its close relative *P. aeruginosa*, *P. putida* cannot grow under anaerobic conditions, but retains the ability to thrive under O_2-limiting conditions (Ugidos *et al*., 2008). Anaerobic growth of *P. aeruginosa* can be supported by anaerobic respiration with nitrate as the terminal electron acceptor or by fermentation of pyruvate and arginine (Galimand *et al*., 1991). In the model, Gram-negative, facultative anaerobic bacterium *E. coli* the availability of O_2 is sensed by the transcription factor FNR (Green *et al*., 2014). Under anaerobic conditions FNR is a dimeric, site-specific, DNA-binding protein that mainly acts to activate expression of genes required for anaerobic growth (Crack *et al*., 2008b). Like *E. coli*, *P. aeruginosa*, which has the ability to grow using anaerobic respiration, possesses a single FNR protein known as ANR (Winteler and Haas, 1996). FNR and ANR are essentially functionally equivalent in that they act as activators of anaerobic gene expression in the absence of O_2 (Winteler and Haas, 1996). Interestingly, although *P. putida* KT2440 cannot grow under anaerobic conditions it possesses three FNR proteins: PP_4265 (ANR), PP_3233 and PP_3287.

The work described here was undertaken to better understand why *P. putida* has three FNR proteins. One hypothesis was that the three FNR proteins of *P. putida* have evolved to control specific sets of genes at different O_2 availabilities. Alternatively, only one of the three *P. putida* FNR proteins, probably ANR, is an O_2 sensor and the other FNR proteins respond to as yet unknown signals by virtue of binding different co-factors/sensory modules. The latter is not without precedent because in *P. aeruginosa* the anaerobic process of denitrification is controlled by two FNR family proteins, ANR and DNR. ANR regulates transcription of *dnr*, which in turn regulates expression of *nir* and *nor* in response to nitric oxide (Trunk *et al*., 2010).

Here it has been shown that all three *P. putida* FNR proteins possess O_2-sensitive [4Fe-4S] clusters that are required for site-specific binding to a common DNA sequence (FF site) (Ibrahim *et al*., 2015). Nevertheless, whilst the mechanism of the reaction of their [4Fe-4S] clusters with O_2 was the same as that of *E. coli* FNR (conversion of [4Fe-4S] to [2Fe-2S]) their sensitivities to O_2 differed. However, whilst the O_2 sensitivity of the ANR [4Fe-4S] cluster resembled that of FNR, the PP_3233

and PP_3287 [4Fe-4S] clusters showed lower sensitivity to O_2 compared to ANR. Phenotypic analysis of *P. putida* mutants that only expressed one FNR protein suggested that strains lacking *anr* were impaired under O_2-limited conditions, whereas those lacking *PP_3233* or *PP_3287* were impaired under aerobic conditions, consistent with the *in vitro* properties of the corresponding proteins (Ibrahim *et al*., 2015).

Like *E. coli* FNR, the iron-sulfur cluster of ANR reacted with nitric oxide *in vitro* and *in vivo* (Ibrahim *et al*., 2015). However, PP_3233 appeared to be insensitive to nitric oxide *in vitro* and *in vivo* and, despite a similar *in vitro* response, PP_3287-dependent reporter gene expression was not affected by the presence of nitric oxide (Ibrahim *et al*., 2015). Therefore, the research reported here suggests that the three *P. putida* FNR proteins are transcription factors that have evolved different iron-sulfur cluster environments such that they have differential responses to O_2 availability.

Under aerobic conditions, many bacteria conserve energy by aerobic respiration. Terminal oxidases play important roles in adaption to different O_2 availabilities. *Escherichia coli* possesses two terminal oxidases: cytochrome *bd-I* (Cyd) with high affinity for O_2 and cytochrome *bo'* (Cyo) with low affinity for O_2 (Bai *et al*., 2014). *Pseudomonas putida* can oxidise the ubiquinones by five terminal oxidases: Cyo (cytochrome bo_3; equivalent to Cyo in *E. coli*), CIO (cyanide-insensitive oxidase; equivalent to Cyd in *E. coli*), aa_3-type oxidase (aa_3) or a Cbb_3-type cytochrome c oxidase (Cbb_3-1 and Cbb_3-2) (Morales *et al*., 2006, Arai *et al*., 2014). As illustrated in Figure 7.1A, the *fnr* is expressed aerobically and anaerobically and is autoregulated (Spiro and Guest, 1987). Expression of genes coding the two terminal oxidases Cyo and Cyd are regulated by FNR as a direct O_2 sensor and ArcAB as an indirect O_2 sensor. Such that *cyo* and *cyd* operons are repressed by FNR, while *cyd* is activated by ArcAB (Bai *et al*., 2014).

The *anr* gene is expressed aerobically and anaerobically like *fnr* (Ibrahim *et al*., 2015). ANR can regulate multiple terminal oxidases (Cyo, CIO and Cbb_3-1,) similar to FNR (Figure 7.1B). Thus, the expression of Cbb_3-1 is activated by ANR while, CIO and Cyo are repressed (Figure 7.1B; Ugidos *et al*., 2008).

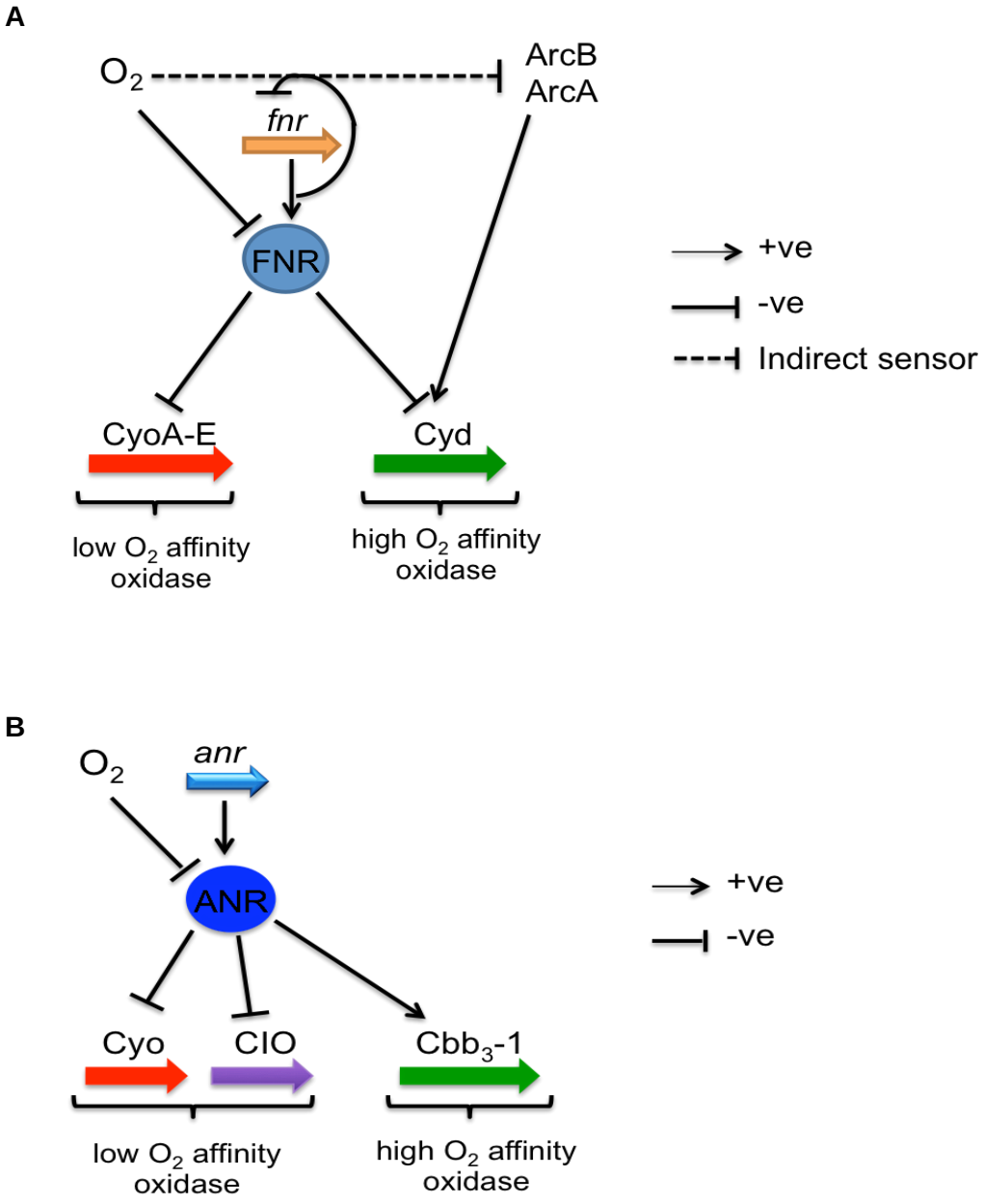

Figure 7.1: Model illustrates the expression of multiple-terminal oxidases. The diagram shows the regulation of genes encoding terminal oxidases by (**A**) FNR (http://www.ecocyc.org) and (**B**) ANR (Ugidos *et al*., 2008).

However, the roles of PP_3233 and PP_3287 are less clear, but the phenotypes of strains expressing just one of these proteins suggest that they operate predominantly under aerobic/micro-aerobic conditions.

Analysis of DNA sequence open reading frame revealed an inverted repeat located at upstream of the *PP_3233* -118.5 relative to the predicated transcript start (TTGAC----GTCAA). This sequence might be the PP_3233 box. A second sequence located at +93.5 (TTGAT----ATCAG) is strongly similar to the Arc box (TTGAC----ATCAG). It has been shown that *P. aeruginosa* ANR can bind to the Arc box (Galimand *et al*., 1991, Winteler and Haas, 1996), suggesting that ANR could bind at this site and repress the transcription of *PP_3233* under O_2-limilted conditions. When the O_2 concentration increases the ANR-DNA complex will breakdown but PP_3233 with its more stable iron-sulfur cluster would remain bound at the putative PP_3233 box and regulate its own expression (Figure 7.2). There is a hybrid sequence TTGAT----GTCAA upstream of *ccoN-1*, which is similar to the putative PP_3233 box and the ANR box suggesting that PP_3233 might contribute in regulation of the CIO and Cbb_3-1 terminal oxidases in addition to ANR (Figure 7.2).

Furthermore, a TTGAT----ATCAA (ANR box) was detected upstream of *PP_3287*, suggesting that *PP_3287* is regulated by ANR anaerobically. The DNA-recognition helices of *P. putida* FNR proteins possess similar motifs to FNR (Glu-209, Ser-212 and Arg-213; FNR number) in ANR and PP_3233, but not PP_3287, which possesses Cys in place of Ser (Figure 3.1). The presence of the cysteine residue suggested that it might contribute to reduction–oxidation (redox) mechanism and thereby function as a redox-sensitive cysteine residue (Xanthoudakis and Curran, 1992, Bandyopadhyay and Gronostajski, 1994).

Transcriptonic and proteomic studies for mutant strains that express only one of three FNR proteins will provide more details about the conditions that induce PP_3233 and PP_3287 target gene expression and the functions of these two proteins under different O_2 concentrations (aerobic and O_2-limited conditions). In addition, using *in vitro* analyses such as footprinting will help us to understand whether they regulate overlapping or distinct regulons. Furthermore, it is important to detect the concentrations of PP_3233 and PP_3287 under different O_2 concentrations by raising antibodies and qRT-PCR. Site-directed mutagenesis of the DNA-recognition helix of PP-3287 could be used to determine the affects of the cysteine residue on DNA-binding affinity. Using EMSAs for PP_3287 under reducing conditions could help to

determine the role of PP_3287 in growth of *P. putida* in diverse environments.

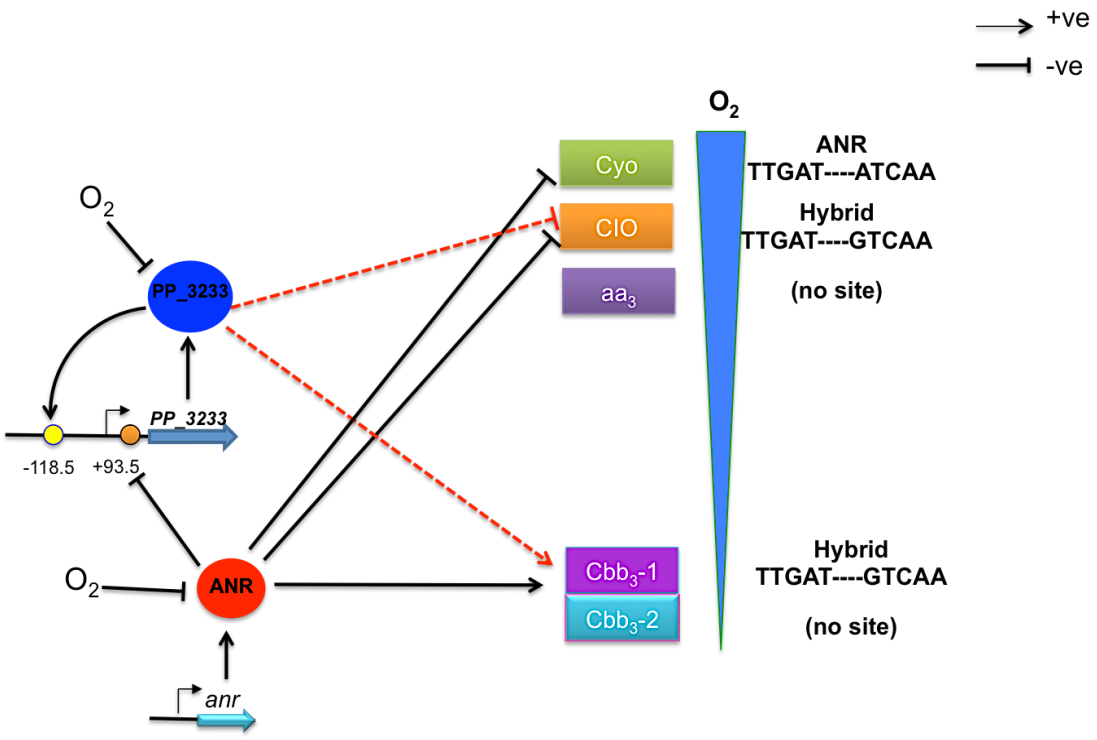

	ANR	PP_3233	Cyo	CIO	Cbb_3-1(2)
Very low O_2	active	-	Off	Off	On
Low O_2	inactive	active	On	Off	On
High O_2	inactive	inactive	On	On	Off

Figure 7.2: Transcription regulation model of ANR and PP_3233 in *Pseudomonas putida* KT2440. In response to anaerobic conditions, ANR is activated and binds to its DNA-binding site. As a result, the expression of terminal oxidases Cyo and CIO are repressed and Cbb_3-1 is activated. Expression of PP_3233 might be repressed by ANR, but when the concentration of O_2 increases the ANR-DNA binding will deactivate allowing PP_3233 with its more stable iron-sulfur cluster to activate its own expression and prolong activation of the high O_2 affinity terminal oxidase Cbb_3-1.

7.2 *Desulfovibrio desulfuricans* HcpR2

Desulfovibrio desulfuricans ATCC27774 is a Gram-negative sulfate reducing bacterium. It is an obligate anaerobic with the ability to utilize different electron acceptors such as nitrate, nitrite and sulfate. Anaerobically, sulfate is consumed first and then nitrate, however the conserved energy from nitrate reduction is higher than sulfate respiration (Cadby *et al*., 2011). *Desulfovibrio desulfuricans* ATCC27774 possesses five FNR-CRP family proteins. Two of these: HcpR and HcpR2 were predicted to regulate the transcription of *nap*, *sat* and *hcp.* The work presented in this thesis was undertaken to understand the role of HcpR2 in controlling the preference of sulfate respiration over nitrate reduction under anaerobic conditions.

Desulfovibrio desulfuricans ATCC27774 HcpR2 has been shown to be an O_2-sensitive transcription factor. Anaerobically, HcpR2 possesses a [4Fe-4S] cluster that is essential for O_2-sensing and DNA-binding. The iron-sulfur cluster of HcpR2 reacts with O_2 via assembly and disassembly of the [4Fe-4S] cluster. Nitric oxide-treated holo-HcpR2 showed lower affinity DNA-binding. Therefore, the results reported here suggest that HcpR2 is a transcription factor that has evolved to respond to O_2 and nitric oxide.

A cascade regulatory model was indicated in *P. aeruginosa* for gene regulation in response to nitrate utilization. *Pseudomonas aeruginosa* ANR possesses a [4Fe-4S] cluster to activate the expression of anaerobic genes (Yoon *et al*., 2007, Schreiber *et al*., 2007). As a result of nitrate reduction, nitric oxide is generated leading to nitrosylated the clusters and loss of the ability to bind DNA and regulate gene expression (Korner *et al*., 2003). DNR (haem protein) is regulated by ANR. As a result, the cascade of ANR-DNR activates the expression of *nir* and *nor* promoters in response to nitric oxide anaerobically (Figure 7.3; Trunk *et al*., 2010, Giardina *et al*., 2011).

The presented work here suggests that HcpR and HcpR2 might operate a similar model, but in the opposite direction to ANR-DNR cascade (Figure 7.4). In response to nitrate, *HcpR* (haem protein equivalent to *P. aeruginosa* DNR) is activated and binds to its DNA-binding site leading to transcription regulation of many genes involved in sulfate and nitrate reduction (Figure 6.3). One of these genes *hcpR2* is activated in response to O_2 or nitric oxide. Consequently, HcpR2 (iron-sulfur cluster protein

equivalent to *P. aeruginosa* ANR) derepresses transcription regulation of *hcp*, which is essential for the repair the iron-sulfur clusters.

To summarize, acquisition of an iron-sulfur cluster under anaerobic conditions and the alteration in DNA-binding in response to O_2 by HcpR2 regulates *hcp* expression. HcpR2 might help the *D. desulfuricans* to survive in oxic environments (low concentration) because high concentration of O_2 is toxic and reduces the viability of the cells. It has been shown that some of SRB family can utilize O_2 to generate ATP, but O_2 could be toxic because of reactive oxygen species (ROS). Therefore, *Desulfovibrio gigas* uses superoxide dismutase enzyme to protect the cells under aerobic conditions (Silva *et al*., 1999, Baumgartner *et al*., 2006). O_2-sensing and transcription regulation by HcpR2 could contribute in development of a new mechanism in *D. desulfuricans* to tolerate and adapt to O_2.

Phenotypic studies of mutant strains that express only HcpR2 under different O_2 and nitric oxide concentrations could reveal further details about the function of HcpR2. An *in vivo* study could help elucidate the role of HcpR2 in adaption to O_2 by measuring *hcpR2* transcript using qRT-PCR and HcpR2 protein by anti-serum raised against HcpR2 under different O_2 concentrations.

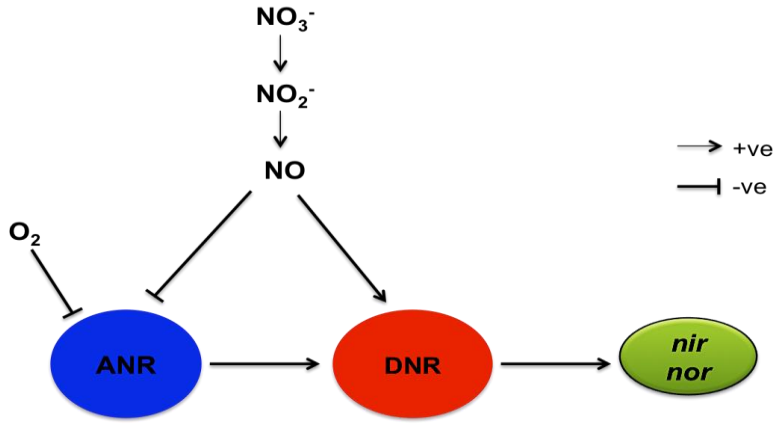

Figure 7.3: The ANR-DNR cascade regulatory model in the *Pseudomonas aeruginosa*. In anaerobic conditions, ANR is active and promotes the expression of *dnr*. In presence of nitrate, DNR is activated by ANR. As a result, *nir* and *nor* promoters are activated by DNR. Figure adapted from Trunk *et al*. (2010).

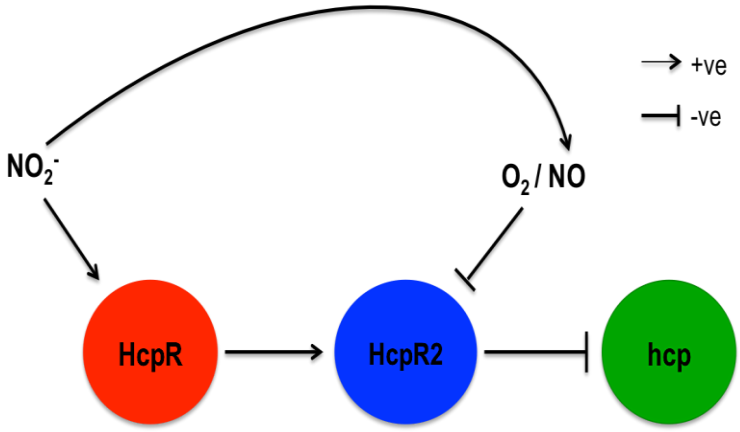

Figure 7.4: Transcription regulation model of HcpR and HcpR2 in *Desulfovibrio desulfuricans*. In response to nitrate, HcpR is activated and binds to its DNA-binding site leading to transcription regulation of many genes that are involved in nitrate and sulfate reduction. In response to O_2/nitric oxide, HcpR2 derepresses the transcription of hcp, which is involved in the repair the iron-sulfur cluster.

References

ACHEBACH, S., SELMER, T. and UNDEN, G. (2005) Properties and significance of apoFNR as a second form of air-inactivated [4Fe-4S].FNR of *Escherichia coli*. *FEBS J,* 272**(16):** 4260-4269.

ACHEBACH, S., TRAN, Q. H., VLAMIS-GARDIKAS, A., MULLNER, M., HOLMGREN, A. and UNDEN, G. (2004) Stimulation of Fe-S cluster insertion into apoFNR by *Escherichia coli* glutaredoxins 1, 2 and 3 *in vitro*. *FEBS Lett,* 565**(1-3):** 203-206.

AONO, S., NAKAJIMA, H., SAITO, K. and OKADA, M. (1996) A novel heme protein that acts as a carbon monoxide-dependent transcriptional activator in *Rhodospirillum rubrum*. *Biochem Biophys Res Commun,* 228**(3):** 752-756.

ARAI, H., KAWAKAMI, T., OSAMURA, T., HIRAI, T., SAKAI, Y. and ISHII, M. (2014) Enzymatic characterisation and *in vivo* function of five terminal oxidases in *Pseudomonas aeruginosa*. *J Bacteriol,* 196**(24):** 4206-4215.

AYALA-CASTRO, C., SAINI, A. and OUTTEN, F. W. (2008) Fe-S cluster assembly pathways in bacteria. *Microbiol Mol Biol Rev,* 72**(1):** 110-125.

BAI, H., ROLFE, M. D., JIA, W., COAKLEY, S., POOLE, R. K., GREEN, J. and HOLCOMBE, M. (2014) Agent-based modeling of oxygen-responsive transcription factors in *Escherichia coli*. *PLoS Comput Biol,* 10**(4):** e1003595.

BANDYOPADHYAY, S. and GRONOSTAJSKI, R. M. (1994) Identification of a conserved oxidation-sensitive cysteine residue in the NFI family of DNA-binding proteins. *J Biol Chem,* 269**(47):** 29949-29955.

BARNARD, A. M., GREEN, J. and BUSBY, S. J. (2003) Transcription regulation by tandem-bound FNR at *Escherichia coli* promoters. *J Bacteriol,* 185**(20):** 5993-6004.

BATES, D. M., POPESCU, C. V., KHOROSHILOVA, N., VOGT, K., BEINERT, H., MUNCK, E. and KILEY, P. J. (2000) Substitution of leucine 28 with histidine in the *Escherichia coli* transcription factor FNR results in increased stability of the $[4Fe\text{-}4S]^{2+}$ cluster to oxygen. *J Biol Chem,* 275**(9):** 6234-6240.

BAUMGARTNER, L. K., REID, R. P., DUPRAZ, C., DECHO, A. W., BUCKLEY, D. H., SPEAR, J. R., PRZEKOP, K. M. and VISSCHER, P. T. (2006) Sulfate reducing bacteria in microbial mats: Changing paradigms, new discoveries. *Sediment Geol,* 185**(3-4):** 131-145.

BEINERT, H. and KILEY, P. J. (1999) Fe-S proteins in sensing and regulatory functions. *Curr Opin Chem Biol,* 3**(2):** 152-157.

BELL, A. and BUSBY, S. (1994) Location and orientation of an activating region in the *Escherichia coli* transcription factor, FNR. *Mol Microbiol,* 11**(2):** 383-390.

BELL, A., GASTON, K., COLE, J. and BUSBY, S. (1989) Cloning of binding sequences for the *Escherichia coli* transcription activators, FNR and CRP: location of bases involved in discrimination between FNR and CRP. *Nucl Acids Res,* 17**(10):** 3865-3874.

BLAKE, T., BARNARD, A., BUSBY, S. J. and GREEN, J. (2002) Transcription activation by FNR: evidence for a functional activating region 2. *J Bacteriol,* 184**(21):** 5855-5861.

BODENMILLER, D. M. and SPIRO, S. (2006) The *yjeB* (*nsrR*) gene of *Escherichia coli* encodes a nitric oxide-sensitive transcriptional regulator. *J Bacteriol,* 188**(3):** 874-881.

BORDOLI, L., KIEFER, F., ARNOLD, K., BENKERT, P., BATTEY, J. and SCHWEDE, T. (2009) Protein structure homology modeling using SWISS-MODEL workspace. *Nat Protoc,* 4**(1):** 1-13.

BOTSFORD, J. L. and HARMAN, J. G. (1992) Cyclic AMP in prokaryotes. *Microbiol Rev,* 56**(1):** 100-122.

BRADFORD, M. M. (1976) A rapid and sensitive method for the quantitation of microgram quantities of protein utilizing the principle of protein-dye binding. *Anal Biochem,* 72**(1-2):** 248-254.

BROWN, N. L., STOYANOV, J. V., KIDD, S. P. and HOBMAN, J. L. (2003) The MerR family of transcriptional regulators. *FEMS Microbiol Rev,* 27**(2-3):** 145-163.

BROWNING, D. F. and BUSBY, S. J. (2004) The regulation of bacterial transcription initiation. *Nat Rev Microbiol,* 2**(1):** 57-65.

BROWNING, D. F., BEATTY, C. M., WOLFE, A. J., COLE, J. A. and BUSBY, S. J. (2002) Independent regulation of the divergent *Escherichia coli nrfA* and *acs*P1 promoters by a nucleoprotein assembly at a shared regulatory region. *Mol Microbiol,* 43**(3):** 687-701.

BUCK, M., GALLEGOS, M. T., STUDHOLME, D. J., GUO, Y. and GRALLA, J. D. (2000) The bacterial enhancer-dependent σ^{54} (σ^{N}) transcription factor. *J Bacteriol,* 182**(15):** 4129-4136.

BURGESS, R. R. (1971) RNA polymerase. *Annu Rev Biochem,* 40**,** 711-740.

BURGESS, R. R., TRAVERS, A. A., DUNN, J. J. and BAUTZ, E. K. (1969) Factor stimulating transcription by RNA polymerase. *Nature,* 221**(5175):** 43-46.

BUSBY, S. and EBRIGHT, R. H. (1997) Transcription activation at class II CAP-dependent promoters. *Mol Microbiol,* 23**(5):** 853-859.

CADBY, I. T. (2014) *The regulation of gene expression in sulfate reducing bacteria.* PhD Thesis, University of Birmingham.

CADBY, I. T., BUSBY, S. J. and COLE, J. A. (2011) An HcpR homologue from *Desulfovibrio desulfuricans* and its possible role in nitrate reduction and nitrosative stress. *Biochem Soc Trans,* 39**(1):** 224-229.

CHAKRABORTY, A., WANG, D., EBRIGHT, Y. W., KORLANN, Y., KORTKHONJIA, E., KIM, T., CHOWDHURY, S., WIGNESHWERARAJ, S., IRSCHIK, H., JANSEN, R., NIXON, B. T., KNIGHT, J., WEISS, S. and EBRIGHT, R. H. (2012) Opening and closing of the bacterial RNA polymerase clamp. *Science,* 337**(6094):** 591-595.

CHO, J.H., KIM, E.K. and SO, J.S. (1995) Improved transformation of *Pseudomonas putida* KT2440 by electroporation. *Biotechnol Tech,* 9**(1):** 41-44.

CONSTANTINIDOU, C., HOBMAN, J. L., GRIFFITHS, L., PATEL, M. D., PENN, C. W., COLE, J. A. and OVERTON, T. W. (2006) A reassessment of the FNR regulon and transcriptomic analysis of the effects of nitrate, nitrite, NarXL, and NarQP as *Escherichia coli* K12 adapts from aerobic to anaerobic growth. *J Biol Chem,* 281**(8):** 4802-4815.

CRACK, J. C., GREEN, J., CHEESMAN, M. R., LE BRUN, N. E. and THOMSON, A. J. (2007) Superoxide-mediated amplification of the oxygen-induced switch from [4Fe-4S] to [2Fe-2S] clusters in the transcriptional regulator FNR. *Proc Natl Acad Sci U S A,* 104**(7):** 2092-2097.

CRACK, J. C., GREEN, J., HUTCHINGS, M. I., THOMSON, A. J. and LE BRUN, N. E. (2012a) Bacterial iron-sulfur regulatory proteins as biological sensor-switches. *Antioxid Redox Signal,* 17**(9):** 1215-1231.

CRACK, J. C., GREEN, J., LE BRUN, N. E. and THOMSON, A. J. (2006) Detection of sulfide release from the oxygen-sensing [4Fe-4S] cluster of FNR. *J Biol Chem,* 281**(28):** 18909-18913.

CRACK, J. C., GREEN, J., THOMSON, A. J. and LE BRUN, N. E. (2012b) Iron-sulfur cluster sensor-regulators. *Curr Opin Chem Biol,* 16**(1-2):** 35-44.

CRACK, J. C., JERVIS, A. J., GASKELL, A. A., WHITE, G. F., GREEN, J., THOMSON, A. J. and LE BRUN, N. E. (2008a) Signal perception by FNR: the role of the iron-sulfur cluster. *Biochem Soc Trans,* 36**(6):** 1144-1148.

CRACK, J. C., LE BRUN, N. E., THOMSON, A. J., GREEN, J. and JERVIS, A. J. (2008b) Reactions of nitric oxide and oxygen with the regulator of fumarate and

nitrate reduction, a global transcriptional regulator, during anaerobic growth of *Escherichia coli*. *Meth Enzymol,* 437**,** 191-209.

CRACK, J. C., SMITH, L. J., STAPLETON, M. R., PECK, J., WATMOUGH, N. J., BUTTNER, M. J., BUXTON, R. S., GREEN, J., OGANESYAN, V. S., THOMSON, A. J. and LE BRUN, N. E. (2011) Mechanistic insight into the nitrosylation of the [4Fe-4S] cluster of WhiB-like proteins. *J Am Chem Soc,* 133**(4):** 1112-1121.

CRACK, J. C., STAPLETON, M. R., GREEN, J., THOMSON, A. J. and LE BRUN, N. E. (2013) Mechanism of $[4Fe\text{-}4S](Cys)_4$ cluster nitrosylation is conserved among NO-responsive regulators. *J Biol Chem,* 288**(16):** 11492-11502.

CRACK, J., GREEN, J. and THOMSON, A. J. (2004) Mechanism of oxygen sensing by the bacterial transcription factor fumarate-nitrate reduction (FNR). *J Biol Chem,* 279**(10):** 9278-9286.

CRAMER, P., BUSHNELL, D. A. and KORNBERG, R. D. (2001) Structural basis of transcription: RNA polymerase II at 2.8 angstrom resolution. *Science,* 292**(5523):** 1863-1876.

CRUZ-RAMOS, H., CRACK, J., WU, G., HUGHES, M. N., SCOTT, C., THOMSON, A. J., GREEN, J. and POOLE, R. K. (2002) NO sensing by FNR: regulation of the *Escherichia coli* NO-detoxifying flavohaemoglobin, Hmp. *EMBO J.,* 21**(13):** 3235-3244.

DADDAOUA, A., MOLINA-SANTIAGO, C., DE LA TORRE, J., KRELL, T. and RAMOS, J. L. (2014) GtrS and GltR form a two-component system: the central role of 2-ketogluconate in the expression of exotoxin A and glucose catabolic enzymes in *Pseudomonas aeruginosa*. *Nucl Acids Res,* 42**(12):** 7654-7663.

DARST, S. A. (2001) Bacterial RNA polymerase. *Curr Opin Struct Biol,* 11**(2):** 155-162.

DAVIS, C. A., CAPP, M. W., RECORD, M. T., JR. and SAECKER, R. M. (2005) The effects of upstream DNA on open complex formation by *Escherichia coli* RNA polymerase. *Proc Natl Acad Sci U S A,* 102**(2):** 285-290.

DEL CASTILLO, T., RAMOS, J. L., RODRIGUEZ-HERVA, J. J., FUHRER, T., SAUER, U. and DUQUE, E. (2007) Convergent peripheral pathways catalyze initial glucose catabolism in *Pseudomonas putida*: genomic and flux analysis. *J Bacteriol,* 189**(14):** 5142-5152.

DELANO, W. (2002) The PyMOL Molecular Graphics System; South San Francisco, CA: DeLano Scientific.

DIBDEN, D. P. and GREEN, J. (2005) *In vivo* cycling of the *Escherichia coli* transcription factor FNR between active and inactive states. *Microbiol,* 151**(12):** 4063-4070.

DOI, R. H. and WANG, L. F. (1986) Multiple procaryotic ribonucleic acid polymerase σ factors. *Microbiol Rev,* 50**(3):** 227-243.

DOS SANTOS, V. A. M., TIMMIS, K. N., TÜMMLER, B. and WEINEL, C. (2004) Genomic features of *Pseudomonas putida* strain KT2440. *Pseudomonas*, 77-112. Springer US.

DUAN, X., YANG, J., REN, B., TAN, G. and DING, H. (2009) Reactivity of nitric oxide with the [4Fe-4S] cluster of dihydroxyacid dehydratase from *Escherichia coli*. *Biochem J,* 417**(3):** 783-789.

EBRIGHT, R. H. (2000) RNA polymerase: structural similarities between bacterial RNA polymerase and eukaryotic RNA polymerase II. *J Mol Biol,* 304**(5):** 687-698.

EGLAND, P. G. and HARWOOD, C. S. (2000) HbaR, a 4-hydroxybenzoate sensor and FNR-CRP superfamily member, regulates anaerobic 4-hydroxybenzoate degradation by *Rhodopseudomonas palustris*. *J Bacteriol,* 182**(1):** 100-106.

EIGLMEIER, K., HONORE, N., IUCHI, S., LIN, E. C. and COLE, S. T. (1989) Molecular genetic analysis of FNR-dependent promoters. *Mol Microbiol,* 3**(7):** 869-878.

ESTREM, S. T., ROSS, W., GAAL, T., CHEN, Z. W., NIU, W., EBRIGHT, R. H. and GOURSE, R. L. (1999) Bacterial promoter architecture: subsite structure of UP elements and interactions with the carboxy-terminal domain of the RNA polymerase alpha subunit. *Genes Dev,* 13**(16):** 2134-2147.

FEKLISTOV, A. and DARST, S. A. (2011) Structural basis for promoter-10 element recognition by the bacterial RNA polymerase sigma subunit. *Cell,* 147**(6):** 1257-1269.

FILENKO, N., SPIRO, S., BROWNING, D. F., SQUIRE, D., OVERTON, T. W., COLE, J. and CONSTANTINIDOU, C. (2007) The NsrR regulon of *Escherichia coli* K-12 includes genes encoding the hybrid cluster protein and the periplasmic, respiratory nitrite reductase. *J Bacteriol,* 189**(12):** 4410-4417.

FISCHER, H.M. (1994) Genetic regulation of nitrogen fixation in rhizobia. *Microbiol Rev,* 58**(3):** 352-386.

FONSECA, P., MORENO, R. and ROJO, F. (2011) Growth of *Pseudomonas putida* at low temperature: global transcriptomic and proteomic analyses. *Environ Microbiol Rep,* 3**(3):** 329-339.

GALIMAND, M., GAMPER, M., ZIMMERMANN, A. and HAAS, D. (1991) Positive FNR-like control of anaerobic arginine degradation and nitrate respiration in *Pseudomonas aeruginosa*. *J Bacteriol,* 173**(5):** 1598-1606.

GIARDINA, G., CASTIGLIONE, N., CARUSO, M., CUTRUZZOLA, F. and RINALDO, S. (2011) The *Pseudomonas aeruginosa* DNR transcription factor: light and shade of nitric oxide-sensing mechanisms. *Biochem Soc Trans,* 39**(1):** 294-298.

GOSTICK, D. O., GREEN, J., IRVINE, A. S., GASSON, M. J. and GUEST, J. R. (1998) A novel regulatory switch mediated by the FNR-like protein of *Lactobacillus casei*. *Microbiol,* 144**(3),** 705-717.

GOURSE, R. L., ROSS, W. and GAAL, T. (2000) UPs and downs in bacterial transcription initiation: the role of the alpha subunit of RNA polymerase in promoter recognition. *Mol Microbiol,* 37**(4):** 687-695.

GREEN, J. and GUEST, J. R. (1994) Regulation of transcription at the ndh promoter of *Escherichia coli* by FNR and novel factors. *Mol Microbiol,* 12**(3):** 433-444.

GREEN, J., ANJUM, M. F. and GUEST, J. R. (1996b) The ndh-binding protein (Nbp) regulates the *ndh* gene of *Escherichia coli* in response to growth phase and is identical to Fis. *Mol Microbiol,* 20**(5):** 1043-1055.

GREEN, J., BENNETT, B., JORDAN, P., RALPH, E. T., THOMSON, A. J. and GUEST, J. R. (1996a) Reconstitution of the [4Fe-4S] cluster in FNR and demonstration of the aerobic-anaerobic transcription switch *in vitro*. *Biochem J,* 316**(3):** 887-92.

GREEN, J., CRACK, J. C., THOMSON, A. J. and LEBRUN, N. E. (2009) Bacterial sensors of oxygen. *Curr Opin Microbiol,* 12**(2):** 145-151.

GREEN, J., IRVINE, A. S., MENG, W. and GUEST, J. R. (1996c) FNR-DNA interactions at natural and semi-synthetic promoters. *Mol Microbiol,* 19**(1):** 125-137.

GREEN, J., ROLFE, M. D. and SMITH, L. J. (2014) Transcriptional regulation of bacterial virulence gene expression by molecular oxygen and nitric oxide. *Virulence,* 5**(8)**: 794-809

GREEN, J., SCOTT, C. and GUEST, J. R. (2001) Functional versatility in the CRP-FNR superfamily of transcription factors: FNR and FLP. *Adv Microb Physiol,* 44**,** 1-34.

GREEN, J., TRAGESER, M., SIX, S., UNDEN, G. and GUEST, J. R. (1991) Characterisation of the FNR protein of *Escherichia coli*, an iron-binding transcriptional regulator. *Proc Biol Sci,* 244**(1310):** 137-144.

GREENE, E., HUBERT, C., NEMATI, M., JENNEMAN, G. and VOORDOUW, G. (2003) Nitrite reductase activity of sulfate- reducing bacteria prevents their

inhibition by nitrate- reducing, sulfide- oxidizing bacteria. *Environ Microbiol,* 5**(7)** 607-617.

GRIES, T. J., KONTUR, W. S., CAPP, M. W., SAECKER, R. M. and RECORD, M. T., JR. (2010) One-step DNA melting in the RNA polymerase cleft opens the initiation bubble to form an unstable open complex. *Proc Natl Acad Sci U S A,* 107**(23):** 10418-10423.

GROSS, C. A., CHAN, C., DOMBROSKI, A., GRUBER, T., SHARP, M., TUPY, J. and YOUNG, B. (1998) The functional and regulatory roles of sigma factors in transcription. *Cold Spring Harb Symp Quant Biol,* 63**,** 141-55.

GUAN, K. and DIXON, J. E. (1991) Eukaryotic proteins expressed in *Escherichia coli*: an improved thrombin cleavage and purification procedure of fusion proteins with glutathione *S*-transferase. *Anal Biochem,* 192**(2):** 262-267.

GUEST, J. R., GREEN, J., IRVINE, A. S. and SPIRO, S. (1996) The FNR modulon and FNR-regulated gene expression. *Regulation of gene expression in Escherichia coli*, 317-342. Springer US.

HARDEN, T. T., WELLS, C. D., FRIEDMAN, L. J., LANDICK, R., HOCHSCHILD, A., KONDEV, J. and GELLES, J. (2016) Bacterial RNA polymerase can retain σ^{70} throughout transcription. *Proc Natl Acad Sci U S A***,** 113**(3):** 602-607.

HAUGEN, S. P., BERKMEN, M. B., ROSS, W., GAAL, T., WARD, C. and GOURSE, R. L. (2006) rRNA promoter regulation by nonoptimal binding of σ region 1.2: an additional recognition element for RNA polymerase. *Cell,* 125**(6):** 1069-1082.

HELMANN, J. D. and CHAMBERLIN, M. J. (1988) Structure and function of bacterial sigma factors. *Annu Rev Biochem,* 57**(1):** 839-872.

HOANG, T. T., KARKHOFF-SCHWEIZER, R. R., KUTCHMA, A. J. and SCHWEIZER, H. P. (1998) A broad-host-range Flp-FRT recombination system for site-specific excision of chromosomally-located DNA sequences: application for isolation of unmarked *Pseudomonas aeruginosa* mutants. *Gene,* 212**(1):** 77-86.

HOFER, B., MULLER, D. and KOSTER, H. (1985) The pathway of *E. coli* RNA polymerase-promoter complex formation as visualized by footprinting. *Nucl Acids Res,* 13**(16):** 5995-6013.

IBRAHIM, S. A., CRACK, J. C., ROLFE, M. D., ACUNA, J. M., THOMSON, A. J., LE BRUN, N. E., SCHOBERT, M., STAPLETON, M. R. and GREEN, J. (2015) Three *Pseudomonas putida* FNR family proteins with different sensitivities to O_2. *J Biol Chem,* 290**(27):** 16812-16823.

IGARASHI, K. and ISHIHAMA, A. (1991) Bipartite functional map of the *E. coli* RNA polymerase alpha subunit: involvement of the C-terminal region in transcription activation by cAMP-CRP. *Cell,* 65**(6):** 1015-1022.

IMLAY, J. A. (2002) How oxygen damages microbes: oxygen tolerance and obligate anaerobiosis. *Adv Microb Physiol,* 46**,** 111-153.

JERVIS, A. J., CRACK, J. C., WHITE, G., ARTYMIUK, P. J., CHEESMAN, M. R., THOMSON, A. J., LE BRUN, N. E. and GREEN, J. (2009) The O_2 sensitivity of the transcription factor FNR is controlled by Ser24 modulating the kinetics of [4Fe-4S] to [2Fe-2S] conversion. *Proc Natl Acad Sci U S A,* 106**(12):** 4659-4664.

JERVIS, A. J. and GREEN, J. (2007) *In vivo* demonstration of FNR dimers in response to lower O_2 availability. *J Bacteriol,* 189**(7):** 2930-2932.

KANG, Y., WEBER, K. D., QIU, Y., KILEY, P. J. and BLATTNER, F. R. (2005) Genome-wide expression analysis indicates that FNR of *Escherichia coli* K-12 regulates a large number of genes of unknown function. *J Bacteriol,* 187**(3):** 1135-1160.

KARGALIOGLU, Y. and IMLAY, J. A. (1994) Importance of anaerobic superoxide dismutase synthesis in facilitating outgrowth of *Escherichia coli* upon entry into an aerobic habitat. *J Bacteriol,* 176**(24):** 7653-7658.

KHOROSHILOVA, N., BEINERT, H. and KILEY, P. J. (1995) Association of a polynuclear iron-sulfur center with a mutant FNR protein enhances DNA binding. *Proc Natl Acad Sci U S A,* 92**(7):** 2499-2503.

KHOROSHILOVA, N., POPESCU, C., MUNCK, E., BEINERT, H. and KILEY, P. J. (1997) Iron-sulfur cluster disassembly in the FNR protein of *Escherichia coli* by O_2: [4Fe-4S] to [2Fe-2S] conversion with loss of biological activity. *Proc Natl Acad Sci U S A,* 94**(12):** 6087-6092.

KILEY, P. J. and REZNIKOFF, W. S. (1991) FNR mutants that activate gene expression in the presence of oxygen. *J Bacteriol,* 173**(1):** 16-22.

KLOTZ, M. G. and HUTCHESON, S. W. (1992) Multiple periplasmic catalases in phytopathogenic strains of *Pseudomonas syringae*. *Appl Environ Microbiol,* 58**(8):** 2468-2473.

KONTUR, W. S., SAECKER, R. M., CAPP, M. W. and RECORD, M. T. (2008) Late steps in the formation of *E. coli* RNA polymerase λP_R promoter open complexes: characterisation of conformational changes by rapid [perturbant] upshift experiments. *J Mol Biol,* 376**(4):** 1034-1047.

KONTUR, W. S., SAECKER, R. M., DAVIS, C. A., CAPP, M. W. and RECORD, M. T. (2006) Solute probes of conformational changes in open complex (RP_o)

formation by *Escherichia coli* RNA polymerase at the λP_R promoter: evidence for unmasking of the active site in the isomerization step and for large-scale coupled folding in the subsequent conversion to RP_o. *Biochem,* 45**(7):** 2161-2177.

KORNER, H., SOFIA, H. J. and ZUMFT, W. G. (2003) Phylogeny of the bacterial superfamily of CRP-FNR transcription regulators: exploiting the metabolic spectrum by controlling alternative gene programs. *FEMS Microbiol Rev,* 27**(5):** 559-592.

KOVACH, M. E., ELZER, P. H., HILL, D. S., ROBERTSON, G. T., FARRIS, M. A., ROOP, R. M. 2nd and PETERSON, K. M. (1995) Four new derivatives of the broad-host-range cloning vector pBBR1MCS, carrying different antibiotic-resistance cassettes. *Gene,* 166**(1):** 175-176.

KOVACIC, R. T. (1987) The 0 °C closed complexes between *Escherichia coli* RNA polymerase and two promoters, T7-A3 and *lacUV5*. *J Biol Chem,* 262**(28):** 13654-13661.

KUREISHI, A., DIVER, J. M., BECKTHOLD, B., SCHOLLAARDT, T. and BRYAN, L. E. (1994) Cloning and nucleotide sequence of *Pseudomonas aeruginosa* DNA gyrase *gyrA* gene from strain PAO1 and quinolone-resistant clinical isolates. *Antimicrob Agents Chemother,* 38**(9):** 1944-1952.

KUROKI, M., IGARASHI, Y., ISHII, M. and ARAI, H. (2014) Fine-tuned regulation of the dissimilatory nitrite reductase gene by oxygen and nitric oxide in *Pseudomonas aeruginosa*. *Environ Microbiol Rep,* 6**(6):** 792-801.

LAMBERG, K. E. and KILEY, P. J. (2000) FNR-dependent activation of the class II *dmsA* and *narG* promoters of *Escherichia coli* requires FNR-activating regions 1 and 3. *Mol Microbiol,* 38**(4):** 817-827.

LAEMMLI, U. K. (1970) Cleavage of structural proteins during the assembly of the head of bacteriophage T4. *nature,* 227**(5259):** 680-685.

LAWSON, C. L., SWIGON, D., MURAKAMI, K. S., DARST, S. A., BERMAN, H. M. and EBRIGHT, R. H. (2004) Catabolite activator protein: DNA binding and transcription activation. *Curr Opin Struct Biol,* 14**(1):** 10-20.

LAZAZZERA, B. A., BATES, D. M. and KILEY, P. J. (1993) The activity of the *Escherichia coli* transcription factor FNR is regulated by a change in oligomeric state. *Genes Dev,* 7**(10):** 1993-2005.

LAZAZZERA, B. A., BEINERT, H., KHOROSHILOVA, N., KENNEDY, M. C. and KILEY, P. J. (1996) DNA binding and dimerization of the Fe-S-containing FNR protein from *Escherichia coli* are regulated by oxygen. *J Biol Chem,* 271**(5):** 2762-2768.

LEE, D. J., WING, H. J., SAVERY, N. J. and BUSBY, S. J. (2000) Analysis of interactions between Activating Region 1 of *Escherichia coli* FNR protein and the C-terminal domain of the RNA polymerase alpha subunit: use of alanine scanning and suppression genetics. *Mol Microbiol,* 37**(5):** 1032-1040.

LESSIE, T. G. and PHIBBS, P. V. JR. (1984) Alternative pathways of carbohydrate utilization in *pseudomonads*. *Annu Rev Microbiol,* 38**(1):** 359-388.

LI, B., WING, H., LEE, D., WU, H. C. and BUSBY, S. (1998) Transcription activation by *Escherichia coli* FNR protein: similarities to, and differences from, the CRP paradigm. *Nucl Acids Res,* 26**(9):** 2075-2081.

LOBO, S. A., MELO, A. M., CARITA, J. N., TEIXEIRA, M. and SARAIVA, L. M. (2007) The anaerobe *Desulfovibrio desulfuricans* ATCC 27774 grows at nearly atmospheric oxygen levels. *FEBS letters,* 581**(3):** 433-436.

LODGE, J., WILLIAMS, R., BELL, A., CHAN, B. and BUSBY, S. (1990) Comparison of promoter activities in *Escherichia coli* and *Pseudomonas aeruginosa* use of a new broad host range promoter probe plasmid. *FEMS Microbiol Lett,* 67**(3):** 221-225.

LODISH, H. (2013) *Molecular cell biology*. 7th edition. New York, Macmillan.

LOPEZ, O., MORERA, C., MIRANDA-RIOS, J., GIRARD, L., ROMERO, D. and SOBERON, M. (2001) Regulation of gene expression in response to oxygen in *Rhizobium etli*: role of FnrN in *fixNOQP* expression and in symbiotic nitrogen fixation. *J Bacteriol,* 183**(24):** 6999-7006.

MARIETOU, A., GRIFFITHS, L. and COLE, J. (2009) Preferential reduction of the thermodynamically less favorable electron acceptor, sulfate, by a nitrate-reducing strain of the sulfate-reducing bacterium *Desulfovibrio desulfuricans* 27774. *J Bacteriol,* 191**(3):** 882-889.

MARTINEZ-ANTONIO, A. and COLLADO-VIDES, J. (2003) Identifying global regulators in transcriptional regulatory networks in bacteria. *Curr Opin Microbiol,* 6**(5):** 482-489.

MARTÍNEZ- GARCÍA, E. and DE LORENZO, V. (2011) Engineering multiple genomic deletions in Gram- negative bacteria: analysis of the multi- resistant antibiotic profile of *Pseudomonas putida* KT2440. *Environ Microbiol,* 13**(10):** 2702-2716.

MECSAS, J., COWING, D. W. and GROSS, C. A. (1991) Development of RNA polymerase-promoter contacts during open complex formation. *J Mol Biol,* 220**(3):** 585-597.

MEKLER, V., KORTKHONJIA, E., MUKHOPADHYAY, J., KNIGHT, J., REVYAKIN, A., KAPANIDIS, A. N., NIU, W., EBRIGHT, Y. W., LEVY, R. and

EBRIGHT, R. H. (2002) Structural organization of bacterial RNA polymerase holoenzyme and the RNA polymerase-promoter open complex. *Cell,* 108**(5):** 599-614.

MENG, W., GREEN, J. and GUEST, J. R. (1997) FNR-dependent repression of ndh gene expression requires two upstream FNR-binding sites. *Microbiol,* 143**(5):** 1521-1532.

METTERT, E. L., OUTTEN, F. W., WANTA, B. and KILEY, P. J. (2008) The impact of O_2 on the Fe-S cluster biogenesis requirements of *Escherichia coli* FNR. *J Mol Biol,* 384**(4):** 798-811.

MILLER, J. H. (1993) *A Short Course in Bacterial Genetics: Laboratory Manual and Handbook for Escherichia coli and Related Bacteria*. United State of America. Cold Spring Harbor Laboratory Press.

MITCHELL, G. J., JONES, J. G. and COLE, J. A. (1986) Distribution and regulation of nitrate and nitrite reduction by *Desulfovibrio* and *Desulfotomaculum* species. *Arch Microbiol,* 144**(1):** 35-40.

MORALES, G., UGIDOS, A. and ROJO, F. (2006) Inactivation of the *Pseudomonas putida* cytochrome *o* ubiquinol oxidase leads to a significant change in the transcriptome and to increased expression of the CIO and *cbb3*-1 terminal oxidases. *Environ Microbiol,* 8**(10):** 1764-1774.

MURAKAMI, K. S. (2013) X-ray crystal structure of *Escherichia coli* RNA polymerase σ^{70} holoenzyme. *J Biol Chem,* 288**(13):** 9126-9134.

MURAKAMI, K. S. (2015) Structural biology of bacterial RNA polymerase. *Biomolecules,* 5**(2):** 848-864.

MURAKAMI, K. S. and DARST, S. A. (2003) Bacterial RNA polymerases: the wholo story. *Curr Opin Struct Biol,* 13**(1):** 31-39.

MUYZER, G. and STAMS, A. J. (2008) The ecology and biotechnology of sulfate-reducing bacteria. *Nat Rev Microbiol,* 6**(6):** 441-454.

MYERS, K. S., YAN, H., ONG, I. M., CHUNG, D., LIANG, K., TRAN, F., KELES, S., LANDICK, R. and KILEY, P. J. (2013) Genome-scale analysis of *Escherichia coli* FNR reveals complex features of transcription factor binding. *PLoS Genet,* 9**(6):** e1003565.

NELSON, K. E., WEINEL, C., PAULSEN, I. T., DODSON, R. J., HILBERT, H., MARTINS DOS SANTOS, V. A., FOUTS, D. E., GILL, S. R., POP, M., HOLMES, M., BRINKAC, L., BEANAN, M., DEBOY, R. T., DAUGHERTY, S., KOLONAY, J., MADUPU, R., NELSON, W., WHITE, O., PETERSON, J., KHOURI, H., HANCE, I., CHRIS LEE, P., HOLTZAPPLE, E., SCANLAN, D., TRAN, K., MOAZZEZ, A., UTTERBACK, T., RIZZO, M., LEE, K., KOSACK, D., MOESTL,

D., WEDLER, H., LAUBER, J., STJEPANDIC, D., HOHEISEL, J., STRAETZ, M., HEIM, S., KIEWITZ, C., EISEN, J. A., TIMMIS, K. N., DUSTERHOFT, A., TUMMLER, B. and FRASER, C. M. (2002) Complete genome sequence and comparative analysis of the metabolically versatile *Pseudomonas putida* KT2440. *Environ Microbiol,* 4**(12):** 799-808.

O'CALLAGHAN, J., REEN, F. J., ADAMS, C. and O'GARA, F. (2011) Low oxygen induces the type III secretion system in *Pseudomonas aeruginosa* via modulation of the small RNAs *rsmZ* and *rsmY*. *Microbiol,* 157**(12):** 3417-3428.

ODOM, J. M. and PECK, H. D. JR. (1981) Localization of dehydrogenases, reductases, and electron transfer components in the sulfate-reducing bacterium *Desulfovibrio gigas*. *J Bacteriol,* 147**(1):** 161-169.

PARTRIDGE, J. D., SANGUINETTI, G., DIBDEN, D. P., ROBERTS, R. E., POOLE, R. K. and GREEN, J. (2007) Transition of *Escherichia coli* from aerobic to micro-aerobic conditions involves fast and slow reacting regulatory components. *J Biol Chem,* 282**(15):** 11230-11237.

PARTRIDGE, J. D., SCOTT, C., TANG, Y., POOLE, R. K. and GREEN, J. (2006) *Escherichia coli* transcriptome dynamics during the transition from anaerobic to aerobic conditions. *J Biol Chem,* 281**(38):** 27806-27815.

PEREZ-RUEDA, E. and COLLADO-VIDES, J. (2000) The repertoire of DNA-binding transcriptional regulators in *Escherichia coli* K-12. *Nucl Acids Res,* 28**(8):** 1838-1847.

PIRES, R. H., VENCESLAU, S. S., MORAIS, F., TEIXEIRA, M., XAVIER, A. V. and PEREIRA, I. A. (2006) Characterisation of the *Desulfovibrio desulfuricans* ATCC 27774 DsrMKJOP complex a membrane-bound redox complex involved in the sulfate respiratory pathway. *Biochem,* 45**(1):** 249-262.

POOLE, R. K. (2005) Nitric oxide and nitrosative stress tolerance in bacteria. *Biochem Soc Trans,* 33**(1):** 176-180.

POPOVYCH, N., TZENG, S. R., TONELLI, M., EBRIGHT, R. H. and KALODIMOS, C. G. (2009) Structural basis for cAMP-mediated allosteric control of the catabolite activator protein. *Proc Natl Acad Sci U S A,* 106**(17):** 6927-6932.

PRESTON, G. M. (2000) *Pseudomonas syringae* pv. *tomato*: the right pathogen, of the right plant, at the right time. *Mol Plant Pathol,* 1**(5):** 263-275.

PULLAN, S. T., GIDLEY, M. D., JONES, R. A., BARRETT, J., STEVANIN, T. M., READ, R. C., GREEN, J. and POOLE, R. K. (2007) Nitric oxide in chemostat-cultured *Escherichia coli* is sensed by FNR and other global regulators: unaltered methionine biosynthesis indicates lack of S nitrosation. *J Bacteriol,* 189**(5):** 1845-1855.

RALPH, E. T., GUEST, J. R. and GREEN, J. (1998) Altering the anaerobic transcription factor FNR confers a hemolytic phenotype on *Escherichia coli* K12. *Proc Natl Acad Sci U S A,* 95**(18):** 10449-10452.

RALPH, E. T., SCOTT, C., JORDAN, P. A., THOMSON, A. J., GUEST, J. R. and GREEN, J. (2001) Anaerobic acquisition of [4Fe-4S] clusters by the inactive FNR(C20S) variant and restoration of activity by second-site amino acid substitutions. *Mol Microbiol,* 39**(5):** 1199-1211.

REINHART, F., ACHEBACH, S., KOCH, T. and UNDEN, G. (2008) Reduced apo-fumarate nitrate reductase regulator (apoFNR) as the major form of FNR in aerobically growing *Escherichia coli*. *J Bacteriol,* 190**(3):** 879-886.

ROE, J. H., BURGESS, R. R. and RECORD, M. T. JR. (1985) Temperature dependence of the rate constants of the *Escherichia coli* RNA polymerase λP_R promoter interaction. Assignment of the kinetic steps corresponding to protein conformational change and DNA opening. *J Mol Biol,* 184**(3):** 441-453.

ROSS, W., GOSINK, K. K., SALOMON, J., IGARASHI, K., ZOU, C., ISHIHAMA, A., SEVERINOV, K. and GOURSE, R. L. (1993) A third recognition element in bacterial promoters: DNA binding by the alpha subunit of RNA polymerase. *Science,* 262**(5138):** 1407-1413.

ROSS, W. and GOURSE, R. L. (2005) Sequence-independent upstream DNA-αCTD interactions strongly stimulate *Escherichia coli* RNA polymerase-*lacUV5* promoter association. *Proc Natl Acad Sci U S A,* 102**(2):** 291-296.

RUFF, E. F., RECORD, M. T. JR. and ARTSIMOVITCH, I. (2015) Initial events in bacterial transcription initiation. *Biomolecules,* 5**(2):** 1035-1062.

SAECKER, R. M., TSODIKOV, O. V., MCQUADE, K. L., SCHLAX, P. E., CAPP, M. W. and RECORD, M. T. (2002) Kinetic studies and structural models of the association of *E. coli* σ^{70} RNA polymerase with the λP_R promoter: Large scale conformational changes in forming the kinetically significant intermediates. *J Molecul Biol,* 319**(3):** 649-671.

SASS, A. M., SCHMERK, C., AGNOLI, K., NORVILLE, P. J., EBERL, L., VALVANO, M. A. and MAHENTHIRALINGAM, E. (2013) The unexpected discovery of a novel low-oxygen-activated locus for the anoxic persistence of *Burkholderia cenocepacia*. *ISME J,* 7**(8):** 1568-1581.

SAWERS, G. (1999) The aerobic/anaerobic interface. *Curr Opin Microbiol,* 2**(2):** 181-187.

SAWERS, G., KAISER, M., SIRKO, A. and FREUNDLICH, M. (1997) Transcriptional activation by FNR and CRP: reciprocity of binding-site recognition. *Mol Microbiol,* 23**(4):** 835-845.

SAYLE, R. A. and MILNER-WHITE, E. J. (1995) RASMOL: biomolecular graphics for all. *Trends Biochem Sci,* 20**(9):** 374.

SCHELLHORN, H. E. and HASSAN, H. M. (1988) Transcriptional regulation of *katE* in *Escherichia coli* K-12. *J Bacteriol,* 170**(9):** 4286-4292.

SCHICKOR, P., METZGER, W., WEREL, W., LEDERER, H. and HEUMANN, H. (1990) Topography of intermediates in transcription initiation of *E. coli*. *EMBO J,* 9**(7):** 2215-2220.

SCHNIDER, U., KEEL, C., BLUMER, C., TROXLER, J., DEFAGO, G. and HAAS, D. (1995) Amplification of the housekeeping sigma factor in *Pseudomonas fluorescens* CHA0 enhances antibiotic production and improves biocontrol abilities. *J Bacteriol,* 177**(18):** 5387-5392.

SCHREIBER, K., KRIEGER, R., BENKERT, B., ESCHBACH, M., ARAI, H., SCHOBERT, M. and JAHN, D. (2007) The anaerobic regulatory network required for *Pseudomonas aeruginosa* nitrate respiration. *J Bacteriol,* 189**(11):** 4310-4314.

SCHWARTZ, C. J., DJAMAN, O., IMLAY, J. A. and KILEY, P. J. (2000) The cysteine desulfurase, IscS, has a major role *in vivo* Fe-S cluster formation in *Escherichia coli*. *Proc Natl Acad Sci U S A,* 97**(16):** 9009-9014.

SCOTT, C., PARTRIDGE, J. D., STEPHENSON, J. R. and GREEN, J. (2003) DNA target sequence and FNR-dependent gene expression. *FEBS Lett,* 541**(1-3):** 97-101.

SHARROCKS, A. D., GREEN, J. and GUEST, J. R. (1990) *In vivo* and *in vitro* mutants of FNR the anaerobic transcriptional regulator of *E. coli*. *FEBS Lett,* 270**(1-2):** 119-122.

SHARROCKS, A. D., GREEN, J. and GUEST, J. R. (1991) FNR activates and represses transcription *in vitro*. *Proc Biol Sci,* 245**(1314):** 219-226.

SIEVERS, F., WILM, A., DINEEN, D., GIBSON, T. J., KARPLUS, K., LI, W., LOPEZ, R., MCWILLIAM, H., REMMERT, M. and SÖDING, J. (2011) Fast, scalable generation of high- quality protein multiple sequence alignments using Clustal Omega. *Mol Syst Biol,* 7**(1)**.

SILVA, G., OLIVEIRA, S., GOMES, C. M., PACHECO, I., LIU, M. Y., XAVIER, A. V., TEIXEIRA, M., LEGALL, J. and RODRIGUES-POUSADA, C. (1999) *Desulfovibrio gigas* neelaredoxin. A novel superoxide dismutase integrated in a putative oxygen sensory operon of an anaerobe. *Eur J Biochem,* 259**(1-2):** 235-243.

SINGH, A. K., SHIN, J. H., LEE, K. L., IMLAY, J. A. and ROE, J. H. (2013) Comparative study of SoxR activation by redox-active compounds. *Mol Microbiol,* 90**(5):** 983-996.

SMITH, L. J., STAPLETON, M. R., FULLSTONE, G. J., CRACK, J. C., THOMSON, A. J., LE BRUN, N. E., HUNT, D. M., HARVEY, E., ADINOLFI, S., BUXTON, R. S. and GREEN, J. (2010) *Mycobacterium tuberculosis* WhiB1 is an essential DNA-binding protein with a nitric oxide-sensitive iron-sulfur cluster. *Biochem J,* 432**(3):** 417-427.

SPIRO, S. (1994) The FNR family of transcriptional regulators. *Antonie Van Leeuwenhoek,* 66**(1-3):** 23-36.

SPIRO, S., GASTON, K. L., BELL, A. I., ROBERTS, R. E., BUSBY, S. J. and GUEST, J. R. (1990) Interconversion of the DNA-binding specificities of two related transcription regulators, CRP and FNR. *Mol Microbiol,* 4**(11):** 1831-1838.

SPIRO, S. and GUEST, J. R. (1987) Regulation and over-expression of the *fnr* gene of *Escherichia coli*. *J Gen Microbiol,* 133**,** 3279-88.

SPIRO, S. and GUEST, J. R. (1990) FNR and its role in oxygen-regulated gene expression in *Escherichia coli*. *FEMS Microbiol Rev,* 6**(12):** 399-428.

SPIRO, S. and GUEST, J. R. (1991) Adaptive responses to oxygen limitation in *Escherichia coli*. *Trends Biochem Sci,* 16**(8):** 310-314.

STALON, V. and MERCENIER, A. (1984) L-arginine utilization by *Pseudomonas* species. *J Gen Microbiol,* 130**(1):** 69-76.

STALON, V., RAMOS, F., PIERARD, A. and WIAME, J. M. (1967) The occurrence of a catabolic and an anabolic ornithine carbamoyltransferase in *Pseudomonas*. *Biochim Biophys Acta,* 139**(1):** 91-97.

STEENKAMP, D. J. and PECK, H. D. JR. (1980) The association of hydrogenase and dithionite reductase activities with the nitrite reductase of *Desulfovibrio desulfuricans*. *Biochem Biophys Res Commun,* 94**(1):** 41-48.

STOVER, C. K., PHAM, X. Q., ERWIN, A. L., MIZOGUCHI, S. D., WARRENER, P., HICKEY, M. J., BRINKMAN, F. S., HUFNAGLE, W. O., KOWALIK, D. J., LAGROU, M., GARBER, R. L., GOLTRY, L., TOLENTINO, E., WESTBROCK-WADMAN, S., YUAN, Y., BRODY, L. L., COULTER, S. N., FOLGER, K. R., KAS, A., LARBIG, K., LIM, R., SMITH, K., SPENCER, D., WONG, G. K., WU, Z., PAULSEN, I. T., REIZER, J., SAIER, M. H., HANCOCK, R. E., LORY, S. and OLSON, M. V. (2000) Complete genome sequence of *Pseudomonas aeruginosa* PAO1, an opportunistic pathogen. *Nature,* 406**(6799):** 959-964.

SUN, H., SPRING, S., LAPIDUS, A., DAVENPORT, K., DEL RIO, T. G., TICE, H., NOLAN, M., COPELAND, A., CHENG, J. F., LUCAS, S., TAPIA, R., GOODWIN, L., PITLUCK, S., IVANOVA, N., PAGANI, I., MAVROMATIS, K., OVCHINNIKOVA, G., PATI, A., CHEN, A., PALANIAPPAN, K., HAUSER, L., CHANG, Y. J., JEFFRIES, C. D., DETTER, J. C., HAN, C., ROHDE, M.,

BRAMBILLA, E., GOKER, M., WOYKE, T., BRISTOW, J., EISEN, J. A., MARKOWITZ, V., HUGENHOLTZ, P., KYRPIDES, N. C., KLENK, H. P. and LAND, M. (2010) Complete genome sequence of *Desulfarculus baarsii* type strain (2st14). *Stand Genomic Sci,* 3**(3):** 276-284.

SUTTON, V. R., METTERT, E. L., BEINERT, H. and KILEY, P. J. (2004) Kinetic analysis of the oxidative conversion of the $[4Fe\text{-}4S]^{2+}$ cluster of FNR to a $[2Fe\text{-}2S]^{2+}$ Cluster. *J Bacteriol,* 186**(23):** 8018-8025.

SWEENEY, W. V. and RABINOWITZ, J. C. (1980) Proteins containing [4Fe-4S] clusters: an overview. *Annu Rev Biochem,* 49**(1):** 139-161.

THAUER, R. K., JUNGERMANN, K. and DECKER, K. (1977) Energy conservation in chemotrophic anaerobic bacteria. *Bacteriol Rev,* 41**(1):** 100-180.

TILLEY, G. J., CAMBA, R., BURGESS, B. K. and ARMSTRONG, F. A. (2001) Influence of electrochemical properties in determining the sensitivity of [4Fe-4S] clusters in proteins to oxidative damage. *Biochem J,* 360**(3):** 717-726.

TIMMIS, K. N. (2002) *Pseudomonas putida*: a cosmopolitan opportunist par excellence. *Environ Microbiol,* 4**(12):** 779-781.

TRAVERS, A. A. and BURGESS, R. R. (1969) Cyclic re-use of the RNA polymerase sigma factor. *Nature,* 222**(5193):** 537-540.

TRIBELLI, P. M., HAY, A. G. and LOPEZ, N. I. (2013) The global anaerobic regulator ANR, is involved in cell attachment and aggregation influencing the first stages of biofilm development in *Pseudomonas extremaustralis*. *PLoS One,* 8**(10):** e76685.

TRUN, N. and TREMPY, J. (2009) *Fundamental Bacterial Genetics*. Blackwell.

TRUNK, K., BENKERT, B., QUACK, N., MUNCH, R., SCHEER, M., GARBE, J., JANSCH, L., TROST, M., WEHLAND, J., BUER, J., JAHN, M., SCHOBERT, M. and JAHN, D. (2010) Anaerobic adaptation in *Pseudomonas aeruginosa*: definition of the ANR and DNR regulons. *Environ Microbiol,* 12**(6):** 1719-1733.

UGIDOS, A., MORALES, G., RIAL, E., WILLIAMS, H. D. and ROJO, F. (2008) The coordinate regulation of multiple terminal oxidases by the *Pseudomonas putida* ANR global regulator. *Environ Microbiol,* 10**(7):** 1690-1702.

UNDEN, G. and DUCHENE, A. (1987) On the role of cyclic AMP and the FNR protein in *Escherichia coli* growing anaerobically. *Arch Microbiol,* 147**(2):** 195-200.

UNDEN, G. and TRAGESER, M. (1991) Oxygen regulated gene expression in *Escherichia coli*: control of anaerobic respiration by the FNR protein. *Antonie Van Leeuwenhoek,* 59**(2):** 65-76.

VALLET-GELY, I., SHARP, J. S. and DOVE, S. L. (2007) Local and global regulators linking anaerobiosis to *cupA* fimbrial gene expression in *Pseudomonas aeruginosa*. *J Bacteriol,* 189**(23):** 8667-8676.

VANDER WAUVEN, C., PIERARD, A., KLEY-RAYMANN, M. and HAAS, D. (1984) *Pseudomonas aeruginosa* mutants affected in anaerobic growth on arginine: evidence for a four-gene cluster encoding the arginine deiminase pathway. *J Bacteriol,* 160**(3):** 928-934.

VARGHESE, S., TANG, Y. and IMLAY, J. A. (2003) Contrasting sensitivities of *Escherichia coli* aconitases A and B to oxidation and iron depletion. *J Bacteriol,* 185**(1):** 221-230.

VASSYLYEV, D. G., SEKINE, S., LAPTENKO, O., LEE, J., VASSYLYEVA, M. N., BORUKHOV, S. and YOKOYAMA, S. (2002) Crystal structure of a bacterial RNA polymerase holoenzyme at 2.6 A resolution. *Nature,* 417**(6890):** 712-719.

VICENTE, M. and CANOVAS, J. L. (1973) Glucolysis in *Pseudomonas putida*: physiological role of alternative routes from the analysis of defective mutants. *J Bacteriol,* 116**(2):** 908-914.

VOLBEDA, A., DARNAULT, C., RENOUX, O., NICOLET, Y. and FONTECILLA-CAMPS, J. C. (2015) The crystal structure of the global anaerobic transcriptional regulator FNR explains its extremely fine-tuned monomer-dimer equilibrium. *Sci Adv,* 1**(11):** e1501086.

VOLLACK, K. U., HARTIG, E., KORNER, H. and ZUMFT, W. G. (1999) Multiple transcription factors of the FNR family in denitrifying *Pseudomonas stutzeri*: characterisation of four fnr-like genes, regulatory responses and cognate metabolic processes. *Mol Microbiol,* 31**(2):** 1681-1694.

VRENTAS, C. E., GAAL, T., ROSS, W., EBRIGHT, R. H. and GOURSE, R. L. (2005) Response of RNA polymerase to ppGpp: requirement for the ω subunit and relief of this requirement by DksA. *Genes Dev,* 19**(19):** 2378-2387.

WILLIAMS, H. D., ZLOSNIK, J. E. and RYALL, B. (2007) Oxygen, cyanide and energy generation in the cystic fibrosis pathogen *Pseudomonas aeruginosa*. *Adv Microb Physiol,* 52**,** 1-71.

WILLIAMS, R., BELL, A., SIMS, G. and BUSBY, S. (1991) The role of two surface exposed loops in transcription activation by the *Escherichia coli* CRP and FNR proteins. *Nucl Acids Res,* 19**(24):** 6705-6712.

WILLIAMS, S. M., SAVERY, N. J., BUSBY, S. J. and WING, H. J. (1997) Transcription activation at class I FNR-dependent promoters: identification of the activating surface of FNR and the corresponding contact site in the C-terminal

domain of the RNA polymerase alpha subunit. *Nucl Acids Res,* 25**(20):** 4028-4034.

WILLIAMS, S. M., WING, H. J. and BUSBY, S. J. (1998) Repression of transcription initiation by *Escherichia coli* FNR protein: repression by FNR can be simple. *FEMS Microbiol Lett,* 163**(2):** 203-208.

WING, H. J., GREEN, J., GUEST, J. R. and BUSBY, S. J. (2000) Role of activating region 1 of *Escherichia coli* FNR protein in transcription activation at class II promoters. *J Biol Chem,* 275**(37):** 29061-29065.

WING, H. J., WILLIAMS, S. M. and BUSBY, S. J. (1995) Spacing requirements for transcription activation by *Escherichia coli* FNR protein. *J Bacteriol,* 177**(23):** 6704-6710.

WINTELER, H. V. and HAAS, D. (1996) The homologous regulators ANR of *Pseudomonas aeruginosa* and FNR of *Escherichia coli* have overlapping but distinct specificities for anaerobically inducible promoters. *Microbiol,* 142**(3):** 685-693.

WONG, S. M. and MEKALANOS, J. J. (2000) Genetic footprinting with mariner-based transposition in *Pseudomonas aeruginosa*. *Proc Natl Acad Sci U S A,* 97**(18):** 10191-10196.

XANTHOUDAKIS, S. and CURRAN, T. (1992) Identification and characterisation of Ref-1, a nuclear protein that facilitates AP-1 DNA-binding activity. *EMBO J,* 11**(2):** 653-665.

YE, R., HAAS, D., KA, J., KRISHNAPILLAI, V., ZIMMERMANN, A., BAIRD, C. and TIEDJE, J. (1995) Anaerobic activation of the entire denitrification pathway in *Pseudomonas aeruginosa* requires ANR, an analog of FNR. *J Bacteriol,* 177**(12):** 3606-3609.

YOON, S. S., KARABULUT, A. C., LIPSCOMB, J. D., HENNIGAN, R. F., LYMAR, S. V., GROCE, S. L., HERR, A. B., HOWELL, M. L., KILEY, P. J., SCHURR, M. J., GASTON, B., CHOI, K. H., SCHWEIZER, H. P. and HASSETT, D. J. (2007) Two-pronged survival strategy for the major cystic fibrosis pathogen, *Pseudomonas aeruginosa*, lacking the capacity to degrade nitric oxide during anaerobic respiration. *EMBO J,* 26**(15):** 3662-3672.

ZHANG, B., CRACK, J. C., SUBRAMANIAN, S., GREEN, J., THOMSON, A. J., LE BRUN, N. E. and JOHNSON, M. K. (2012) Reversible cycling between cysteine persulfide-ligated [2Fe-2S] and cysteine-ligated [4Fe-4S] clusters in the FNR regulatory protein. *Proc Natl Acad Sci U S A,* 109**(39):** 15734-15739.

ZHANG, G., CAMPBELL, E. A., MINAKHIN, L., RICHTER, C., SEVERINOV, K. and DARST, S. A. (1999) Crystal structure of *Thermus aquaticus* core RNA polymerase at 3.3 A resolution. *Cell,* 98**(6):** 811-824.

ZHENG, L., WHITE, R. H., CASH, V. L., JACK, R. F. and DEAN, D. R. (1993) Cysteine desulfurase activity indicates a role for NIFS in metallocluster biosynthesis. *Proc Natl Acad Sci U S A,* 90**(7):** 2754-2758.

ZHOU, A., CHEN, Y. I., ZANE, G. M., HE, Z., HEMME, C. L., JOACHIMIAK, M. P., BAUMOHL, J. K., HE, Q., FIELDS, M. W., ARKIN, A. P., WALL, J. D., HAZEN, T. C. and ZHOU, J. (2012) Functional characterisation of CRP/FNR-type global transcriptional regulators in *Desulfovibrio vulgaris* Hildenborough. *Appl Environ Microbiol,* 78**(4):** 1168-1177.

ZIEGELHOFFER, E. C. and KILEY, P. J. (1995) *In vitro* analysis of a constitutively active mutant form of the *Escherichia coli* global transcription factor FNR. *J Mol Biol,* 245**(4):** 351-361.

ZIMMERMANN, A., REIMMANN, C., GALIMAND, M. and HAAS, D. (1991) Anaerobic growth and cyanide synthesis of *Pseudomonas aeruginosa* depend on ANR, a regulatory gene homologous with FNR of *Escherichia coli*. *Mol Microbiol,* 5**(6):** 1483-1490.

Appendix

Table S1: Amino acid analysis of ANR

Amino acid	nmole/mL	µg/mL	Mg/mL
Cysteic acid	-	-	-
Hydroxyproline	-	-	-
Aspartic acid	316	36.3	0.0363
Threonine	150	15.2	0.0152
Serine	277	24.1	0.0241
Glutamic acid	451	58.2	0.0582
Proline	153	14.9	0.0149
Glycine	351	20.0	0.0200
Alanine	288	20.5	0.0205
Cystine	22.9	5.10	0.00510
Valine	212	21.0	0.0210
Methionine	89.3	11.7	0.0117
Isoleucine	207	23.4	0.0234
Leucine	407	46.1	0.0461
Tyrosine	50.1	8.18	0.00818
Phenylalanine	112	16.5	0.0165
Histidine	85.8	11.8	0.0118
Tryptophan	-	-	-
Lysine	140	17.9	0.0179
Arginine	192	30.0	0.0300
Totals	**3500**	**381**	**0.381**

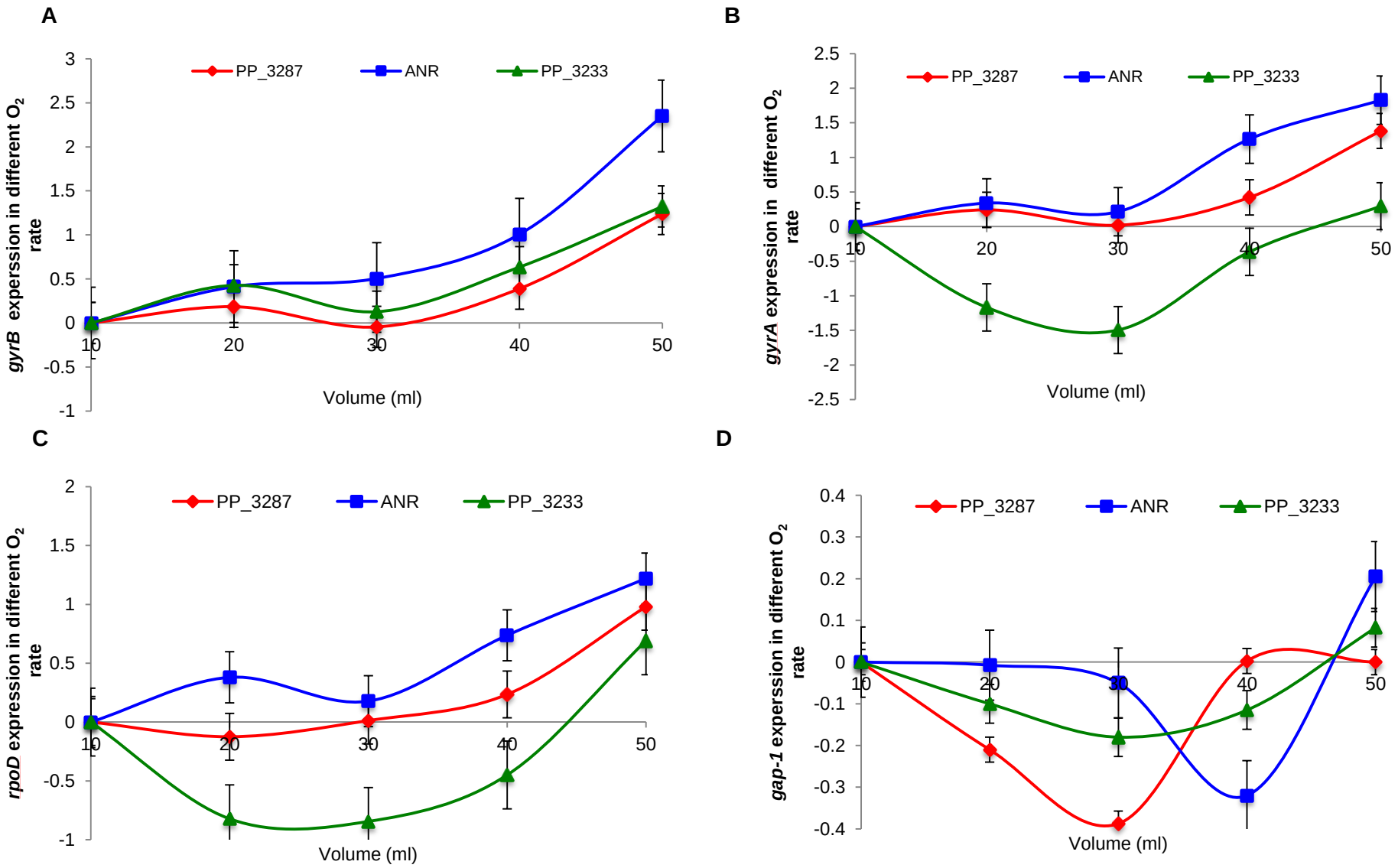
A
PP_3287
ANR
PP_3233
gyrB experssion in different O2 rate
Volume (ml)
B
gyrA expression in different O2 rate
Volume (ml)
C
rpoD expression in different O2 rate
Volume (ml)
D
gap-1 experssion in different O2 rate
Volume (ml)

Figure S1: Expression of *gryB*, *gyrA*, *rpoD* and *gap-1* respectively for *P. putida* mutant strains under different O_2 concentration. Cultures of *P. putida* JRG6723, JRG6722 or JRG6721 that express ANR^+, PP_3233^+ or PP_3287^+ were grown in 50 mL shaking conical flask containing 10, 20, 30, 40 or 50 mL of LB medium with tetracycline 35 µg/mL at 30°C/200 rpm. RNA samples purified and diluted to 20 ng/µl after measuring the concentrations (Section 2.5.9B). Error bars are the standard division from the mean of (n=4).